





Universitat Autònoma de Barcelona

ADVERTIMENT. L'accés als continguts d'aquesta tesi queda condicionat a l'acceptació de les condicions d'ús establertes per la següent llicència Creative Commons:  http://cat.creativecommons.org/?page_id=184

ADVERTENCIA. El acceso a los contenidos de esta tesis queda condicionado a la aceptación de las condiciones de uso establecidas por la siguiente licencia Creative Commons:  <http://es.creativecommons.org/blog/licencias/>

WARNING. The access to the contents of this doctoral thesis it is limited to the acceptance of the use conditions set by the following Creative Commons license:  <https://creativecommons.org/licenses/?lang=en>



UNIVERSITAT AUTÒNOMA DE BARCELONA

Genetic dissection of *ETHQV8.1*, a QTL related with climacteric fruit ripening in melon

PhD thesis

Dissertation presented by Miguel Santo Domingo Martínez for the degree of Doctor of Plant Biology and Biotechnology by Universitat Autònoma de Barcelona (UAB).

This work was performed in Centre de Recerca en Agrigenòmica (Crag), Bellaterra.

PhD candidate

Miguel Santo Domingo Martínez

Supervisors

Jordi Garcia Mas & Marta Pujol Abajo

Tutor

Jordi Garcia Mas

Content

List of Figures	1
List of Tables	5
List of Supplementary material	6
List of Abbreviations.....	10
Summary.....	13
General introduction.....	21
Melon.....	23
Fruit ripening	26
Fruit ripening in climacteric species: tomato as a model	27
Fruit ripening in non-climacteric species: strawberry as a model.....	32
Fruit ripening in melon: co-existence of climacteric and-non climacteric varieties....	36
New approaches in plant breeding	40
Omics.....	40
New breeding techniques	42
Objectives.....	47
Chapter 1.....	51
Chapter 1.1.....	57
Abstract.....	61
Introduction	63
Results and discussion.....	65
Materials and methods.....	78
Conclusion.....	81
Supplementary material	83
Digital supplementary material	85
References	86
Chapter 1.2.....	93
Abstract.....	97
Introduction	99
Results and discussion.....	100
Materials and methods.....	114
Conclusion.....	118
Supplementary material	119
Digital supplementary material	119
References	120

Chapter 2	129
Abstract	133
Introduction	135
Materials and Methods	136
Results	142
Discussion	151
Supplementary material	158
Digital supplementary material	164
References	165
Chapter 3	181
Chapter 3.1	185
Abstract	189
Introduction	191
Results	192
Discussion	202
Materials and methods	207
Supplementary material	212
Digital supplementary material	217
References	218
Chapter 3.2	223
Abstract	227
Introduction	229
Materials and methods	231
Results	235
Discussion	242
Conclusion	245
Supplementary material	246
Digital supplementary material	247
References	248
Chapter 4	253
Abstract	257
Introduction	259
Materials and methods	260
Results	262
Discussion	271
Supplementary material	277

Digital supplementary material	283
References	284
General discussion	293
General references	301
Conclusions	327

List of Figures

Figure I.1. Network of the *Cucumis melo* clade. Each colored circle represents a haplotype, colors represent geographical origin and black circles represent groups of modern cultivars. Modified from Endl *et al* (2018).

Figure I.2. Schematic representation of the different layers affecting fruit ripening in tomato.

Figure I.3. Schematic representation of the different layers affecting fruit ripening in strawberry.

Figure I.4. Schematic representation of the different layers affecting fruit ripening in melon.

Figure I.5. Current situation of edited crops legislation worldwide, showing the population of the ten most populated countries in 2022. Adapted from Buchholzer and Frommer (2022).

Figure 1.1.1. Breeding scheme followed to develop the PS IL collection.

Figure 1.1.2. A) Genotypic characterization of the IL collection. Purple represents the genotype of the recurrent parent Ved and green, the genotype of the donor parent PS. B) Representative images of the ILs.

Figure 1.1.3. Segregation of qualitative traits and genomic location of the responsible major gene.

Figure 1.1.4. Boxplot representing the SSC values for PS ILs.

Figure 1.1.5. Boxplot representing the values of morphological traits for PS ILs.

Figure 1.1.6. Boxplot representing the values of climacteric ripening traits for PS ILs.

Figure 1.2.1. Fruit quality, fruit morphology and fruit ripening related phenotypes of the parental lines PS and Ved in 2020 and 2021.

Figure 1.2.2. Simplified breeding scheme for the development of the VED IL population.

Figure 1.2.3. **A)** Graphical representation of the genotypes of the introgression lines and the two parental lines. **B)** External and internal appearance of each of the introgression lines and the parental lines.

Figure 1.2.4. Fruit quality related phenotypes of the VED IL population in 2020 and 2021.

Figure 1.2.5. Fruit morphology related phenotypes of the VED IL population in both years 2020 and 2021.

Figure 1.2.6. Ripening related phenotypes of the VED IL population in 2020 and 2021.

Figure 2.1. **A)** Genotype of the 26 recombinant F2 plants found in the region of *ETHQV8.1*. **B)** Analysis marker by marker of the four quantitative ripening-related phenotypes.

Figure 2.2. **A)** Genotype of the selected recombinant families, Ved and PS8.2 in the region of the QTL *ETHQV8.1*. **B)** Boxplot of EALF phenotype in the selected recombinant families, Ved and PS8.2. **C)** Analysis marker by marker of the four quantitative ripening-related phenotypes.

Figure 2.3. **A)** Relative expression data of *CmERF024* in the four genotypes at different points of the fruit development and ripening. **B)** Earliness of abscission layer formation (EALF) of the four analyzed genotypes.

Figure 2.4. **A)** Representation of the gene structure of *CmERF024*, together with the two mutant alleles with their DNA and protein sequences. **B)** and **C)** Earliness of abscission layer formation in two different locations.

Figure 2.5. Gene Ontology analysis of **A)** the genes co-expressed with *CmERF024* during melon fruit development, and **B)** the high confident targets of *CmERF024*.

Figure 3.1.1. Phenotypic evaluation of the three parental lines PS, SC and Ved used in the study.

Figure 3.1.2. External and internal visualization of the fruits of the lines used in this study, including the parental lines.

Figure 3.1.3. A) Representation of the phenotype “earliness of abscission layer formation” in the ILs. B), C), and D) Interaction plots showing the two-by-two interactions.

Figure 3.1.4. A) Ethylene production, B) earliness of ethylene production and C) slope of the log₁₀ transformed data in the exponential part of the peak of the ILs.

Figure 3.1.5. Production of esters and aldehydes, showing both total relative production.

Figure 3.2.1. Graphic representation of the breeding scheme followed to develop the IL population.

Figure 3.2.2. Phenotypes of the parental lines ‘Védrantais’ (Ved), ‘Ginseng makuwa’ (Mak) and ‘Piel de Sapo’ (PS)

Figure 3.2.3. External and internal appearance of the six lines characterized in 2021.

Figure 3.2.4. Fruit quality related phenotypes of the parental line Ved and the evaluated ILs at harvest.

Figure 3.2.5. Interaction plots showing the interactions between *ETHQV8.1* and *MAK10.1* for the analyzed phenotypes.

Figure 3.2.6. Ripening related phenotypes of the parental line Ved and the evaluated ILs 1QPS8, 1QMAK10 and 2QPSMAK8.10

Figure 3.2.7. Ethylene related phenotypes of the parental line Ved and the evaluated ILs 1QPS8, 1QMAK10 and 2QPSMAK8.10.

Figure 4.1. Ethylene production (A,B) and respiration rate (C,D) of the four analyzed genotypes (Ved, PS, PS8.2 and VED8.2) during fruit development and ripening, measured in summer 2020 and 2021.

Figure 4.2. PCA of the metabolic profiling of the flesh samples of the analyzed genotypes in season 2021.

Figure 4.3. Summary of the relative abundance of the primary metabolites during the fruit development of the four analyzed lines in 2020.

Content

Figure 4.4. Summary of the relative abundance of the primary metabolites during the fruit development of the four analyzed lines in 2021

Figure 4.5. Abundance profile of the metabolites considered as most related with ripening.

Figure 4.6. Correlation heatmap of the clusters obtained in the RNA-seq data analysis and the metabolic profiling data of the two parental lines PS and Ved in 2020 season.

List of Tables

Table 1.1.1. QTLs identified for quantitative traits in the PS IL population.

Table 1.1.2. Phenotypic traits evaluated in the PS IL collection.

Table 1.2.1. Summary of the developed introgression lines population, with average introgression size per chromosome in physical and genetic distance.

Table 1.2.2. Summary of the QTLs mapped in the population for the quantitative traits.

Table 1.2.3. Different phenotypes analyzed in this study, divided in three groups.

Table 2.1. Phenotypes analyzed in the experiment.

Table 2.2. List of high confident targets that co-expressed with CmERF024 with a putative binding peak in their promoter region.

Table 3.1.1. Melon lines used in this work. SC = Songwan Charmi, VED = Védrantais.

Table 3.1.2. Multiple linear model used to analyze the earliness of abscission layer formation (EALF) in the ILs. $R^2 = 0.86$.

Table 3.1.3. Traits evaluated in the experiment.

Table 3.2.1. Summary of the ILs used or developed in the present study. All lines share the genetic background of 'Védrantais'.

Table 3.2.2. Phenotypes evaluated in the present study.

List of Supplementary material

Figure 1.1.S1. Images of the parental lines used to develop the IL collection.

Figure 1.1.S2. Effect of the QTL *CDQP7.1* on chlorophyll degradation.

Table 1.1.S1. Average and SD values of phenotypic traits analyzed in the IL collection and the parental lines PS and Ved.

Table 1.1.S2. Genotypes of the IL collection.

Table 1.1.S3. Description of the IL collection.

Table 1.1.S4. General description of some IL collections.

Table 1.1.S5. Information about the SNPs used to develop and genotype the IL collection.

Table 1.2.S1. Phenotypical data of the analyzed quantitative traits in the whole studied population.

Table 1.2.S2. Genotypes of the IL population.

Table 1.2.S3. Quantitative phenotypes of the Introgression Lines evaluated in 2019.

Table 1.2.S4. Composition of modified MS medium used for in vitro culture.

Figure 2.S1. Principal component analysis of the RNA-seq experiment.

Figure 2.S2. Different clusters obtained in the RNA-seq experiment by WGCNA.

Figure 2.S3. Predicted protein structure of *CmERF024* using ‘Alphafold’ (Jumper *et al*, 2021).

Figure 2.S4. Consensus binding motif of *CmERF024*.

Figure 2.S5. Relative expression by qRT-PCR of three high confident targets of *CmERF024* in the parental lines ‘Védrantais’ and ‘Piel de Sapo’ and the introgression lines (ILs) PS8.2 and VED8.2 during fruit development.

Figure 2.S6. Phylogenetic tree of the homologous gene family members of *CmERF024* (MELO3C024520) in melon, tomato and Arabidopsis.

Table 2.S1. List of primers used in this study.

Table 2.S2. Information of the RNA-seq experiment by sample.

Table 2.S3. Summary of the trimmed and uniquely aligned reads in the melon reference genome v4.0 in the DAP-seq experiment.

Table 2.S4. Summary of the alignment in the resequenced recombinant lines R14-F3, R15-F3 and R68-F3.

Table 2.S5. Phenotypic data of the analyzed plants.

Table 2.S6. Different alleles in each position of *ETHQV8.1* using both resequencing data and SNPs markers of the resequenced families.

Table 2.S7. Structural variants analysis of the resequenced lines R14-F3, R15-F3 and R68-F3, and PS8.2.

Table 2.S8. Binding peaks found in the DAP-seq experiments.

Table 2.S9. Expression clusters obtained with WGCNA in the RNA-seq experiment.

Table 2.S10. Significant GO terms found for *CmERF024* co-expression cluster.

Table 2.S11. Significant GO terms found for the HTC gene list.

Additional File 2.1. Raw data of the RNA-seq experiment, aligned with STAR against the reference genome v4.0.

Additional File 2.2. FASTA DNA and protein sequences of *CmERF024* in ‘Piel de Sapo’ and ‘Védrantais’.

Figure 3.1.S1. Representation of the breeding scheme followed to develop the double and triple ILs from the initial lines 1QSC3, 1QSC6, 1QVED8 and 2QSC36.

Figure 3.1.S2. Principal Component Analysis of the three main climacteric symptoms in the population.

Figure 3.1.S3. General “less than additive” trend observed in the population for the earliness of abscission layer formation.

Figure 3.1.S4. Phenotype evaluation of the level of abscission.

Figure 3.1.S5. Principal component analysis for the aroma profile of the population in rind and flesh

Figure 3.1.S6. Phenotypic evaluation of **A)** fruit weight, **B)** soluble solid content and **C)** firmness in the population analyzed in the study.

Table 3.1.S1. Phenotypes of the lines used in this study, along with the parental lines.

Table 3.1.S2. Production of each analyzed compound (ng/g), total production (ng/g) and number of different compounds produced in each line.

Table 3.1.S3. Quantity and percentage of volatile compounds found in flesh tissue and rind tissue.

Table 3.1.S4. Compounds related to melon aroma, and their single effect, and their production in flesh tissue and rind tissue.

Table 3.1.S5. Linear model for the phenotype DAPE, DAPP and SLOPE, showing single effects and interaction between QTLs

Table 3.1.S6. Linear model for the production of benzeacetaldehyde in rind (**A**), eucalyptol in flesh (**B**), phenylethyl alcohol in flesh (**C**), propanoic acid, 2-methyl-, ethyl ester in flesh (**D**) and 1-octen-3-ol in flesh (**E**), showing single effects of the QTLs.

Table 3.1.S7. Primers used to genotype the three QTLs.

Table 3.2.S1. Markers used for Marker Assisted Selection, with the respective primers design for PACE2.0 genotyping system.

Table 3.2.S2. Summary of the Marker Assisted Selection (MAS) results for the construction of the entire IL population.

Table 3.2.S3. Mean and standard deviation (SD) of the different analyzed phenotypes in the parental lines and the introgression lines.

Table 3.2.S4. Multiple linear models for the analyzed phenotypes Figure 4.S1

Figure 4.S1. Abundance profile of the metabolites not considered as related with ripening in 2021. Error bars represent standard deviation of three to six replicates.

Figure 4.S2. Clusters of metabolite profiles in the four lines in 2021

Figure 4.S3. Clusters of metabolite profiles in the parental lines PS and Ved in 2020.

Figure 4.S4. Summary of the citric acid behavior from the onset of ripening to fully ripe fruits in different crops

Table 4.S1. Pearman's correlation between the metabolite profiles in 2020 and 2021.

Table 4.S2. Mean values and standard deviation of the relative abundance of each detected metabolite after PQN normalization

Table 4.S3. PCA loadings of all the analyzed metabolites in 2021.

Table 4.S4. Differently abundant metabolites in season 2021, classified by cluster.

Table 4.S5. Differently abundant metabolites between the parents PS and Ved in season 2020, classified by cluster.

List of Abbreviations

ABA	Abscisic acid
ABS	Level of abscission
ACC	1-aminocyclopropane-1-carboxylic acid
ACO	ACC oxidase
ACS	ACC synthase
ANOVA	Analysis of variance
ARF	Auxin responsive factor
ARO	Aroma production
ATAC-seq	Assay of Transposase-Accessible Chromatin sequencing
BC	Back-cross
bp	Base pair
Bt	<i>Bacillus thuringiensis</i>
Cas	CRISPR associated protein
CD	Chlorophyll degradation
Chr	Chromosome
cM	centiMorgan
CMV	Cucumber mosaic virus
CRISPR	Clustered regularly interspaced short palindromic repeats
CSSL	Chromosome segment substitution line
DAP	Days after pollination
DAPE	Earliness of ethylene production
DAPP	Earliness of the ethylene peak
DAP-seq	DNA affinity purification sequencing
DBS	Double-strand break
DEG	Differentially expressed gene
DHL	Double haploid line
DNA	Deoxyribonucleic acid
EALF	Earliness of abscission layer formation
EARO	Earliness of aroma production
ECC	Earliness of the change of the rind color
ECD	Earliness of chlorophyll degradation

ECOL	Rind color of the immature fruit
ERF	Ethylene responsive transcription factor
ETH	Ethylene production
EYELL	Earliness of yellowing of the rind
FA	Fruit area
FC	Flesh color
FIR	Flesh firmness
FL	Fruit length
FP	Fruit perimeter
FPKM	Fragments per kilobase of transcript per million
FS	Fruit shape
FW	Fruit weight
FWI	Fruit width
GABA	γ -aminobutyric acid
GC-MS	Gas chromatography – mass spectrometry
GMO	Genetically modified organism
GO	Gene ontology
gRNA	Guide RNA
GWAS	Genome-wide association study
HAR	Harvest date
HCT	High confident target
IAA	Indole-3-acetic acid
IL	Introgression line
KEGG	Kyoto encyclopedia of genes and genomes
KO	Knock-out
Mak	Ginsen Makuwa
MAS	Marker assisted selection
MegN	Meganucleases
MOT	Mottled rind
mRNA	Messenger RNA
NBT	New breeding technique
NE	Not edited
NIL	Near isogenic line

Content

PCA	Principal component analysis
PCR	Polymerase chain reaction
PhD	Philosophie doctor
PPT	L-phosphinotricin
PQN	Probabilistic quotient normalization
PS	Piel de Sapo
qRT-PCR	Quantitative reverse transcription polymerase chain reaction
QTL	Quantitative trait locus
RAPD	Random amplified polymorphic DNA
RFLP	Restriction fragment length polymorphism
RIL	Recombinant inbred line
RNA	Ribonucleic acid
RNA-seq	Ribonucleic acid sequencing
RT-PCR	Reverse transcription polymerase chain reaction
SAM	S-adenosyl-L-methionine
SC	Songwan Charmi
SD	Standard deviation
SLOPE	Slope of the log ₁₀ transformed data in the exponential part of the peak
SNP	Single nucleotide polymorphism
SPME	Solid phase micro extraction
SSC	Soluble solid content
SUT	Presence of sutures
TALEN	Transcription activator-like effector nuclease
TCA	Tricarboxylic acid cycle
TF	Transcription factor
TOF	Time of flight
Ved	Védrantais
VOC	Volatile organic compound
WGCNA	Weighted correlation network analysis
YELL	Yellowing of the rind
ZFN	Zinc finger nuclease

Summary

Summary

Fruit ripening is an essential process in crop plants, as it allows seed dispersion. Also, it has an economic importance due to its effect in fruit shelf-life and food waste. In flesh fruits there are two types of ripening: climacteric, with a characteristic peak of ethylene at the onset of ripening, coupled to an increase in cellular respiration; and non-climacteric, without ethylene peak production nor increase in respiration during the process. Tomato is considered the model fruit for climacteric ripening research, while strawberry is the model crop for non-climacteric ripening studies. Melon (*Cucumis melo* L.), apart from being an economically important crop worldwide, has the advantage of covering both climacteric and non-climacteric behaviors in the same species, making it a suitable candidate for genetic and genomic studies regarding fruit ripening.

To study this trait, we have developed two reciprocal introgression line (IL) populations with a high coverage of the donor genome, and segregating for ripening behavior, using as parental lines the climacteric ‘Védrantais’ (Ved) and the non-climacteric ‘Piel de Sapo’ (PS). In both IL populations, a previously reported QTL, *ETHQV8.1*, has been validated altering ripening behavior, as well as other QTLs controlling ripening and fruit morphology traits. Starting from the IL population with Ved genetic background, we have fine-mapped *ETHQV8.1* to a 3.6 Kbp region containing a single annotated gene, ethylene responsive transcription factor 024 (*CmERF024*). Studying its expression in both IL populations and using the CRISPR/Cas9 technique recently developed in melon, we reported *CmERF024* as the causal gene of *ETHQV8.1*. When highly expressed, *CmERF024* induced a climacteric response, milder when the gene was less or not expressed, apparently affecting chromatin structure and DNA accessibility.

To further investigate the role of *ETHQV8.1*, we have stacked this QTL with three previously reported QTLs affecting ripening in both Ved (*MAK10.1*) and PS (*ETHQB3.5* and *ETHQV6.3*) genetic backgrounds. The epistatic interactions between these QTLs controlled climacteric fruit ripening in melon, covering a broad spectrum of behaviors both in climacteric and non-climacteric genetic backgrounds. These results suggest that a small set of QTLs is sufficient to shape quantitative traits, proving powerful knowledge for applying in plant breeding.

Finally, to explore the relationships among ethylene production, respiration rate and primary metabolism, we have performed a metabolic profiling of Ved and PS, together

Summary

with the ILs covering *ETHQV8.1*. The results showed that *ETHQV8.1* is able to alter primary metabolism, ethylene production and cellular respiration, suggesting a crosstalk between the three processes. Also, some metabolites seemed especially relevant for the process, as citrate, and others may be interesting targets for melon plant breeding programs, as GABA.

As a summary, this PhD thesis has been focused on dissecting *ETHQV8.1*, a QTL related with climacteric ripening in melon. Combining molecular breeding with new breeding techniques we have validated the causal gene, *CmERF024*, which can delay significantly fruit ripening and potentially extend shelf-life. We have also analyzed its role in plant metabolism and its interactions with other known QTLs, providing a useful knowledge for melon breeding.

Resumen

La maduración del fruto es un proceso esencial en las plantas de cultivo, ya que permite la dispersión de las semillas. Además tiene importancia económica debido a sus efectos en la vida útil de los frutos y el desperdicio de comida. Hay dos tipos de maduración: climatérica, que produce un pico de producción de etileno durante la maduración acoplado a un aumento en la respiración celular; y no climatérica, que no produce ese pico de etileno ni el aumento en la respiración durante el proceso. El tomate es el organismo modelo en estudios de maduración climatérica, mientras la fresa es el modelo para frutos no climatéricos. El melón (*Cucumis melo* L.), aparte de ser un cultivo importante económicamente, posee variedades climatéricas y no climatéricas dentro de la misma especie, haciéndolo un perfecto candidato para estudios genéticos y genómicos sobre la maduración de frutos.

Para estudiar este proceso, hemos desarrollado dos poblaciones recíprocas de líneas de introgresión (IL) con una alta cobertura del genoma y segregando para rasgos relacionados con la maduración, utilizando la variedad climatérica ‘Védrantais’ (Ved) y la no climatérica ‘Piel de Sapo’ (PS) como parentales. En ambas poblaciones hemos validado *ETHQV8.1*, un QTL descrito anteriormente alterando la maduración, además de otros QTLs afectando la maduración y la morfología del fruto. Utilizando la población de ILs en fondo genético Ved, hemos realizado un mapeo fino de *ETHQV8.1* acortando el QTL hasta una región de 3.6 Kbp que contiene únicamente un gen anotado, ‘ethylene responsive transcription factor 024’ (*CmERF024*). Estudiando su expresión en las poblaciones de ILs, y utilizando la técnica CRISPR/Cas9 de edición genómica (recientemente desarrollada para melón), hemos identificado *CmERF024* como el gen causal de *ETHQV8.1*. Cuando *CmERF024* se expresa, produce una respuesta climatérica, y cuanto se expresa poco o no se expresa, más suave es el climaterio, afectando aparentemente a la estructura de la cromatina y la accesibilidad del ADN.

Para profundizar en el rol de *ETHQV8.1*, hemos piramidado este QTL con otros tres QTLs que han sido identificados como reguladores de la maduración en fondo genético Ved (*MAK10.1*) y PS (*ETHQB3.5* y *ETHQV6.3*). La interacción epistática entre estos QTLs controla la maduración en melón, cubriendo un amplio espectro de comportamientos en fondo genético climatérico y no climatérico. Los resultados obtenidos sugieren que un pequeño número de QTLs es suficiente para regular rasgos cuantitativos, siendo una herramienta potente para la mejora genética del melón.

Summary

Finalmente, hemos querido explorar las relaciones entre la producción de etileno, la respiración celular y el metabolismo primario realizando un perfilado metabólico de Ved, PS y las ILs cubriendo *ETHQV8.1*. Los resultados muestran que *ETHQV8.1* es capaz de alterar el metabolismo primario y la respiración, aparte del perfil de producción de etileno, sugiriendo una relación entre estos procesos. Además, algunos metabolitos parecen especialmente relevantes en el proceso de maduración, como el citrato; y otros pueden ser objetivos interesantes en programas de mejora, como el GABA.

En resumen, esta tesis doctoral se ha centrado en el estudio de *ETHQV8.1*, un QTL relacionado con la maduración climatérica en melón. Combinando la mejora asistida por marcadores con nuevas técnicas de mejora, hemos identificado *CmERF024* como el gen causal, capaz de retrasar significativamente la maduración y potencialmente extendiendo la vida útil del melón. También hemos analizado su papel en el metabolismo y sus interacciones con otros QTLs, proporcionando nuevos conocimientos y herramientas para la mejora del melón.

Resum

La maduració dels fruits es un procés essencial de les plantes cultivades, permetent la dispersió de les llavors. A més, té una importància econòmica deguda als seus efectes en la vida útil dels fruits i el malbaratament d'aliments. Existeixen dos tipus de maduració: la climatèrica, amb un pic d'etilè produït durant la maduració, acoplat a un augment a la respiració cel·lular; i la no climatèrica, sense la producció d'aquest pic d'etilè ni augment a la respiració. El tomàquet és l'organisme model per estudiar la maduració climatèrica, mentre que la maduixa ho és pels estudis de la maduració no climatèrica. El meló (*Cucumis melo* L.), a més de ser un cultiu important econòmicament, posseeix varietats climatèriques i no climatèriques dins la mateixa espècie, fent-lo un candidat perfecte pels estudis genètics i genòmics sobre la maduració dels fruits.

Per estudiar aquest procés, hem desenvolupat dues poblacions recíproques de línies d'introgessió (ILs), amb una elevada cobertura del genoma y segregant per a trets relacionats amb la maduració, utilitzant com a pares la varietat climatèrica 'Védrañtais' (Ved) i la no climatèrica 'Piel de Sapo' (PS). Amb ambdues poblacions hem validat *ETHQV8.1*, un QTL descrit anteriorment que altera la maduració, a més d'altres QTLs que afecten la maduració i al morfologia dels fruits. Utilitzant la població d'ILs amb fons genètic Ved, hem dut a terme un mapeig fi d'*ETHQV8.1* fins a una regió de 3.6 Kbp que conté un únic gen anotat, 'ethylene responsive transcription factor 024' (*CmERF024*). Analitzant la seva expressió a les poblacions d'ILs i emprant la tècnica CRISPR/Cas9 d'edició gènica (desenvolupada recentment a meló), hem identificat *CmERF024* com a gen causal d'*ETHQV8.1*. Quan *CmERF024* s'expressa, produeix una resposta climatèrica, i quan s'expressa poc o no s'expressa, el climateri es més suau, afectant, aparentment, l'accessibilitat i l'estructura de la cromatina mitjançant el control transcripcional d'histones.

Per aprofundir en el rol d'*ETHQV8.1*, hem piramidat aquest QTL amb altres identificats com a reguladors de la maduració en fons genètic Ved (*MAK10.1*) i PS (*ETHQB3.5* i *ETHQV6.3*). La interacció epistàtica d'aquests QTLs controla la maduració al meló, cobrint un ampli espectre de comportaments en ambdós fons. Els resultats obtinguts suggereixen que un petit nombre de QTLs es suficient per regular caràcters quantitius, essent una eina potent per a la millora del meló.

Summary

Finalment, hem volgut explorar les relacions entre la producció d'etilè, la respiració cel·lular i el metabolisme primari obtenint el perfil metabòlic de Ved, PS i les ILs cobrint *ETHQV8.1*. Els resultats posen de manifest que *ETHQV8.1* és capaç d'alterar el metabolisme primari i la respiració, a més del perfil de producció d'etilè, suggerint una relació entre aquests processos. A més, alguns metabòlits semblen especialment rellevants pel procés de maduració, com el citrat; i altres poden ser objectius interessants per a programes de millora, com el GABA.

En resum, aquesta tesi doctoral ha estat focalitzada en l'estudi d'*ETHQV8.1*, un QTL relacionat amb la maduració climatèrica del meló. Combinant la millora assistida per marcadors amb noves eines de millora, hem identificat *CmERF024* com a gen causal d'*ETHQV8.1*, capaç de retardar significativament la maduració i potencialment allargant la vida útil del meló. També hem analitzat el seu paper en el metabolisme i les seves interaccions amb altres QTLs, proporcionant nous coneixements i eines aplicables a la millora genètica del meló.

General introduction

Melon

Origin

Melon (*Cucumis melo* L.) is a diploid species ($2n = 2n = 24$) with an estimated genome of 450 Mbp (Arumuganathan & Earle, 1991) and a sequenced reference genome of 357.65 Mbp (Gacria-Mas *et al*, 2012; Castanera *et al*, 2020), member of the *Cucurbitaceae* family. This dicot plant family consists of around 1,000 different species, classified in 96 genera (Renner & Schaefer, 2016). Originated in late cretaceous, most of its members are annual vines with tendrils derived from modified shoots (Sousa-Baena *et al*, 2018). Apart from melon, many *Cucurbitaceae* species have a significant importance in human diet, as pumpkin (*Cucurbita pepo*), watermelon (*Citrullus lanatus*) or cucumber (*Cucumis sativus*). Moreover, other species have also additional non-culinary importance, as the sponge gourd (*Luffa aegyptiaca*), which can be consumed as a vegetable as well as be used as a plant-based sponge.

The origin of this species is dated about 2.8 million years ago, when it separated from its closest relatives, *C. pirocarpus* from Australia and *C. trigonous* from India (Endl *et al*, 2018). A million years later, *C. melo* was separated in two subspecies, *C. melo* subsp. *Meloides* (known as African *agrestis*) and *C. melo* subsp. *Melo*, this last split also in two clades, Australian *agrestis* and Asian *agrestis*. It has been suggested that domestication started around 5,000-6,000 years ago in Africa, and maybe earlier in Asia, presenting two independent domestication events. Other authors suggest three independent domestication events, two in India, leading to the subspecies *melo* and *agrestis*, and one in Africa (Zhao *et al*, 2019). Most of the modern cultivars ('*Inodorous*', '*Cantaloupensis*', '*Reticulatus*', '*Makuwa*', etc.) derive from the Asian domestication event, showing also some hybridization between the two domesticated lineages in some modern African cultivars (Figure I.1) (Endl *et al*, 2018).

Economic importance

In the last 40 years, melon production has grown steadily, from around 8.8 million tons in 1980 to 28.5 million tons in 2020 (FAOSTAT, 2020), being Spain the 7th producer worldwide in the last five years, although the production is decreasing in this country. Moreover, Spain has been the world leader melon exporter during the last years, mainly exporting to other countries in the European Union. In 2020, Spain exported 435,000 tons

General introduction

of melons for a value of around 1,000 million euros (Ministerio de Agricultura, Ganadería y Pesca, 2021).

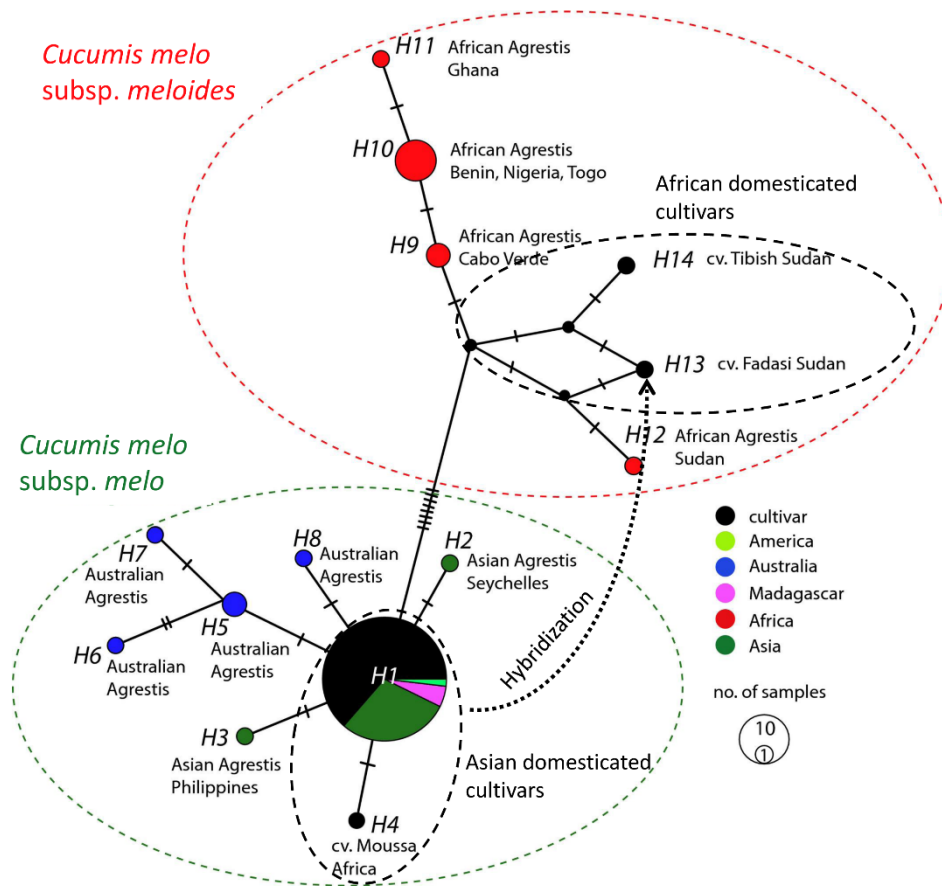


Figure I.1. Network of the *Cucumis melo* clade. Each colored circle represents a haplotype, colors represent geographical origin and black circles represent groups of modern cultivars. Modified from Endl *et al* (2018).

Due to this economic weight in Spain, melon breeding needs to be implemented to keep improving existing cultivars. The main focuses of melon breeding have classically been to improve the yield, to develop disease resistant varieties and to improve organoleptic quality. In recent years, the effects of climate change are becoming more evident, pointing out the necessity to keep improving cultivars to adapt to the changing environmental conditions. Another recent goal of melon breeding is to minimize the environmental impact of its production, reducing fruit losses all along the productive chain, from the production field to the final consumer.

The increasing importance of adaptation and/or mitigation of climate change makes melon breeding a necessary tool to maintain, and even increase, the economic contribution that melon production has in farmers' economy.

Molecular breeding

In order to improve melon cultivars in breeding programs, several mapping populations have been developed. With these populations, important agronomical traits can be associated with molecular markers, making melon breeding faster and easier.

The first type of molecular markers developed in melon were restriction fragment length polymorphisms (RFLPs) (Neuhaussen, 1992). Few years later, the first melon genetic map was published using RFLPs, random amplified polymorphic DNA (RAPD) markers, one isoenzyme, four disease resistance markers and one morphological marker (Baudracco-Arnas & Pitrat, 1996). From there, many genetic maps were published in the following years to map fruit quality and disease resistance QTLs, among other traits (Wang *et al*, 1997; Dannin-Poleg *et al*, 2002; Harel-Beja *et al*, 2010). A qualitative jump was done in 2012, when the first melon reference genome was published (Garcia-Mas *et al*, 2012), and even more with the subsequent versions (Argyris *et al*, 2015; Ruggieri *et al*, 2018; Castanera *et al*, 2020). This advance has allowed to develop a high number of molecular markers based on the DNA sequence and construct high-density genetic maps (Nimmakalaya *et al*, 2016; Chang *et al*, 2017; Pereira *et al*, 2018). Recently, more than 1,000 melon genotypes have been resequenced, providing a significant resource for genetic studies in this species (Zhao *et al*, 2019).

Apart from the classical populations used to construct genetic maps (F₂, recombinant inbred lines (RIL), or double haploid lines (DHL)), the ease to develop molecular markers based in SNPs, together with the already known RFLPs and RAPDs, has allowed to develop collections of introgression lines (IL). IL populations allow to study and map different traits minimizing the effect of the genetic background. This approach has led to the identification of several QTLs related with agronomical traits (Perpiñá *et al*, 2016; Castro *et al*, 2019), disease resistance (Essafi *et al*, 2009), fruit shape (Díaz *et al*, 2014), fruit quality (Obando-Ulloa *et al*, 2009) or fruit ripening (Perpiñá *et al*, 2017; Vegas *et al*, 2013; Ríos *et al*, 2017), as well as identifying some causal genes of these QTLs (Giner *et al*, 2017; Ríos *et al*, 2017).

Fruit ripening

In the life cycle of a plant, sexual reproduction is a key phase as it allows the development of new individuals combining the genetic information of the parents. Even in monoecious plants, as melon, recombination during meiosis increases genetic diversity of the offspring.

Melon is cultivated as a fruit crop. In this type of plants, fruits allow the seeds to develop and, when they are fully developed, fruits are in charge of seed dispersion. During fruit development, after fertilization, there are two different phases (Gillaspy *et al*, 1993; Higashi *et al*, 1999). The first phase is fruit growth, divided in two steps. First, cells experience a high mitotic activity, dividing at a high rate; and second, cells increase their size producing the major grow of the fruit. Once the fruit has obtained its final size and the seeds are fully developed, the fruit acquires the ability to ripe in a second phase.

Fruit ripening, as the last step of fruit development, is a key step for the plant. During this step, as the seeds are already developed, the fruit suffers a set of physiological changes that make it suitable and attractive for animal consumption with the final goal of seed dispersion. These changes also make the fruit attractive for human consumption, having a big effect on the economy. Classically there are two types of fruit ripening: climacteric and non-climacteric (Brady, 1987). During climacteric fruit ripening, the physiological changes suffered by the fruit are induced by a rise in the respiration rate coordinated by ethylene. In non-climacteric fruits, by contrast, these changes are not caused by an increase in the respiration rate and are not controlled by ethylene. Despite the type of fruit ripening, all fruits suffer similar changes during ripening, such as cell wall degradation leading to a softening of the fruit, changes in color due to chlorophyll degradation, sugars accumulation and volatiles production (Goulao & Oliveira, 2008; Nath *et al*, 2014). In each plant species, these changes are controlled by different pathways or processes, being tomato (*Solanum lycopersicum*) and strawberry (*Fragaria x ananassa*) the model plants for studying climacteric and non-climacteric fruit ripening, respectively.

According to Lü *et al* (2018), the use of ethylene as a regulator of fleshy fruit ripening has evolved multiple times in the history of angiosperms. Evolving from senescence or floral organ regulatory pathways, different transcriptional feedback circuits have evolved to control the role of ethylene during fruit ripening, while other processes, as histone methylation, may play conserved roles in this stage of fruit development.

Fruit ripening in climacteric species: tomato as a model

Tomato, as the model plant for fruit studies, is the most studied plant and several processes have been associated with ripening in this species.

Hormonal control

Phytohormones (plant hormones) have been long known as the main regulators of plant development, and therefore fruit ripening. Although in climacteric fruits as tomato ethylene plays a central role (discussed later), other hormones are also involved.

Auxins can delay tomato fruit ripening. Modifying the expression of auxin responsive factors (*ARFs*), ripening behavior is modulated, indicating a crosstalk between auxins and ethylene (Jones *et al*, 2002; Hao *et al*, 2015; Breitel *et al*, 2016). Also, one of these studies (Breitel *et al*, 2016) indicates a triple crosstalk between auxins, ethylene, and abscisic acid (ABA). ABA has been also associated with climacteric ripening, promoting the expression of ethylene synthesis genes (Zhang *et al*, 2009; Kou *et al*, 2021).

But, as commented before, ethylene is the main hormone controlling fruit ripening in climacteric fruits, being also the most studied of all phytohormones during this physiological process.

Ethylene production and perception

Ethylene has been widely studied in tomato as one of the core controllers of climacteric fruit ripening. Ethylene production in plants is well-studied (Bleecker & Kende, 2000). This gaseous plant hormone is synthesized from the methionine cycle. In the first step, S-adenosyl-L-methionine (SAM) is transformed into 1-aminocyclopropane-1-carboxylic acid (ACC) by *ACC synthase* (*ACS*). In a second step, ACC is oxidized by *ACC oxidase* (*ACO*) into ethylene. This pathway is tightly regulated, both by positive and negative feedbacks (Kende, 1993). During fruit growth, ethylene production is maintained in a residual level by a negative feedback regulation, known as system 1. Once the fruit has achieved the capacity to ripe, there is a transition to system 2 of ethylene production, where it is autocatalytically produced regulated as a positive feedback loop (Barry *et al*, 2000). Along this process, several isoforms of *ACS* participate in the different steps with different expression pattern. *ACS1A* and *ACS6* are responsible of the ethylene production in system 1 (Barry *et al*, 2000). Once the fruit has the competence to ripe, *ACS4* is induced, acting together with *ACS1A*. When fruit ripening starts, the main contributor to

General introduction

ethylene production is *ACS2*, regulated by ethylene (Barry *et al*, 2000). Each isoform of *ACS* is not only regulated transcriptionally, but also post-transcriptionally and post-translationally (Olson *et al*, 1995, Oetiker *et al*, 1997). The other family of genes, *ACO*, have also different expression patterns in the plant, being *ACO1* the main isoform acting during fruit ripening (Barry *et al*, 1996).

Another important ethylene-related process is ethylene perception and signal transduction. This process has been deeply studied in the model plant *Arabidopsis thaliana*, and some of this knowledge can be translated to tomato fruits. *Never-ripe* (*Nr*) mutant was described in the fifties as a non-ripening mutant (Rick, 1956), and later the causal gene was suggested as an ethylene receptor homolog of the *Arabidopsis ETR1* (Yen *et al*, 1995). From there, several ethylene receptors have been described, from *ETR1* to *ETR6*, being *ETR3* (or *NR*) the causal gene of *Nr* mutant (Klee, 2004; Lashbrook *et al*, 1998; Payton *et al*, 1996; Tieman & Klee, 1999; Wilkinson *et al*, 1997; Zhou *et al*, 1996). With distinctive characteristics, these receptors are differentially expressed in tissues at various stages of development, giving all the tissues the ability to respond to ethylene. During fruit ripening, *NR* and *ETR4* are the major components of the *ETR* protein pool, indicating their major role at this stage of fruit development (Tieman & Klee, 1999; Wilkinson *et al*, 1995). Another tomato ripening mutant, *Green ripe* or *Gr*, present a similar phenotype as *Nr*, suggesting the causal gene is also an ethylene receptor specific for floral and fruit tissues (Kerr, 1982). The gene was later identified demonstrating its role in ethylene perception, although its specific function is still unknown (Barry & Giovannoni, 2006).

After ethylene perception, signal transduction must take place to translate the external stimulus into cellular responses. The first step of this process is carried out by *Constitutive Triple Response* (*CTR*) proteins. In tomato, four *CTR* genes have been described (from *CTR1* to *CTR4*) (Adam-Phillips *et al*, 2004), acting as negative regulators of ethylene signaling. When ethylene is not present, these proteins inhibit the signal transduction, and when the hormone is present, they stop acting, allowing the signal to go into the cell. Located in the endoplasmic reticulum membrane, tomato *CTR* proteins are able to interact with *ETR* proteins, showing some redundancy in their roles transmitting the ethylene signal (Zhong *et al*, 2008).

Once the ethylene signal is transduced, a set of transcription factors (TF) are responsible of transforming the signal into a cellular response. The main classes of TFs are the

Ethylene-Insensitive 3 (EIN3), that includes *EIN3-like (EIL)*, and *Ethylene-Response Factors (ERF)* gene families. *EIN3* in tomato is a positive regulator of ethylene responses, whose mutant presents ethylene insensitivity (Chao *et al*, 1997). The regulation of its action is conducted by its degradation by *EIN3-binding F-box 1* and *2 (EBF1* and *EBF2)*, which are also regulated by *EIN3* in a feedback loop (Gagne *et al*, 2004). *EIN3* is able to bind the promoter of several ripening-related genes, as *ERF1* and *ACO1* (Solano *et al*, 1998) indicating a central role in controlling fruit ripening in tomato. *ERFs* are considered the last steps of ethylene responses, but their specific roles are still unknown. Some members of this family (apart from *ERF1*) have been studied for their relationship with fruit ripening (Liu *et al*, 2016) showing expression patterns associated with ripening, some of them being induced at the onset of ripening, and some at later stages of the process. Among all of them (in tomato the family has 77 members), *ERF.E1*, *ERF.E2* and *ERF.E4* are the main *ERFs* associated with fruit ripening (Liu *et al*, 2016).

Transcription factors

Apart from the main ethylene pathway (ethylene synthesis, perception, transduction and response), a set of transcription factors have been identified as key regulators of tomato fruit ripening.

In late sixties, a ripening mutant was identified, *ripening inhibitor* or *rin* (Robinson, 1968). This mutant presented fruits that fail to ripe, as well as some other phenotypes (Vrebalov *et al*, 2002). The positional cloning on this locus led to the identification of two *MADS-box* TFs (*MADS-RIN* and *MADS-MC*) as causing the phenotypes. In the mutant, a deletion between these two genes was causing the production of a chimeric protein consisting of the first amino acids of *MADS-RIN* and the last amino acids of *MADS-MC*. This chimeric protein was affecting severely the ripening process, preventing the fruit to ripe (Vrebalov *et al*, 2002). Years later, when CRISPR/Cas9 gene editing technology was developed, a knock-out mutant of *MADS-RIN* presented a milder phenotype than *rin*, with partial ripening (Wang *et al*, 2020). These two different observations indicated that the spontaneous *rin* mutation was more likely a gain-of-function mutation (a dominant repressor) than a knock-out mutation, suggesting that, although *MADS-RIN* is an important gene controlling fruit ripening, it is not essential as it was initially thought.

General introduction

Some years later after the description of *rin* mutant, another mutant was described: *non-ripening* or *nor* (Tigchelaar *et al*, 1973) with a strong ripening-inhibiting phenotype. The mutation produces a frameshift in the *NAC-NOR* transcription factor, resulting in a truncated protein of 186 amino acids instead of the original 355 (Kumar *et al*, 2018). When studied later (Gao *et al*, 2019; Wang *et al*, 2020), it was found that a CRISPR knock-out mutant of *NAC-NOR* did not present a strong phenotype, similar to *MADS-RIN*. In the *nor* spontaneous mutant, the protein still maintains its DNA-binding activity, possibly interfering with the normal transcriptional activation of *NAC-NOR* controlled genes, avoiding other activators to bind their promoters. This transcriptional suppression would not be present in the CRISPR mutant, explaining its milder phenotype (Gao *et al*, 2019; Wang *et al*, 2020). Another member of the *NAC-NOR* family, *NOR-like 1*, has been also associated with fruit ripening, (Gao *et al*, 2018).

A third tomato ripening mutant is *colorless non-ripening* or *cnr*, described in late nineties (Thompson *et al*, 1999), also with a strong phenotype producing yellow fruits. This mutation has been characterized as an epimutation in the promoter of a *SQUAMOSA promoter binding protein-like*, *SBL-CNR*, producing a hypermethylation that dramatically decreases its expression (Manning *et al*, 2006). After CRISPR knock-out development (Gao *et al*, 2019, Wang *et al*, 2020) the effect of these new alleles was different than the *cnr* mutant. In these mutants it was observed that the expression of ripening related genes was not as reduced as in *cnr* and they showed a quite mild phenotype, indicating a less important role of this gene in tomato fruit ripening.

Other transcription factors are known to participate in fruit ripening (Li *et al*, 2021). For example, *MADS box FRUITFULL homologs 1* and *2* (*FUL1* and *FUL2*) can directly interact with *MADS-RIN* promoting tomato fruit ripening (Fujisawa *et al*, 2014).

Epigenomic changes

As seen in the *cnr* spontaneous mutant, epigenomic changes can have a strong effect in fruit ripening. In that case, the hypermethylation of the promoter of *SBL-CNR* leads to an inhibition of fruit ripening. In tomato, a diverse set of epigenomic changes have been associated with fruit ripening in the last years.

DNA methylation is well-known as a central process regulating plant development. During fruit ripening, tomato fruits undergo a general hypomethylation process that activates ripening-related genes and inhibits others (Lang *et al*, 2017). The responsible

for this epigenomic change has been identified as *DEMETER-like DNA methylase 2*, *DML2* (Liu *et al*, 2015). With CRISPR knock-out mutants, it has been demonstrated the role of *DML2* in the activation of ripening-related transcription factors, as *MADS-RIN*, *NAC-NOR* or *SBL-CNR* (Liu *et al*, 2015), and the repression of other genes, as *CAP10B* or *RBCS-2A* (Lang *et al*, 2017). *DML2* is also regulated by another epigenomic modification, the N⁶-Methyladenosine modification, adjusting mRNA stability (Shao *et al*, 2012). These results expose the importance of DNA methylation and demethylation in controlling fruit ripening in tomato.

Other epigenomic changes are related with histones. On one hand, the replacement of histone with histone variants is associated with tomato coloration during ripening, where histone variant *H2A.Z* regulates the expression of several genes of the carotenoid biosynthetic pathway (Yang *et al*, 2021). On the other hand, histone post-translational modifications are known as regulators of plant development. Removing methylation in H3K27 promotes fruit ripening by inducing the expression of ripening-related genes, as *ACS2* (Li *et al*, 2020). Also, a histone deacetylase, *HDT3*, participates in tomato fruit ripening by controlling ethylene production and carotenoid accumulation (Guo *et al*, 2017), and another protein, *HAF1*, has a similar role (Aiese Cigliano *et al*, 2013), indicating the important role of histone regulation in fruit development and ripening.

Metabolic control

Another layer of control of fruit ripening is the metabolic state of the cell. Indeed, some metabolites can modulate the ripening response of fleshy fruits.

More studied in non-climacteric fruits, as strawberry, in tomato some advances in this field have been also achieved. In this species, sucrose has a regulating role during fruit ripening. In *rin* mutants, several sucrose metabolism genes were differentially expressed, indicating a relationship between sucrose and ripening. More interestingly, in a tomato line with a silenced invertase gene (one of the main enzymes in sucrose metabolism), *MADS-RIN* expression was also affected, fruit ripening was delayed and ethylene production altered (Qin *et al*, 2016). These experiments demonstrated that sugar metabolism can directly regulate fruit ripening, specifically sucrose. A cooperative role of ABA and sucrose in fruit ripening has also been established, indicating a crosstalk between sucrose and hormonal signaling during fruit ripening (Jia *et al*, 2016).

General introduction

Other metabolites are also regulators of tomato fruit ripening, such as polyamines, which have been extensively studied. These metabolites have been reported as significantly important during tomato ripening when studying *rin* and *nor* ripening mutants (Osorio *et al*, 2020). As polyamines and ethylene are synthesized from SAM and they have opposite roles, there can be a balance between these processes. Also, some studies indicate that polyamines control fruit ripening by delaying tomato ripening or over-ripening (Li *et al*, 1992; Tassoni *et al*, 2006; Gupta *et al*, 2019).

With all these layers of regulation, climacteric fruit ripening in tomato is a complex process (Figure I.2).

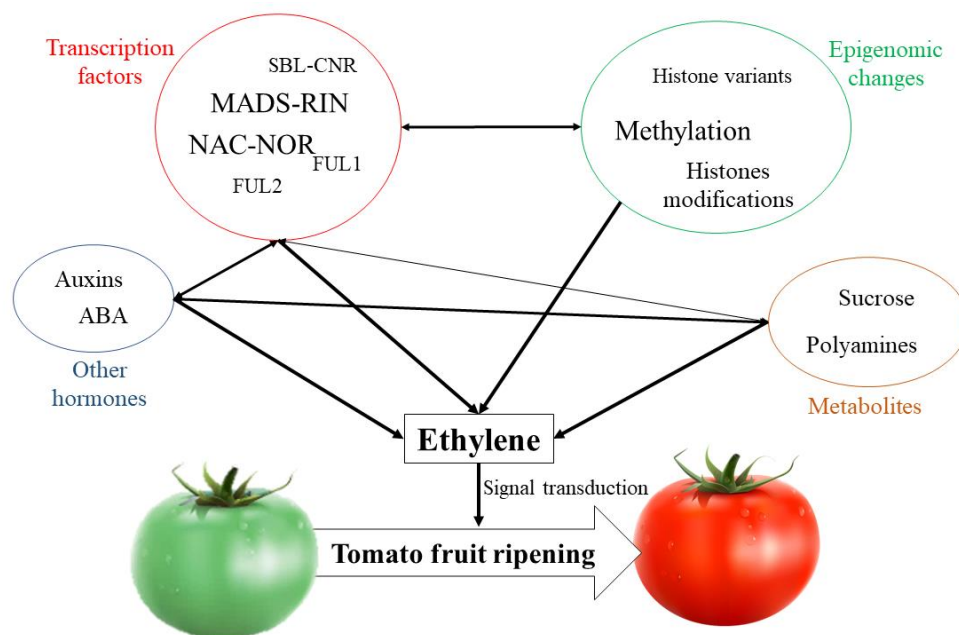


Figure I.2. Schematic representation of the different layers affecting fruit ripening in tomato.

Fruit ripening in non-climacteric species: strawberry as a model

Although non-climacteric fruit ripening is less understood than the climacteric one, some studies have been performed to dissect the control of this process in non-climacteric fruits.

Strawberry (*Fragaria x ananassa*) is considered the model plant regarding non-climacteric fruits. Same as in tomato, some physiological changes take place during the last stages of fruit development, as color change or volatile production (Woodward, 1972). These changes are also regulated in different layers.

Hormonal control

During strawberry fruit development, several phytohormones are controlling the process of growth. Auxins and gibberellins have their major levels at the beginning of fruit development, decreasing during fruit growth (Symons *et al*, 2012). At the onset of fruit ripening, auxin levels are almost zero, while gibberellins are also low but still detectable (Symons *et al*, 2012). Once ripening has started (considering this point as the beginning of the color change), gibberellins continue decreasing, and ABA is the hormone that leads the process, being accumulated in the receptacle (Symons *et al*, 2012; Gu *et al*, 2019). Also, the treatment with auxins or gibberellins demonstrated the role of these hormones in inhibiting strawberry fruit ripening (Symons *et al*, 2012; Gu *et al*, 2019).

ABA is considered the main hormone regulating non-climacteric fruit ripening in strawberry (Bai *et al*, 2021). The importance of this phytohormone in fruit ripening was demonstrated by injecting either ABA, an ABA accelerator or an ABA inhibitor, producing an advance in ripening with the two first, and a delay with the third one (Jia *et al*, 2011). This effect of ABA inducing fruit ripening was also demonstrated by the modification of both ABA synthesis and perception pathways (Jia *et al*, 2011). Its role as a central regulator may be explained by its capacity to interact with the rest of plant hormones. Interaction of ABA and auxins has been reported, and also with gibberellic acid (GA), during both fruit growth and ripening (Liao *et al*, 2018). It can also interact with ethylene (Jiang *et al*, 2003). Although non-climacteric ripening in strawberry is considered ethylene-independent, this gaseous hormone can trigger secondary ripening processes, as reducing fruit firmness by increasing the respiratory rate of fruits (Tian *et al*, 2000). The interaction between ABA and other hormones, including ethylene, would regulate the intensity and timing of fruit ripening in the non-climacteric strawberry.

Transcription factors

Another layer of regulation is the transcriptome. Several transcription factors control the transcription of ripening related genes, as well as hormone synthesis or hormone responsive genes.

The *Myb* family seems to play important roles in strawberry ripening. During fruit ripening, *MYB1* is responsible for the change of coloration by promoting the accumulation of anthocyanins (Aharoni *et al*, 2001). Moreover, other members of this family control the abundance of other primary and secondary metabolites, as eugenol or citric acid, during fruit ripening (Medina-Puche *et al*, 2015; Zhang *et al*, 2018; Wang *et*

General introduction

al, 2022; Liu *et al*, 2022b). Another member of this family, *GAMYB*, a *MYB* transcription factor controlled by gibberellins, can alter the initiation of ripening and primary and secondary metabolism when it is down-regulated (Vallarino *et al*, 2015).

Other transcription factors are also involved in strawberry fruit ripening. The *NAC* transcription factor *Ripening Inducing Factor (RIF)* controls different ripening-related processes, as sugar accumulation or flesh softening, by regulating ABA biosynthesis and signaling, as well as cell wall degradation or volatiles production (Martín-Pizarro *et al*, 2021). A *Teosinte branched 1, Cycloidea and Proliferating cell factor (TCP)*, *TCP9*, is also involved in the biosynthesis of ABA and cell wall degradation processes (Xie *et al*, 2020). It can also physically interact with another transcription factor, *MYC1*, to modulate the synthesis of anthocyanins, the main contributors to fruit coloration in strawberry (Xie *et al*, 2020; Pillet & Folta, 2015). *MADS-box* transcription factors are also present in the regulation of non-climacteric ripening in strawberry. Suppression of *MADS9* gene alters fruit ripening delaying the color changes (Seymour *et al*, 2011). This gene can also alter the morphology of sepals, indicating a role in plant development (Seymour *et al*, 2011).

Epigenomic changes

Same as in other fruit crops, epigenomic changes are controlling fruit ripening in strawberry. Although less studied than in tomato, some advances have been done recently in the field of fruit epigenomics in this crop.

A general DNA demethylation has been observed during strawberry fruit ripening (Cheng *et al*, 2018). In this fruit, this DNA demethylation is caused by a down-regulation of RNA-directed DNA methylation instead of the up-regulation of DNA demethylases as in tomato (Cheng *et al*, 2018, Liu *et al*, 2015; Lang *et al*, 2017).

Histone modifications take place also during ripening (Mu *et al*, 2021). At this stage of fruit development, histone acetylation and methylation regulate fruit softening by controlling the expression of cell wall degradation enzymes (Mu *et al*, 2021).

N⁶-Methyladenosine modification displays a dramatic change during strawberry fruit ripening (Zhou *et al*, 2021). Many genes suffer this epigenomic modification during ripening, including some of the ABA biosynthesis and signaling pathways (Zhou *et al*, 2021).

Metabolic control

Apart from being one of the main metabolites in primary metabolism, sucrose has also a signaling role in fruit ripening. In strawberry, it is known that sucrose acts alone or together with ABA to control non-climacteric fruit ripening (Jia *et al*, 2011; Jia *et al*, 2013; Luo *et al*, 2020b). Same as ABA, sucrose is able to accelerate fruit ripening in sucrose-treated strawberries, and even more when treated together with ABA (Jia *et al*, 2013; Luo *et al*, 2020b). The effect of sucrose has been widely studied (Luo *et al*, 2019; Jia *et al*, 2016; Luo *et al*, 2020a; Durán-Soria *et al*, 2020), and interaction with a *MYB* transcription factor has been reported (Wei *et al*, 2018). All this evidence indicate a key role of sucrose, together with ABA, in the regulation of fruit ripening in strawberry.

As in tomato, polyamines are other type of regulators of ripening. They are able to control a diverse set of hormones, like auxins, ethylene and ABA, which ends in the regulation of non-climacteric ripening (Guo *et al*, 2018). Different polyamines have different roles. While spermine and spermidine promote fruit coloration and ripening, putrescine inhibits these processes (Gao *et al*, 2018; Gao *et al*, 2021).

All the knowledge generated in non-climacteric strawberry indicates that, contrary to tomato, ABA is the main hormone regulating fruit ripening, while ethylene would play minor roles (Figure I.3). The regulation of ABA by transcription factors and sucrose may be an interesting point to focus for fruit ripening behavior modification in strawberry breeding programs.

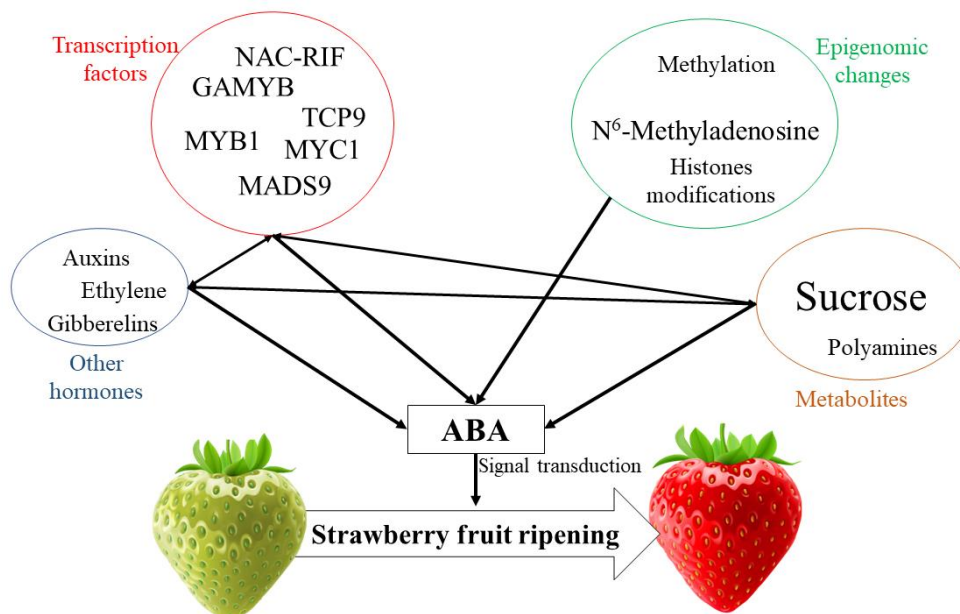


Figure I.3. Schematic representation of the different layers affecting fruit ripening in strawberry.

Fruit ripening in melon: co-existence of climacteric and-non climacteric varieties

Lately, melon has emerged as a new model to study fruit ripening. In this species, there are both climacteric and non-climacteric varieties, making melon suitable for genetic studies to dissect the regulation of fruit ripening that cannot be done in model species (Ezura & Owino, 2008).

Genetic studies

The co-existence of both types of ripening in melon allows the development of segregating populations to map QTLs associated with fruit ripening. This approach has been used several times, dissecting the genetic control of this process.

The scientific interest in controlling fruit ripening in melon using genetics started in the nineties. Using the climacteric variety ‘Védraçais’ (Ved), member of the *cantaloupensis* group, the development of an *ACO* antisense transgenic line demonstrated the effect of ethylene in this climacteric variety (Ayub *et al*, 1996). The transgenic line presented a delayed ripening with effects in flesh firmness, while the wild type and the transgenic line treated with ethylene presented similar phenotypes (Ayub *et al*, 1996). This experiment allowed the association of ethylene sensing with fruit ripening in a climacteric variety. On the other hand, non-climacteric varieties, as ‘Piel de Sapo’ (PS) or ‘Honey Dew’, from the *inodorous* group, are not able to produce a climacteric increase of ethylene production (Vegas *et al*, 2013; Pratt *et al*, 1977). Related with fruit ripening, in melon there are traits that are dependent on ethylene, and other traits are independent, as seen using *ACO* antisense melon lines (Pech *et al*, 2008). Flesh color change, sugar accumulation and a minor part of fruit softening are ethylene-independent processes, while a major part of softening, the abscission layer formation or the production of aromatic volatiles are ethylene-dependent (Pech *et al*, 2008).

Knowing this differential behavior on ethylene production and sensing affecting ripening-related symptoms, a set of segregating populations have been developed to map these different traits. The first mapping of ethylene related traits in melon was described in 2002 (Zheng *et al*, 2002). Using F2 and two BC1 populations, they could associate two different RFLPs with two QTLs of ethylene production (Zhen *et al*, 2002).

After this first mapping, several new populations have been developed, finding a set of QTLs affecting melon fruit ripening. An introgression line (IL) population developed from the non-climacteric varieties ‘Piel de Sapo’ (PS) and ‘Songwan Charmi’ (SC, PI161375) (Eduardo *et al*, 2005) was used to detect a ripening-related QTL in chromosome 3, *eth3.5*, which did not colocalize with any known ethylene-related gene (Moreno *et al*, 2008). Studying that introgression line, they discovered that ethylene production and climacteric behavior were caused by two different loci, *ETHQB3.5* and *ETHQV6.3*, located in chromosome 3 and 6 respectively, and that they interact to promote a climacteric response in a PS non-climacteric background (Vegas *et al*, 2013). Although the causal gene of *ETHQB3.5* has not been identified yet, *CmNAC-Nor* has been confirmed as the causal gene of *ETHQV6.3* (Ríos *et al*, 2017). This gene is a homologue of tomato *NAC-NOR*, responsible of the *nor* phenotype, indicating a key role of this family of transcription factors in regulating fruit ripening also in melon (Ríos *et al*, 2017). Recently it has been established that *NAC-Nor* in melon is also required for seed development, as its knock-out could not develop viable seeds (Liu *et al*, 2022a).

Another IL population, developed with the climacteric Ved as recurrent parent and the climacteric variety ‘Ginsen Makuwa’ (Mak, derived from PI420176) as the donor parent (Perpiñá *et al*, 2016), also showed segregation for ripening behavior. One introgression line covering the proximal part of chromosome 10 presented a modified climacteric behavior, MAK-10 (Perpiñá *et al*, 2017). This line displayed a delayed climacteric response, also affecting flesh firmness and aroma (Perpiñá *et al*, 2017). They named this QTL *MAK10_1*.

Besides, to dissect the genetics underlying climacteric ripening in melon a recombinant inbred line (RIL) population was developed using as parental lines PS and Ved (Pereira *et al*, 2018). Mapping ripening-related traits in this population, a major QTL was found in chromosome 8, *ETHQV8.1* (Pereira *et al*, 2020). This QTL, found also in a genome-wide association study (GWAS) (Pereira *et al*, 2020), caused an increased climacteric behavior when the Ved allele was present, and it also had an effect in the aroma production (Pereira *et al*, 2020; Mayobre *et al*, 2021). With several candidate genes in the interval of the QTL, two of them (a negative regulator of the ethylene signal transduction *CTR1-like* and a demethylase *ROS1*) have effects in fruit ripening, although the causal gene of the QTL was still unclear (Giordano *et al*, 2022). Knock-out mutants of both genes presented an advance in fruit ripening, expected in the case of *CTR1-like*, but

General introduction

unexpected in the case of *ROSI* (Giordano *et al*, 2022). In the same study, they mapped also a minor QTL affecting ripening in chromosome 7, and others affecting certain climacteric symptoms, as flesh firmness and abscission (Pereira *et al*, 2020).

Other studies have found QTLs related with other ripening-related traits, as sugar content (Obando-Ulloa *et al*, 2009; Harel-Beja *et al*, 2010) or fruit firmness (Moreno *et al*, 2008; Dai *et al*, 2022).

Hormonal regulation

Apart from the well-known role of ethylene in melon fruit ripening, other hormones have also a role in this process in melon.

ABA content in fruits varies during development. With a high concentration at the beginning of fruit development, it quickly decreases and then it increases sharply before climacteric ripening (Sun *et al*, 2013), suggesting a role in this last stage of development. After fruit detachment, ABA also can promote ethylene production, respiration, and sugar accumulation, demonstrating the role of this hormone in fruit ripening in a dose dependent manner (Sun *et al*, 2013). Studies in transgenic lines reported some relationship between ethylene and ABA. The transgenic antisense *ACO* line with a reduced ethylene production resulted in a modified ABA concentration (Martínez-Madrid *et al*, 2002). More recently, knocking-out *NAC-Nor*, consequently modifying ripening behavior, also turned out in a decrease in ABA content, probably caused by the downregulation of biosynthetic genes (Wang *et al*, 2022).

This crosstalk of the two ripening-promoting hormones and their regulation in both ways, seem to be coordinating melon fruit ripening, combining both climacteric and non-climacteric models.

Other layers of regulation

Apart from the already mentioned *NAC-Nor* transcription factor, another TF family has been associated with the regulation of fruit ripening in melon. Two members of the *ethylene insensitive 3-like (EIL3)* family are able to directly promote the expression of *ACO1*, which would probably lead to an increase in ethylene production (Huang *et al*, 2010). *WRKY* transcription factors are also associated with melon fruit ripening. In a comparative study of fruit transcriptomics and metabolomics, one transcription factor,

WRKY49, was reported to control β -carotene accumulation in melon by regulating the expression of a phytoene synthase (Duan *et al.*, 2022).

In addition, the epigenomic regulation has been recently reported as another layer of control of melon fruit ripening. The knock-out of a demethylase, *ROS1*, caused a differential methylation pattern in the promoter of ripening-related genes, leading to an advance in climacteric ripening in Ved (Giordano *et al.*, 2022).

Although less studied than the model plants, melon is recently becoming an important alternative model to study fruit ripening (Ezura & Owino, 2008). With several genetic studies, a set of QTLs are known to control fruit ripening, although the causal genes for several of them are still unknown. The combination of these genetic studies, together with other physiological ones, are bringing to light the complex regulation of fruit ripening in melon (Figure I.4).

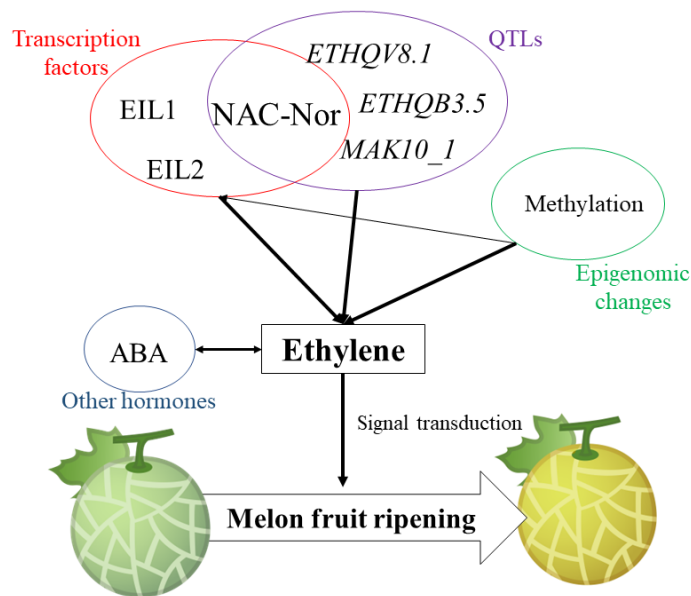


Figure I.4. Schematic representation of the different layers affecting fruit ripening in melon.

Understanding the genetic factors that regulate this process is a challenge for plant scientists, with crucial applications in plant breeding. The work of both breeders and plant scientists can lead to the control of many fruit traits, not only focused on the market, but also in the mitigation of climate change. The reduction of food waste at post-harvest is heavily affected by fruit ripening, so understanding and controlling this process might reduce emissions all along the productive chain.

New approaches in plant breeding

In the last years, new technologies have been developed that can substantially help plant breeders. On one hand, phenotyping has evolved with the development of omics, which can be used for a more accurate measure of individual traits. On the other hand, new breeding techniques (NBTs) allow the modification of traits by making specific changes in the DNA, accelerating the process of plant breeding.

Omics

Omics are defined as the collective characterization and/or quantification of pools of biological molecules with the goal of understanding the function, structure, and dynamics of an organism or a part of an organism. This set of disciplines, as transcriptomics, proteomics or metabolomics, can help breeders to achieve their goal: figure out how plants function and use this knowledge to improve them.

Transcriptomics

Transcriptomics are the technologies used to study the sum of RNAs in an organism, or a part of an organism. These techniques, as RNA-seq, allow the quantification of gene expression as a first layer of gene function regulation.

The study of gene expression can help positional cloning by identifying candidate genes. This approach has been used several times in different species. In rice, the fine mapping of a QTL and a posterior gene expression analysis led to the identification of a gene controlling grain size and yield (Li *et al*, 2011). In wheat, a similar approach using ILs led to the identification of two candidate genes for a major QTL controlling dormancy (Barrero *et al*, 2015). Moving to fruit crops, in tomato a set of candidate genes for heat stress was reported by merging transcriptomic analysis with genetic mapping in a multiparental population (Bineau *et al*, 2021). In grape, a meta-QTL controlling veraison time was analyzed using RNA-seq data, reporting a set of candidate genes (Delfino *et al*, 2019). This approach has been also applied in melon, finding several candidate genes controlling fruit quality traits in an IL population (Zarid *et al*, 2020).

Another use of transcriptomic data is to find candidate genes for a certain process, without previous knowledge of the genome position. For example, an RNA-seq analysis of olive tree during fungal infection allowed the identification of putative genes involved in that process (Jiménez-Ruiz *et al*, 2017). In addition, several studies in tomato comparing

cultivars to identify candidate genes have been performed to study salt tolerance (Sun *et al*, 2010) or flowering time (Wang *et al*, 2021a).

Proteomics

As transcriptomics, proteomics can help breeders to identify candidate genes for their further use in plant breeding. Proteomics is the study of the total pool of proteins of a plant, or a part of a plant, that acts as another layer of regulation of gene function.

These techniques have helped to understand several processes, as drought tolerance, fruit ripening or disease resistance. With a mass spectrometry approach, Hajheidari *et al* (2007) uncovered the role of redox reactions and gliadins in wheat drought tolerance. A similar approach, together with a transcriptomic analysis, helped to understand the importance of consumption of storage substances for drought tolerance in rice (Shu *et al*, 2011). Targeted proteomics in tomato led to the identification of an ethylene receptor, *ETR3*, that might be important for fruit ripening (Chen *et al*, 2019). In another fruit crop, strawberry, proteomics allowed the identification of candidate genes associated with pathogen resistance (Koehler *et al*, 2012).

All these studies converge in one point, the identification of candidate genes associated with several traits or processes. The identification of these genes may encourage their use in plant breeding for improving different crops.

Metabolomics

Metabolomics, or the study of the pool of metabolites, has emerged as a powerful tool for plant breeding, for improving both plant yield and nutritional content (Alseekh *et al*, 2018). This approach has several applications in plant breeding.

First, it can help to discover metabolic pathways. The biosynthetic genes of dhurrin (a toxic metabolite) in sorghum was identified by metabolite profiling and transcriptome analyses (Nielsen *et al*, 2016). Another biosynthetic route that has been elucidated using metabolomics is the entire cholesterol biosynthetic pathway in tomato, by studying the sterol profiling (Sonawane *et al*, 2017), opening its modification to improve nutritional content as this pathway is a key precursor for a large number of metabolites.

Second, metabolic profiling can help breeders by associating certain metabolites to desirable traits. In maize, a clear relationship between some metabolites (as sucrose or histidine) and yield has been established (Yesbergenova-Cuny *et al*, 2016), allowing the

General introduction

use of these metabolic markers to improve kernel yield. In another study integrating proteomics and metabolomics, it was reported that the content of sucrose synthesized in leaves could improve organoleptic quality in apple (Li *et al*, 2016). A similar integrative approach with genomic, transcriptomic and metabolomic data led to the discovery of novel lipid-related genes that had a big effect in consumer acceptance by modulating volatile production in tomato (Garbowicz *et al*, 2018).

A particularly important growing field for plant metabolomics is stress responses, as climate change is modifying substantially the environment where crops grow. Integrative analysis involving metabolomics has linked several metabolites with abiotic stress responses. Under drought stress, the metabolic flux from glycolysis to acetate is increased to stimulate the jasmonate signaling pathway, connecting metabolism, epigenetic changes and hormone signaling (Kim *et al*, 2017). A similar study demonstrated the importance of soluble sugars in drought stress response in sugarcane (Vital *et al*, 2017).

All this knowledge about plant metabolism has motivated the development of engineered fortified crops. One example is the Golden Rice, an engineered rice with three carotenoid biosynthetic enzymes that accumulates higher levels of vitamin A (Ye *et al*, 2000; Moghissi *et al*, 2016). Other examples of engineered crops are vitamin fortified cassava, maize and potato (Sayre *et al*, 2011; Bai *et al*, 2011).

New breeding techniques

The progress in science and technology is allowing the development of new strategies in plant breeding. Apart from the classical breeding and marker-assisted selection, the generation of transgenic or cisgenic plants, together with gene editing, is opening a wide new range of possibilities for improving crops.

Trans- and cis-genesis

The first genetically engineered plant was tobacco, in 1983, expressing an antibiotic resistance gene (Bevan *et al*, 1983). Until some years later, transgenic crops were not approved for human consumption. The first commercialized transgenic crop was a virus resistant tobacco in China in 1992, but it was revoked a few years later (Zhou, 2000). The first transgenic fruit crop in the market was FlavSavrTM tomato, produced in 1992 and approved in 1994, with a delay in tissue softening by an antisense polygalacturonase gene (Kramer & Radenbauhg, 1994). After these first transgenic crops in early 90s, more have arrived at the market, especially maize and soybean, but also fruit crops as apples and

squash (ISAAA, 2017). The cultivated area of transgenic crops worldwide has grown steadily from the beginning, being USA and Brazil the leading countries (ISAAA, 2017). Mostly, transgenic crops are engineered to improve their disease resistance, as Bt cotton, maize, and soybean, resistant to insects by expressing a gene from *Bacillus thuringiensis* (Koch *et al*, 2015).

Other type of GMOs are cisgenic plants, which incorporate genetic information from the same species. Cisgenesis technology can be used to introduce different alleles of genes conferring new characteristics to the plant. This approach has been used to develop a scab resistant apple line by introducing a resistant allele in a susceptible variety (Belfanti *et al*, 2004). A similar experiment achieved the development of a potato late blight resistant line from a susceptible genotype (van der Vossen *et al*, 2005). Cisgenesis has important applications in disease resistance, as many of these resistances are conferred by major genes in a dominant way, and it could substitute marker assisted introgression of beneficial alleles.

Genome editing

Genome editing is becoming a revolution in plant sciences. There are several targeted nucleases with reported applications in plant breeding, as *meganucleases* (*MegN*), *zinc finger nucleases* (*ZFN*), *transcription activator-like effector nuclease* (*TALEN*), and clustered regularly interspaced short palindromic sequences (*CRISPR*)/*CRISPR-associated proteins* (*Cas*) (Khalil 2020), being the last one a significant improvement respect to the others.

Meganucleases were the first used nucleases for genome editing in plants (Puchta *et al*, 1996), where double-strand breaks (DBSs) would lead to mutations in DNA sequence. This principle can be applied for plant genome manipulation. However, redesigning meganucleases for targeted mutagenesis is not easy, as DNA-binding domain overlaps with the effector domain, making difficult to alter the recognition of DNA sequences (Prieto *et al*, 2007).

Zinc finger nucleases are easier to modify, presenting an improvement respect to meganucleases, and they are combinatorial, so in theory they could be used to mutate any genomic sequence (Maeder *et al*, 2008). *ZFN* technology has been used mostly in *A. thaliana*. In crop species, *ZFN* edited plants have been developed with a mutated malate

General introduction

dehydrogenase in tomato (Shukla *et al*, 2013), and low phytate lines in maize (Shukla *et al*, 2009), demonstrating their potential for plant breeding.

TALEN technology allows to freely design the DNA binding domain, with the potential of produce DSBs in any DNA sequence. With this technique, several genes were edited in rice, mostly producing small deletions (Shan *et al*, 2013). More applications have been reported in rice (Li *et al*, 2012) and in potato (Nicolia *et al*, 2015).

Although some advances were done with the three technologies mentioned above, the biggest step in plant editing was the development of CRISPR/*Cas*. While *MegN*, *ZFN* and *TALEN* required the re-designing of DNA binding domains, with CRISPR/*Cas* technology this re-design is not needed, as the nuclease is carried to the target DNA sequence by a RNA molecule, called guide RNA (gRNA). Firstly described as an antiviral machinery in bacteria (Mojica *et al*, 2005; Mojica *et al*, 2009), its application in DNA engineering was soon developed (Doudna & Charpentier, 2014). This method consists of a nuclease (*Cas*) that binds a short RNA molecule that guides the whole complex to its complementary DNA sequence, where it produces a double strand break leading to mutations. By changing the sequence of the gRNA, potentially all the genomes could be edited in a fast and easy way. The application of CRISPR/*Cas* gene editing in agriculture has evolved a lot in a few years. There are many examples of modified traits in several crops (Mohan *et al*, 2022). In tomato, many genes have been edited to improve agricultural traits, as yield, nutritional value or tolerance to biotic and abiotic stresses (Chaudhuri *et al*, 2022). One successful example in tomato is the first CRISPR-edited commercialized crop. This tomato has a mutation in a calmodulin-binding domain gene that produces a knock-out, modifying the flux of the γ -aminobutyric acid (GABA) shunt. Therefore, the concentration of GABA is increased, with a potential benefit for consumers' health (Nonaka *et al*, 2019). Two years after the publication, this CRISPR-edited tomato was commercialized in Japan (Waltz, 2021). Apart from this example, many crops are susceptible of CRISPR-based plant breeding, including some *Cucurbitaceae* family members as melon (Liu *et al*, 2022a, Giordano *et al*, 2022) and cucumber (Shnaider *et al*, 2022).

All this advances in genome editing, especially CRISPR/*Cas* technology, together with the development of new *Cas* proteins with specific functions, have opened a new field for breeders. The combination of classical and new breeding techniques has the potential and

the goal of providing safe food for a growing worldwide population in the present climate change scenario.

Regulatory frame

Although the potential of new breeding techniques is virtually unlimited, differences in regulation among countries are creating inequalities worldwide. GMOs are regulated worldwide, with several steps until approval for human consumption.

In the case of transgenic crops, each country has its own legislation regarding production and labeling. Generally, in America (both North and South), transgenic plants regulation is soft, being in this continent the major transgenic crops' producers (USA, Brazil, Argentina and Canada). In Asia, some countries have also approved some biotech crops, as China, India or Pakistan. South Africa and Australia also have transgenic crops production. In Europe, where the legislation regarding transgenics is harder, only two countries are currently producing transgenic crops: Spain and Portugal, and for only one crop, Bt corn.

In the case of edited crops, particularly CRISPR-edited ones, the scenario is different. With these technologies, once the DNA has been edited, normally the transgene or transgenes are removed, ending with an edited non-transgenic plant with no foreign DNA. For this reason, together with the difficulty (or impossibility) of discerning an edited plant from a mutagenized one by classical methods, regulation worldwide is different than in transgenic plants. In most countries, these edited plants are not regulated as GMOs, so they can be approved in a case-by-case fashion (Buchholzer & Frommer, 2022), such as China, India, Brazil, Nigeria or USA; while in others they are under consideration, as Bangladesh and Indonesia (Figure I.5). On the other hand, in the European Union, edited non-transgenic plants have the consideration of GMOs regarding regulation (Figure I.5) (Tarja Laaninen, 2021), although at present the legislation is being reevaluated.

The general trend worldwide is towards a softer regulation for edited crops than for transgenic ones. Especially in the most populated countries (Figure I.5), where access to food might be a problem in the near future, CRISPR/*Cas* gene editing has been proved a powerful tool to improve the existing cultivars.

General introduction

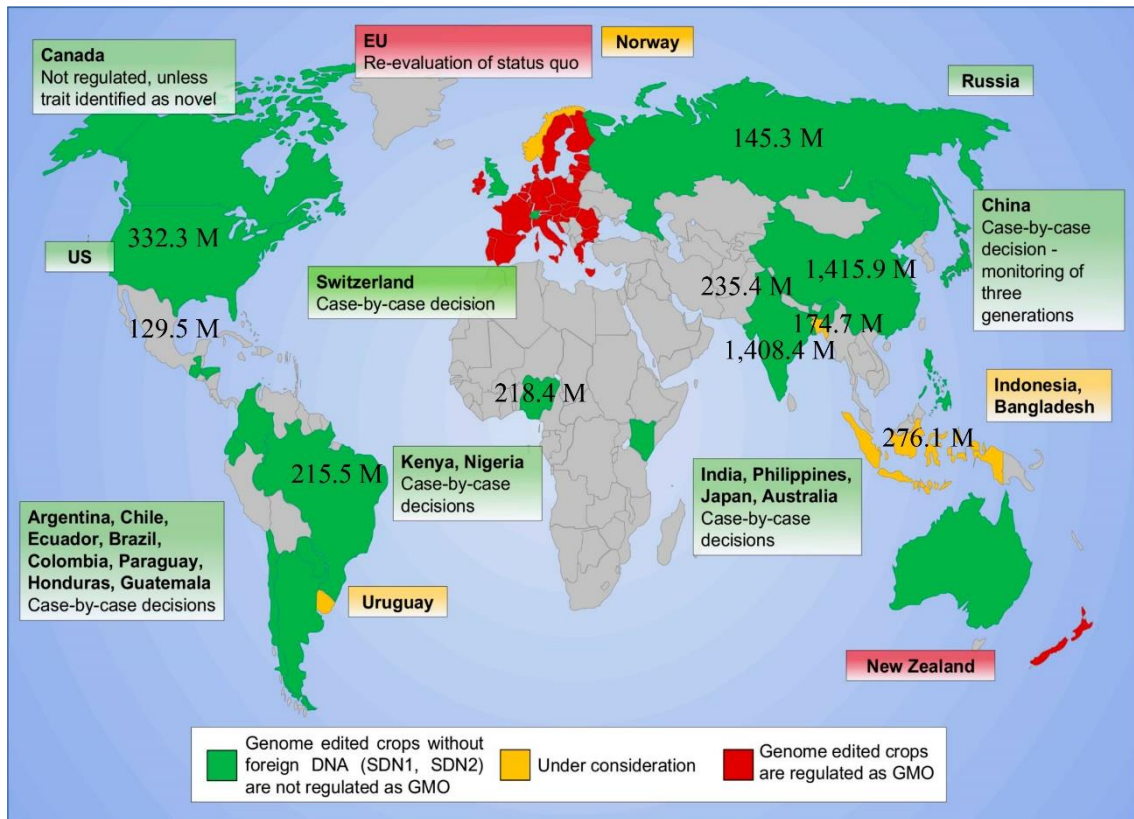


Figure I.5. Current situation of edited crops legislation worldwide, showing the population of the ten most populated countries in 2022. Adapted from Buchholzer & Frommer (2022).

Objectives

The main objective of this PhD thesis is to characterize *ETHQV8.1*, previously described as a major QTL controlling fruit ripening in melon in a ‘Védrantais’ x ‘Piel de Sapo’ RIL population. To achieve this goal, four specific objectives were proposed:

1. Completion and characterization of the ripening behavior of two reciprocal IL populations funded by ‘Védrantais’ and ‘Piel de Sapo’.
2. Characterization of *ETHQV8.1*.
 - a. Fine mapping of *ETHQV8.1* in the introgression line containing the QTL in the Védrantais background.
 - b. Identification and functional validation of a candidate gene using CRISPR/Cas9 gene editing technology.
 - c. Study the gene function to dissect the molecular mechanism of fruit ripening.
3. Interaction studies between *ETHQV8.1* and three other ripening-related QTLs in the ‘Piel de Sapo’ and ‘Védrantais’ genetic backgrounds.
4. Study of the effect of *ETHQV8.1* in the physiology of the fruit.

Chapter 1

Development of two reciprocal IL populations using
‘Védrantais’ and ‘Piel de Sapo’ as parents, and
characterization of ripening, morphology and quality traits

Background

The availability of different genetic resources allows the identification and mapping of QTLs associated with traits of agronomical interest. Introgression line (IL) populations are a powerful tool to validate QTLs and a robust starting point for other genetic studies. In melon, new IL populations might be an excellent complement to previous developed populations for studying melon fruit ripening, as a recombinant inbred lines (RIL) population developed with the same parents, or previous IL populations founded with the same recurrent parental line.

Results

From an initial cross of the parental lines ‘Védrantais’ and ‘Piel de Sapo’, we have developed both populations in three or four backcross generations and a final selfing to fix homozygous regions. In a total of six or seven generations we have obtained two populations, PS ILs and VED ILs, with Ved and PS as recurrent parents, respectively, covering around 98% of the genome with introgressions of the donor parent in around 35 different lines. After a QTL mapping, we could validate known QTLs, as *ETHQV8.1* and *ETHQV6.3* affecting climacteric ripening, and major genes controlling flesh or rind color. Also, we have mapped new QTLs affecting climacteric ripening and fruit morphology.

Conclusions

The development of these two IL populations represents an important resource for melon breeding and genomics. The validation of known QTLs and major genes demonstrates the efficacy of this kind of populations to unravel the genetic control of several segregating traits, as fruit ripening or morphology. Also, ILs are a powerful genetic resource for other genetic studies, as fine mapping to find causal genes or to study QTL interactions, due to the minimizing of background effects affecting the studied traits. For plant breeding, ILs can be a good starting point to develop new varieties by marker-assisted introgression of target alleles.

Chapter 1.1

A novel introgression line collection to unravel the genetics of climacteric ripening and fruit quality in melon

A novel introgression line collection to unravel the genetics of climacteric ripening and fruit quality in melon

Lara Pereira^{1*}, Miguel Santo Domingo^{1*}, Jason Argyris^{1,2}, Carlos Mayobre¹, Ana Montserrat Martín-Hernández^{1,2}, Marta Pujol^{1,2§}, Jordi Garcia-Mas^{1,2§}

¹ Centre for Research in Agricultural Genomics (CRAG) CSIC-IRTA-UAB-UB, Edifici CRAG, Campus UAB, 08193 Bellaterra, Barcelona, Spain.

² Institut de Recerca i Tecnologia Agroalimentàries (IRTA), Bellaterra, Barcelona, Spain.

* These authors share first authorship

§ Corresponding authors addresses:

Marta Pujol, marta.pujol@irta.cat Phone: +34 935636600

Jordi Garcia-Mas, jordi.garcia@irta.cat Phone: +34 935636600

Orcid data:

Lara Pereira (0000-0001-5184-8587)

Miguel Santo Domingo (0000-0001-7447-9331)

Jason Argyris (0000-0003-2685-9959)

Carlos Mayobre (0000-0001-5511-9728)

Ana Montserrat Martín-Hernández (0000-0003-2616-3847)

Marta Pujol (0000-0002-3595-5363)

Jordi Garcia-Mas (0000-0001-7101-9049)

Scientific Reports **11**, Article number: 11364 (2021), doi: 10.1038/s41598-021-90783-6

Abstract

Introgression lines are valuable germplasm for scientists and breeders, since they ease genetic studies such as QTL interactions and positional cloning as well as the introduction of favorable alleles into elite varieties. We develop a novel introgression line collection in melon using two commercial European varieties, the *cantalupensis* ‘Védraçais’ as recurrent parent and the *inodorus* ‘Piel de Sapo’ as donor parent. The collection contains 34 introgression lines, covering 99% of the donor genome. The mean introgression size is 18.16 Mbp and ~3 lines were obtained per chromosome, on average. The great segregation of these lines for multiple fruit quality traits allowed us to identify eight QTLs, of which one modified sugar content, four altered fruit morphology and three were involved in climacteric ripening. In addition, we confirmed the genomic location of five major genes previously described, which control mainly fruit appearance, such as mottled rind and external color. Several QTLs had been reported before in other populations sharing parental lines, validating its relevance, while others were newly detected in our work. These introgression lines would be useful to perform additional genetic studies, as fine mapping and gene pyramiding, especially for important complex traits such as fruit weight and climacteric ripening.

Keywords: introgression line, melon, germplasm, fruit quality, climacteric ripening.

Introduction

Understanding the genetics beyond interesting traits, from human diseases to crop yield, has been one of the main goals of modern science. Genetic variation is studied and correlated with phenotypes, in order to identify the genomic regions controlling traits of interest. In plants, due to the ease of crossing, many types of segregating populations can be developed depending on the goal of the research and the availability of time and resources. In species with short generation periods, as cereals and vegetable crops, populations with increased complexity are usually developed, as Recombinant Inbred Line (RIL) (Harel-Beja *et al*, 2010), Nested Association Mapping (McMullen *et al*, 2009), Multi-parent Advanced Generation Intercrosses (Huang *et al*, 2015) and Introgression Line (IL) (Eduardo *et al*, 2005; Barrantes *et al*, 2014) populations. IL collections are immortal lines that share a high proportion of genetic background from a recurrent parent, differing only in a specific region of the genome (introgression), inherited from the donor parent. Ideally, the complete genome of the donor parent is covered by the ILs conforming the collection. They are considered a powerful resource since, besides QTL mapping experiments, they allow to perform subsequent specific studies as QTL validation (Díaz *et al*, 2017), QTL interactions (Lin *et al*, 2000; Monforte *et al*, 2001) and fine mapping (Giner *et al*, 2017; Ríos *et al*, 2017).

IL populations (also referred as Near Isogenic Lines, NILs) have been used as genetic resources in multiple species for several decades (Briggle, 1969; Suge, 1972; Pegg & Cronshaw, 1976), from model plants as *Arabidopsis thaliana* (Keurentjes *et al*, 2007), rice (Li *et al*, 2005) and tomato (Bernacchi *et al*, 1998) to less studied and even orphan crops, as strawberry (Urrutia *et al*, 2015), peach (Serra *et al*, 2016) and groundnut (Foncéka *et al*, 2009). They have proven their efficiency to map and characterize traits related with disease resistance, plant architecture and fruit morphology and quality. Furthermore, they have been commonly used in breeding programs to introduce desired exotic alleles from donor accessions, where the recurrent parent is typically an elite line.

Generally, ILs are developed by genotyping the target introgression as well as the recurrent parent background with molecular markers. The rapid increase in marker availability and high-throughput genotyping techniques have changed the methods used to develop these populations. Recently, the trend has been to minimize the number of needed backcrosses by increasing the size of the initial screened populations and the number of markers, in order to decrease the number of non-desired contaminations in

narrow non-genotyped regions of the genome (Barrantes *et al*, 2014; Urrutia *et al*, 2015; Serra *et al*, 2016).

IL populations have been developed and widely used throughout the last years in melon (Eduardo *et al*, 2005, 2007; Obando-Ulloa *et al*, 2009, 2010; Vegas *et al*, 2013; Perpiñá *et al*, 2016, 2017; Giner *et al*, 2017; Ríos *et al*, 2017; Castro *et al*, 2019). Melon is a diploid species with a relatively small genome (450 Mbp) and $2n=2x=24$ (Garcia-Mas *et al*, 2012). Melon has become an alternative model species to study certain traits, as climacteric ripening (Ezura & Owino, 2008) and sex determination (Martin *et al*, 2009). An IL collection, developed from a cultivated variety (spp. *melo*) as recurrent parent and an exotic Korean accession (spp. *agrestis*) as donor parent (Eduardo *et al*, 2005), has been used to fine map and clone two genes controlling climacteric ripening (Ríos *et al*, 2017) and resistance to *Cucumber Mosaic Virus* (Giner *et al*, 2017). In addition, pyramiding of multiple QTLs controlling or modulating the same trait was achieved through crosses of several ILs; e.g., the QTL *ETHQV6.3*, corresponding to *CmNAC-NOR* (Ríos *et al*, 2017) and involved in climacteric ripening, interacts with a second QTL (*ETHQB3.5*), leading to a more intense climacteric phenotype when both introgressions are combined in the same IL (Vegas *et al*, 2013).

Most of the populations developed in melon have been funded by a cross between an elite cultivar and an exotic accession. A recent study using a RIL population between two European cultivars, “Védrantais” (Ved), a typical French variety belonging to the *cantalupensis* group, and “Piel de Sapo” (PS), a Spanish variety from the *inodorus* group, showed segregation for traits related with fruit quality and climacteric ripening (Pereira *et al* 2018, 2020). Climacteric ripening is a complex and polygenic trait that partially determines the overall fruit quality. Melon is one of the few species where both climacteric and non-climacteric varieties coexist, offering an excellent model to dissect the genetics of the trait (Ezura & Owino, 2008). Climacteric ripening is defined by an autocatalytic synthesis of the plant hormone ethylene at the onset of the ripening stage, followed by a peak of respiration (Lelièvre *et al*, 1997). In climacteric melons, these biochemical signals trigger multiple phenotypic changes such as chlorophyll degradation, production of several volatiles that lead to a sweet aroma, abscission layer formation in the pedicel and degradation of cell wall resulting in a loss of flesh firmness (Pech *et al*, 2008).

The aim of this work was to develop an IL collection using Ved as recurrent parent and PS as donor parent in order to identify and validate QTLs controlling fruit quality and climacteric ripening in melon. This advanced germplasm resources would be useful in the future to further characterize these genetic factors through fine mapping and QTL interaction studies.

Results and discussion

Parent phenotypes

Two commercial lines, Ved and PS, were selected as parents to develop the IL collection due to the segregation of several relevant traits among them, such as ripening behavior and external appearance. They represent the two most common and consumed melons in Europe. Ved produces a round, medium-size fruit with intermediate sugar content (6-9 °Brix), whereas PS fruits are elongated, its fruit weight is higher as well as its sugar content (9-12 °Brix) (Table 1.1.S1). The external appearance of the fruit also varies: Ved presents white/cream rind with marked sutures and PS mottled green rind (Figure 1.1.S1). The flesh color is orange in Ved and white in PS.

Interestingly, these two varieties represent the two extremes of ripening behavior in melon (Pereira *et al*, 2020). Ved is a typical climacteric variety, presenting the characteristic ethylene peak at the onset of ripening closely followed by classical phenotypic consequences such as intense sweet aroma, abscission layer formation, chlorophyll degradation and loss of flesh firmness. PS is completely non-climacteric, the ethylene production during ripening remains undetectable and it lacks the phenotypic changes associated to climacteric ripening, except loss of flesh firmness, a trait partially ethylene-independent (Pech *et al*, 2008).

Development of the PS IL collection

IL collections are a highly valuable resource for both research and breeding, although their development is more complex and expensive than other populations. In the last years, many IL collections have been described for different species, including melon, which have been successfully used to map and characterize QTLs (Barrantes *et al*, 2016; Argyris *et al*, 2017; Urrutia *et al*, 2017). Here, we developed a new IL collection to gain insight about the genetic control of fruit quality.

In the BC₁ population, the number of introgressions ranged from 4 to 17 per line, with a mean of 11.5 and a median of 12, indicating that on average one recombination per

chromosome and meiosis had occurred. The use of marker-assisted selection in the first BC generation reduced substantially the risk of carrying non-detected contaminations. The percentage of Ved genome ranged from 13.0 to 80.1%, with an average of 48.7%. The observed heterozygosity was $H_0 = 0.46$ and 16 SNPs showed significant segregation distortion. The highest segregation distortion was observed in the centromeric region of chromosome 12 ($\chi^2 = 43.3$), which presented a minimum observed heterozygosity of 0.31. A set of 25 BC₁ plants (7.8%) were selected, presenting a mean of 8 introgressions and 62.2% of Ved background genome. After two more cycles of backcross and marker assisted selection to BC₂ and BC₃ (Figure 1.1.1), the number of introgressions in the 64 selected lines was notably reduced to a mean of 2.6 introgressions and they carried an 85.7% of Ved genome on average. In the next generation, a set of 100 plants were selected, carrying 1.8 introgressions and 88.3% of Ved genome on average, and most of the final ILs were recovered from their progenies. Due to various complications (misbehaved SNPs, loss of plants due to pests or bad fruit set), a 6% of PS genome remained uncovered in the IL collection. Lines from previous generations were used to obtain six new ILs, and four of them were phenotyped in 2019.

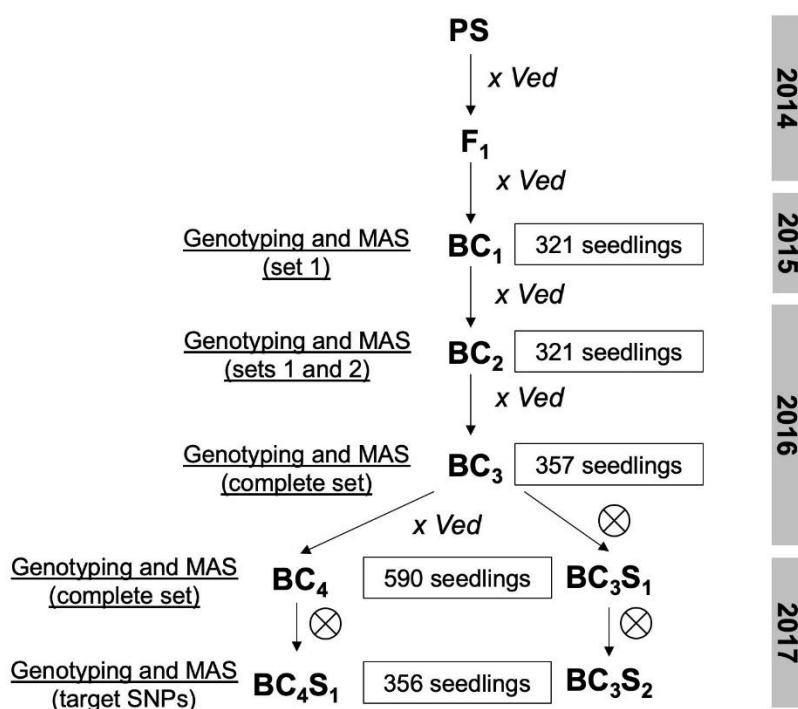


Figure 1.1.1. Breeding scheme followed to develop the IL collection

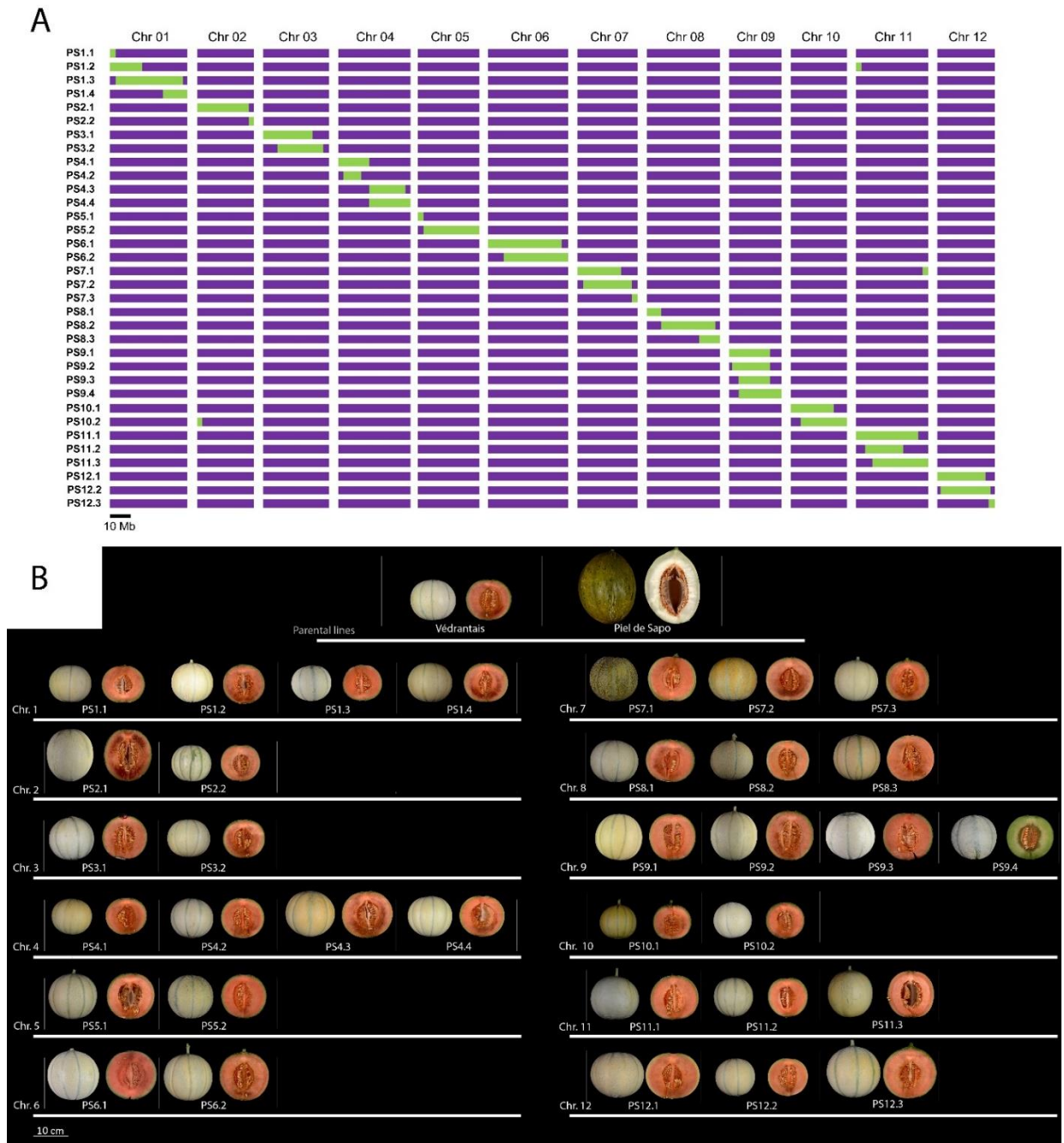


Figure 1.1.2. A) Genotypic characterization of the IL collection. Purple represents the genotype of the recurrent parent Ved and green, the genotype of the donor parent PS. B) Representative images of the ILs

The most remarkable parameters for an IL collection are the number of ILs per chromosome, which is directly correlated with the resolution and with the required resources for phenotyping, the size of the introgressions, which also defines the resolution, and the number of generations needed to obtain the ILs, which is related with undesired introgressions in non-target regions. The PS IL collection, comprised by 34 lines, covered the complete genome of PS except the last 3.8 Mbp of chromosome 3

(Figure 1.1.2A; Table 1.1.S2). A mean of 2.8 ILs per chromosome was obtained, with a large range of introgression length from 2.46 to 35.32 Mbp (Table 1.1.S3). Considering the overlapping of introgressions from different ILs, we could define 42 genomic bins. In comparison to other IL collections, this is an intermediate size, below the 6 ILs per chromosome obtained in a strawberry IL collection (Urrutia *et al*, 2015) but higher than the 1.3 ILs per chromosome from other recently described melon IL collections (Perpiñá *et al*, 2016; Castro *et al*, 2019) (Table 1.1.S4). The size in genetic distance units, inferred from a genetic map in a RIL population using the same parents (Pereira *et al*, 2018), ranged from 17.6 to 129.2 cM, with an average of 63.8 cM. As we could expect, the introgressions in the telomeric regions were smaller in terms of physical distance but larger in genetic distance, as opposed to the introgressions covering the pericentromeric regions (Figure 1.1.2A). The size of the introgressions was slightly higher than the genetic distance value obtained in other IL collections (mean of 38.7 cM), but similar in physical distance (Eduardo *et al*, 2005; Barrantes *et al*, 2014; Urrutia *et al*, 2015; Perpiñá *et al*, 2016). This discordance could be attributed to the strategy used to select the SNPs for the marker-assisted selection, which was mainly based on physical distances (markers homogeneously distributed across the chromosomes). The number of generations used to obtain the ILs in our work was generally six (BC₃S₂ and BC₄S₁), as in most other IL collections (Table 1.1.S4). The percentage of covered PS genome is ~ 99%, slightly higher than in other IL collections.

QTL mapping

Fruit quality

Several traits contributing to fruit quality were segregating in the IL collection, including several external characteristics of the fruit as color and morphology (Figure 1.1.2B, Table 1.1.S1). Qualitative phenotypes determining the external appearance of the fruit were already appreciated during the development of the IL collection. The mapping of these traits to the corresponding genomic region was easily performed even in pre-ILs due to its simple inheritance and high heritability, and the phenotyping of the complete collection performed in 2018 and 2019 confirmed the preliminary results.

PS2.2 presented mottled rind, observed as dark green spots during early stages of fruit development and turning to bright yellow spots in ripe fruits (Figure 1.1.3A). This major gene, *Mt-2*, was delimited to the interval 24.77 - 27.06 Mbp on chromosome 2. *Mt-2* was also mapped to chromosome 2 in previous studies (Périn *et al*, 1999; Pereira *et al*, 2018).

PS10.1 fruits were white during fruit development as Ved but turned to a light-yellow during fruit ripening instead of cream (Figure 1.1.3B). The interval of this major gene (0 - 5.10 Mbp on chromosome 10), contains *CmKFB*, which controls flavonoids biosynthesis in melon rind (Feder *et al*, 2015).

PS11.1 and PS11.3 presented smooth rind, without sutures (Figure 1.1.3C), in contrast to Ved and the rest of the IL collection. The responsible major gene could be mapped to the interval shared by both lines on chromosome 11, from 21.26 – 29.79 Mbp. *MELO3C019694*, located within the introgressions of PS11.1 and PS11.3, was proposed as responsible for the presence of sutures, due to a delay in gene expression during the initial stages of fruit development (Zhao *et al*, 2019). The same trait has been studied in other cucurbits, especially in *Cucurbita pepo* (Esteras *et al*, 2012), but the biological process causing the sutures has not been described yet.

PS9.3 was the only IL in our collection without orange flesh (Figure 1.1.3D); however, unlike the donor parent PS, PS9.3 flesh is green. This phenotype is explained by the oligogenic inheritance of flesh color in ripe fruits. Three phenotypes, orange, white and green flesh, can be observed depending on the allelic combination of two genes that act epistatically. A dominant gene on chromosome 9 already cloned, *Gf* or *CmOr* (Tzuri *et al*, 2015), controls the presence of orange color, conferred by a high content of carotenoids and is located in the position 21.68 Mbp of chromosome 9 (version v3.6.1 of the melon genome). The non-orange allele, which is recessive, allows the manifestation of the second gene, called *Wf*, to control white (dominant) or green (recessive) flesh color (Monforte *et al*, 2004; Cuevas *et al*, 2009; Galpaz *et al*, 2017). *Wf* has been mapped using several populations to an interval of 5 Mbp on chromosome 8 (Monforte *et al* 2004; Cuevas *et al* 2009) and *MELO3C003069* has been proposed as candidate gene (Galpaz *et al*, 2017). Ved genotype is *Gf/Gf wf/wf* and PS genotype is *gf/gf Wf/Wf*; therefore, the genotype of IL PS9.3, carrying a PS introgression in *Gf* locus, is the double recessive *gf/gf wf/wf*, leading to green color instead of the white color observed in PS.

PS5.1 was the only IL in which soluble solid content significantly differed from Ved (Figure 1.1.4). The QTL on chromosome 5, spanning from the beginning of the chromosome to 2.83 Mbp, reduced soluble solid content 34.3% when compared to Ved, dropping from 8.78 to 5.77 °Brix (Table 1.1.1). *SSCQP5.1*, the identified QTL controlling soluble solid content, colocalizes with a previously described QTL on chromosome 5,

sscqsc5.1 (Argyris *et al*, 2017); however, the PS allele, conferring lower soluble solid content in our IL collection, had the opposite effect in the PS x “Trigonus” and PS x “Songwhan Charmi” analyzed by Argryris *et al* (2017). Remarkably, none of the ILs showed a soluble solid content significantly higher than Ved, even though PS does. PS8.2 presented consistently higher levels of soluble solid content, with 10.59 °Brix on average, but the difference with respect to Ved was not significant.

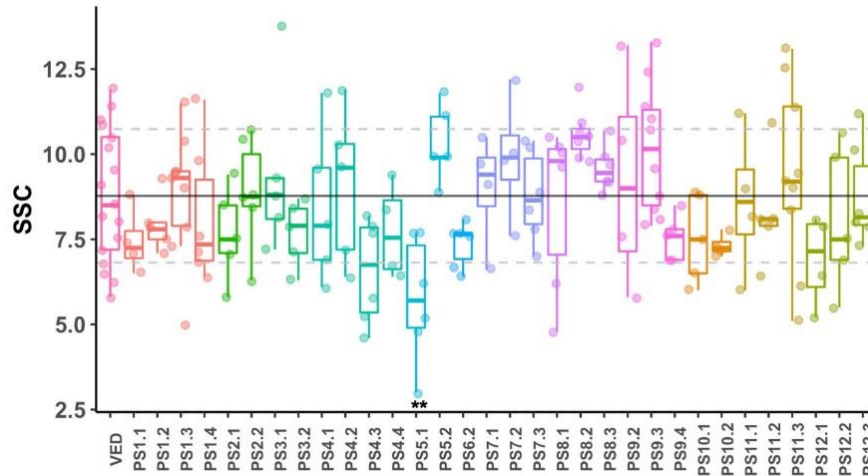


Figure 1.1.4. Boxplot representing the SSC values for ILs. Each dot represents a replicate, the black solid line corresponds to the average and the grey dashed lines to the average \pm SD of the recurrent parent Ved. Significant differences are marked with asterisks: * <0.1 , ** <0.05 , *** <0.01

Fruit morphology

Fruit weight is one of the most relevant traits for the industry since it defines yield and also drives consumer’s preferences. Although a few genes controlling fruit weight have been cloned in the model fruit crop tomato (Frery *et al*, 2000; Chakrabarti *et al*, 2013; Mu *et al*, 2017), the genetic basis of the trait in melon remains poorly understood. Several QTLs have been described in different populations through both QTL mapping and genome-wide association studies, however the underlying genes responsible of the phenotype remain unknown (Monforte *et al*, 2014). In the PS IL population, we identified three QTLs affecting fruit weight, carried by ILs PS2.2, PS4.1 and PS10.1 (Figure 1.1.5). The two latter ILs were also significantly different to Ved in the other size-related traits as fruit area, fruit perimeter and fruit length, whereas PS4.1 also for fruit width.

PS2.2 borne fruits with an average weight of 435 g, 37.8% reduction as compared to Ved (Table 1.1.1 and Figure 1.1.5). *FWQP2.2* was delimited to the distal region of chromosome 2, from 24.77 – 27.06 Mbp. No QTLs were identified for the other size-

Chapter 1: Introgression Lines

related traits in the same genomic region, although some of the fruits actually presented lower values (Figure 1.1.5); these traits were more variable than fruit weight, possibly causing a lack of statistical power. A meta-QTL for fruit weight was defined previously on chromosome 2, colocalizing with the gene *a*, which causes sex determination in female flower. Thus, in those populations the fruit weight difference may be a consequence of sex determination (Boualem *et al*, 2008; Monforte *et al*, 2014). However, the QTL described in our IL collection does not colocalize with *a* (*MELO3C015444*), indicating that the underlying gene has to be distinct.

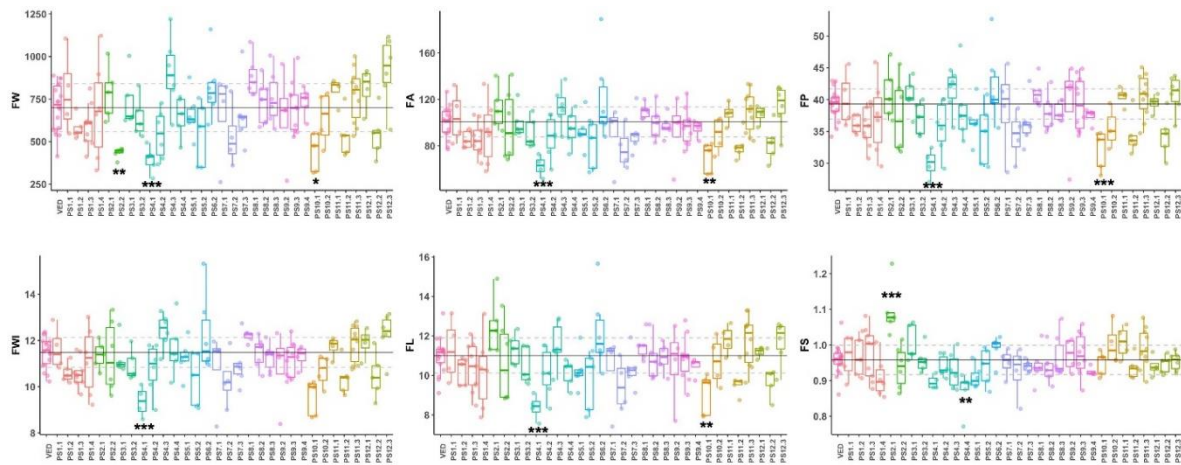


Figure 1.1.5. Boxplot representing the values of morphological traits for ILs. Each dot represents a replicate, the black solid line corresponds to the average and the grey dashed lines to the average \pm SD of the recurrent parent Ved. Significant differences are marked with asterisks: * <0.1 , ** <0.05 , *** <0.01

PS4.1 fruits weighed 394.8 g and showed a significantly smaller size than Ved (Table 1.1.1 and Figure 1.1.5). The reduction in average values for the IL as compared to Ved was about 43.5% for fruit weight, 37.7% for fruit area, 23.7% for fruit perimeter, 18% for fruit length and 24.4% for fruit width. Since both dimensions were similarly decreased, the fruit shape was not affected. PS4.1 covers from the beginning of the chromosome 4 to 14.92 Mbp; however, PS4.2, which did not show any fruit size difference compared to Ved, spans from 2.44 to 10.97 Mbp. Therefore, *FWQP4.1* could be located either from 0 – 2.44 Mbp or from 10.97 – 14.97 Mbp.

PS10.1 carried fruits with a smaller size and a flattened shape in comparison to Ved. Fruit weight, fruit area, fruit perimeter and fruit length were reduced between 18 and 36%, whereas fruit width was not affected. *FWQP10.1* was located on chromosome 10 from 0 to 5.25 Mbp (Table 1.1.1).

Table 1.1.1. QTLs identified for quantitative traits in the IL population

Trait	QTL	IL	Chr	Genomic		Ved Mean	% difference	p-value (Dunnett test)
				interval (Mbp)	IL mean			
SSC	<i>SSCQP5.1</i>	PS5.1	5	0.00-2.83	5.77	8.78	-34.28	0.0138
FW	<i>FWQP2.2</i>	PS2.2	2	24.77-27.06	435	699.09	-37.78	0.0189
	<i>FWQP4.1</i>	PS4.1	4	0.00-2.45	394.8		-43.53	0.0078
	<i>FWQP10.1</i>	PS10.1	10	0.00-5.25	442.4		-36.72	0.0533
FA	<i>FAQP4.1</i>	PS4.1	4	0.00-2.45	62.66	100.64	-37.74	0.0054
	<i>FAQP10.1</i>	PS10.1	10	0.00-5.25	69.97		-30.47	0.0252
FP	<i>FPQP4.1</i>	PS4.1	4	0.00-2.45	29.99	39.33	-23.75	<0.0001
	<i>FPQP10.1</i>	PS10.1	10	0.00-5.25	32.15		-18.26	0.0080
FL	<i>FLQP4.1</i>	PS4.1	4	0.00-2.45	8.38	11.01	-23.89	0.0037
	<i>FLQP10.1</i>	PS10.1	10	0.00-5.25	9.07		-17.62	0.0494
FWI	<i>FWIQP4.1</i>	PS4.1	4	0.00-2.45	9.36	11.48	-18.47	0.0019
FS	<i>FSQP2.1</i>	PS2.1	2	0.00-16.42	1.1	0.96	14.58	<0.0001
	<i>FSQP4.4</i>	PS4.4	4	27.25-34.32	0.87		-9.38	0.0163
EALF	<i>EALFQP6.2</i>	PS6.2	6	7.47-38.30	37.6	33.89	10.95	0.0499
	<i>EALFQP8.2</i>	PS8.2	8	6.89-25.00	41.75		23.19	<0.0001
EARO	<i>EAROQP8.2</i>	PS6.2	6	7.47-38.30	36.67	33.67	8.91	0.0569
	<i>EAROQP8.2</i>	PS8.2	8	6.89-25.00	38.67		14.85	<0.0001
ECD	<i>ECDQP8.2</i>	PS8.2	8	6.89-25.00	36.83	33.22	10.87	0.0582
HAR	<i>HARQP6.2</i>	PS6.2	6	7.47-38.30	42.33	37.78	12.04	0.0385
	<i>HARQP8.2</i>	PS8.2	8	6.89-25.00	45.5		20.43	<0.0001
FIR	<i>FIRQP2.1</i>	PS2.1	2	0.00-16.42	0.68	2.99	-77.26	< 0.0001
	<i>FIRQP8.2</i>	PS8.2	8	6.89-25.00	4.44		48.49	0.0181
	<i>FIRQP8.3</i>	PS8.3	8	25.00-34.77	4.3		43.81	0.0835

* The color gradient corresponds with the percentage of reduction (red) or increase (blue) in the IL phenotype when comparing to Ved

Surprisingly, in these three ILs the alleles from PS were reducing fruit weight. Nevertheless, undoubtedly some alleles contributing to develop large fruits must be present in PS genome, since its fruit weight is nearly double than Ved fruits. We observed a trend in four ILs which showed a median fruit weight higher than average plus one standard deviation of Ved fruit weight. PS4.3, PS8.1, PS12.1 and PS12.3 fruits weighed 905, 880, 812.82 and 916.67 g, respectively, representing increases in fruit weight between 16.3 and 31.1 % as compared to Ved (Figure 1.1.5). However, the values presented a substantial variation within each line, probably preventing from detecting significant differences. The larger size of these fruits was visually obvious (Figure 1.1.2B) and also other size-related traits as fruit area and fruit perimeter showed this trend (Figure 1.1.5).

Two QTLs were identified for fruit shape. PS2.1 presented more elongated fruits, with an average fruit shape index of 1.10 which represents an increase of 14.58% as compared to Ved. *FSQP2.1* was delimited from the beginning of chromosome 2 to position 16.42 Mbp. This QTL does colocalize with the locus *a* previously mentioned (Boualem *et al*, 2008). However, both Ved and PS are andromonoecious, indicating that the genetic variation causing fruit shape differences may be due to a different underlying gene. PS4.4 carried flatter fruits with a fruit shape index of 0.87, a reduction of 9.38% as compared to Ved (Table 1.1.1 and Figure 1.1.5). *FSQP4.4* was located on chromosome 4, from 27.25 to 34.32 Mbp. To our knowledge, no previous fruit shape QTLs have been mapped to chromosome 4 in melon.

Curiously, none of the ILs fruit weight QTLs were identified in the Ved x PS RIL population (Pereira *et al*, 2018). The discrepancy may be due to QTL x QTL interactions, which could make some QTLs undetectable in certain genetic backgrounds. Similarly, fruit weight QTLs detected in the RIL population where not detected in the ILs, but *FWQU5.1* and *FWQU8.1*, would correspond to ILs PS5.2 and PS8.1; PS5.2 presented a high variation between replicates, possibly preventing from detecting a QTL at significant levels. PS8.1, already mentioned, showed an increase in fruit weight of ~180 g, considerably higher to the 92.4 g additive effect of PS observed in the Ved x PS RIL population (Pereira *et al*, 2018). The high variation between replicates and its limited number could cause lack of statistical power to detect a QTL confidently, but the observed trend in fruit weight suggests that PS allele in PS8.1 contributes to large fruits, in agreement with the Ved x PS RIL population. In addition, a QTL for fruit weight was

also detected in the same region of chromosome 8 in an F2 obtained by crossing a wild and a cultivated *agrestis* accessions, as well as a domestication sweep in a diversity panel of accessions (Zhao *et al*, 2019). Additional QTLs on chromosomes 6, 7 and 11 detected in the RIL population, where the Ved allele reduced fruit size, were undetectable in our IL collection. However, the fruit shape QTL on chromosome 2 was identified in both populations.

Fruit ripening

Melon has emerged as an alternative model to decipher the genetic control of fruit ripening, since both climacteric and non-climacteric varieties are found within the species. PS is a non-climacteric variety and Ved is highly climacteric and produces a large amount of ethylene at the onset of ripening (Périn *et al*, 2002; Saladié *et al*, 2015). The hypothesis of a quantitative composition of climacteric ripening, with the ethylene production and associated phenotypes varying in a continuum spectrum, rather than a qualitative presence-absence, is gaining relevance in recent studies (Ríos *et al*, 2017; Pereira *et al*, 2020). The PS IL collection added evidence to this hypothesis, since all ILs from the collection were climacteric. Nearly all the harvested fruits were aromatic and produced abscission layer, two of the most evident and typical traits of climacteric melons. However, PS7.1 did not present consistently the change of color due to chlorophyll degradation during ripening. As mentioned before, a major gene controlling rind color in immature fruit is located in the proximal arm of chromosome 7. Both PS7.1 and PS7.2 carried the PS allele of *Wi*, the major gene conferring green color during fruit development. We observed that PS7.2 degraded chlorophyll and turned yellow; this phenotype is completely different from Ved, whose white color turns to cream/light orange during ripening, and from PS, whose green color is maintained during ripening. Interestingly, not all PS7.1 fruits turned to yellow but some stayed green during ripening (Figure 1.1.S2). We defined the QTL *CDQP7.1* for chlorophyll degradation on chromosome 7, from the beginning of the chromosome to 2.62 Mbp.

In addition to the presence-absence of climacteric symptoms, we also recorded its earliness (ECD, EARO, EALF), earliness of harvest (HAR) and flesh firmness (FIR) after harvest to quantify the intensity of climacteric ripening.

PS8.2 showed the most delayed and the less intense climacteric characteristics in the IL collection. It presented a delay of 3-8 days in the appearance of climacteric symptoms, from ~33 DAP in Ved to ~39 DAP in PS8.2, representing about a 20% reduction. The

increase in flesh firmness was as high as 48.5%. The QTL was defined from 6.89 to 25.00 Mbp on chromosome 8 (Table 1.1.1; Figure 1.1.6).

PS6.2 also presented a delayed ripening of about 4 days, although the earliness of chlorophyll degradation and flesh firmness were not affected. The QTL was delimited from 7.47 to 38.30 Mbp on chromosome 6 (Figure 1.1.6; Table 1.1.1).

Two lines, PS2.1 and PS8.3, differed from Ved on flesh firmness, although their climacteric behavior was otherwise unaffected. PS2.1 showed a huge decrease in flesh firmness, being the only QTL for which PS allele enhances a climacteric characteristic (Figure 1.1.6; Table 1.1.1). However, cell wall degradation and the subsequent decrease of flesh firmness is only partially dependent on ethylene in melon (Pech *et al*, 2008) and flesh firmness in Ved and PS is similar. So, this QTL could be the main factor controlling cell wall degradation and allowing the softening of the flesh in the non-climacteric PS. *FIRQP2.1* is located at the beginning of chromosome 2 (0 – 16.42 Mbp). PS8.3 presented an increase in flesh firmness of about 44%, similarly to PS8.2, with which shares ~7 Mbp. However, the overall reduction of climacteric intensity in PS8.2 was not observed in PS8.3. We cannot discern whether the QTL causing this reduction in flesh firmness is exclusive of PS8.3 or shared between both lines, so the overlapping region was included in the interval of the QTL, namely from 25.0 to 34.77 Mbp.

Several QTLs related to climacteric ripening have been already mapped in melon (Périn *et al*, 2002; Vegas *et al*, 2013; Perpiñá *et al*, 2016). In the Ved x PS RIL population, several QTLs controlling or modulating ethylene production and/or climacteric traits as aroma production, fruit abscission and chlorophyll degradation have been identified (Pereira *et al*, 2020). In contrast with the low rate of overlapping observed for fruit morphology QTLs, all mapped QTLs affecting climacteric ripening were identified using both the Ved x PS RIL population and the PS IL collection, in similar genomic intervals (Pereira *et al*, 2020). Among them, *ETHQV8.1*, carried by PS8.2, was clearly and consistently the most relevant in both populations, presenting a delay in both the ethylene peak (measured only in the RIL population) and the appearance of climacteric traits (quantified in the RIL and IL collections).

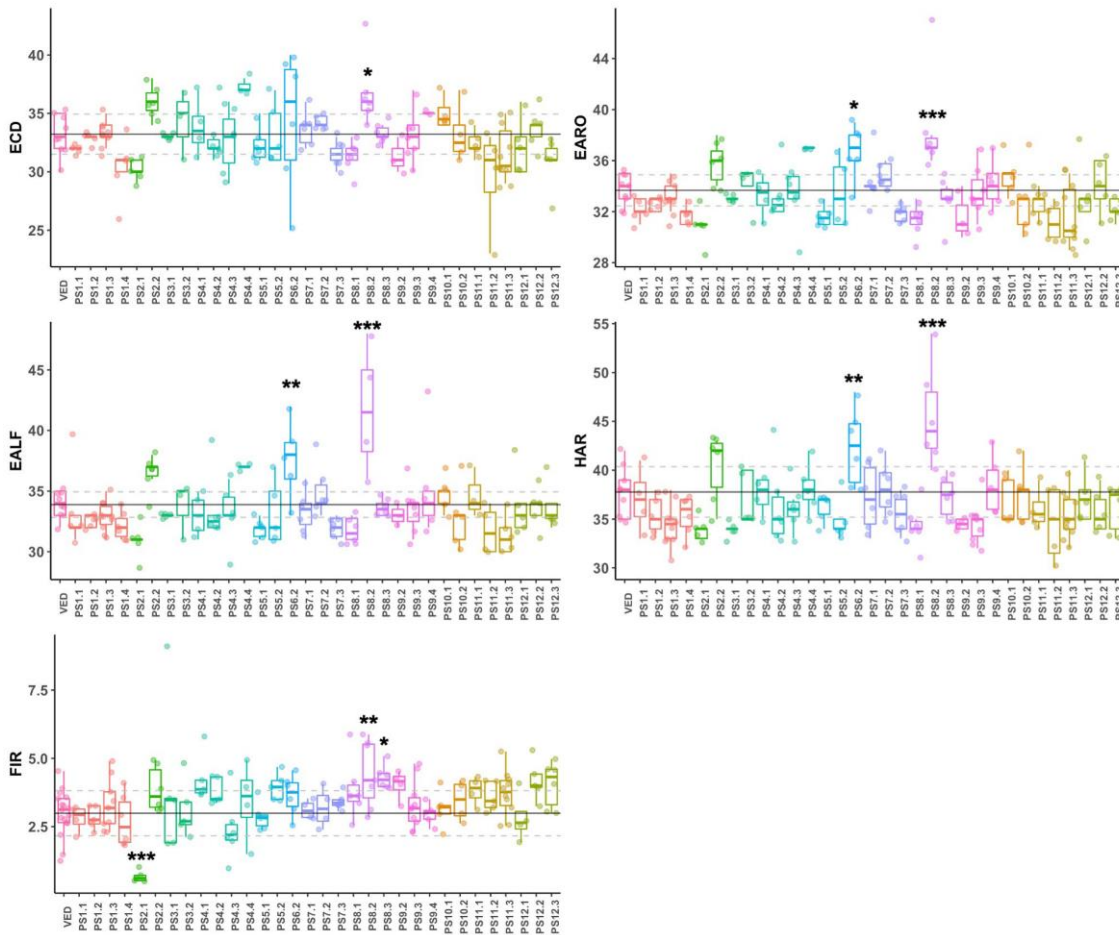


Figure 1.1.6. Boxplot representing the values of climacteric ripening traits for ILs. Each dot represents a replicate, the black solid line corresponds to the average and the grey dashed lines to the average \pm SD of the recurrent parent Ved. Significant differences are marked with asterisks: * < 0.1 , ** < 0.05 , *** < 0.01

Other melon IL collections have explored the genetic basis of fruit ripening (Vegas *et al*, 2013; Perpiñá *et al*, 2016; Castro *et al*, 2019). In total, they mapped three ripening QTLs on chromosomes 3, 6 and 10. These populations shared one parent with our IL collection, and yet we were able to identify two different QTLs on chromosomes 7 (*CDQP7.1* for chlorophyll degradation, Figure 1.1.S2) and 8 (several ripening traits, Table 1.1.1), supporting the complex genetic architecture of fruit ripening in melon. In addition, the partial effect of some of these QTLs, as observed in PS7.1, may be useful in breeding programs, allowing to modify only the desired trait without altering overall ripening behavior.

Materials and methods

Plant material and breeding scheme

Seedlings were planted in fertipots and maintained under controlled conditions in an indoor greenhouse facility (Crag, Barcelona) during approximately three weeks. After this period, selected plants were grown in a greenhouse in Caldes de Montbui (Barcelona) during spring and summer seasons (April-October). Plants were pruned weekly and pollinations were executed manually, allowing to develop only one fruit per plant.

The IL collection was founded by a cross between two commercial varieties, “Védrantais” (Ved), a French melon from the *cantalupensis* group, and “Piel de Sapo” T111 (PS), a Spanish melon from the *inodorus* group. Pollen from the F₁ plants was used to pollinate female flowers from Ved, obtaining BC₁ seed with the cytoplasm from the recurrent parent. After BC₁, Ved was generally used as male and the pre-IL as female. Seedlings of the BC₁ progenies were screened and a subset of plants was selected following these hierarchical criteria: 1) the complete genome of PS should be contained at least twice in the selected individuals; 2) the lines should carry the lowest possible number of introgressions; 3) the lines should contain the highest possible percentage of Ved genome. The chosen individuals were backcrossed again to obtain the BC₂ progeny. Analogous cycles of screening and selection were performed for the subsequent progenies following the breeding scheme presented in Figure 1.1.1. When the lines contained three or less introgressions, they were self-pollinated to identify lines carrying a unique introgression in homozygosity within the progeny. Depending on the introgression line, three or four backcrosses followed by one or two self-pollinations were needed to obtain the target introgression line in homozygosity without additional non-target introgressions in other chromosomes.

DNA extraction and genotyping

DNA extractions were performed from young leaves following the CTAB protocol (Doyle, 1991) with some modifications (Pereira *et al*, 2018).

The progenies of BC₁, BC₂ and most part of the BC₃ seedlings were analyzed with an initial set of 48 SNPs (set 1) homogeneously distributed within the 12 melon chromosomes (Table 1.1.S5a). The selected plants from BC₂ and BC₃ generations were subsequently genotyped with an additional set of 48 SNPs (set 2) (Table 1.1.S5b). SNPs were identified and designed from resequencing data of both parental lines (Sanseverino *et al*, 2015) and their positions are referred to the melon reference genome v3.6.1

(<http://www.melonomics.net>). SNPs producing sub-optimal genotypes were substituted by other SNPs located nearby. The progenies of BC₃S₁, BC₄, BC₃S₂ and BC₄S₁, screened in 2017, were genotyped with the complete set of SNPs (Table 1.1.S5c), which was comprised mostly by sets 1 and 2. Additional SNPs were used whenever necessary to genotype overlapping introgressions (Table 1.1.S5d). Plants were genotyped with SNPs using the KASPar SNP Genotyping System (KBiosciences, Herts, UK). KASPar primers were designed following LGC Genomics protocol. The genotyping was performed using the high-throughput genotyping system Biomark HD, based on the Fluidigm technology, with 48x48 (2015 and 2016) and 96x96 (2017) chips. In the last phases of screening and selection, when most part of the genome was already fixed for Ved, only SNPs contained within the known introgressions were genotyped with the same KASPar primers but using qPCR in a LightCycler 480 Real-time PCR System, according to the technical instructions provided by the supplier (Roche Diagnostics, Spain).

To calculate the size of the introgressions and the intervals delimiting the QTLs, two assumptions were done; we supposed that the haplotypes of the non-genotyped extremes of the chromosome were the same than the first or last SNP genotyped; and we used the intermediate position between two genotyped SNPs as the virtual recombination breakpoint. The approximate genetic size of the introgressions was calculated using as a reference a genetic map obtained from a Ved x PS RIL population (Pereira *et al*, 2018).

Experimental design and phenotyping of fruit quality and climacteric ripening traits

Phenotyping of most part of the IL collection was performed in greenhouse conditions in Caldes de Montbui (Barcelona) during the summer of 2018. The experiment consisted of randomized blocks including from five to seven plants of each IL and 13 plants of the recurrent parent, Ved. Four ILs that were not fully developed in 2018 were grown and phenotyped under the same conditions, along with the Ved controls, in the summer of 2019. Lastly, two more ILs were obtained in 2019 yet not phenotyped in the current study; these two ILs are included in the description of the collection but excluded from the QTL analysis.

Qualitative traits related with fruit appearance were visually inspected and recorded as presence or absence (Table 1.1.2). These traits were rind color of immature fruit (ECOL), yellowing of the rind (YELL), presence of sutures (SUT) and mottled rind (MOT). Flesh color of mature fruits (FC) was recorded as orange, white or green. All fruits were weighed (FW), photographed and scanned at harvest. The scanned images were analyzed

in Tomato Analyzer 3.0 (Rodríguez *et al*, 2010) to extract the values of morphological traits: fruit perimeter (FP), fruit area (FA), fruit length (FL) and fruit width (FWI); fruit shape (FS) was calculated as FL/FWI. To measure the soluble solid content (SSC), four 1-cm cylinders of flesh were obtained from the central part of the fruit in a proximal-distal section and the SSC value was estimated by a hand refractometer from manually extracted juice.

Table 1.1.2 Phenotypic traits evaluated in the IL collection

Category	Trait (units*)	Code
	Presence of sutures	SUT
	Rind color of immature fruit	ECOL
	Mottled rind	MOT
	Yellowing of the rind	YELL
	Soluble solids content (° Brix)	SSC
Fruit quality	Flesh color	FC
	Fruit weight (g)	FW
	Fruit 80ecn (cm ²)	FA
	Fruit perimeter (cm)	FP
	Fruit width (cm)	FWI
	Fruit length (cm)	FL
Fruit morphology	Fruit shape	FS
	Chlorophyll degradation	CD
	Earliness of chlorophyll degradation (DAP)	ECD
	Aroma production	ARO
	Earliness of aroma production (DAP)	EARO
	Earliness of abscission layer formation (DAP)	EALF
Climacteric	Earliness of harvesting (DAP)	HAR
ripening	Flesh firmness (kg · cm ⁻²)	FIR

*DAP: days after pollination

Ripening-related traits were evaluated as qualitative (presence or absence) or quantitative (earliness of appearance of the trait in days after pollination, DAP). The visual inspection of melon fruits attached to the plant was performed daily, from approximately 25 DAP until harvest. Chlorophyll degradation (CD) and its earliness (ECD) were recorded when degreening was obvious in visual inspections. Aroma production (ARO) and its earliness (EARO) were evaluated every other day by smelling the fruits. Earliness of abscission

layer formation (EALF) was recorded as well after daily visual inspection when a scar in the pedicel was clearly formed. The harvest date was determined by the following criteria and registered (HAR): (a) abscission date when the fruit abscised; (b) after five days of the appearance of the abscission layer; (c) at 55-60 days after pollination when fruits were non-climacteric. The firmness of fruit flesh (FIR) was measured at harvest using a penetrometer (Fruit TestTM, Wagner Instruments), in at least three regions of the fruit (distal, proximal and median), and the mean value was registered.

QTL and major gene mapping and statistical analyses

A QTL was designated when the mean of one or more IIs carrying the corresponding region was significantly different to Ved mean using Dunnett's test. When two IIs overlapped in a certain region of the introgression, the overlapping interval defined the QTL if both lines were significantly different to Ved but was excluded when only one line presented the phenotype. The statistical analysis was implemented in R (version 3.6.3) using the functions `aov` and `glht` from the packages `stats` and `multcomp`, respectively. Three levels of significance (0.1, 0.05 and 0.001) were used and the p-values were specified. The genomic intervals of the QTLs and major genes were calculated using the intermediate position between 81ecnologed SNPs as the virtual recombination breakpoint.

Conclusion

We have developed a new IL collection, using as parental lines two elite European cultivars. A RIL population derived from the same parental lines has proven its effectiveness to identify relevant fruit quality QTLs. Multiple QTLs and major genes controlling several aspects of fruit quality have been identified and the germplasm generated in this work could ease further fine mapping and positional cloning. In addition, these lines could be used to pyramid QTLs controlling complex traits such as fruit size or climacteric ripening, allowing to better understand the genetic interactions among them. Lastly, the PS IL collection may be an excellent resource for breeding programs. Generally, IIs are developed using wild or exotic material, which carry detrimental alleles by linkage drag. By using two commercial varieties of high quality and yet segregating for many relevant traits, we avoided the unfavorable alleles that could be linked to the target gene in other non-commercial materials.

Authors' contributions

MP and JG-M conceived and designed the research. LP, MSD, JA and CM performed the experiments and data analyses. LP wrote the original draft. MSD, MP and JG-M reviewed and edited the manuscript. AMM-H and JG-M contributed to funding acquisition. All authors read and approved the manuscript.

Supplementary material

Figures

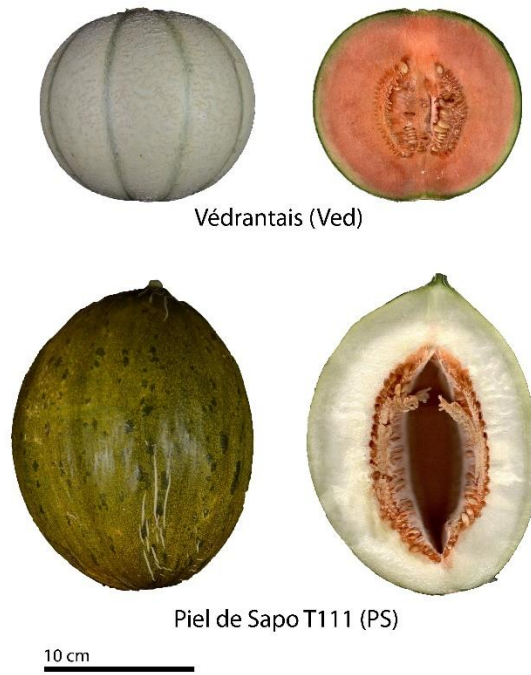


Figure 1.1.S1. Images of the parental lines used to develop the IL collection

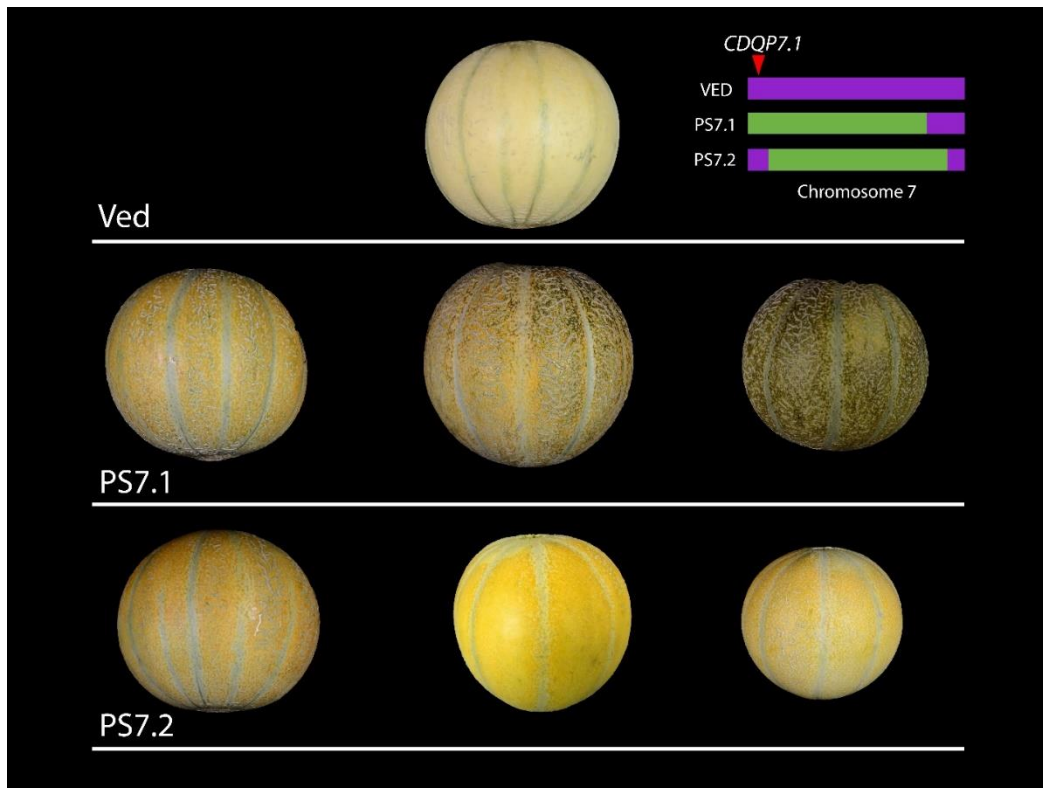


Figure 1.1.S2. Effect of the QTL *CDQP7.1* on chlorophyll degradation.

Tables**Table 1.1.S3.** Description of the IL collection

Chr	Number of IIs	Introgression size (Mbp)			Introgression size (cM)		
		Average	Min	Max	Average	Min	Max
1	4	15.43	2.46	32.02	53.4	22.1	82.2
2	2	13.75	2.73	24.77	63.9	14.7	113.0
3	2	22.69	21.76	23.62	77.1	75.8	78.4
4	4	15.00	8.53	19.40	68.5	44.2	86.6
5	2	14.66	2.76	26.57	62.6	29.3	95.8
6	2	33.07	30.83	35.32	109.8	90.5	129.2
7	3	15.69	2.98	23.36	56.9	30.2	77.2
8	3	14.21	6.89	25.98	51.2	37.2	58.8
9	4	18.24	14.91	20.52	46.0	17.6	70.8
10	2	19.22	17.98	20.47	59.7	24.9	94.6
11	3	24.94	18.56	29.79	71.5	29.7	105.3
12	3	17.11	4.58	23.75	59.1	47.1	73.5
Total	34	18.16	2.46	35.32	62.8	14.7	129.2

Table 1.1.S4. General description of some IL collections

Species	Donor parental	Needed generations ¹	Ils/chr ²	First MAS-generation	Reference
Tomato	<i>S. pimpinellifolium</i>	6	4.6	BC2	(Barrantes <i>et al</i> 2014)
Eggplant	<i>S. incanum</i>	7	2.1	BC1	(Gramazio <i>et al</i> 2017)
Peach	Almond “Texas”	3	3.5 ²	BC1	(Serra <i>et al</i> 2016)
Strawberry	<i>Fragaria bucharica</i>	4	6	BC1	(Urrutia <i>et al</i> 2015)
Melon	PI 162375 “Songwhan Charmi”	6	4.75	BC1	(Eduardo <i>et al</i> 2005)
Melon	PI 420176 “Ginsen Makuwa”	6	1.3	BC2	(Perpiñá <i>et al</i> 2016)
Melon	PI 273438 “Queen’s pocket melon”	6	1.3	BC2	(Castro <i>et al</i> 2019)
Melon	“Piel de Sapo” T111	6	2.8	BC1	This work

¹The number of generations needed to develop the population

²Only homozygous IIs were considered

Digital supplementary material

Table 1.1.S1. Average and SD values of phenotypic traits analyzed in the IL collection and the parental lines PS and Ved

Table 1.1.S2. Genotypes of the IL collection

Table 1.1.S5. Information about the SNPs used to develop and genotype the IL collection

References

- Argyris JM, Díaz A, Ruggieri V, *et al* (2017) QTL Analyses in Multiple Populations Employed for the Fine Mapping and Identification of Candidate Genes at a Locus Affecting Sugar Accumulation in Melon (*Cucumis melo* L .). *Front Plant Sci* 8:1–20. <https://doi.org/10.3389/fpls.2017.01679>
- Barrantes W, Fernández-del-Carmen A, López-Casado G, *et al* (2014) Highly efficient genomics-assisted development of a library of introgression lines of *Solanum pimpinellifolium*. *Mol Breed* 34:1817–1831. <https://doi.org/10.1007/s11032-014-0141-0>
- Barrantes W, López-Casado G, García-Martínez S, *et al* (2016) Exploring new alleles involved in tomato fruit quality in an introgression line library of *solanum pimpinellifolium*. *Front Plant Sci* 7:1–12. <https://doi.org/10.3389/fpls.2016.01172>
- Bernacchi D, Beck-Bunn T, Emmatty D, *et al* (1998) Advanced backcross QTL analysis of tomato. II. Evaluation of near-isogenic lines carrying single-donor introgressions for desirable wild QTL-alleles derived from *Lycopersicon hirsutum* and *L. pimpinellifolium*. *Theor Appl Genet* 97:170–180. <https://doi.org/10.1007/s001220050882>
- Boualem A, Fergany M, Fernandez R, *et al* (2008) A conserved mutation in an ethylene biosynthesis enzyme leads to andromonoecy in melons. *Science* (80-) 321:836–838. <https://doi.org/10.1126/science.1159023>
- Briggle LW (1969) Near-Isogenic Lines of Wheat with Genes for Resistance to *Erysiphe graminis* f. sp. *tritici*. *Crop Sci* 9:70–72
- Castro G, Perpiñá G, Monforte AJ, *et al* (2019) New melon introgression lines in a Piel de Sapo genetic background with desirable agronomical traits from dudaim melons. *Euphytica* 215:. <https://doi.org/10.1007/s10681-019-2479-1>
- Chakrabarti M, Zhang N, Sauvage C, *et al* (2013) A cytochrome P450 regulates a domestication trait in cultivated tomato. *Proc Natl Acad Sci U S A* 110:17125–17130. <https://doi.org/10.1073/pnas.1307313110>
- Cuevas HE, Staub JE, Simon PW, Zalapa JE (2009) A consensus linkage map identifies genomic regions controlling fruit maturity and beta-carotene-associated flesh color

- in melon (*Cucumis melo* L.). *Theor Appl Genet* 119:741–756. <https://doi.org/10.1007/s00122-009-1085-3>
- Díaz A, Hernández M, Dolcet R, *et al* (2017) Quantitative trait loci analysis of melon (*Cucumis melo* L.) domestication - related traits. *Theor Appl Genet* 130:1837–1856. <https://doi.org/10.1007/s00122-017-2928-y>
- Doyle J (1991) DNA Protocols for Plants. In: Hewitt GM, Johnston AWB, Young JPW (eds) *Molecular Techniques in Taxonomy*. Springer Berlin Heidelberg, Berlin, Heidelberg, pp 283–293
- Eduardo I, Arús P, Monforte AJ (2005) Development of a genomic library of near isogenic lines (NILs) in melon (*Cucumis melo* L.) from the exotic accession PI161375. *Theor Appl Genet* 112:139–148. <https://doi.org/10.1007/s00122-005-0116-y>
- Eduardo I, Arús P, Monforte AJ, *et al* (2007) Estimating the genetic architecture of fruit quality traits in melon using a genomic library of near isogenic lines. *J Am Soc Hortic Sci* 132:80–89. <https://doi.org/10.21273/jashs.132.1.80>
- Esteras C, Gomez P, Monforte AJ, *et al* (2012) High-throughput SNP genotyping in *Cucurbita pepo* for map construction and quantitative trait loci mapping. *BMC Genomics* 13:80. <https://doi.org/10.1186/1471-2164-13-80>
- Ezura H, Owino WO (2008) Melon, an alternative model plant for elucidating fruit ripening. *Plant Sci* 175:121–129. <https://doi.org/10.1016/j.plantsci.2008.02.004>
- Feder A, Burger J, Gao S, *et al* (2015) A Kelch Domain-Containing F-Box Coding Gene Negatively Regulates Flavonoid Accumulation in Muskmelon. *Plant Physiol* 169:1714–1726. <https://doi.org/10.1104/pp.15.01008>
- Foncéka D, Hodo-Abalo T, Rivallan R, *et al* (2009) Genetic mapping of wild introgressions into cultivated peanut: A way toward enlarging the genetic basis of a recent allotetraploid. *BMC Plant Biol* 9:1–13. <https://doi.org/10.1186/1471-2229-9-103>
- Frary A, Nesbitt TC, Frary A, *et al* (2000) fw2.2: A quantitative trait locus key to the evolution of tomato fruit size. *Science* (80-) 289:85–88. <https://doi.org/10.1126/science.289.5476.85>

Chapter 1: Introgression Lines

- Galpaz N, Gonda I, Shem-Tov D, *et al* (2017) Deciphering genetic factors that determine melon fruit-quality traits using RNA-Seq based high-resolution QTL and eQTL mapping. *ARPN J Eng Appl Sci* 12:3218–3221. <https://doi.org/10.1111/ijlh.12426>
- Garcia-Mas J, Benjak A, Sanseverino W, *et al* (2012) The genome of melon (*Cucumis melo* L.). *Proc Natl Acad Sci U S A* 109:11872–7. <https://doi.org/10.1073/pnas.1205415109>
- Giner A, Pascual L, Bourgeois M, *et al* (2017) A mutation in the melon Vacuolar Protein Sorting 41 prevents systemic infection of Cucumber mosaic virus. *Sci Rep* 7:1–12. <https://doi.org/10.1038/s41598-017-10783-3>
- Gramazio P, Prohens J, Plazas M, Mangino G (2017) Development and Genetic Characterization of Advanced Backcross Materials and An Introgression Line Population of *Solanum incanum* in a *S. melongena* Background. 8:1–15. <https://doi.org/10.3389/fpls.2017.01477>
- Harel-Beja R, Tzuri G, Portnoy V, *et al* (2010) A genetic map of melon highly enriched with fruit quality QTLs and EST markers, including sugar and carotenoid metabolism genes. *Theor Appl Genet* 121:511–33. <https://doi.org/10.1007/s00122-010-1327-4>
- Huang BE, Verbyla KL, Verbyla AP, *et al* (2015) MAGIC populations in crops: current status and future prospects. *Theor Appl Genet* 128:999–1017. <https://doi.org/10.1007/s00122-015-2506-0>
- Keurentjes JJB, Bentsink L, Alonso-Blanco C, *et al* (2007) Development of a near-isogenic line population of *Arabidopsis thaliana* and comparison of mapping power with a recombinant inbred line population. *Genetics* 175:891–905. <https://doi.org/10.1534/genetics.106.066423>
- Kubicki B (1962) Inheritance of some characters in muskmelons (*Cucumis melo*). *Genet Pol* 3:265–74
- Lelièvre J-M, Latchè A, Jones B, *et al* (1997) Ethylene and fruit ripening. *Physiol Plant* 101:727–739. <https://doi.org/10.1111/j.1399-3054.1997.tb01057.x>
- Li ZK, Fu BY, Gao YM, *et al* (2005) Genome-wide introgression lines and their use in genetic and molecular dissection of complex phenotypes in rice (*Oryza sativa* L.).

- Plant Mol Biol 59:33–52. <https://doi.org/10.1007/s11103-005-8519-3>
- Lin HX, Yamamoto T, Sasaki T, Yano M (2000) Characterization and detection of epistatic interactions of 3 QTLs, Hd1, Hd2, and Hd3, controlling heading date in rice using nearly isogenic lines. *Theor Appl Genet* 101:1021–1028. <https://doi.org/10.1007/s001220051576>
- Martin A, Troadec C, Boualem A, *et al* (2009) A transposon-induced epigenetic change leads to sex determination in melon. *Nature* 461:1135–1138. <https://doi.org/10.1038/nature08498>
- McMullen MD, Kresovich S, Villeda HS, *et al* (2009) Supporting online material for: Genetic Properties of the Maize Nested Association Mapping Population. *Science* (80-) 325:737–741. <https://doi.org/10.1126/science.1174320>
- Monforte a J, Oliver M, Gonzalo MJ, *et al* (2004) Identification of quantitative trait loci involved in fruit quality traits in melon (*Cucumis melo* L.). *Theor Appl Genet* 108:750–8. <https://doi.org/10.1007/s00122-003-1483-x>
- Monforte AJ, Diaz A, Caño-Delgado A, Van Der Knaap E (2014) The genetic basis of fruit morphology in horticultural crops: Lessons from tomato and melon. *J Exp Bot* 65:4625–4637. <https://doi.org/10.1093/jxb/eru017>
- Monforte AJ, Friedman E, Zamir D, Tanksley SD (2001) Comparison of a set of allelic QTL-NILs for chromosome 4 of tomato: Deductions about natural variation and implications for germplasm utilization. *Theor Appl Genet* 102:572–590. <https://doi.org/10.1007/s001220051684>
- Mu Q, Huang Z, Chakrabarti M, *et al* (2017) Fruit weight is controlled by Cell Size Regulator encoding a novel protein that is expressed in maturing tomato fruits. *PLoS Genet* 13:1–26. <https://doi.org/10.1371/journal.pgen.1006930>
- Obando-Ulloa JM, Eduardo I, Monforte AJ, Fernández-Trujillo JP (2009) Identification of QTLs related to sugar and organic acid composition in melon using near-isogenic lines. *Sci Hortic (Amsterdam)* 121:425–433. <https://doi.org/https://doi.org/10.1016/j.scienta.2009.02.023>
- Obando-Ulloa JM, Ruiz J, Monforte AJ, Fernández-Trujillo JP (2010) Aroma profile of a collection of near-isogenic lines of melon (*Cucumis melo* L.). *Food Chem*

- 118:815–822. <https://doi.org/https://doi.org/10.1016/j.foodchem.2009.05.068>
- Pech JC, Bouzayen M, Latché A (2008) Climacteric fruit ripening: Ethylene-dependent and independent regulation of ripening pathways in melon fruit. *Plant Sci* 175:114–120. <https://doi.org/https://doi.org/10.1016/j.plantsci.2008.01.003>
- Pegg GF, Cronshaw DK (1976) Ethylene production in tomato plants infected with *Verticillium albo-atrum*. *Physiol Plant Pathol* 8:279–295
- Pereira L, Domingo MS, Ruggieri V, *et al* (2020) Genetic dissection of climacteric fruit ripening in a melon population segregating for ripening behavior. *Hortic Res.* <https://doi.org/10.1038/s41438-020-00411-z>
- Pereira L, Ruggieri V, Pérez S, *et al* (2018) QTL mapping of melon fruit quality traits using a high-density GBS-based genetic map. *BMC Plant Biol.* <https://doi.org/10.1186/s12870-018-1537-5>
- Périn C, Dogimont C, Giovinazzo N, *et al* (1999) Genetic Control and Linkages of Some Fruit Characters in Melon. *Cucurbit Genet Coop Rep* 22:16–18
- Périn C, Gomez-Jimenez M, Hagen L, *et al* (2002) Molecular and Genetic Characterization of a Non- Climacteric Phenotype in Melon Reveals Two Loci Conferring Altered Ethylene Response in Fruit 1. *Plant Physiol* 129:300–309
- Perpiñá G, Cebolla-Cornejo J, Esteras C, *et al* (2017) “MAK-10”: A long shelf-life charentais breeding line developed by introgression of a genomic region from Makuwa Melon. *HortScience* 52:1633–1638. <https://doi.org/10.21273/HORTSCI12068-17>
- Perpiñá G, Esteras C, Gibon Y, *et al* (2016) A new genomic library of melon introgression lines in a cantaloupe genetic background for dissecting desirable agronomical traits. *BMC Plant Biol* 16:1–21. <https://doi.org/10.1186/s12870-016-0842-0>
- Ríos P, Argyris J, Vegas J, *et al* (2017) ETHQV6.3 is involved in melon climacteric fruit ripening and is encoded by a NAC domain transcription factor. *Plant J* 91:671–683. <https://doi.org/10.1111/tpj.13596>
- Rodríguez GR, Moysenko JB, Robbins MD, *et al* (2010) Tomato Analyzer: A Useful Software Application to Collect Accurate and Detailed Morphological and Colorimetric Data from Two-dimensional Objects. *JoVE* e1856.

<https://doi.org/doi:10.3791/1856>

- Saladié M, Cañizares J, Phillips MA, *et al* (2015) Comparative transcriptional profiling analysis of developing melon (*Cucumis melo* L.) fruit from climacteric and non-climacteric varieties. *BMC Genomics* 16:1–20. <https://doi.org/10.1186/s12864-015-1649-3>
- Sanseverino W, Hénaff E, Vives C, *et al* (2015) Transposon insertions, structural variations, and SNPs contribute to the evolution of the melon genome. *Mol Biol Evol* 32:2760–2774. <https://doi.org/10.1093/molbev/msv152>
- Serra O, Donoso JM, Picañol R, *et al* (2016) Marker-assisted introgression (MAI) of almond genes into the peach background: a fast method to mine and integrate novel variation from exotic sources in long intergeneration species. *Tree Genet Genomes* 12:. <https://doi.org/10.1007/s11295-016-1056-1>
- Suge H (1972) EFFECT OF UZU (UZ) GENE ON THE LEVEL OF ENDOGENOUS GIBBERELLINS IN BARLEY. *Japanese J Genet* 47:423–430
- Tzuri G, Zhou X, Chayut N, *et al* (2015) A “golden” SNP in CmOr governs the fruit flesh color of melon (*Cucumis melo*). *Plant J* 82:267–279. <https://doi.org/10.1111/tpj.12814>
- Urrutia M, Bonet J, Arús P, Monfort A (2015) A near-isogenic line (NIL) collection in diploid strawberry and its use in the genetic analysis of morphologic, phenotypic and nutritional characters. *Theor Appl Genet* 128:1261–1275. <https://doi.org/10.1007/s00122-015-2503-3>
- Urrutia M, Rambla JL, Alexiou KG, *et al* (2017) Genetic analysis of the wild strawberry (*Fragaria vesca*) volatile composition. *Plant Physiol Biochem* 121:99–117. <https://doi.org/10.1016/j.plaphy.2017.10.015>
- Vegas J, Garcia-Mas J, Monforte AJ (2013) Interaction between QTLs induces an advance in ethylene biosynthesis during melon fruit ripening. *Theor Appl Genet* 126:1531–1544. <https://doi.org/10.1007/s00122-013-2071-3>
- Zhao G, Lian Q, Zhang Z, *et al* (2019) A comprehensive genome variation map of melon identifies multiple domestication events and loci influencing agronomic traits. *Nat Genet* 51:1607–1615. <https://doi.org/10.1038/s41588-019-0522-8>

Chapter 1.2

Fruit morphology and ripening-related QTLs in a newly developed introgression line collection of the elite varieties ‘Védrantais’ and ‘Piel de Sapo’

Fruit morphology and ripening-related QTLs in a newly developed introgression line collection of the elite varieties ‘Védrantais’ and ‘Piel de Sapo’

Miguel Santo Domingo^{1§}, Carlos Mayobre^{1§}, Lara Pereira¹, Jason Argyris^{1,2}, Laura Valverde¹, Ana Montserrat Martín-Hernández^{1,2}, Jordi Garcia-Mas^{1,2*} and Marta Pujol^{1,2*}

¹ Centre for Research in Agricultural Genomics (CRAG) CSIC-IRTA-UAB-UB, Edifici CRAG, Campus UAB, 08193 Bellaterra, Barcelona, Spain.

² Institut de Recerca i Tecnologia Agroalimentàries (IRTA), 08193 Bellaterra, Barcelona, Spain.

§ These authors contributed equally

* Corresponding authors

Corresponding authors addresses:

Jordi Garcia-Mas, jordi.garcia@irta.cat Phone: +34 935636600

Marta Pujol, marta.pujol@irta.cat Phone: +34 935636600

Manuscript accepted for publication at *Plants* (ISSN: 2223-7747)

Abstract

Melon is an economically important crop with widely diverse fruit morphology and ripening characteristics. Its diploid sequenced genome and multiple genomic tools make this species suitable to study the genetic architecture of fruit traits. With the development of this introgression line population, of the elite varieties ‘Piel de Sapo’ and ‘Védraçais’, we present a powerful tool to study fruit morphology and ripening traits that can also facilitate the characterization or pyramiding of QTLs in *inodorous* melon types. The population consists of 36 lines covering almost 98% of the melon genome, with an average of three introgressions per chromosome and segregating for multiple fruit traits: morphology, ripening and quality. High variability in fruit morphology was found within the population, with 24 QTLs affecting six different traits, confirming previously reported QTLs and two newly detected QTLs, *FLQW5.1* and *FWQW7.1*. We detected 20 QTLs affecting fruit ripening traits, six of them reported for the first time, two affecting the timing of yellowing of the rind (*EYELLQW1.1* and *EYELLQW8.1*) and four at the end of chromosome 8 affecting aroma, abscission and harvest date (*EAROQW8.3*, *EALFQW8.3*, *ABSQW8.3* and *HARQW8.3*). We also confirmed the location of several QTLs, such as fruit quality-related QTLs affecting rind and flesh color and appearance and flesh firmness.

Keywords

Introgression lines, *Cucumis melo*, fruit quality, climacteric ripening

Introduction

Cultivated fruit and vegetables are an essential part of the human and animal diet, so it is crucial to improve yield as well as the quality of their edible parts. To help breeders, molecular tools have been developed in many crop species to map and associate a trait with a genomic region. With these tools, molecular plant breeding has emerged as a relevant strategy to accelerate plant breeding, and the use of molecular markers has led to the discovery of the molecular mechanisms of diverse traits (Bhoite *et al*, 2018; Cai *et al*, 2019; Zhaoming *et al*, 2017).

Several mapping populations have been used in modern plant breeding, such as Recombinant Inbred Lines (RILs) (Fukino *et al*, 2004; Kuang *et al*, 2022; Clark *et al*, 2022) and F2 populations (Endelman *et al*, 2016; Zhang *et al*, 2022). RILs have been widely used for mapping QTLs associated with traits such as yield in wheat (Wang *et al*, 2009) and leaf type in soybean (Wang *et al*, 2019), while F2 populations have also been used in the study of yield in rice (Li *et al*, 2000) and fruit quality traits in pomegranate (Harel-Beja *et al*, 2015). In RILs and F2 populations, the genome of the two founding parents is equally represented, but in other mapping populations the genomes of the parents are not equally represented, such as Introgression Lines (ILs) (Eshed *et al*, 1995; Perpiñá *et al*, 2016) and Chromosome Segment Substitution Lines (CSSLs) (Balakrishnan *et al*, 2019; Xu *et al*, 2010).

IL populations make it possible to mendelize and study different traits without the effect of other interacting loci. This has been used widely for different traits and crops such as fruit weight and soluble solid content in tomato (Eshed *et al*, 1995), flowering time in maize (Szalma *et al*, 2007), grain weight in rice (Fujita *et al*, 2022) or CMV resistance in melon (Essafi *et al*, 2009; Giner *et al*, 2017). In addition, it allows pyramiding of different QTLs and studying their interactions, as has been done for studying resistance to bacterial blight in rice (Babar *et al*, 2022) or resistance to *Aphanomyces euteiches* in pea (Lavaud *et al*, 2016). ILs are developed by multiple backcrosses with the same parental line (the recurrent parent) and a last step of self-pollination to fix the heterozygous regions, giving a set of perpetual lines sharing most of the genome of the recurrent parent, but having an introgression in a given chromosome from the other parental line (donor parent). Ideally, with a complete set of ILs, the donor genome should be fully covered.

In melon, many mapping populations have been developed to study fruit quality (Pereira *et al.*, 2018; Oren *et al.*, 2020; Dai *et al.*, 2022; Argyris *et al.*, 2017; Pereira *et al.*, 2021) and fruit morphology (Pereira *et al.*, 2021; Castro *et al.*, 2019; Martínez-Martínez *et al.*, 2022). For melon breeding, fruit ripening represents a key complex trait, and several studies have been conducted to identify the genes underlying this process (Pereira *et al.*, 2021; Pereira *et al.*, 2020; Perpiñá *et al.*, 2017). Melon presents intra-specific segregation of climacteric ripening, allowing the development of populations segregating for ripening behavior (Pereira *et al.*, 2020; Pereira *et al.*, 2021). Recently, three genes involved in melon ripening (*CmCTR1*, *CmROSI* and *CmNAC-NOR*) have been validated through CRISPR/Cas9 (Giordano *et al.*, 2022; Liu *et al.*, 2022) and a collection of lines pyramided with three ripening-related QTLs introgressed in a non-climacteric background has been developed to understand the interaction of these QTLs (Santo Domingo *et al.*, 2022).

Here we developed a novel IL population with ‘Piel de Sapo’ (PS) as the recurrent parent and ‘Védraçais’ (Ved) as donor parent. These two elite cultivars were chosen due to their differences in fruit morphology and ripening behavior. PS is a large, oval, white-fleshed melon with non-climacteric ripening behavior, while Ved is a small, round, aromatic, orange-fleshed melon with typical climacteric behavior. This is a new high-value genomic resource for breeding *inodorous* varieties and offers some insights into the genomic architecture of fruit quality, fruit morphology and fruit ripening behavior in melon.

Results and discussion

Phenotyping of the parental lines

PS and Ved were used as parental lines for the population, with PS the recurrent and Ved the donor parent. Both varieties are considered elite cultivars, as they are widely consumed for their taste and aroma, but with distinctive characteristics.

Over the two-year period of analysis, 2020 and 2021, PS produced consistently larger fruits than Ved, even though the PS fruits were smaller in the 2021 season (FW; Figure 1.2.1A) (Table 1.2.S1). The soluble solid content was highly dependent on the environmental conditions. In 2020, there were no significant differences between the cultivars, while PS fruits accumulated more soluble solids than Ved in 2021 (SSC; Figure 1.2.1B) (Table 1.2.S1). This SSC variability has been observed in previous studies: the mean value in PS is generally around 10-11° Brix, but in some environments it can reach

values lower than 9 or higher than 13 (Argyris *et al*, 2017; Pereira *et al*, 2021; Eduardo *et al*, 2007; Leida *et al*, 2015). In Ved, the variation has also been found to be highly dependent on the location and the season, from around 7 to 13° Brix (Pereira *et al*, 2021; Perpiñá *et al*, 2017; Santo Domingo *et al*, 2022) This high dependence on the environment can make it difficult to map QTLs related with this trait.

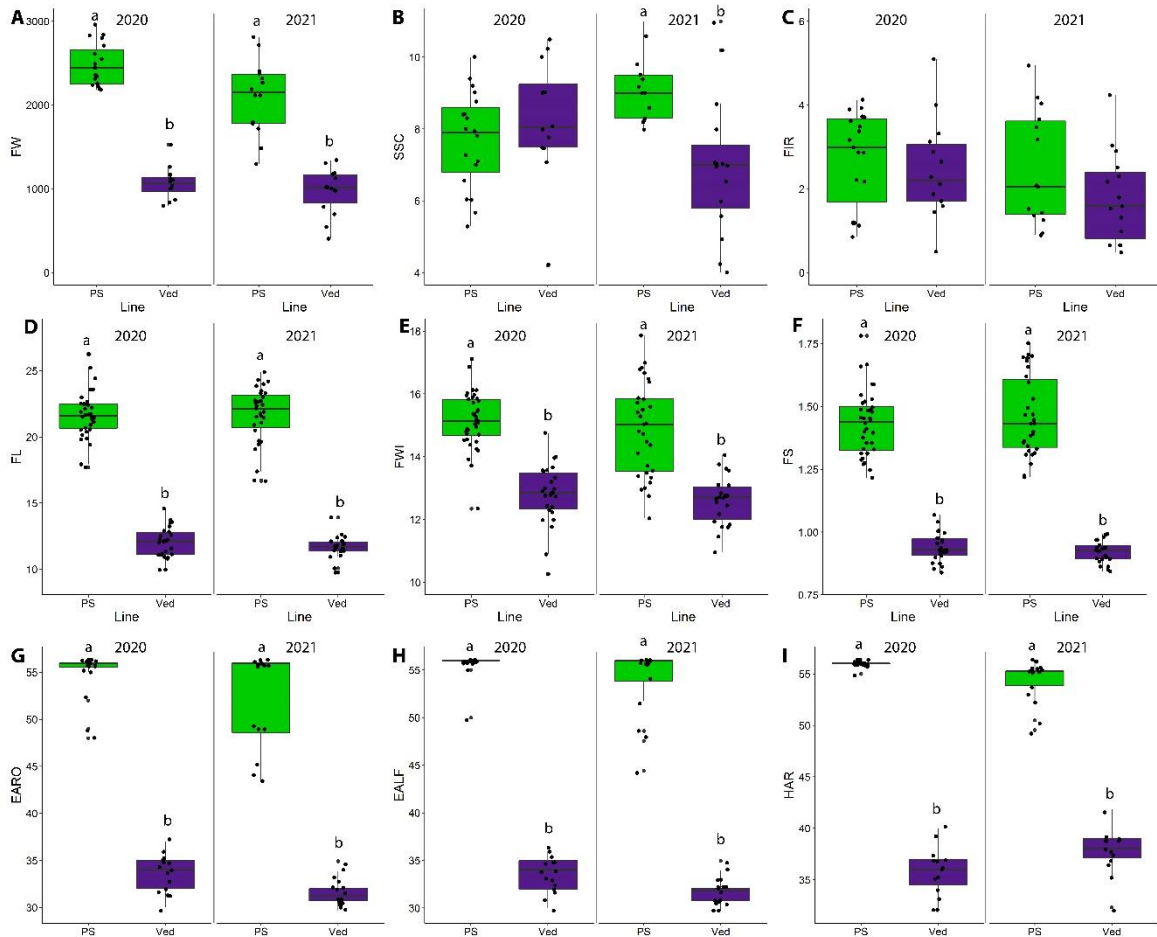


Figure 1.2.1. Fruit quality, fruit morphology and fruit ripening related phenotypes of the parental lines PS and Ved in 2020 and 2021. **A)** Fruit weight (FW) (g). **B)** Soluble solid content (°Brix) (SSC). **C)** Flesh firmness (kg cm^{-2}) (FIR). **D)** Fruit length (cm) (FL). **E)** Fruit width (cm) (FWI). **F)** Fruit shape (FS). **G)** Presence of aroma (days after pollination) (EARO). **H)** Abscission layer formation (days after pollination) (EALF). **I)** Harvest date (days after pollination) (HAR). Different letters represent significantly different groups ($p\text{-value} < 0.05$).

No significant differences were found in firmness of the flesh between cultivars or between years (FIR; Figure 1.2.1C) (Table 1.2.S1). This trait is also highly dependent on the environment, especially in PS, where it has been found to vary significantly between years, while Ved tends to be more stable (Pereira *et al*, 2020; Santo Domingo *et al*, 2022).

Chapter 1: Introgression Lines

When we looked at fruit shape, PS produced more oval melons than Ved in both years, with longer and wider fruits in PS, while Ved produced rounded (FS close to 1) smaller fruits (FL, FWI, FS; Figure 1.2.1D, E, F) (Table 1.2.S1).

The biggest differences between the parental lines were observed in traits related to ripening behavior. In climacteric melons, the production of ethylene is coupled to certain ripening related traits, such as the production of aroma (EARO) and the abscission layer formation (EALF), also affecting the harvest date (HAR) (Pereira *et al*, 2021). While Ved ripened at around 35 days after pollination in both years, PS ripened around 20 days later, generally without producing aroma or abscission layer (Figure 1.2.1G, H, I) (Table 1.2.S1).

Development of the IL collection

For the development of the IL population, we used the same sets of SNPs as in Pereira *et al* (2021). Starting the Ved x PS cross in 2014, six or seven generations were needed to complete the population, depending on the IL (Figure 1.2.2).

The BC1 generation carried a mean of 50.2% of the PS genome, ranging from 10.6% to 76.6%, and an average of 11.8 introgressions, varying between 5 and 17 introgressions per plant. Twenty BC1 plants with a mean of 8.3 introgressions and 65.5% of the recurrent parent were selected for the next round of backcrossing. In the BC2 generation, 46 seedlings carrying a mean of 5.3 introgressions and 77.3% of the PS genome were selected for the next round of backcrossing. In the BC3 generation, 55 plants carrying an average of 3.4 introgressions and 82.4% of PS genome were selected. Some BC3 plants were backcrossed while others were self-pollinated. During the spring season of 2017, both BC3S1 and BC4 generations were genotyped, and 92 plants with an average of 2.2 introgressions and 87.9% of PS genome were selected. Seven BC3 families were also recovered in order to cover gaps in the genome. At this point, five lines carried the desired single introgression. To complete the population, in summer 2017 several interesting progenies were genotyped using the complete set of SNPs or a customized number of SNPs, depending on the line. With this new screening, 18 new ILs were obtained. In 2018, 24 additional families were genotyped and 29 ILs were finalized (considering the ILs obtained in 2017). Also in 2018, three more families were genotyped with the complete set of SNPs to cover gaps in the genome. Finally, five ILs were added to the population in 2019, and two more in 2020, which were derived from the lines selected for covering gaps or unfinished lines.

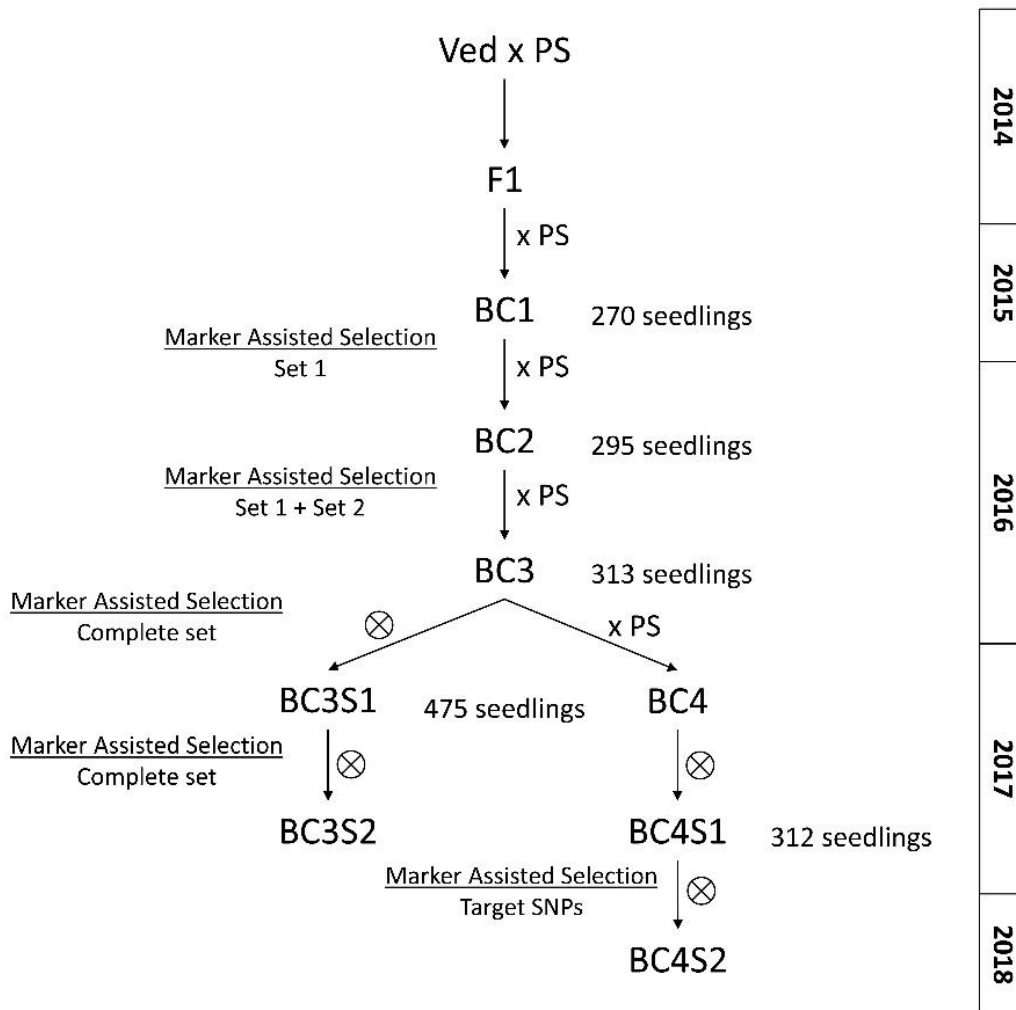


Figure 1.2.2. Simplified breeding scheme for the development of the IL population

In the BC1 generation, the mean heterozygosity was $H_0 = 0.48$ and segregation distortion was observed for 10 SNPs. The highest distortion, $\chi^2 = 18$, was in the SNP chr7_16723157. The H_0 of this SNP, located at the position 18,255,891 bp on chromosome 7, was 0.63 with a predominance of the Ved allele. Segregation distortion has previously been observed in melon in different chromosomes, including chromosome 7 (Nimmakalaya *et al*, 2016). For the other SNPs that had segregation distortion, the H_0 ranged from 0.41 to 0.44, below the mean.

Finally, a set of 36 ILs was developed covering 97.89% of the genome, with an average of three unique introgressions per chromosome (Table 1.2.S2). The information and graphical representation of the population are given in Table 1.2.1 and Figure 1.2.3.

Table 1.2.1. Summary of the developed introgression lines population, with average introgression size per chromosome in physical and genetic distance.

Chr	Number of ILs	Introgression size (bp)			Introgression size* (cM)		
		Average	Min	Max	Average	Min	Max
1	4	15,012,079	7,083,403	23,611,517	49.5	37.7	58.3
2	4	12,741,987	2,293,836	23,903,255	57.1	14.7	100.6
3	2	11,857,082	6,062,824	17,651,340	53.2	36.8	69.7
4	3	17,188,567	11,842,362	24,802,312	69.6	65.5	75.1
5	4	9,353,072	2,799,579	22,919,604	45.5	24.9	63.3
6	4	9,574,343	2,430,563	27,849,153	38.2	21.9	66.7
7	3	19,189,571	8,232,872	25,979,214	81.8	67.5	100.8
8	4	12,919,496	1,895,546	25,002,865	47.8	12.9	92.1
9	2	23,045,254	20,847,233	25,243,276	85.6	61.7	109.5
10	2	15,007,760	5,108,239	24,907,280	70.3	54.0	86.6
11	2	25,057,113	20,321,128	29,793,099	89.6	54.0	99.4
12	2	13,781,830	4,579,847	22,983,813	51.9	47.1	56.8
Total	36	14,584,344	1,895,546	29,793,099	58.5	12.9	109.5

*Genetic distance based on the genetic map in Pereira *et al* (2018).

Phenotyping of the IL population and QTL mapping

In 2019, a first phenotypic analysis of a subgroup of 17 ILs was performed (Table 1.2.S3). In summer 2020, the available collection of 35 ILs was properly characterized and phenotyped (Table 1.2.S1) and the population was genotyped using the complete set of SNPs with some modifications of SNPs that did not work properly (Table 1.2.S2). Finally, in 2021, six unfinished lines from 2020 were phenotyped again together with a newly developed line covering a gap on chromosome 5 (Table 1.2.S1).

Mottled rind is a characteristic of the parental line PS. Within the IL collection, only VED2.3 did not have mottled rind (Figure 1.2.4A). This QTL was mapped at the end of chromosome 2, at the interval 20.37 – 24.77 Mbp. A major gene, *Mt-2*, has been previously described close to this region (Pereira *et al*, 2018; Pereira *et al*, 2021; Périn *et al*, 1999), and a candidate gene *MELO3C026282.2*, encoding a protein essential for chloroplast development, has recently been reported as the causal gene of this QTL (Shen *et al*, 2021).

Both VED7.1 and VED7.2 had white immature rind compared to the green rind of PS and the rest of the ILs. This QTL was mapped to the interval 2.62 – 20.73 Mbp on chromosome 7 (Figure 1.2.4B). This region includes the major gene *Wi*, previously described as controlling this trait (Kubicki *et al*, 1962). This interval colocalized with the

region identified in two other populations of the same parental lines (Pereira *et al*, 2018; Pereira *et al*, 2021).

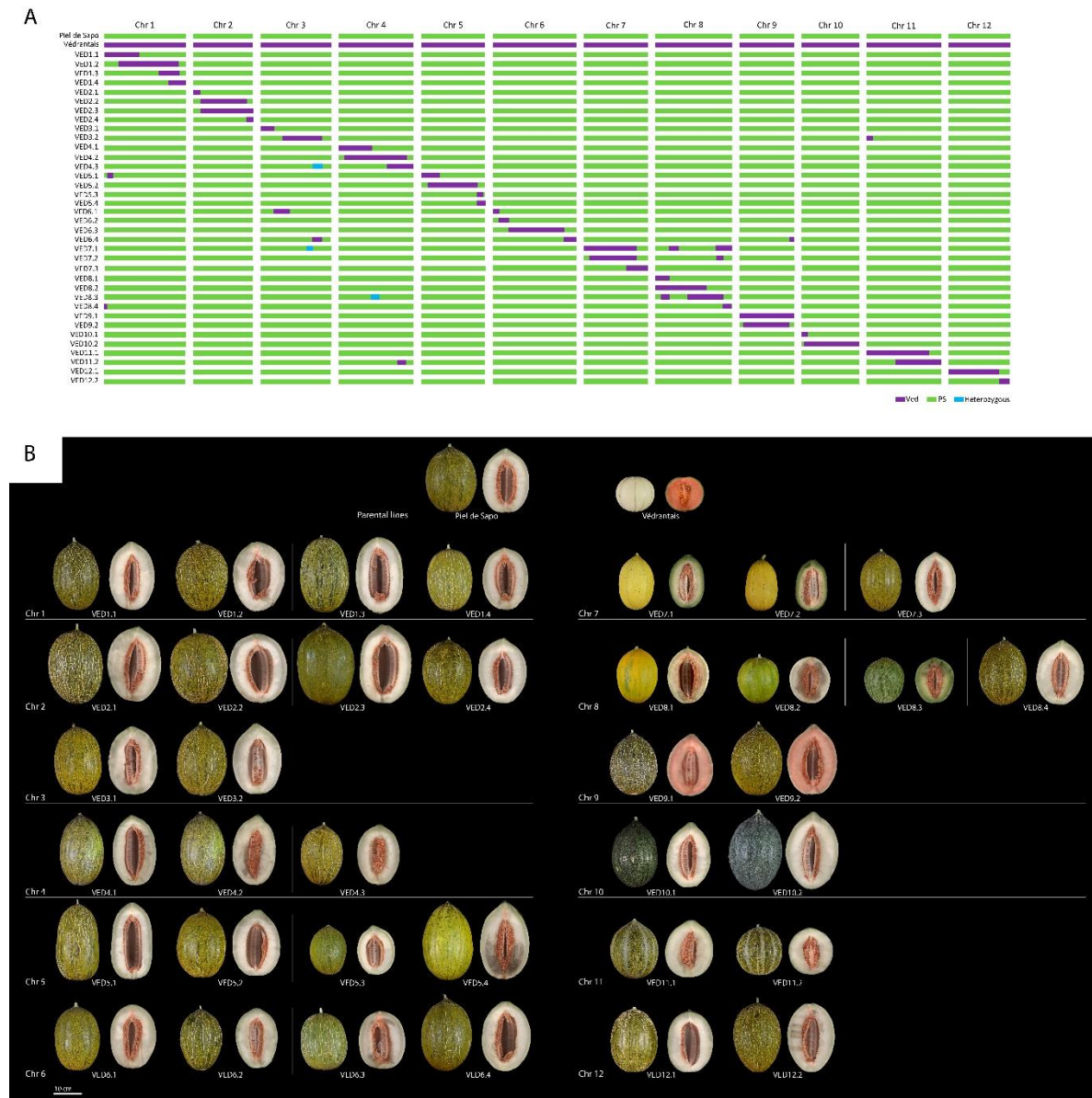


Figure 1.2.3. A) Graphical representation of the genotypes of the introgression lines and the two parental lines. B) External and internal appearance of each of the introgression lines and the parental lines.

Also related to the external color of the fruit, the entire population turned yellow during ripening (from around 25 DAP), except for VED10.1 and VED10.2, which remained dark green until harvest. This behavior has been related to flavonoid biosynthesis (Feder *et al*, 2015). This trait was mapped on chromosome 10, in the interval 1.76 – 5.11 Mbp (Figure 1.2.4C), colocalizing with the previously described causal gene *CmKBF* (Feder *et al*, 2015).

Chapter 1: Introgression Lines

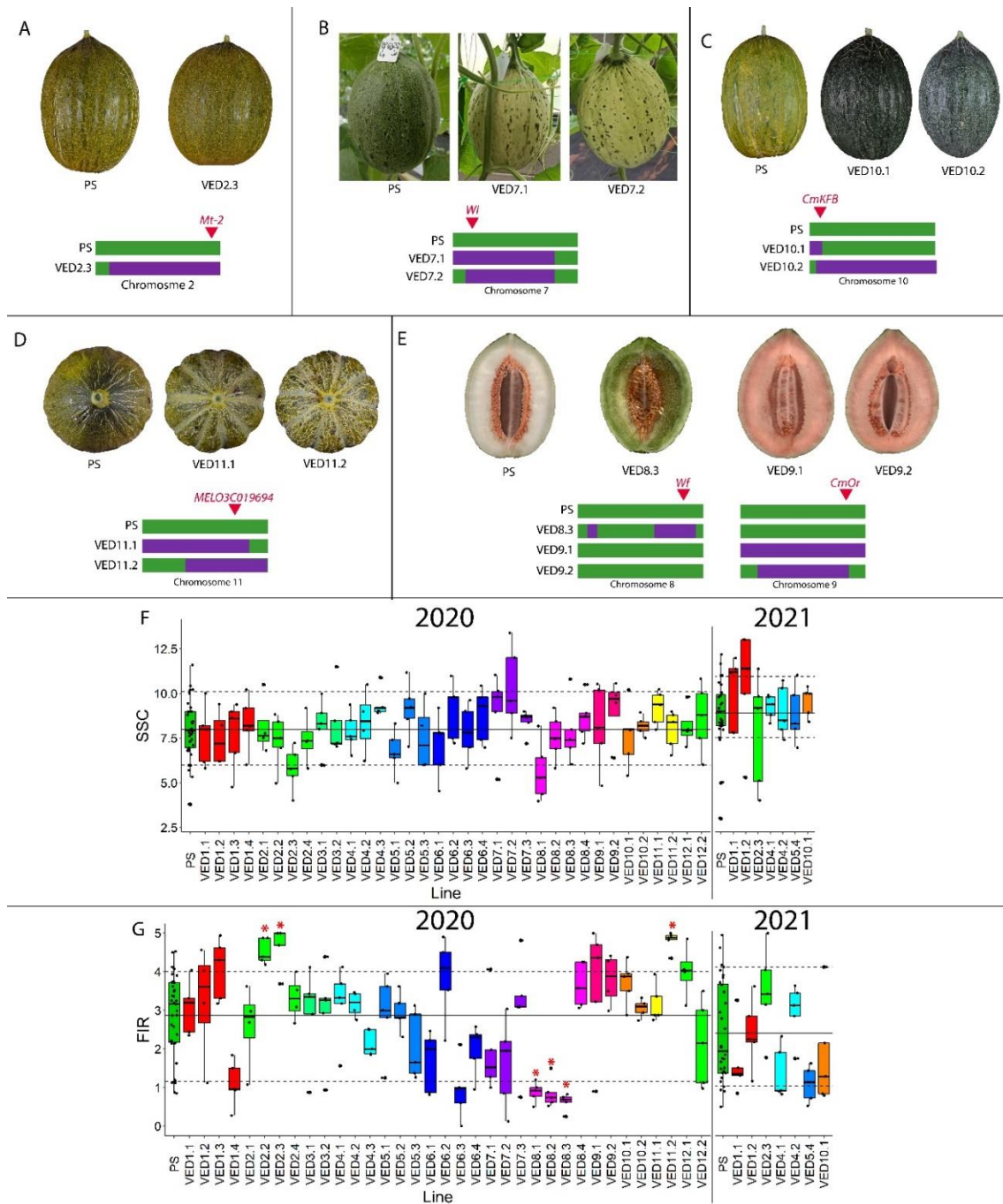


Figure 1.2.4. Fruit quality related phenotypes of the population in 2020 and 2021. **A)** Presence of spots in the rind, with a representation of chromosome 2 and the reported causal gene. **B)** Immature rind color, with a representation of chromosome 7 and the reported causal gene. **C)** Yellowing of the rind, with a representation of chromosome 10 and the reported causal gene. **D)** Presence of sutures in the rind, with a representation of chromosome 11 and the reported causal gene. **E)** Flesh color, with a representation of chromosomes 8 and 9 and the reported causal genes. **F)** Soluble solid content (SSC) in °Brix. **G)** Flesh firmness (FIR) in kg cm⁻². Red asterisk in F and G indicates p-value < 0.05.

Table 1.2.2. Summary of the QTLs mapped in the population for the quantitative traits. ^aThe color gradient corresponds to the percentage of reduction (red) or increase (blue) in the IL phenotype when compared to PS.

Trait	QTL	IL	Year	Chr.	Genomic interval (Mbp)	IL mean	PS Mean	% difference ^a	p-value
FW	<i>FWQW7.1</i>	VED7.1	2020	7	2.62 - 20.73	1090.4	2175.6	-50.0	0.0131
		VED7.2	2020			963.6		-55.7	0.0148
FP	<i>FPQW4.1</i>	VED4.3	2020	4	22.48 - 27.25	54.17	62.48	-13.30	0.0183
		VED4.4	2020			54.58		-12.64	0.0259
	<i>FPQW8.1</i>	VED8.1	2020	8	0 - 6.89	54.65		-12.53	0.0053
	<i>FPQW7.1</i>	VED7.1	2020	7	2.62 - 20.73	48.66		-22.12	0.0004
		VED7.2	2020			48.08		-23.05	0.0002
	<i>FPQW8.2</i>	VED8.3	2020	8	31.12 - 34.62	45.2		-27.66	0.0002
<i>FPQW11.1</i>	VED11.2	2020	11	29.79 - 34.46	54.89	-12.15	0.0071		
FA	<i>FAQW4.1</i>	VED4.1	2021	4	0 - 14.92	71.52	62.2	14.98	0.0216
		VED4.3	2020			191.39		-24.59	0.0336
	VED4.4	2020	193.09	-23.92	0.0053				
	<i>FAQW5.1</i>	VED5.3	2020		27.63 - 29.32	200.19		-21.12	0.0203
	<i>FAQW8.1</i>	VED8.1	2020	8	0 - 6.89	202.38		-20.26	0.0163
	<i>FAQW7.1</i>	VED7.1	2020	7	2.62 - 20.73	156.19		-38.46	0.0006
		VED7.2	2020			150.7		-40.62	0.0004
	<i>FAQW8.2</i>	VED8.3	2020	8	31.12 - 34.62	136.38		-46.26	0.0002
	<i>FAQW11.1</i>	VED11.2	2020	11	29.79 - 34.46	197.52		-22.17	0.0097
	FL	<i>FLQW5.1</i>	VED5.3	2020	5	27.63 - 29.32		18.3	21.66
VED6.3			2020	6			7.47 - 35.32	18.1	
<i>FLQW8.1</i>		VED8.1	2020	8	0 - 6.89	18.33	-15.37	0.0461	
<i>FLQW7.1</i>		VED7.1	2020	7	2.62 - 20.73	16.71	-22.85	0.0187	
		VED7.2	2020			16.76	-22.62	0.0167	
<i>FLQW8.2</i>		VED8.3	2020	8	31.12 - 34.62	15.02	-30.66	0.0131	
<i>FLQW11.1</i>	VED11.2	2020	11	29.79 - 34.46	17.04	-21.33	0.0171		
FWI	<i>FWIQW4.1</i>	VED4.4	2020	4	30.00 - 34.31	13.42	15.16	-11.48	0.0473
	<i>FWIQW7.1</i>	VED7.1	2020	7	2.62 - 20.73	12.07		-20.38	0.0171
		VED7.2	2020			11.41		-24.73	0.0130
<i>FWIQW8.1</i>	VED8.3	2020	8	31.12 - 34.62	11.45	-24.47	0.0179		
FS	<i>FSQW6.1</i>	VED6.3	2020	6	7.47 - 35.32	1.19	1.43	-16.78	0.0011
	<i>FSQW11.1</i>	VED11.2	2020	11	29.79 - 34.46	1.15		-19.58	<0.0001
FIR	<i>FIRQW2.1</i>	VED2.2	2020	2	3.16 - 24.77	4.52	2.86	58.04	0.0298
		VED2.3	2020			4.59		60.49	0.0475
	<i>FIRQW8.1</i>	VED8.1	2020	8	0 - 6.89	0.88		-69.23	0.0459
	<i>FIRQW8.2</i>	VED8.2	2020	8	6.89 - 14.98	0.85		-70.03	0.0334
	<i>FIRQW8.3</i>	VED8.3	2020	8	14.96 - 34.62	0.62		-78.32	0.0130
<i>FIRQW11.1</i>	VED11.2	2020	11	29.79 - 34.46	4.8	67.83	0.0171		
EARO	<i>EAROQW6.1</i>	VED6.3	2020	6	7.47 - 35.32	49.5	55.36	-10.59	0.0078
	<i>EAROQW8.1</i>	VED8.1	2020	8	0 - 6.89	40.89		-26.14	<0.0001
	<i>EAROQW8.2</i>	VED8.2	2020	8	6.89 - 14.98	46.1		-16.73	<0.0001
	<i>EAROQW8.3</i>	VED7.1	2020	8	31.12 - 34.62	47.17		-14.79	0.0063
		VED7.2	2020			46.8		-15.46	0.0007
	VED8.3	2020			46.9	-15.28	0.0001		

Chapter 1: Introgression Lines

EYELL	<i>EYELLQW1.1</i>	VED1.3	2020	1	29.95 - 34.47	29	26	0.12	0.0181	
		VED1.4	2020			31		0.19	0.0076	
	<i>EYELLQW8.1</i>	VED8.3	2020	8	25.00 - 29.53	37		0.42	0.0004	
	<i>EYELLQW10.1</i>	VED10.1	2020	10	1.76 - 5.11	43		0.65	0.0083	
		VED10.2	2020			54		1.08	0.0011	
	<i>EYELLQW10.1</i>	VED10.1	2021	10	1.76 - 5.11	56	27	1.07	0.0002	
EALF	<i>EALFQW6.1</i>	VED6.3	2020	6	7.47 - 35.32	49.38	55.81	-11.52	<0.0001	
	<i>EALFQW8.1</i>	VED8.1	2020	8	2.63 - 6.89	41.43		-25.76	<0.0001	
		VED8.3	2020			44.56		-20.16	<0.0001	
	<i>EALFQW8.2</i>	VED8.2	2020	8	6.89 - 14.98	47.33		-15.19	<0.0001	
	<i>EALFQW8.3</i>		VED7.1	2020				49.83	-10.71	0.0016
			VED7.2	2020	8	31.12 - 34.62		48.6	-12.92	0.0002
		VED8.3	2020			44.56	-20.16	<0.0001		
ABS	<i>ABSQW6.1</i>	VED6.3	2020	6	7.47 - 35.32	1	0.11	0.89	0.0031	
	<i>ABSQW8.1</i>	VED8.1	2020	8	2.63 - 6.89	1.11		1.00	0.0008	
		VED8.3	2020			2.44		2.33	<0.0001	
	<i>ABSQW8.2</i>	VED8.2	2020	8	6.89 - 14.98	1		0.89	<0.0001	
	<i>ABSQW8.3</i>		VED7.1	2020				0.83	0.72	0.0369
			VED7.2	2020	8	31.12 - 34.62		1.2	1.09	0.0049
		VED8.3	2020			2.44	2.33	<0.0001		
HAR	<i>HARQW6.1</i>	VED6.3	2020	6	7.47 - 35.32	52.75	55.97	-5.75	<0.0001	
	<i>HARQW8.1</i>	VED8.1	2020	8	2.63 - 6.89	46.43		-17.05	<0.0001	
		VED8.3	2020			47		-16.02	<0.0001	
	<i>HARQW8.2</i>	VED8.2	2020	8	6.89 - 14.98	52.63		-5.97	0.0002	
	<i>HARQW8.3</i>	VED7.2	2020	8	31.12 - 34.62	52		-7.09	<0.0001	
VED8.3		2020			47	-16.02	<0.0001			

Regarding the external aspect of the rind, VED11.1 and VED11.2 had sutures, while the rest of the population had smooth rind. This trait was mapped to a region on chromosome 11, in the interval 14.14 – 29.79 Mbp (Figure 1.2.4D). This region colocalized with QTLs reported in previous studies (Pereira *et al*, 2018; Pereira *et al*, 2021) and contains *MELO3C019694.2*, a gene that has been proposed as a candidate gene for this trait (Zhao *et al*, 2019).

As for the internal appearance of the melon, we detected three different flesh colors (Figure 1.2.3B). While PS and most of the population had white flesh, other ILs had orange or green flesh. The flesh of VED8.3 was green when mature, mapping this QTL to chromosome 8 at the interval 25.00 – 32.87 Mbp. This region colocalizes with previously reported QTLs controlling this trait (Monforte *et al*, 2004; Cuevas *et al*, 2009) and contains two genes that have been proposed as candidate genes for *Wf*, *MELO3C003069.2* (Galpaz *et al*, 2018) and *MELO3C003097.2* (Zhao *et al*, 2019). The

orange flesh of VED9.1 and VED9.2 was similar to the Ved parental line, and this QTL was mapped in the interval 1.62 – 22.56 Mbp on chromosome 9 (Figure 1.2.4E). The gene *CmOr* (*Gf*), located in our mapping interval on chromosome 9, has been reported as controlling the accumulation of carotenoids in melon flesh, provoking the orange coloration (Tzuri *et al*, 2015). The color of the flesh in melon is controlled by two genes under dominant epistasis, being *Gf* dominant over *Wf*. When *Gf* is not present (*gf/gf*), then white is dominant over green (Monforte *et al*, 2004; Cuevas *et al*, 2009; Galpaz *et al*, 2018). In our population, PS has the alleles *gf/gf Wf/Wf* and Ved is *Gf/Gf wf/wf*, so VED8.3 had the alleles *gf/gf wf/wf*, resulting in green flesh, and VED9.1 and VED9.2 had *Gf/Gf Wf/Wf*, being orange fleshed.

Focusing on the other quality traits, we did not detect any significant difference regarding SSC in the population, even though a certain level of variability was observed (Figure 1.2.4F) (Table 1.2.S1). We did, however, map several QTLs related with fruit firmness (Table 1.2.2). The flesh in three of the ILs on chromosome 8 (VED8.1, VED8.2 and VED8.3) was less firm compared to PS (*FIRQW8.1*, *FIRQW8.2* and *FIRQW8.3*), probably caused by their climacteric behavior (Table 1.2.S1). The effect of *FIRQW8.1* and *FIRQW8.3* was observed in our first phenotyping in 2019 (Table 1.2.S3). Three other ILs (VED2.2, VED2.3 and VED11.2) had an increase in firmness (*FIRQW2.1* and *FIRQW11.1*). In VED2.2 and VED2.3 this was significantly higher than in PS, as was the case for VED2.3 firmness in 2021, although this was not significant. *FIRQW2.1* was mapped to the interval 3.16 - 24.77 Mbp on chromosome 2. This QTL was also detected in the reciprocal IL population containing introgressions of PS in the background of Ved (Pereira *et al*, 2021), with the overlapping region of both populations being 3.16 – 16.42 Mbp. VED11.2 fruit flesh was significantly firmer than PS, with a QTL (*FIRQW11.1*) on chromosome 11 at the interval 29.79 – 34.46 Mbp (Figure 1.2.4G, Table 1.2.S1), that colocalized with a previously reported flesh firmness QTL (Nimmakalaya *et al*, 2016).

Fruit morphology traits

Fruit morphology is an important characteristic for fruit consumption, varying from the small round pocket melons to the elongated big-sized varieties. Our parental lines had significantly different morphologic phenotypes in both evaluated years (Figure 1.2.1D, E, F) and the IL population segregated for these traits.

On chromosome 7, there was a significant decrease of 50% of fruit weight in VED7.1 and VED7.2 between 2.62 - 20.73 Mbp, containing QTL *FWQW7.1* (Table 1.2.S1, Figure

(Pereira *et al*, 2021). Both QTLs on chromosome 4, *FPQW4.2* and *FPQP4.1* consistently affect fruit size producing bigger melons when the Ved allele is present.

On chromosome 8 we identified two different QTLs for fruit morphology, one in VED8.1 and the other one in VED8.3. The QTL in VED8.1 produced flatter melons (Table 1.2.S1, Figure 1.2.5) and significant changes in FP, FA and FL; it was mapped in the interval 0 - 6.89 Mb at the beginning of the chromosome. This QTL collocated with a previously known QTL for fruit shape in an F2 population with PS as one of the parents (Díaz *et al*, 2017). Although not affecting the shape of the fruit, a QTL for fruit weight has also been mapped in the same region producing smaller melons (Pereira *et al*, 2018). The second QTL, affecting VED8.3, was located at 31.12 - 34.62 Mbp (Table 1.2.S1, Figure 1.2.5), and affects fruit size (FA, FP, FL and FWI) producing smaller melons. This distal part of chromosome 8 has already been reported as one of the main controllers of melon fruit shape (Ramamurthy *et al*, 2015). Close to this region, a gene controlling fruit shape has been characterized, *CmOFP13* (Martínez-Martínez *et al*, 2022). Our QTL does not colocalize with this gene, so the causal gene for the QTL covered by VED8.3 must be a different one. Both QTLs on chromosome 8 affecting fruit shape were also detected in 2019 (Table 1.2.S3).

A QTL mapped on chromosome 5 in the interval 27.63 - 29.32 Mbp (*FLQW5.1*) decreased the fruit length, and consequently the fruit area (Table 1.2.S1, Figure 1.2.5). To our knowledge, this is the first time that a QTL controlling fruit morphology has been mapped to the distal part of chromosome 5 in melon (Table 1.2.2).

We detected two QTLs affecting fruit shape on chromosome 6 in the interval 7.47- 35.32 Mbp, *FSQV6.1* and *FLQV6.1*. VED6.3 produced rounded melons than PS, significantly decreasing FL and FS (Table 1.2.S1, Figure 1.2.5). An association between this region of chromosome 6 and fruit shape has been reported previously in two different RIL populations (Pereira *et al*, 2018; Oren *et al*, 2020) and a F2 population (Díaz *et al*, 2017). *FSQV6.1* was also detected in 2019 (Table 1.2.S3).

The last fruit morphology related QTL (*FSQV11.1*) was detected on chromosome 11 (29.79 - 34.46 Mb). VED11.2 produced rounder, and also smaller melons affecting FS, FL, FA and FP. This QTL has been previously reported in a RIL population funded by the same parents (Pereira *et al*, 2018).

The presence of QTLs affecting all traits related to fruit morphology, together with other QTLs affecting only some dimensions, brings out the complex genetic architecture of fruit shape and morphology in melon. Some unstable QTLs were detected, as the QTL affecting size in VED4.2 (*FPQW4.1* and *FAQW4.1*). This dependence on the environment in QTL mapping for morphological traits has been reported before in melon when using different populations, as RILs (Pereira *et al*, 2018) and ILs (Perpiñá *et al*, 2016), and also in tomato (Barrantes *et al*, 2016). Moreover, in tomato, genetic interactions among OFP, SUN and TRM5 genes have been described affecting cellular elongation, division, and thus fruit shape (Snouffer *et al*, 2020). This variable behavior, together with genetic interactions between QTLs, explains the difficulty in controlling those traits in the field.

Ripening traits

The analysis of ripening was centered around four related phenotypes: earliness of aroma production (EARO), earliness of abscission layer formation (EALF), harvest date (HAR) and the level of abscission (ABS). As PS is a non-climacteric melon, most of the fruits did not produce aroma nor an abscission layer, and were harvested at 55 DAP, around 20 days later than Ved, when they were fully ripe (Figure 1.2.1G, H, I). There were high levels of abscission only in the climacteric line Ved, and we detected segregation for these four traits in the IL population, obtaining climacteric ILs.

A QTL on chromosome 6 in the region 7.47- 35.32 Mbp affected all ripening related traits. VED6.3 produced climacteric melons, with aroma and abscission layer around 50 DAP (Table 1.2.S1, Figure 1.2.6). A QTL related to climacteric ripening has been previously reported in this region in two ILs populations. One was with the same parental lines, where the allele of PS delayed ripening in a Ved background (Pereira *et al*, 2021), and another in an IL population with the same recurrent parent PS, where the introgression of the alleles of PI 161375 induced a climacteric response (Moreno *et al*, 2008; Vegas *et al*, 2013). The causal gene for this QTL has been characterized and identified as the transcription factor *CmNAC-NOR* (Ríos *et al*, 2017; Liu *et al*, 2022).

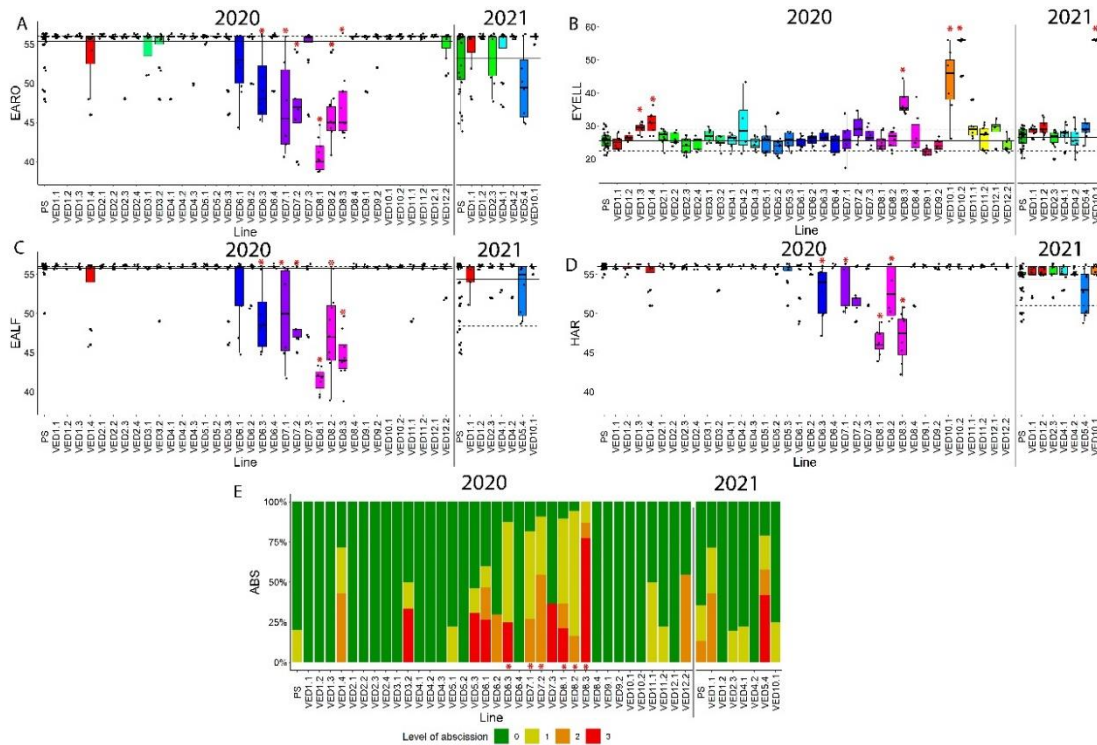


Figure 1.2.6. Ripening related phenotypes of the population in 2020 and 2021. Red asterisk indicates p -value < 0.05 . **A)** Earliness of aroma (EARO) in days after pollination (DAP). **B)** Earliness of yellowing of the rind (EYELL) in DAP. **C)** Abscission layer formation (EALF) in DAP. **D)** Harvest date (HAR) in DAP. **E)** Level of abscission (ABS).

The other chromosome governing climacteric ripening in this IL population was chromosome 8. VED8.1, VED8.2 and VED8.3 had climacteric behavior, similar in VED8.1 and VED8.2, while VED8.3 differed. The climacteric behavior of VED8.1 and VED8.2 was typical, with a sweet aroma and gradual abscission layer formed between 40 and 45 days (Table 1.2.2, Figure 1.2.6, Table 1.2.S1). We considered that there were two different QTLs, one in the interval 2.63 - 6.89 Mbp, and another in the interval 6.89 - 14.98 Mbp, due to the existence of a validated QTL in the second region that is not covered by VED8.1, *ETHQV8.1* (Pereira *et al*, 2020; Santo Domingo *et al*, 2022). These two QTLs were also identified in the 2019 season, affecting VED8.1 and VED8.2 (Table 1.2.S3). The first QTL, affecting VED8.1, has been previously reported in a RIL population (Oren *et al*, 2022). Affecting VED8.2, the second one was identified in a RIL population with the same parental lines as this study. Widely studied, it has been validated in several seasons both in climacteric and non-climacteric backgrounds (Pereira *et al*, 2020). There are three candidates which have been proposed as the causal gene: *MELO3C024516.2*, *MELO3C024518.2* and *MELO3C024520.2*, encoding a demethylase, a negative regulator of ethylene signaling and an ethylene responsive transcription factor,

respectively (Pereira *et al*, 2020). Two of these candidate genes, *MELO3C024516.2* and *MELO3C024518.2*, have been studied through CRISPR/Cas9 knock-out lines, suggesting an involvement of both genes in fruit ripening (Giordano *et al*, 2022). A third QTL was mapped on chromosome 8 in the interval 31.12 - 34.62 Mbp, affecting VED8.3, VED7.1 and VED7.2. Both VED7.1 and VED7.2 have undesired introgressions on chromosome 8, in the same region as VED8.3 (Figure 1.2.3A). These three lines behaved similarly, with abrupt climacteric ripening, extreme flesh softening and very quick abscission - one day after the aroma was detected the fruits abscised from the plant. This indicates a unique QTL in the three lines, located in the shared region. To our knowledge this QTL is newly reported, as this region was previously reported being involved in flesh firmness but no effect in the climacteric ripening had been described (Pereira *et al*, 2020; Nimmakalaya *et al*, 2016; Moreno *et al*, 2008).

The last phenotype related with fruit ripening is the earliness of yellowing of the rind (EYELL). This phenotype is caused by the biosynthesis of flavonoids (Feder *et al*, 2015). As shown in Figure 4, there is a major gene controlling this trait on chromosome 10, which we detected in 2020 and 2021 in VED10.1 and VED10.2 (Figure 1.2.6B). In the case of VED10.1 in 2020, the region where the gene is located was still segregating, explaining the high variance in this line (Figure 1.2.6B). Apart from these two ILs, we detected two more QTLs affecting the timing of the yellowing of the rind (Table 1.2.2, Figure 1.2.6B). One QTL on chromosome 1, *EYELLQW1.1*, delays this change, while the other *EYELLQW8.1* on chromosome 8, has a greater effect (Table 1.2.2). To our knowledge, these are two newly reported QTLs.

Materials and methods

Plant material and breeding scheme

Seedlings were planted and maintained for two weeks in biodegradable pots under controlled conditions at CRAG (Barcelona). After genotyping, selected plants were transported to a greenhouse in Caldes de Montbui (Barcelona) and grown in coconut fiber sacks in the spring and summer seasons. These plants were pruned weekly and manually pollinated. Only one fruit per plant was allowed to develop to optimize fruit growth and seed production.

The IL population was made from a cross between two elite commercial cultivars, “Védrantais” (Ved), a French variety belonging to the *cantalupensis* group, and “Piel de

Sapo” T111 (PS), a Spanish cultivar in the *inodorous* group. Pollen from male flowers of F1 plants was used to pollinate female flowers from the recurrent parent PS, obtaining BC1 seed, from which the pre-IL female flowers were generally pollinated with pollen from PS flowers. Seedlings of the BC1 progenies were screened and plants were selected following these criteria: 1) those having the complete genome of the donor parent at least twice; 2) the lines carrying the lowest possible number of introgressions in their genome; 3) the lines with the highest possible percentage of the recurrent parent genome. Chosen individuals were backcrossed again with PS to obtain BC2 progeny. Several cycles of genotyping and selection were subsequently carried out for the progenies, as shown in Figure 2. For lines with less than three introgressions, self-pollination was used to identify plants carrying a single introgression in homozygosity in their progeny. Depending on the line, three or four backcrosses followed by one or two self-pollinations were carried out in order to obtain the final IL. Lines with undesired introgressions were backcrossed and self-pollinated again.

In vitro plant culture

Selected plantlets were maintained *in vitro* for several months. Plants were introduced in sterile tubes with modified MS medium (Table 1.2.S4). Rooted plantlets were cut and transferred to fresh media every three weeks. Before the acclimatation, plants were multiplied to have enough replicates for the experiment. For the acclimatation, they were transferred to soil in a closed portable greenhouse for two days. Over the following five days, the greenhouse was opened slightly every day until they were totally acclimated.

DNA extraction and genotyping

Depending on the objective, we used two different DNA extraction procedures: CTAB protocol for high-throughput genotyping and long-term storage (Doyle, 1990) with some modifications (Pereira *et al*, 2018), and an alkaline-lysis protocol for single-SNP genotyping and short-term storage (Lu *et al*, 2020).

Progenies of BC1, BC1 and BC3 were genotyped using a set of 48 SNPs, called set 1 (Pereira *et al*, 2021). The selected plants from the BC2 and BC3 generations were then genotyped with an additional set of 48 SNPs (set 2) (Pereira *et al*, 2021). SNPs were designed from resequencing data of both parents (Sanseverino *et al*, 2015) and their positions relate to the melon reference genome v3.6.1. The progenies of BC3S1, BC4, BC3S2 and BC4S1, screened in 2017, were genotyped with the complete set of 96 SNPs (Pereira *et al*, 2021). Seedlings were genotyped with customized sets of SNPs using two

similar systems: i) KASPar SNP Genotyping System (KBiosciences, Herts, UK), and ii) PACE2.0 SNP Genotyping System (3CR Bioscience, Essex, UK). Primers were designed for both systems following the LGC Genomics protocol. High-throughput genotyping was using the Biomark HD genotyping system, based on the Fluidigm technology. In the last phases of genotyping, only SNPs within the known introgressions were genotyped. The same primers were used for qPCR in a LightCycler 480 Real-time PCR System, according to the technical instructions provided by the supplier (Roche Diagnostics, Spain).

The size of the introgressions was calculated following two assumptions: i) the haplotypes of the non-genotyped extremes of the chromosome are the same as the first or last genotyped SNP, and ii) the recombination point is in the intermediate position between two genotyped SNPs. The approximate genetic size of the introgressions was calculated using as a reference the Ved x PS RIL population genetic map (Pereira *et al*, 2018).

Experimental design and phenotyping

The major part of the IL population was phenotyped in the summer of 2020 in Caldes de Montbui (Barcelona), with additional phenotyping of some ILs in the summer of 2019 and 2021. During the three seasons, plants were randomly planted, with at least eight replicates per IL, and 40 PS plants. More than five fruits were characterized per line.

The phenotypes were organized in three categories of trait: fruit quality, fruit morphology and fruit ripening (Table 1.2.3).

Fruit quality traits were separated between qualitative and quantitative. Qualitative traits were evaluated visually: mottled rind (MOT), external color of the immature fruit (ECOL), yellowing of the rind (YELL), presence of sutures (SUT) and flesh color (FC) (Table 1.2.3). Two additional phenotypes related with quality were treated as quantitative: soluble solid content (SSC) and firmness of the flesh (FIR) (Table 1.2.3). SSC was measured at harvest with an optical refractometer from manually extracted juice from at least three 1 cm cylinders of fruit flesh. FIR was also measured at harvest using a penetrometer. Four measurements were recorded per sample, and the average value was used for the analysis.

Table 1.2.3. Different phenotypes analyzed in this study, divided in three groups.

Group	Phenotype	Units*	Symbol
Fruit quality traits	Mottled rind		MOT
	Yellowing of the rind		YELL
	Presence of sutures		SUT
	Flesh color		COL
	External color of immature fruit		ECOL
	Soluble solid content	° Brix	SSC
	Firmness	kg cm ⁻²	FIR
Fruit morphology traits	Fruit area	Cm ²	FA
	Fruit perimeter	cm	FP
	Fruit length	cm	FL
	Fruit width	cm	FWI
	Fruit shape		FS
	Fruit weight	g	FWI
Fruit ripening traits	Presence of aroma	DAP	EARO
	Earliness of yellowing of the rind	DAP	EYELL
	Abscission layer formation	DAP	EALF
	Level of abscission	**	ABS
	Harvest date	DAP	HAR

*DAP = Days after pollination

**Semi-quantitative trait, from 0 to 3.

For fruit morphology traits, scanned images of the fruits were analyzed with the Tomato analyzer software (Brewer *et al*, 2006), and five phenotypes were annotated: fruit area (FA), fruit perimeter (FP), fruit length (FL), fruit width (FW) and fruit shape (FS) estimated as the ratio of fruit length to fruit width. Fruit weight (FW) was also measured at harvest.

For fruit ripening traits, fruits were examined daily from 20 days after pollination (DAP) until harvest date. Presence of aroma (EARO) was recorded as the first day aroma could be detected by smelling the fruit. Abscission layer formation (EALF) was recorded as the first day the abscission layer was detected by visual inspection. The earliness of the yellowing of the rind (EYELL) was recorded as the first day the bottom of the fruit started to turn yellow. Abscission level (ABS) was treated as semi-quantitative using a scale from

0 to 3, 0 being the total absence of the layer and 3, complete abscission from the plant. Harvest date (HAR) was fixed using the following criteria: i) for fruits with no abscission layer formation, HAR was fixed at 56 DAP, ii) for fruits that completely abscised from the plant, HAR was the abscission day, and iii) for fruits with partial abscission layer formation, HAR was fixed at five days after the abscission layer was detected visually. EARO and EALF, if not present, were considered as the same day as HAR.

Data analysis

All the statistical analyses and graphical representations were obtained using the software R v3.5.3 with the RStudio v1.0.143 interface (R Core Team, 2020).

Data analyses were performed with a non-parametrical test, due to the non-normal distribution of data. Wilcoxon signed-rank test was used to compare each IL with PS, and then a Holm method was used to correct p-values for multiple comparisons. In general, significance was fixed at p-value <0.05.

Conclusion

The existence of different types of populations allows scientists and breeders to better understand the genetic architecture of complex traits, such as fruit morphology and fruit ripening, which can be applied in breeding programs. With the development of this IL population, we have validated known QTLs and discovered new ones implicated in a diverse set of traits that can be useful for melon breeders. IL populations are a powerful tool to fine-map QTLs and identify candidate genes as a previous step to develop new varieties using marker-assisted selection to introgress natural alleles in elite cultivars, or gene-editing to generate new alleles.

Supplementary material

Table 1.2.S4. Composition of modified MS medium used for in vitro culture.

Compound	Concentration
DUCHEFA M 0.231 MS + B5 vitamin	4.41 g/L
CuSO ₄ .5H ₂ O	1 mg/L
2-(N-Morpholino)ethanesulfonic acid, 4-Morpholineethanesulfonic acid monohydrate (MES)	0.6 g/L
Sucrose	30 g/L
Agar	8 g/L
pH	5.8

Digital supplementary material

Table 1.2.S1. Phenotypical data of the analyzed quantitative traits in the whole studied population.

Table 1.2.S2. Genotypes of the IL population.

Table 1.2.S3. Quantitative phenotypes of the Introgression Lines evaluated in 2019.ç

Acknowledgements

The authors thank Fuensanta García and Àngel Montejo for technical assistance in field and lab operations and Martí Bernardo for assistance in data analyses.

Author's contributions

MP and JG-M conceived and designed the research. MSD, CM, LP, JA and LV performed the experiments and data analyses. AMM-H contributed to the management of the plant material. MSD wrote the original draft. CM, LP, MP and JG-M reviewed and edited the manuscript. All authors read and approved the manuscript.

References

- Argyris, J.M.; Díaz, A.; Ruggieri, V.; Fernández, M.; Jahrmann, T.; Gibon, Y.; Picó, B.; Martín-Hernández, A.M.; Monforte, A.J.; Garcia-Mas, J. QTL Analyses in Multiple Populations Employed for the Fine Mapping and Identification of Candidate Genes at a Locus Affecting Sugar Accumulation in Melon (*Cucumis Melo* L.). *Frontiers in Plant Science* **2017**, *8*.
- Babar, A.D.; Zaka, A.; Naveed, S.A.; Ahmad, N.; Aslam, K.; Asif, M.; Maqsood, U.; Vera Cruz, C.M.; Arif, M. Development of Basmati Lines by the Introgression of Three Bacterial Blight Resistant Genes through Marker-Assisted Breeding. *Euphytica* **2022**, *218*, 59, doi:[10.1007/s10681-022-03013-z](https://doi.org/10.1007/s10681-022-03013-z).
- Balakrishnan, D.; Surapaneni, M.; Mesapogu, S.; Neelamraju, S. Development and Use of Chromosome Segment Substitution Lines as a Genetic Resource for Crop Improvement. *Theor Appl Genet* **2019**, *132*, 1–25, doi:[10.1007/s00122-018-3219-y](https://doi.org/10.1007/s00122-018-3219-y).
- Barrantes, W.; López-Casado, G.; García-Martínez, S.; Alonso, A.; Rubio, F.; Ruiz, J.J.; Fernández-Muñoz, R.; Granell, A.; Monforte, A.J. Exploring New Alleles Involved in Tomato Fruit Quality in an Introgression Line Library of *Solanum pimpinellifolium*. *Frontiers in Plant Science* **2016**, *7*.
- Bhoite, R.; Onyemaobi, I.; Si, P.; Siddique, K.H.M.; Yan, G. Identification and Validation of QTL and Their Associated Genes for Pre-Emergent Metribuzin Tolerance in Hexaploid Wheat (*Triticum Aestivum* L.). *BMC Genetics* **2018**, *19*, 102, doi:[10.1186/s12863-018-0690-z](https://doi.org/10.1186/s12863-018-0690-z).
- Brewer, M.T.; Lang, L.; Fujimura, K.; Dujmovic, N.; Gray, S.; van der Knaap, E. Development of a Controlled Vocabulary and Software Application to Analyze Fruit Shape Variation in Tomato and Other Plant Species. *Plant Physiology* **2006**, *141*, 15–25, doi:[10.1104/pp.106.077867](https://doi.org/10.1104/pp.106.077867).
- Cai, Z.; Cheng, Y.; Xian, P.; Lin, R.; Xia, Q.; He, X.; Liang, Q.; Lian, T.; Ma, Q.; Nian, H. Fine-Mapping QTLs and the Validation of Candidate Genes for Aluminum Tolerance Using a High-Density Genetic Map. *Plant Soil* **2019**, *444*, 119–137, doi:[10.1007/s11104-019-04261-0](https://doi.org/10.1007/s11104-019-04261-0).

- Castro, G.; Perpiñá, G.; Monforte, A.J.; Picó, B.; Esteras, C. New Melon Introgression Lines in a Piel de Sapo Genetic Background with Desirable Agronomical Traits from Dudaim Melons. *Euphytica* **2019**, *215*, 169, doi:[10.1007/s10681-019-2479-1](https://doi.org/10.1007/s10681-019-2479-1).
- Clark, C.B.; Wang, W.; Wang, Y.; Fear, G.J.; Wen, Z.; Wang, D.; Ren, B.; Ma, J. Identification and Molecular Mapping of a Major Quantitative Trait Locus Underlying Branch Angle in Soybean. *Theor Appl Genet* **2022**, *135*, 777–784, doi:[10.1007/s00122-021-03995-9](https://doi.org/10.1007/s00122-021-03995-9).
- Cuevas, H.E.; Staub, J.E.; Simon, P.W.; Zalapa, J.E. A Consensus Linkage Map Identifies Genomic Regions Controlling Fruit Maturity and Beta-Carotene-Associated Flesh Color in Melon (*Cucumis Melo* L.). *Theor Appl Genet* **2009**, *119*, 741–756, doi:[10.1007/s00122-009-1085-3](https://doi.org/10.1007/s00122-009-1085-3).
- Dai, D.; Zeng, S.; Wang, L.; Li, J.; Ji, P.; Liu, H.; Sheng, Y. Identification of Fruit Firmness QTL Ff2.1 by SLAF-BSA and QTL Mapping in Melon. *Euphytica* **2022**, *218*, 52, doi:[10.1007/s10681-022-02999-w](https://doi.org/10.1007/s10681-022-02999-w).
- Díaz, A.; Martín-Hernández, A.M.; Dolcet-Sanjuan, R.; Garcés-Claver, A.; Álvarez, J.M.; Garcia-Mas, J.; Picó, B.; Monforte, A.J. Quantitative Trait Loci Analysis of Melon (*Cucumis Melo* L.) Domestication-Related Traits. *Theor Appl Genet* **2017**, *130*, 1837–1856, doi:[10.1007/s00122-017-2928-y](https://doi.org/10.1007/s00122-017-2928-y).
- Doyle, J. J. Isolation of plant DNA from fresh tissue. *Focus* **1990**, *12*, 13–15.
- Eduardo, I.; Arús, P.; Monforte, A.J.; Obando, J.; Fernández-Trujillo, J.P.; Martínez, J.A.; Alarcón, A.L.; Álvarez, J.M.; Knaap, E. van der Estimating the Genetic Architecture of Fruit Quality Traits in Melon Using a Genomic Library of Near Isogenic Lines. *Journal of the American Society for Horticultural Science* **2007**, *132*, 80–89, doi:[10.21273/JASHS.132.1.80](https://doi.org/10.21273/JASHS.132.1.80).
- Endelman, J.B.; Jansky, S.H. Genetic Mapping with an Inbred Line-Derived F2 Population in Potato. *Theor Appl Genet* **2016**, *129*, 935–943, doi:[10.1007/s00122-016-2673-7](https://doi.org/10.1007/s00122-016-2673-7).
- Eshed, Y.; Zamir, D. An Introgression Line Population of *Lycopersicon Pennellii* in the Cultivated Tomato Enables the Identification and Fine Mapping of Yield-

- Associated QTL. *Genetics* **1995**, *141*, 1147–1162, doi:[10.1093/genetics/141.3.1147](https://doi.org/10.1093/genetics/141.3.1147).
- Essafi, A.; Díaz-Pendón, J.A.; Moriones, E.; Monforte, A.J.; Garcia-Mas, J.; Martín-Hernández, A.M. Dissection of the Oligogenic Resistance to Cucumber Mosaic Virus in the Melon Accession PI 161375. *Theor Appl Genet* **2009**, *118*, 275–284, doi:[10.1007/s00122-008-0897-x](https://doi.org/10.1007/s00122-008-0897-x).
- Feder, A.; Burger, J.; Gao, S.; Lewinsohn, E.; Katzir, N.; Schaffer, A.A.; Meir, A.; Davidovich-Rikanati, R.; Portnoy, V.; Gal-On, A.; *et al* A Kelch Domain-Containing F-Box Coding Gene Negatively Regulates Flavonoid Accumulation in Muskmelon. *Plant Physiology* **2015**, *169*, 1714–1726, doi:[10.1104/pp.15.01008](https://doi.org/10.1104/pp.15.01008).
- Fujita, D.; Tagle, A.G.; Koide, Y.; Simon, E.V.; Fukuta, Y.; Ishimaru, T.; Kobayashi, N. Characterization of QTLs for Grain Weight from New Plant Type Rice Cultivars through the Development of Near-Isogenic Lines with an IR 64 Background. *Euphytica* **2022**, *218*, 50, doi:[10.1007/s10681-022-03008-w](https://doi.org/10.1007/s10681-022-03008-w).
- Fukino, N.; Kuniyama, M.; Matsumoto, S. Characterization of Recombinant Inbred Lines Derived from Crosses in Melon (*Cucumis Melo* L.), ‘PMAR No. 5’ × ‘Harukei No. 3.’ *Breeding Science* **2004**, *54*, 141–145, doi:[10.1270/jsbbs.54.141](https://doi.org/10.1270/jsbbs.54.141).
- Galpaz, N.; Gonda, I.; Shem-Tov, D.; Barad, O.; Tzuri, G.; Lev, S.; Fei, Z.; Xu, Y.; Mao, L.; Jiao, C.; *et al* Deciphering Genetic Factors That Determine Melon Fruit-Quality Traits Using RNA-Seq-Based High-Resolution QTL and EQTL Mapping. *The Plant Journal* **2018**, *94*, 169–191, doi:[10.1111/tbj.13838](https://doi.org/10.1111/tbj.13838).
- Giner, A.; Pascual, L.; Bourgeois, M.; Gyetvai, G.; Rios, P.; Picó, B.; Troadec, C.; Bendahmane, A.; Garcia-Mas, J.; Martín-Hernández, A.M. A Mutation in the Melon Vacuolar Protein Sorting 41prevents Systemic Infection of Cucumber Mosaic Virus. *Sci Rep* **2017**, *7*, 10471, doi:[10.1038/s41598-017-10783-3](https://doi.org/10.1038/s41598-017-10783-3).
- Giordano, A.; Santo Domingo, M.; Quadrana, L.; Pujol, M.; Martín-Hernández, A.M.; Garcia-Mas, J. CRISPR/Cas9 Gene Editing Uncovers the Roles of CONSTITUTIVE TRIPLE RESPONSE 1 and REPRESSOR OF SILENCING 1 in Melon Fruit Ripening and Epigenetic Regulation. *Journal of Experimental Botany* **2022**, *73*, 4022–4033, doi:[10.1093/jxb/erac148](https://doi.org/10.1093/jxb/erac148).

- Gur, A.; Tzuri, G.; Meir, A.; Sa'ar, U.; Portnoy, V.; Katzir, N.; Schaffer, A.A.; Li, L.; Burger, J.; Tadmor, Y. Genome-Wide Linkage-Disequilibrium Mapping to the Candidate Gene Level in Melon (*Cucumis Melo*). *Sci Rep* **2017**, *7*, 9770, doi:[10.1038/s41598-017-09987-4](https://doi.org/10.1038/s41598-017-09987-4).
- Harel-Beja, R.; Sherman, A.; Rubinstein, M.; Eshed, R.; Bar-Ya'akov, I.; Trainin, T.; Ophir, R.; Holland, D. A Novel Genetic Map of Pomegranate Based on Transcript Markers Enriched with QTLs for Fruit Quality Traits. *Tree Genetics & Genomes* **2015**, *11*, 109, doi:[10.1007/s11295-015-0936-0](https://doi.org/10.1007/s11295-015-0936-0).
- Harel-Beja, R.; Tzuri, G.; Portnoy, V.; Lotan-Pompan, M.; Lev, S.; Cohen, S.; Dai, N.; Yeselson, L.; Meir, A.; Libhaber, S.E.; *et al* A Genetic Map of Melon Highly Enriched with Fruit Quality QTLs and EST Markers, Including Sugar and Carotenoid Metabolism Genes. *Theor Appl Genet* **2010**, *121*, 511–533, doi:[10.1007/s00122-010-1327-4](https://doi.org/10.1007/s00122-010-1327-4).
- Kuang, L.; Ahmad, N.; Su, B.; Huang, L.; Li, K.; Wang, H.; Wang, X.; Dun, X. Discovery of Genomic Regions and Candidate Genes Controlling Root Development Using a Recombinant Inbred Line Population in Rapeseed (*Brassica Napus L.*). *International Journal of Molecular Sciences* **2022**, *23*, 4781, doi:[10.3390/ijms23094781](https://doi.org/10.3390/ijms23094781).
- Kubicki, B. Inheritance of some characters in muskmelons (*Cucumis melo*). *Genet Pol* **1962**, *265–274*.
- Lavaud, C.; Baviere, M.; Le Roy, G.; Hervé, M.R.; Moussart, A.; Delourme, R.; Pilet-Nayel, M.-L. Single and Multiple Resistance QTL Delay Symptom Appearance and Slow down Root Colonization by *Aphanomyces Euteiches* in Pea near Isogenic Lines. *BMC Plant Biology* **2016**, *16*, 166, doi:[10.1186/s12870-016-0822-4](https://doi.org/10.1186/s12870-016-0822-4).
- Leida, C.; Moser, C.; Esteras, C.; Sulpice, R.; Lunn, J.E.; de Langen, F.; Monforte, A.J.; Picó, B. Variability of Candidate Genes, Genetic Structure and Association with Sugar Accumulation and Climacteric Behavior in a Broad Germplasm Collection of Melon (*Cucumis Melo L.*). *BMC Genetics* **2015**, *16*, 28, doi:[10.1186/s12863-015-0183-2](https://doi.org/10.1186/s12863-015-0183-2).

- Li, J.X.; Yu, S.B.; Xu, C.G.; Tan, Y.F.; Gao, Y.J.; Li, X.H.; Zhang, Q. Analyzing Quantitative Trait Loci for Yield Using a Vegetatively Replicated F₂ Population from a Cross between the Parents of an Elite Rice Hybrid. *Theor Appl Genet* **2000**, *101*, 248–254, doi:[10.1007/s001220051476](https://doi.org/10.1007/s001220051476).
- Liu, B.; Santo Domingo, M.; Mayobre, C.; Martín-Hernández, A.M.; Pujol, M.; Garcia-Mas, J. Knock-Out of CmNAC-NOR Affects Melon Climacteric Fruit Ripening. *Frontiers in Plant Science* **2022**, *13*.
- Lu, J.; Hou, J.; Ouyang, Y.; Luo, H.; Zhao, J.; Mao, C.; Han, M.; Wang, L.; Xiao, J.; Yang, Y.; *et al* A Direct PCR-Based SNP Marker-Assisted Selection System (D-MAS) for Different Crops. *Mol Breeding* **2020**, *40*, 9, doi:[10.1007/s11032-019-1091-3](https://doi.org/10.1007/s11032-019-1091-3).
- Martínez-Martínez, C.; Gonzalo, M.J.; Sipowicz, P.; Campos, M.; Martínez-Fernández, I.; Leida, C.; Zouine, M.; Alexiou, K.G.; Garcia-Mas, J.; Gómez, M.D.; *et al* A Cryptic Variation in a Member of the Ovate Family Proteins Is Underlying the Melon Fruit Shape QTL Fsqs8.1. *Theor Appl Genet* **2022**, *135*, 785–801, doi:[10.1007/s00122-021-03998-6](https://doi.org/10.1007/s00122-021-03998-6).
- Monforte, A.J.; Oliver, M.; Gonzalo, M.J.; Alvarez, J.M.; Dolcet-Sanjuan, R.; Arús, P. Identification of Quantitative Trait Loci Involved in Fruit Quality Traits in Melon (*Cucumis Melo* L.). *Theor Appl Genet* **2004**, *108*, 750–758, doi:[10.1007/s00122-003-1483-x](https://doi.org/10.1007/s00122-003-1483-x).
- Moreno, E.; Obando, J.M.; Dos-Santos, N.; Fernández-Trujillo, J.P.; Monforte, A.J.; Garcia-Mas, J. Candidate Genes and QTLs for Fruit Ripening and Softening in Melon. *Theor Appl Genet* **2008**, *116*, 589–602, doi:[10.1007/s00122-007-0694-y](https://doi.org/10.1007/s00122-007-0694-y).
- Nimmakayala, P.; Tomason, Y.R.; Abburi, V.L.; Alvarado, A.; Saminathan, T.; Vajja, V.G.; Salazar, G.; Panicker, G.K.; Levi, A.; Wechter, W.P.; *et al* Genome-Wide Differentiation of Various Melon Horticultural Groups for Use in GWAS for Fruit Firmness and Construction of a High Resolution Genetic Map. *Frontiers in Plant Science* **2016**, *7*.
- Oren, E.; Tzuri, G.; Dafna, A.; Meir, A.; Kumar, R.; Katzir, N.; Elkind, Y.; Freilich, S.; Schaffer, A.A.; Tadmor, Y.; *et al* High-Density NGS-Based Map Construction

- and Genetic Dissection of Fruit Shape and Rind Netting in Cucumis Melo. *Theor Appl Genet* **2020**, *133*, 1927–1945, doi:[10.1007/s00122-020-03567-3](https://doi.org/10.1007/s00122-020-03567-3).
- Oren, E.; Tzuri, G.; Dafna, A.; Rees, E.R.; Song, B.; Freilich, S.; Elkind, Y.; Isaacson, T.; Schaffer, A.A.; Tadmor, Y.; *et al* QTL Mapping and Genomic Analyses of Earliness and Fruit Ripening Traits in a Melon Recombinant Inbred Lines Population Supported by de Novo Assembly of Their Parental Genomes. *Horticulture Research* **2022**, *9*, uhab081, doi:[10.1093/hr/uhab081](https://doi.org/10.1093/hr/uhab081).
- Pereira, L.; Ruggieri, V.; Pérez, S.; Alexiou, K.G.; Fernández, M.; Jahrmann, T.; Pujol, M.; Garcia-Mas, J. QTL Mapping of Melon Fruit Quality Traits Using a High-Density GBS-Based Genetic Map. *BMC Plant Biology* **2018**, *18*, 324, doi:[10.1186/s12870-018-1537-5](https://doi.org/10.1186/s12870-018-1537-5).
- Pereira, L.; Santo Domingo, M.; Argyris, J.; Mayobre, C.; Valverde, L.; Martín-Hernández, A.M.; Pujol, M.; Garcia-Mas, J. A Novel Introgression Line Collection to Unravel the Genetics of Climacteric Ripening and Fruit Quality in Melon. *Sci Rep* **2021**, *11*, 11364, doi:[10.1038/s41598-021-90783-6](https://doi.org/10.1038/s41598-021-90783-6).
- Pereira, L.; Santo Domingo, M.; Ruggieri, V.; Argyris, J.; Phillips, M.A.; Zhao, G.; Lian, Q.; Xu, Y.; He, Y.; Huang, S.; *et al* Genetic Dissection of Climacteric Fruit Ripening in a Melon Population Segregating for Ripening Behavior. *Horticulture Research* **2020**, *7*, 187, doi:[10.1038/s41438-020-00411-z](https://doi.org/10.1038/s41438-020-00411-z).
- Périn, C., Dogimont, N., Giovinnazo, D., Besombes, D., Guitton, L. *et al* Genetic Control and Linkages of Some Fruit Characters in Melon – The Cucurbit Genetics Cooperative (CGC), **1999**, Available at: <https://cucurbit.info/1999/07/genetic-control-and-linkages-of-some-fruit-characters-in-melon/>
- Perpiñá, G.; Cebolla-Cornejo, J.; Esteras, C.; Monforte, A.J.; Picó, B. ‘MAK-10’: A Long Shelf-Life Charentais Breeding Line Developed by Introgression of a Genomic Region from Makuwa Melon. *HortScience* **2017**, *52*, 1633–1638, doi:[10.21273/HORTSCI12068-17](https://doi.org/10.21273/HORTSCI12068-17).
- Perpiñá, G.; Esteras, C.; Gibon, Y.; Monforte, A.J.; Picó, B. A New Genomic Library of Melon Introgression Lines in a Cantaloupe Genetic Background for Dissecting Desirable Agronomical Traits. *BMC Plant Biology* **2016**, *16*, 154, doi:[10.1186/s12870-016-0842-0](https://doi.org/10.1186/s12870-016-0842-0).

- R Core Team. R: A language and environment for statistical computing. R Foundation for Statistical Computing **2020**, Vienna, Austria. URL <https://www.R-project.org/>.
- Ramamurthy, R.K.; Waters, B.M. Identification of Fruit Quality and Morphology QTLs in Melon (*Cucumis Melo*) Using a Population Derived from *Flexuosus* and *Cantalupensis* Botanical Groups. *Euphytica* **2015**, *204*, 163–177, doi:[10.1007/s10681-015-1361-z](https://doi.org/10.1007/s10681-015-1361-z).
- Ríos, P.; Argyris, J.; Vegas, J.; Leida, C.; Kenigswald, M.; Tzuri, G.; Troadec, C.; Bendahmane, A.; Katzir, N.; Picó, B.; *et al* ETHQV6.3 Is Involved in Melon Climacteric Fruit Ripening and Is Encoded by a NAC Domain Transcription Factor. *The Plant Journal* **2017**, *91*, 671–683, doi:[10.1111/tpj.13596](https://doi.org/10.1111/tpj.13596).
- Sanseverino, W.; Hénaff, E.; Vives, C.; Pinosio, S.; Burgos-Paz, W.; Morgante, M.; Ramos-Onsins, S.E.; Garcia-Mas, J.; Casacuberta, J.M. Transposon Insertions, Structural Variations, and SNPs Contribute to the Evolution of the Melon Genome. *Molecular Biology and Evolution* **2015**, *32*, 2760–2774, doi:[10.1093/molbev/msv152](https://doi.org/10.1093/molbev/msv152).
- Santo Domingo, M.; Areco, L.; Mayobre, C.; Valverde, L.; Martín-Hernández, A.M.; Pujol, M.; Garcia-Mas, J. Modulating Climacteric Intensity in Melon through QTL Stacking. *Horticulture Research* **2022**, *9*, uhac131, doi:[10.1093/hr/uhac131](https://doi.org/10.1093/hr/uhac131).
- Shen, J.; Xu, X.; Zhang, Y.; Niu, X.; Shou, W. Genetic Mapping and Identification of the Candidate Genes for Mottled Rind in *Cucumis Melo* L. *Frontiers in Plant Science* **2021**, *12*.
- Snouffer, A.; Kraus, C.; van der Knaap, E. The Shape of Things to Come: Ovate Family Proteins Regulate Plant Organ Shape. *Current Opinion in Plant Biology* **2020**, *53*, 98–105, doi:[10.1016/j.pbi.2019.10.005](https://doi.org/10.1016/j.pbi.2019.10.005).
- Szalma, S.J.; Hostert, B.M.; LeDeaux, J.R.; Stuber, C.W.; Holland, J.B. QTL Mapping with Near-Isogenic Lines in Maize. *Theor Appl Genet* **2007**, *114*, 1211–1228, doi:[10.1007/s00122-007-0512-6](https://doi.org/10.1007/s00122-007-0512-6).
- Tzuri, G.; Zhou, X.; Chayut, N.; Yuan, H.; Portnoy, V.; Meir, A.; Sa'ar, U.; Baumkoler, F.; Mazourek, M.; Lewinsohn, E.; *et al* A 'Golden' SNP in CmOr Governs the

- Fruit Flesh Color of Melon (*Cucumis Melo*). *The Plant Journal* **2015**, *82*, 267–279, doi:[10.1111/tpj.12814](https://doi.org/10.1111/tpj.12814).
- Vegas, J.; Garcia-Mas, J.; Monforte, A.J. Interaction between QTLs Induces an Advance in Ethylene Biosynthesis during Melon Fruit Ripening. *Theor Appl Genet* **2013**, *126*, 1531–1544, doi:[10.1007/s00122-013-2071-3](https://doi.org/10.1007/s00122-013-2071-3).
- Wang, L.; Cheng, Y.; Ma, Q.; Mu, Y.; Huang, Z.; Xia, Q.; Zhang, G.; Nian, H. QTL Fine-Mapping of Soybean (*Glycine Max L.*) Leaf Type Associated Traits in Two RILs Populations. *BMC Genomics* **2019**, *20*, 260, doi:[10.1186/s12864-019-5610-8](https://doi.org/10.1186/s12864-019-5610-8).
- Wang, R.X.; Hai, L.; Zhang, X.Y.; You, G.X.; Yan, C.S.; Xiao, S.H. QTL Mapping for Grain Filling Rate and Yield-Related Traits in RILs of the Chinese Winter Wheat Population Heshangmai × Yu8679. *Theor Appl Genet* **2009**, *118*, 313–325, doi:[10.1007/s00122-008-0901-5](https://doi.org/10.1007/s00122-008-0901-5).
- Xu, J.; Zhao, Q.; Du, P.; Xu, C.; Wang, B.; Feng, Q.; Liu, Q.; Tang, S.; Gu, M.; Han, B.; *et al* Developing High Throughput Genotyped Chromosome Segment Substitution Lines Based on Population Whole-Genome Re-Sequencing in Rice (*Oryza Sativa L.*). *BMC Genomics* **2010**, *11*, 656, doi:[10.1186/1471-2164-11-656](https://doi.org/10.1186/1471-2164-11-656).
- Zhang, H.; Zang, J.; Huo, Y.; Zhang, Z.; Chen, H.; Chen, X.; Liu, J. Identification of the Potential Genes Regulating Seed Germination Speed in Maize. *Plants* **2022**, *11*, 556, doi:[10.3390/plants11040556](https://doi.org/10.3390/plants11040556).
- Zhao, G.; Lian, Q.; Zhang, Z.; Fu, Q.; He, Y.; Ma, S.; Ruggieri, V.; Monforte, A.J.; Wang, P.; Julca, I.; *et al* A Comprehensive Genome Variation Map of Melon Identifies Multiple Domestication Events and Loci Influencing Agronomic Traits. *Nat Genet* **2019**, *51*, 1607–1615, doi:[10.1038/s41588-019-0522-8](https://doi.org/10.1038/s41588-019-0522-8).
- Zhaoming, Q.; Xiaoying, Z.; Huidong, Q.; Dawei, X.; Xue, H.; Hongwei, J.; Zhengong, Y.; Zhanguo, Z.; Jinzhu, Z.; Rongsheng, Z.; *et al* Identification and Validation of Major QTLs and Epistatic Interactions for Seed Oil Content in Soybeans under Multiple Environments Based on a High-Density Map. *Euphytica* **2017**, *213*, 162, doi:[10.1007/s10681-017-1952-y](https://doi.org/10.1007/s10681-017-1952-y).

Chapter 2

Ethylene-responsive transcription factor 024, identified as the causal gene of *ETHQV8.1*, acts as a key regulator of melon fruit ripening

Ethylene-responsive transcription factor 024, identified as the causal gene of *ETHQV8.1*, acts as a key regulator of melon fruit ripening.

Miguel Santo Domingo¹, Luis Orduña², David Navarro², Carlos Mayobre¹, Antonio Santiago², Laura Valverde¹, José Tomás Matus², Marta Pujol^{1,3} and Jordi García-Mas^{1,3}.

¹Centre for Research in Agricultural Genomics (CRAG) CSIC-IRTA-UAB-UB, Edifici CRAG, Campus UAB, Bellaterra, 08193 Barcelona, Spain

²Institute for Integrative Systems Biology (I2SysBio), Universitat de València-CSIC, Paterna, 46908, Valencia, Spain

³Institut de Recerca i Tecnologia Agoralimentàries (IRTA), Edifici CRAG, Campus UAB, Bellaterra, 08193 Barcelona, Spain

Abstract

Fruit ripening is an essential process in plant development as it allows seed dispersion at the end of the fruit development. It is also a crucial factor in fruit shelf life, fruit ripening behavior being one of the main goals in plant breeding. Ethylene is a hormone that plays a key role in fruit ripening, and together with the respiration pattern determines whether the fruit ripens as climacteric or non-climacteric. In melon (*Cucumis melo*) there are both climacteric and non-climacteric varieties, making it an ideal crop to study fruit ripening from a genetic point of view. In a previous work, a major QTL for fruit ripening was identified in chromosome 8: *ETHQV8.1*, covering a region of 182.2 Kbp. *ETHQV8.1* was validated and fine-mapped using Introgression Lines (ILs) funded by the same parental lines and F2 populations, narrowing down the interval to a region of 3.6 Kbp containing a single gene: MELO3C024520.2. Annotated as *Ethylene Responsive Transcription Factor 024* or *ERF024*, its expression was correlated with climacteric ripening behavior. In ‘Védrantais’, it had a peak of expression at 30 days after pollination (DAP), at the beginning of climacteric ripening, while in ‘Piel de Sapo’ it was barely expressed. We also observed expression in the ILs, correlated with their ripening behavior. To validate *ERF024* as the causal gene of *ETHQV8.1*, gene editing using *CRISPR/Cas9* was performed. A knock-out line with two null alleles was obtained, and a preliminary phenotyping experiment suggested *CmERF024* as the causal gene of *ETHQV8.1*. In order to investigate the gene function, a DAP-seq experiment was performed to identify genes regulated by *ERF024*, together with a gene co-expression analysis based on RNA-seq data. 26 genes were found being co-expressed with *ERF024* and containing a binding peak in their promoter, considering them High Confident Targets (HCT). A Gene Ontology analysis of these HCTs revealed a significant enrichment of DNA structure-related terms, suggesting an important role of *CmERF024* in the control of DNA structural changes associated with the transcriptomic switch happening during climacteric fruit ripening in melon.

Introduction

Melon (*Cucumis melo* L.) is a member of the Cucurbitaceae family, which includes melons, cucumbers, watermelons or pumpkins. This family is of great importance for human diet, and therefore economically significant. Mostly, the edible parts of these plants are the fruits, some of them raw (as melon or cucumber) and other ones cooked (as pumpkin or squash).

In fruit development, we can differentiate several stages: fruit set, fruit growth (divided in two phases: cell division and cell expansion) and fruit ripening (Quinet *et al*, 2019). These processes are controlled by different phytohormones, as auxin, gibberellin and ethylene. Ethylene is a gaseous plant hormone that has a key role on fruit ripening. Depending on the ethylene produced by fruits during ripening, they can be categorized as climacteric or non-climacteric. In the case of climacteric fruit ripening, being tomato the model species, a model controlling ethylene production and therefore fruit development and ripening has been proposed (Barry *et al*, 2000; Cara & Giovannoni, 2008; Liu *et al*, 2015a). Two systems of ethylene production have been described, system 1 and 2 (McMurchie *et al*, 1972; Liu *et al*, 2015a). In climacteric fruits, during fruit development system 1 maintains the hormone at low levels, and when fruits achieve the competence to ripe there is a transition to system 2, where ethylene increases by an autocatalytic production triggering the physiological changes of climacteric ripening. Several genes have been associated with this transition, as the ethylene receptors *ETR4* and *ETR6* (Kevani *et al*, 2007) or the transcription factor *MADS-RIN* (Vrebalov *et al*, 2002). In non-climacteric fruits, with strawberry as the model plant, ethylene may also play a role in the control of fruit ripening, but much less information is available (Sun *et al*, 2013; Kou *et al*, 2021).

In the case of melon, there are both climacteric and non-climacteric varieties in the same species, making it a suitable alternative model species to study fruit ripening. During climacteric fruit ripening in melon there is a peak of ethylene production, triggering physiological changes in the fruit, as the production of volatile compounds or the formation of the abscission layer (Pech *et al*, 2008). Non-climacteric varieties do not have this peak of ethylene production, but they also suffer some physiological changes that are ethylene-independent, as the accumulation of sugars or secondary metabolites, as carotenoids (Pech *et al*, 2008). Due to the diversity found in melon and the importance of ripening in fruit shelf-life, several studies have been performed to dissect the genetics of

fruit ripening. Some QTLs have been mapped in the genome using different populations (Vegas *et al.*, 2013; Rios *et al.*, 2017; Perpiñá *et al.*, 2017; Pereira *et al.*, 2020; Pereira *et al.*, 2021), and some interaction studies among ripening related QTLs have been done (Vegas *et al.*, 2013; Santo Domingo *et al.*, 2022). These studies allowed the identification of the causal gene of one QTL, *ETHQV6.3*, encoding a *CmNAC-NOR* transcription factor (MELO3C016540.2) (Rios *et al.*, 2017; Liu *et al.*, 2022a), suggesting the importance of transcription factors in controlling melon fruit ripening. Also, the study of another major ripening QTL, *ETHQV8.1*, has brought to light the importance of epigenomic changes controlling climacteric ripening in melon, although the causal gene has not been identified yet (Giordano *et al.*, 2022).

Apart from the classical genetic approaches to study QTLs, new technologies have emerged in the last years that can help in the validation of candidate genes. RNA-seq or other transcriptomic studies have been widely used to study QTLs and identify candidate genes (Wen *et al.*, 2019; Galpaz *et al.*, 2018), combining QTL mapping with gene expression data. Also, other approaches have been used, as metabolomic studies together with QTL mapping (Alseekh *et al.*, 2015) or proteomics (Consoli *et al.*, 2002). CRISPR/*Cas9* gene editing (Doudna & Charpentier, 2014) has become a revolution in plant breeding as novel alleles of agronomic important genes can be developed. This technology has been widely used to study gene function in several crops, as tomato (Wang *et al.*, 2019) or rice (Romero & Garcia-Arias 2019), and recently it has been implemented in melon (Giordano *et al.*, 2022; Liu *et al.*, 2022a; Wang *et al.*, 2022).

The goal of this work is to dissect *ETHQV8.1*, a major QTL governing climacteric fruit ripening in melon (Pereira *et al.*, 2020; Pereira *et al.*; 2021, Santo Domingo *et al.*, accepted). A fine mapping strategy was followed to identify the gene, followed by a CRISPR/*Cas9* validation and RNA-seq and DAP-seq analysis to study its role during fruit ripening.

Materials and Methods

Plant material

Four melon genotypes were used in this work: the commercial varieties 'Piel de Sapo' T111 (PS) and 'Védrantais' (Ved), and two Introgression Lines (ILs) PS8.2 (Pereira *et al.*, 2021) and VED8.2 (Santo Domingo *et al.*, accepted) with the introgressions covering *ETHQV8.1* from PS and Ved respectively, in the reciprocal genetic background.

Ved and PS8.2 were used in the fine mapping experiment, while PS and Ved were used in the RNA-seq and DAP-seq experiments. The four genotypes were used in gene expression analyses. Ved was also used for gene editing.

Plant growth conditions

Seedlings were germinated and grown at CRAG (Barcelona) during two weeks before genotyping. After selection, plants were transported to Caldes de Montbui (Barcelona) and grown in coconut fiber sacks under greenhouse conditions. Plants were pruned twice a week and hand-pollinated until one fruit per plant was set to optimize fruit growth and development.

Two generations per year were performed for seed production, and one generation per year for fruit phenotyping experiments.

For the fine mapping experiment, the hybrid from the cross Ved x PS8.2 was grown during winter under greenhouse conditions to generate enough F2 seeds. In the F2 population, two weeks old 3,456 seedlings were genotyped, and selected plants were grown in Caldes de Montbui (Barcelona) in coconut fiber sacks. All recombinant plants were self-pollinated to obtain F3 seeds. The nine most informative plants were selected for the progeny test, where 48 seedlings of each family were genotyped and grown for phenotyping. More than 6 melons were evaluated of each family in the phenotyping experiment.

In case of plants coming from *in vitro* plant culture, plantlets were acclimated in small greenhouses at CRAG for 5 days, reducing the humidity level every 24 h. After acclimation, plants were grown under greenhouse conditions at Caldes the Montbui in coconut fiber sacks and at CRAG in big pots

DNA extraction

Three different DNA extraction protocols were used, depending on the final use of the extracted DNA.

For a quick genotyping with SNPs, an alkaline-lysis protocol was performed. Briefly, grinded material was digested with NaOH at 96°C for 1 minute, and then neutralized with Tris-HCL (Lu *et al*, 2020).

For long-term storage and PCR genotyping, a Doyle extraction was performed with some modifications (Pereira *et al*, 2018). Briefly, grinded material was incubated with CTAB

at 65 °C for 40 min, then the DNA was purified with chloroform, and cleaned with isopropanol and ethanol (Doyle, 1991).

For high-quality and high-quantity DNA required for the DAP-seq experiment and genome resequencing, also a CTAB protocol was used (Doyle, 1991), but followed by a phenol-chloroform-isoamyl alcohol cleaning step.

Genotyping

Plants used for the fine mapping were genotyped using SNP markers. Two equivalent systems were used: i) KASPar SNP genotyping system (KBiosciences, UK) and ii) PACE2.0 SNP genotyping system (3CR Bioscience, UK). Both systems are based in an allele-specific PCR with different fluorochromes depending on the allele. Primers were designed following manufacturer instructions and are listed in Table 2.S1A.

For the fine mapping experiment, all the seedlings were genotyped using the flanking markers of *ETHQV8.1* chr08_9603217 and chr08_9757323 at positions 8,625,397 and 8,807,601 bp in chromosome 8 (melon reference genome v4.0), respectively. Once grown in greenhouse conditions, DNA was extracted again, and they were genotyped within the interval with the markers listed in Table 2.S1A.

For the progeny test in 2020, the 9 most informative families were selected (R5, R14, R15, R17, R24, R42, R57, R68 and R79) and 48 seeds of each family were germinated, along with the parental lines Ved and PS8.2. These plants were genotyped with a customized set of markers each family, consisting of the flanking markers of the QTL and the markers harboring the recombination point. Recombinant homozygous plants were selected.

For the CRISPR/*Cas9* experiment, plants were genotyped in two steps. First a PCR was done to detect the construct inserted in the genomic DNA. Then, selected plants were Sanger sequenced in the region of MELO3C024520.2 to detect the edits. Primers used in these experiments are listed in Table 2.S1B. Also, ploidy level was evaluated by flow-cytometry analysis at Iribov Innovations (Heerhugowaard, the Netherlands). Edited plants were selected, as well as some not edited that were used as NE controls (transformed and not edited Ved) for gene function validation studies.

Phenotyping

Fruits were evaluated concerning their ripening behavior and quality. Five ripening-related traits were considered (ECD, EARO, EALF, ABS, and HAR), and three fruit quality related phenotypes were recorded (FW, SSC and FIR) (Table 2.1).

Table 2.1. Phenotypes analyzed in the experiment.

Group	Phenotype	Units	Symbol
Fruit quality	Fruit weight	g	FW
	Soluble solid content	° Brix	SSC
	Flesh firmness	kg cm ⁻²	FIR
Fruit ripening	Earliness of chlorophyll degradation	Days after pollination (DAP)	ECD
	Earliness of aroma production		EARO
	Earliness of abscission layer formation		EALF
	Harvest date		HAR
	Level of abscission		-

All of them were treated as quantitative, except level of abscission (ABS), which was considered semi-quantitative in a scale from 0 (no abscission layer formation) to 3 (complete abscission from the plant). Harvest date was fixed using the following criteria: i) the days after pollination (DAPs) when the fruit abscised from the plant; ii) 5 DAPs after the abscission layer was observed if the abscission layer was partially formed; and iii) 56 DAPs if there was not abscission layer.

FW, SSC and FIR were evaluated at harvest. FW was measured using a balance, SSC was measured with an optical refractometer (Atago™) from fresh extracted juice, and FIR was measured at 4 different parts of the fruit with a manual penetrometer (Fruit Test™, Wagner Instruments), and the mean value was annotated.

RNA extraction and Real time PCR

RNA was extracted from three biological replicates per genotype (PS, Ved, PS8.2 and VED8.2) in four stages of the development of the fruit: 15 DAP, 25 DAP, 30 DAP and Harvest date. RNA was extracted from fruit flesh using Spectrum™ Plant Total RNA Kit, from Sigma-Aldrich (Sant Louis, USA), and a DNase treatment was performed with TURBO DNA-free Kit (Thermo-Fisher Scientific, USA).

Extracted RNA was retro-transcribed to cDNA using PrimeScript™ RT-PCR Kit from Takara Bio INC (Kusatsu, Japan). RT-PCRs were performed in a LightCycler480 from Roche (Basel, Switzerland) using SYBR Green MasterMix, following manufacturer specifications, using *CmRPS15* as housekeeping gene (Kong *et al*, 2016).

RNA-seq

Extracted RNA from PS and Ved at different time-points was used for RNA-seq analysis (Table 2.S2A). After Quality Control, RNA was sequenced by Novogene Co (Cambridgeshire, UK) using the PE150 strategy. A total of more than 1,180 million high-quality reads were obtained (177.2 Gb), distributed evenly among samples (Table 2.S2B). After trimming with ‘fastp’ (Chen *et al*, 2018), trimmed reads were aligned to the reference melon genome v4.0 (Ruggieri *et al*, 2018) using ‘STAR’ (Dobin *et al*, 2013), aligning uniquely around 95% of the reads (Table 2.S2C). Ved-71 was considered an outlier in its group (Ved-30 DAP) in the PCA analysis due to its clustering with Ved at harvest (Figure 2.S1), and it was withdrawn in the subsequent analyses. Counts matrix was calculated using ‘featureCounts’ package (Liao *et al*, 2014) (Additional File 2.1) and filtered by low expression (≥ 5 reads in ≥ 3 samples). For finding differentially expressed genes (DEGs), two approaches were followed, both based on a negative binomial distribution: i) DEGs identified using ‘ImpulseDE2’ (Fischer *et al*, 2018); and ii) DEGs identified using ‘DESeq2’ comparing the two genotypes in each time point. After pooling the DEGs identified by both strategies, a clustering approach was followed using ‘WGCNA’ (Langfelder & Horvath, 2008). A total of 11,869 genes were considered as DEGs. FPKM normalized gene counts were then analyzed using WGNA with the parameters: power = 13, mergedCutHeight = 0.15, and deepSplit = 2, finding a total of 24 DEGs’ clusters (Figure 2.S2).

DAP-seq

For de DAP-seq experiment, the protocol from Bartlett *et al*, 2017 was followed, with minor modifications. First, 5 μ g of high-quality genomic DNA from PS and Ved was fragmented through sonication (Bioruptor plus, IBB), in 30 cycles of 30/90 seconds on/off at 4°C and low power, to obtain fragments around 200 bp. Then, fragmented DNA was cleaned with sodium acetate and ethanol. A step of end repair was performed using Fast DNA End-Repair Kit (Thermo Scientific, USA) and cleaned again. After repairing the ends, adenines were added at 3’ endings using Biotaq (Ecogen, Spain) at 72°C for 30 min. After another cleaning with sodium acetate and ethanol, the adaptor Y (formed by the ligation of primers ‘Adapter A’ and ‘Adapter B’ (Table 2.S1C) was ligated using T4 ligase at room temperature for 3 h. After checking the quality of the libraries by RT-PCR, a PCR was performed with Phusion Green Kit (Thermo Scientific, USA) to erase

methylation marks. Primers used for the construction of the library are listed in Table 2.S1C.

For protein expression, TNT expression reaction (Promega, USA) was performed following manufacturer instructions with pIX-Halo::ERF024 plasmid or pIX-Halo as input samples. After protein expression, the reactions were incubated with HaloTag Beads (Promega, USA) for 1 h and cleaned several times with PBS+NP40 solution. Once the chimeric protein was bound to the beads, the DNA library was added and incubated for 1 h. After several washings with PBS+NP40 solution to remove not-bound DNA, the reaction was incubated at 98°C for 10 min to recover the bound DNA. DNA was then amplified using specific primers and run in an agarose gel 1% (wt/vol). After running the gel for 20 min at 100 mV, the stripe from 200 to 500 bp was extracted using GeneJET Gel Extraction Kit (Thermo Scientific, USA). The resulting DNA was sequenced by Novogene (Cambridgeshire, UK) using a PE150 strategy.

Raw reads were trimmed using ‘fastp’ (Chen *et al*, 2018) and aligned to the reference genome v4.0 (Ruggieri *et al*, 2018) using ‘Hisat2’ algorithm (Kim *et al*, 2019) (Table 2.S3). ‘GEM peak caller’ (Guo *et al*, 2012) was used to determine binding peaks, following a multireplicate strategy (2 replicates and 2 inputs per genotype) with default parameters and fold = 5. Then, peaks were filtered in the region of 1kb upstream the start of the gene and inside the gene based on previous studies performed in *Arabidopsis thaliana* (Yu *et al*, 2016).

Vector construction

To construct the CRISPR/*Cas9* vector, one guide RNA (gRNA) was designed targeting *CmERF024* (MELO3C024520.2) using the ‘Breaking Cas’ tool (<https://bioinfogp.cnb.csic.es/tools/breakingcas/>). 5’-TCAAACCCTCCTCGTTACCG-3’ was selected as the optimum gRNA and the cloning steps were performed as described at Schmil & Puchta (2016). The two generated oligonucleotides (Table 2.S1D) were annealed at room temperature and cloned into the plasmid pEn-Chimera in the *BbsI* site. After the construct was verified by sequencing, the gRNA was cloned in the plasmid pDe-Cas9 using Gateway technology (Katzen, 2007), and verified again by sequencing, obtaining pDe-Cas9-gRNA.

To construct the DAP-seq vector, the *CmERF024* sequence was amplified with *attB1* and *attB2* tails (Table 2.S1E) and cloned into the plasmid pIX-Halo using ‘Gateway’

technology. First, the amplified DNA was cloned in pDONR221 and verified by sequencing. Then it was cloned in pIX-Halo through BP reaction, and verified again by sequencing, obtaining pIX-Halo::ERF024.

Melon transformation

Agrobacterium tumefaciens transformation was performed as described before (Giordano *et al*, 2022). Briefly, the CRISPR/*Cas9* vector was transformed into *A. tumefaciens* (strain AGL-0) for melon transformation and seeds were incubated for 24 h in MS medium. Then, the embryos were removed and the distal half of the cotyledons was cultivated with transformed *A. tumefaciens* for 20 min in liquid MS medium with acetosyringone 200 μ M. Explants were then co-cultivated for 3 days in regeneration medium with hormones (0.5 mg/L 6-benzylaminopurine (BA), 0.1 mg/L indole-3-acetic acid (IAA)) at 28°C (Castelblanque *et al*, 2008). After three days, explants were transferred to fresh selection medium with L-phosphinotricin (PPT), and then transferred to fresh media every three weeks. Selected transgenic plants were grown in controlled conditions in 12/12 h light/dark cycles at 28°C. Individualized plants were transferred to regeneration medium without hormones. When sufficiently grown, DNA was extracted for genotyping.

Resequencing of recombinant lines

Extracted DNA of the recombinant lines R14-F3, R15-F3 and R68-F3 was re-sequenced using DNBSEQTM sequencing technology (BGI, China) using PE150 strategy. After trimming, reads were aligned to the reference genome v4.0 (Ruggieri *et al*, 2018). Around 89 million reads were obtained per sample with more than 60 million 150 bp mapped reads after filtering and an average coverage of 40X (Table 2.S4). SNP mining and structural variants analysis was performed for the target region of *ETHQV8.1*.

Statistical analyses

Data analysis was performed using R v4.4.1 (R Core Team, 2020) with RStudio interface. ANOVA and t-tests were performed using “rstats” package, and plots were made using “ggplot2” package. Gene Ontology analyses were performed using “gprofiler2” package (Kolberg *et al*, 2020). Significance level was considered as p-value < 0.05.

Results

Fine mapping of *ETHQV8.1*

With the objective of dissecting *ETHQV8.1*, we performed a fine mapping in an F2 population funded by the cross of Ved and the IL PS8.2, both sharing the same

background except for a PS introgression in chromosome 8 in PS8.2 (Pereira *et al*, 2020; Pereira *et al*, 2021). PS8.2 has been previously characterized, producing a delay of ripening of around 5 days (Pereira *et al*, 2021).

In the F2 population, we genotyped 3,456 seedlings with the flanking markers, finding 29 recombinants (Figure 2.1A). *ETHQV8.1* was contained in a genetic distance of 0.84 cM and a physical distance of 182.2 Kbp (Pereira *et al*, 2020). 26 out of the 29 recombinants were recovered, due to incomplete fruit set. The genotypes of the 26 recombinant plants are shown in Figure 2.1A.

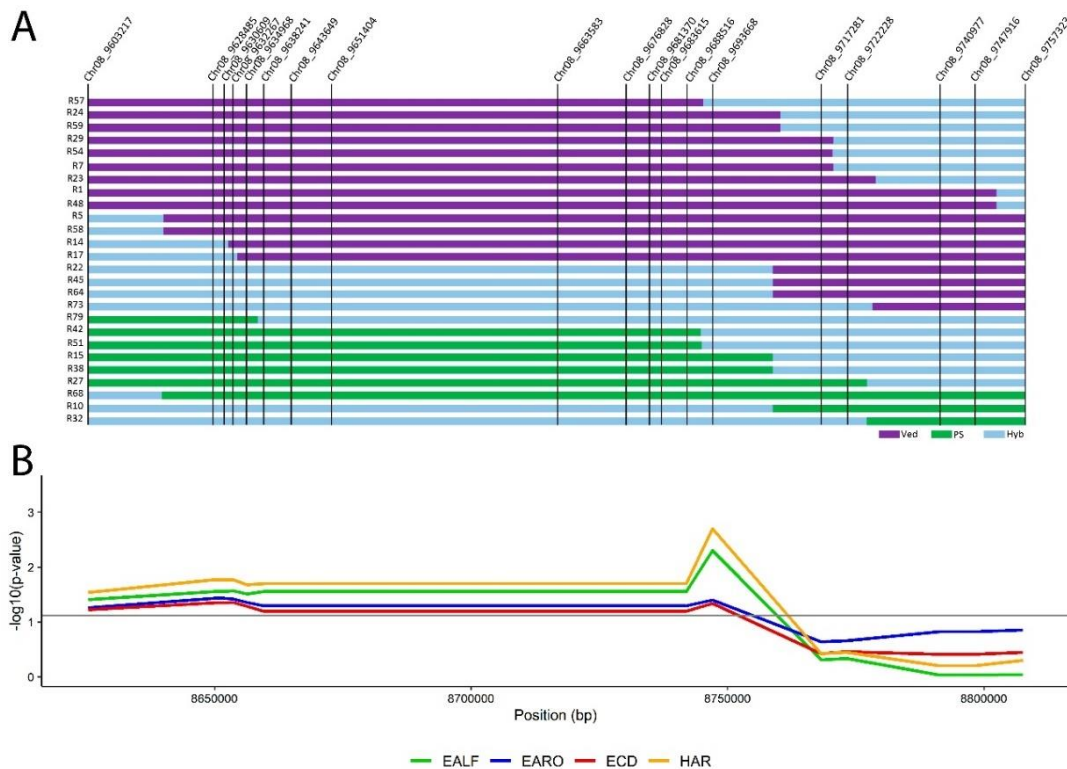


Figure 2.1. **A)** Genotype of the 26 recombinant F2 plants found in the region of *ETHQV8.1*. Markers are named based on their position in melon genome v3.6.1 (Table 2.S1A). **B)** Analysis marker by marker of the four quantitative ripening-related phenotypes earliness of abscission layer formation (EALF), earliness of aroma production (EARO), earliness of chlorophyll degradation (ECD) and harvest date (HAR). In the X-axis, the position in chromosome 8 is represented, and in the Y-axis, the $-\log_{10}(\text{p-value})$. Horizontal line represents $\text{p-value} = 0.05$.

Analyzing the ripening related phenotypes EALF, EARO, ECD and HAR (Table 2.S5A), we detected that from marker Chr08_9717281 to the flanking right marker, there was not association with the phenotypes ($\text{p-value} > 0.05$) (Figure 2.1B). However, phenotypes were associated with markers from 8,625,397 to 8,747,096 bp (markers Chr08_9603217 and Chr08_9693668, respectively) ($\text{p-value} < 0.05$). So, in this first step of the fine mapping we narrowed down the interval from 182.2 kb to 142.9 Kbp, but the QTL

interval still contained 9 annotated genes. Therefore, we proceed with a second step of the fine mapping with the F3 generation. We selected the most informative families (R5-F3, R14-F3, R17-F3, R79-F3, R42-F3, R15-F3, R68-F3, R57-F3 and R24-F3) and, after genotyping the QTL interval, we selected F3 plants that were homozygous at both sides of the recombination point (Figure 2.2A).

After phenotyping, we observed some recombinant families behaving as Ved, other families with a PS8.2-like ripening behavior, and other lines that had an intermediate behavior (Figure 2.2B) (Table 2.S5B). Although we could detect some association between the markers Chr8_9628485 and Chr8_9630609 and the phenotype (Figure 2.2A), we also performed the analysis marker by marker (Figure 2.2C). Comparing the Ved alleles with the PS alleles in all the markers, we could validate the trends observed in the previous analysis. We found a highly significant association of the markers Chr8_9628485 and Chr8_9630609 with the four ripening-related traits (Figure 2.2C). In order to confirm the region, the recombinant families flanking the associated region (R14-F3 and R68-F3), together with the parental lines (Ved and PS8.2), a family with intermediate phenotype (R79-F3) and R15-F3, were selected and their offspring was evaluated again in 2021 (Table 2.S5C). R14-F3, R68-F3 and R79-F3 confirmed their behavior as PS8.2, and R15-F3 confirmed its behavior as Ved, being the only family not consistent with the expected phenotype regarding its genotype, although in both years it ripened a bit later than Ved.

We resequenced the two recombinant lines flanking the associated region (R14-F3 and R68-F3) to confirm our genotypes, and also R15-F3. The results obtained validated the previous SNP genotyping, confirming the recombination point and no other unexpected contaminations in the rest of the genome (Table 2.S6). With the structural variants analysis we could fine tune the recombination points of R14-F3 and R68-F3 (Table 2.S7), narrowing down the interval to a region of 3,566 bp between 8,648,965 and 8,652,531 bp in chromosome 8 (v4.0), but we could not associate a particular variant with the observed phenotype.

To sum up, with the second step of the fine mapping we narrowed down the QTL to a region between 8,648,965 and 8,652,531 bp in chromosome 8 (v4.0). In this region there is only one annotated gene, MELO3C024520.2, annotated as *Ethylene responsive transcription factor 024* or *ERF024*.

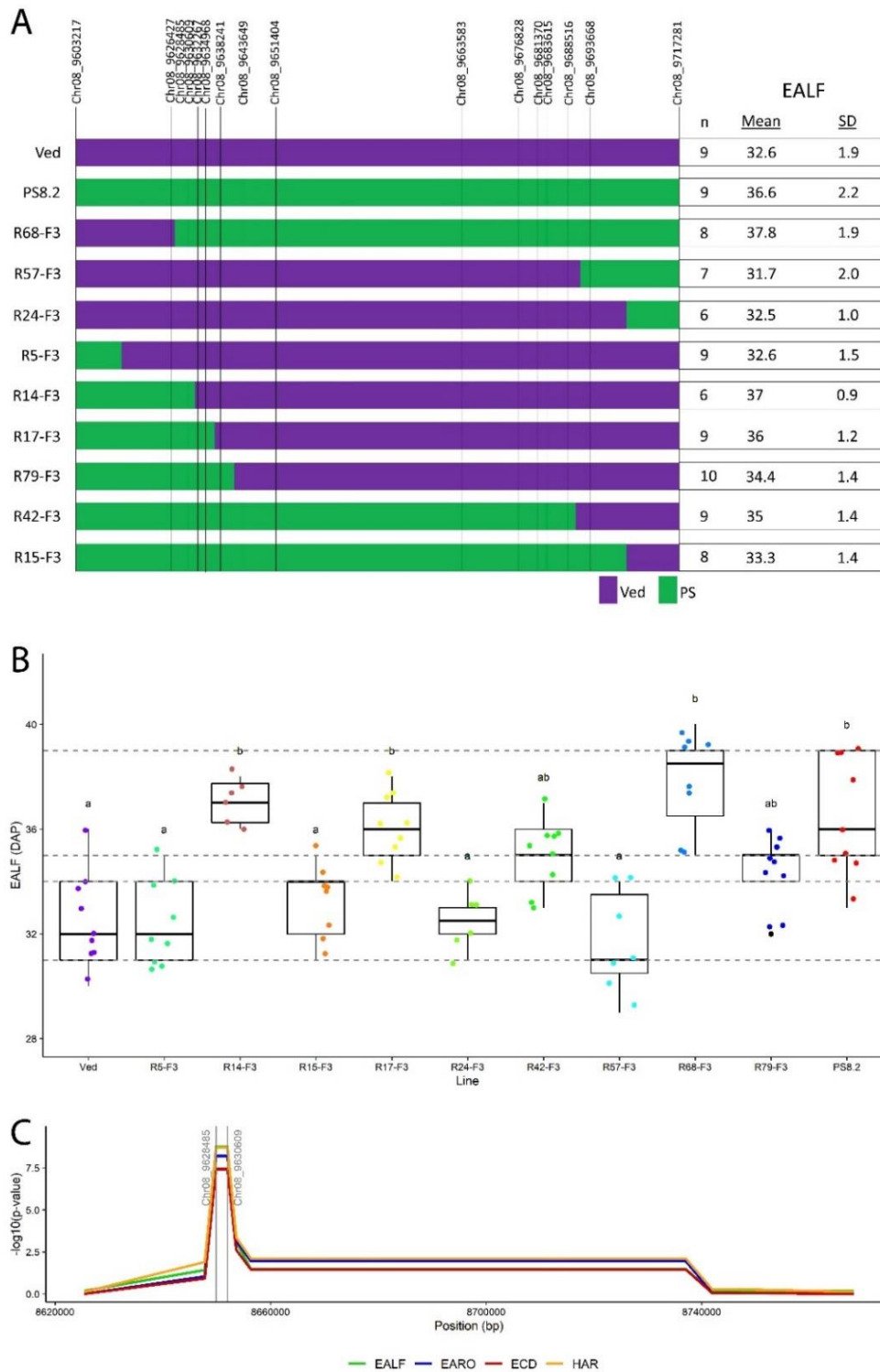


Figure 2.2. **A)** Genotype of the selected recombinant F3 families, Ved and PS8.2 in the region of the QTL *ETHQV8.1*, showing also the mean of the earliness of abscission layer formation (EALF) phenotype. **B)** Boxplot of EALF phenotype in the selected recombinant F3 families, Ved and PS8.2, showing with dashed horizontal lines the Q1 and Q3 of both Ved and PS8.2. Different letters represent significantly different groups (p -value < 0.05). **C)** Analysis marker by marker of the four quantitative ripening-related phenotypes earliness of abscission layer formation (EALF), earliness of aroma production (EARO), earliness of chlorophyll degradation (ECD) and harvest date (HAR). X-axis: the position in chromosome 8 is shown, Y-axis: $-\log_{10}(p\text{-value})$.

CmERF024 validation

We checked the expression of *CmERF024* in the four genotypes (PS, Ved, PS8.2 and VED8.2) by qRT-PCR (Figure 2.3A). We observed a peak of expression happening at 30 DAP for all the genotypes, before the ethylene production known in Ved (Figure 2.2) (Santo Domingo *et al*, 2022), but with differences in their relative expression. In PS8.2 the expression at the peak was significantly lower than in Ved, correlating with the milder climacteric behavior of the IL; and in VED8.2, *CmERF024* was significantly more expressed than in PS, correlating with the climacteric behavior of the IL and the non-climacteric behavior of PS represented by the earliness of abscission layer formation (Figure 2.3B) (Table 2.S5D).

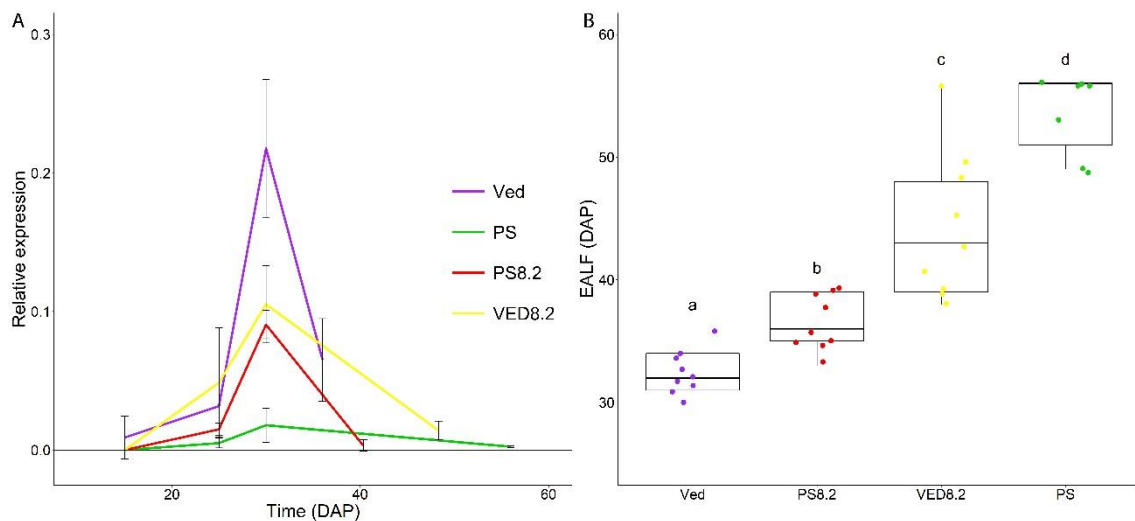


Figure 2.3. **A)** Relative expression data of *CmERF024* in the four genotypes Ved, PS, PS8.2 and VED8.2 at different points of the fruit development and ripening. **B)** Earliness of abscission layer formation (EALF) of the four genotypes. Different letters represent significantly different groups (p-value < 0.05).

These observations supported the hypothesis of *CmERF024* being the causal gene of *ETHQV8.1*. *CmERF024* is a member of AP2/EREBP (*APETALA 2* and *ethylene-responsive element binding protein*) superfamily. Containing only one AP2/EREBP domain, it is part of the *ethylene responsive transcription factor (ERF)* family, with 31 members in the melon genome. With this evidence, we performed CRISPR/Cas9 gene editing to generate knock-out lines in Ved and validate the gene function.

The gRNA was designed upstream the AP2/ERF domain, so the edit should cause a complete knock-out allele (Figure 2.4A, Figure 2.S3). We obtained two different mutant alleles, one with a deletion of 1 bp (ERF024-a), and the other with a 2 bp deletion

(ERF024-b), both predicted to produce knock-outs (Figure 2.4A). Both alleles were obtained in the same plant, which was a bi-allelic knock-out T0 plant. After *in vitro* propagation of this plant, the T0 generation was phenotyped (ERF024-KO), using two different controls: the Védraçais parental line after *in vitro* propagation (Ved), and a transformed but not edited line (Not Edited or NE).

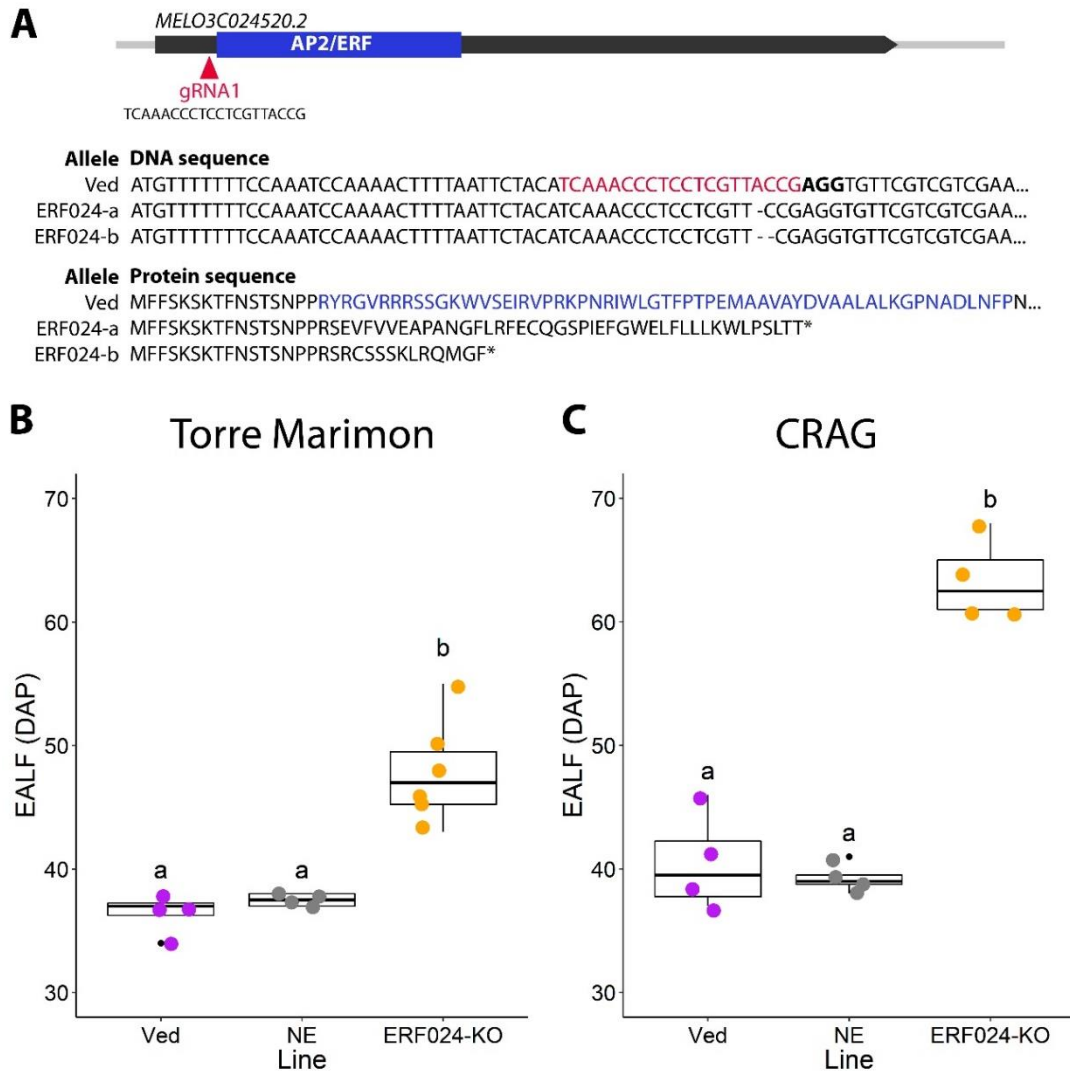


Figure 2.4. **A)** Representation of the gene structure of *CmERF024*, together with the two mutant alleles (ERF024-a, ERF024-b) with their DNA and protein sequences, showing in blue the AP2/ERF domain and in red the position of the gRNA. **B)** and **C)** Earliness of abscission layer formation (EALF) of the two controls (Ved and NE (transformed and not edited Ved)) and the T0 knock-out plant (ERF024-KO) at Torre Marimon (**B**) and at CRAG (**C**). Small letters mean significantly different groups (p -value < 0.05).

This preliminary experiment was performed in two different locations in spring-summer 2022: at CRAG greenhouses (Cerdanyola del Vallès, Spain) and at Torre Marimon greenhouses (Caldes de Montbui, Spain). In Torre Marimon Ved and NE ripened at 37

DAP, and at CRAG both ripened at 40 DAP (Figure 2.4B, C) (Table 2.S5E, F). On the contrary, ERF024-KO had a different behavior. Some of the plants did not show climacteric symptoms when they were harvested due to cracking or rotting. The ones left at the plant presented some mild climacteric symptoms much later than the controls: around 48 DAP at Torre Marimon and at 63 DAP at CRAG (Figure 2.4B, C) (Table 2.S5E, F). The difference was significant between ERF024-KO and each of the controls at both locations confirmed that most likely *CmERF024* is the causal gene of *ETHQV8.1*.

CmERF024 function

Once the gene was validated by CRISPR/*Cas9* edited mutants, we went on studying its function. As it has a DNA-binding domain *AP2/ERF* (Figure 2.4A, Figure 2.S3) and it is annotated as a transcription factor, we performed a DAP-seq experiment to identify the putative target genes. We did the experiment in both genetic backgrounds PS and Ved, and we obtained 41,706 and 52,732 binding peaks, corresponding to 15,540 and 17,956 genes, respectively (Table 2.S8). After filtering for the distance of the binding region from the gene, we obtained 2,243 and 2,685 binding sites for PS and Ved, respectively. The consensus binding motif for both genotypes was RGDCGGRY (Figure 2.S4).

Using RNA-seq data from PS and Ved at different time points (15, 25, 30 DAPs and Harvest date), we considered high confident targets (HCT) the genes with one or more binding motifs in their promoter and co-expressed with *CmERF024*, coinciding with expression clusters 16 and 21 of the RNA-seq analysis, which were then merged into a single cluster (Figure 2.S2) (Table 2.S9). In this HTC gene list, we found several histones and DNA-related proteins (Table 2.2), as well as *CmERF024*, and three of them were validated by qRT-PCR using the parental lines Ved and PS and the ILs (Figure 2.S5).

After gene ontology enrichment analysis with all the genes in the co-expression cluster of *CmERF024* (genes with a peak of expression in Ved at 30 DAP but not in PS, what is considered the onset of ripening in melon (Saladié *et al.*, 2015)), we found a high significance of terms related with DNA conformation, chromatin and nucleosomes (Figure 2.5A) (Table 2.S10), indicating a possible involvement of these DNA-related processes at the onset of fruit ripening. When we analyzed the HTC gene list, the same terms were significant, suggesting a participation of *CmERF024* in these processes (Figure 2.5B) (Table 2.S11).

Table 2.2. List of high confident targets that co-expressed with *CmERF024* with a putative binding peak in their promoter region.

ID	Distance to TSS	logFC	Annotation
MELO3C015882.2	237	2.549	Histone H2A
MELO3C018135.2	262	0.791	Histone H2A
MELO3C024829.2	292	9.681	classical arabinogalactan protein 4
MELO3C031941.2	644	4.303	glycine-rich cell wall structural protein 1.8-like
MELO3C023431.2	211	1.457	haloalkane dehalogenase
MELO3C016426.2	-755	1.263	ferric reduction oxidase 7
MELO3C009714.2	171	0.908	Remorin
MELO3C002236.2	124	0.715	E2F transcription factor-like E2FE
MELO3C005059.2	267	1.669	Histone H4
MELO3C013436.2	120	1.059	DNA helicase
MELO3C026749.2	175	0.783	DNA helicase
MELO3C009536.2	-675	1.953	Protein CHROMOSOME TRANSMISSION FIDELITY 7
MELO3C024520.2	291	3.477	ethylene-responsive transcription factor ERF024
MELO3C003431.2	245	1.361	BnaA05g08570D protein
MELO3C009717.2	148	0.904	tRNA (Guanine-N(7)-)-methyltransferase subunit trm82
MELO3C026208.2	138	0.960	Purple acid phosphatase
MELO3C021372.2	404	4.036	Unknown protein
MELO3C011610.2	107	2.094	Histone H3
MELO3C031246.2	-963	2.169	DNA primase
MELO3C006072.2	211	4.411	acidic endochitinase-like
MELO3C013885.2	29	2.378	poly(U)-specific endoribonuclease-B
MELO3C004866.2	-115	1.157	Histone H2B
MELO3C023490.2	-30	1.220	Elongation factor 4
MELO3C010481.2	194	0.380	Sister chromatid cohesion PDS5-B-B-like protein
MELO3C028557.2	-124	2.053	Kinetochore protein
MELO3C015926.2	107	1.514	DNA helicase

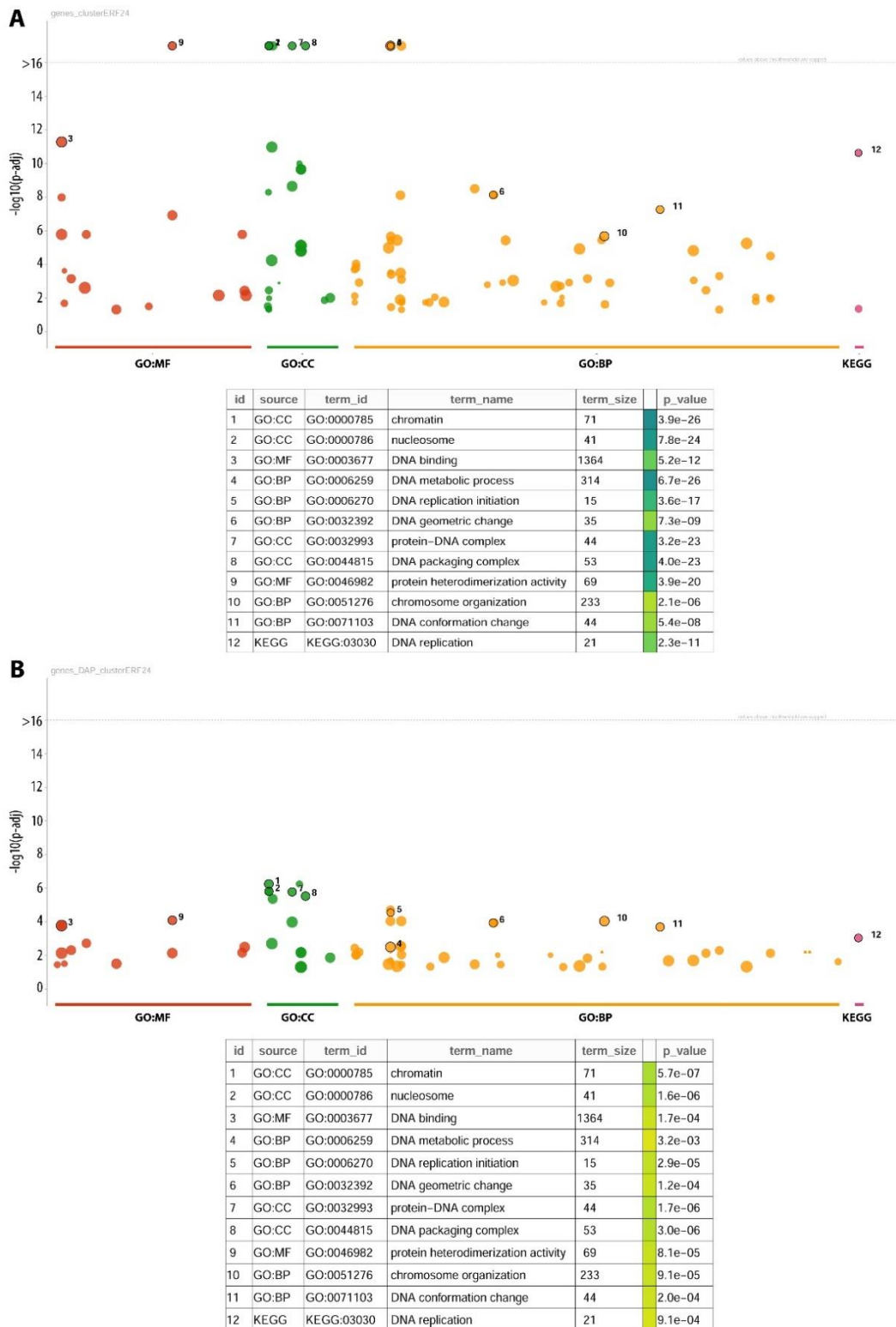


Figure 2.5. Gene Ontology analysis of **A)** the genes co-expressed with *CmERF024* during melon fruit development, and **B)** the high confident targets of *CmERF024*. GO: gene ontology, MF: molecular function, CC: cell compartment, BP: biological process, KEGG: Kyoto encyclopedia of genes and genomes.

Discussion

In this work we present the identification, validation, and characterization of a novel key regulator of melon fruit ripening, *CmERF024*.

Ethylene Responsive transcription Factor 024 is the causal gene of ETHQV8.1

ETHQV8.1 has been previously reported as a key regulator QTL for fruit ripening in melon, using both mapping populations and association studies (Pereira *et al*, 2020; Pereira *et al*, 2021; Santo Domingo *et al*, 2022; Santo Domingo *et al*, accepted). Although other candidate genes annotated in the original QTL interval were also associated with fruit ripening (Giordano *et al*, 2022), there were not enough evidence to determine the causal gene. However, with a two-step fine mapping process, we managed to narrow down the interval to a 3.6 Kbp region containing a single gene, *CmERF024*, proving this strategy as very powerful for gene identification in melon (Hu *et al*, 2022). The use of ILs also allowed us to minimize the effect of the background, facilitating the analysis of the gene effect during phenotyping.

Using the CRISPR/*Cas9* gene editing system we have been also able to validate *CmERF024* in a climacteric background using knock-out lines. Although this tool has been widely used in other crops, such as rice (Huang *et al*, 2022), maize (Liu *et al*, 2022b) or tomato (Li *et al*, 2018; Hendelman *et al*, 2021), there are less examples of gene editing in melon used for candidate gene validation (Giordano *et al*, 2022; Nizan *et al*, 2020). The knock-out T0 lines presented a delayed climacteric response in the two tested locations, in accordance with the phenotypes observed in the ILs, and showed partial dependence on the environment (Figure 2.4B, C). On the contrary of what could be assumed because of its annotation as an ethylene-responsive factor, *CmERF024* seems to act before ethylene is produced (Pereira *et al*, 2020; Santo Domingo *et al*, 2022), having a peak of expression few days before ripening. Expressed mainly at 30 DAP (Figure 2.3A), it may be participating in the transition from fruit growth to fruit ripening. This stage of development has been set as the beginning of ripening in both climacteric and non-climacteric lines, as it coincides with the beginning of sucrose accumulation (Saladié *et al*, 2015). With an expression peak in the climacteric lines but not in PS, *CmERF024* may be triggering the climacteric response in those lines, controlling the expression of genes that will be governing the dramatic transcriptomic shift observed in Ved at the later stages of ripening (Figure 2.S1). The presence of a binding peak in the promoter region

of *CmERF024* also indicates a putative auto-regulation. The peak, covering the 200 bp region between positions 8,651,930 and 8,652,129 bp in chromosome 8 (Table 2.S7) includes two SNPs between Ved and PS: one at position 8,651,955 bp and the other at position 8,652,075 bp, with PS having alleles C and G, and Ved alleles T and A, respectively (Additional File 2.2). These variants could explain the differences in expression between the different lines with shared genomic backgrounds, having *CmERF024* a higher binding efficiency in the Ved allele than in the PS one. This kind of auto-regulation behavior has been reported before in other *ERFs* in other species, as peach (Zhou *et al*, 2020a). However, more experimental work is needed to determine the genetic variant responsible for *CmERF024* differential expression between PS and Ved alleles, as targeted mutagenesis of the different SNPs.

Considering that *CmERF024* acts before ripening, it could be participating in the transition from system 1 to system 2 of ethylene production (McMurchie *et al*, 1972). It is not likely that *CmERF024* is directly regulating ethylene biosynthetic genes because in this case its expression should be coupled to the production of ethylene, not few days before.

Transcription factors play essential roles in fruit development and ripening

CmERF024 is annotated as a transcription factor (TF) of the *AP2/EREBP* (*APETALA 2 and ethylene-responsive element binding protein*) gene superfamily and containing an *AP2/ERF* domain. This family is widely distributed in the plant kingdom, and it is thought that it has been horizontally transferred to other organisms, as bacteria or phages (Wessler, 2005). In plants, *AP2/EREB* TFs are known to have functions in developmental processes (Filkenstein *et al*, 1998; Pandey *et al*, 2005), regulation of primary and secondary metabolism (Licausi *et al*, 2011; Yu *et al*, 2012) and biotic and abiotic stress tolerance (Nakashima *et al*, 2000; Hinz *et al*, 2010). Depending on their structure, they have been divided in four families (Licausi *et al*, 2013), being *ERF024* part of the *ERF* family with one *AP2* domain. This family has also been divided in several groups (Nakano *et al*, 2006) or subfamilies (Sakuma *et al*, 2002) in *Arabidopsis*. The closest homologue of *CmERF024* in *Arabidopsis* (*HARDY* or *At2G36450*) (Figure 2.S6) belongs to the group IIIb (Nakano *et al*, 2006), and it has been reported to improve drought tolerance in both *Arabidopsis* and rice (Karaba *et al*, 2007). On the other hand, the two closest homologues in tomato, *Solyc09g009240* and *Solyc10g083560* (Figure 2.S6), annotated as *Ethylene-Responsive factor 13* and *1*, respectively, are barely expressed during fruit development,

although *Solyc10g083560* is slightly expressed in the columella at breaker stage (Férrandez-Pozo *et al.*, 2017). In melon, the closest homologue is MELO3C00941.2 (Figure 2.S6). This gene, annotated as *ethylene responsive transcription factor 024-like*, is not expressed in fruit flesh in PS, Ved or Harukei (Additional file 2.1) (Yano *et al.*, 2020).

Other members of this family have been reported to control ethylene synthesis in tomato and tobacco (Zhang *et al.*, 2009). *SlERF2/TERF2* is able to bind physically the promoter of *ACS3* of tomato and tobacco, both *in vivo* and *in vitro*, due to the presence of a GCC-box. This interaction induced ethylene production and ethylene-associated responses in both species (Zhang *et al.*, 2009). To our knowledge, no *ERF* has been characterized in melon as being involved in fruit ripening, although one member of the family in watermelon is able to delay climacteric fruit ripening in tomato (Zhou *et al.*, 2020b). When overexpressed in transgenic tomato, *CtERF069* is able to delay flowering time, fruit set and fruit ripening, having the bigger effect in flowering time with a delay of around three weeks (Zhou *et al.*, 2020b). In melon, *CmERF110* has been reported to control sex determination, acting as a mediator between ethylene and sex-determination genes (Tao *et al.*, 2018), but no other *ERF* has been described. In other crops, a set of *ERFs* regulates different traits related with fruit ripening (Zhai *et al.*, 2022). In banana, *MaERF9* is able to control aroma production and softening interacting with another transcription factor, *MaDof23* (Feng *et al.*, 2016). In apple, a set of *ERFs* are controlling secondary metabolism related with fruit ripening, as accumulation of carotenoids and anthocyanins (Zhang *et al.*, 2018; Ma *et al.*, 2021; Dang *et al.*, 2021). Apart from these *AP2/ERF* regulating specific ripening-related traits, there are others with a more general effect. In apple, banana and peach, several *ERFs* are able to target ethylene biosynthetic genes, producing a wider effect in fruit ripening (Yue *et al.*, 2020; Xiao *et al.*, 2013; Guo *et al.*, 2021). An *AP2* TF has also been characterized as a major regulator of fruit ripening in tomato, *SlAP2a* (Karlova *et al.*, 2011). *SlAP2a* is expressed at the onset of ripening in tomato (breaker stage), presenting a similar expression pattern as *CmERF024*. With an RNAi approach, this gene was found to delay fruit ripening, but increasing ethylene production levels (Karlova *et al.*, 2011). Of all the *AP2* and *AP2/ERF* transcription factors mentioned before, none of them seems to have an analogous function as *CmERF024*. Some of them interact directly with ethylene biosynthetic genes, producing a quick and general response, while *CmERF024* did not target ethylene biosynthetic genes, according to DAP-seq data, and

presented a slower response (some lines presented a delay of more than 10 days from *CmERF024* expression to the ethylene peak). Other *ERFs* were only affecting certain ripening-related traits, while our candidate gene is affecting the entire ripening process.

In *Arabidopsis*, *ERFs* are known to bind *GCC boxes* and *dehydration responsive elements (DRE)* (Fujimoto *et al*, 2000; Müller and Munné-Bosch 2015). *HARDY*, the closest homolog of *CmERF024* in *Arabidopsis*, is part of the *DREB* subfamily. Some members of this subfamily can bind the *C-repeat (CRT)* element or *DRE*, being their sequences *GCCGAC* and *ACCGAC*, respectively (Eini *et al*, 2013; Agarwal *et al*, 2017). The consensus binding motif for *CmERF024* in the melon genome was *RCCGDC* (Figure 2.S4), being consistent with the previous reported results in *Arabidopsis*.

Other families of transcription factors have been also related with fruit ripening in several species. A *MADS-box* transcription factor is known as one of the main regulators of tomato fruit ripening (Vrebalov *et al*, 2002; Li *et al*, 2020b). When mutated or silenced, *SIMADS-RIN* triggers a ripening inhibition, delaying carotenoid accumulation. Central roles of *MADS* transcription factors have been observed in other climacteric species like banana or papaya (Liu *et al*, 2021; Fu *et al*, 2021). Also, *NAC* transcription factors have been related with fruit development and ripening. One member of the *NAC* family, *nor*, has a central role in controlling tomato fruit ripening (Gao *et al*, 2020; Wang *et al*, 2020), and other *NAC* transcription factors also have effects in this process (Zhu *et al*, 2014; Ma *et al*, 2014). In melon, the ortholog of *nor* has been also characterized as essential for fruit ripening (Liu *et al*, 2022a), and with different effects depending on the allelic variability (Rios *et al*, 2017; Pereira *et al*, 2021; Santo Domingo *et al*, 2022). There are *NAC* transcription factors related with climacteric ripening in other species, like banana (Shan *et al*, 2014) and peach (Pirone *et al*, 2013). Another main controller of fruit ripening in tomato is *cnr*, also encoding a transcription factor (Lai *et al*, 2020; Wang *et al*, 2020). The role of transcription factors seems to be conserved among different fruit crops, as seen in the case of *NAC* and *MADS* families, being key regulators of fruit ripening in several plant species.

The interactions between these transcription factors have been also addressed. In the case of tomato, *SIMADS-RIN* interacts physically with transcription factors *FUL1/2* and *TAGL1* to control both ethylene-dependent and ethylene-independent fruit ripening processes (Fujisawa *et al*, 2014), and different key regulators of fruit ripening interact epistatically in tomato (Wang *et al*, 2020) and melon (Santo Domingo *et al*, 2022).

In summary, the role of transcription factors in the regulation of fruit ripening has been widely addressed in different species pointing out their great importance in this process, as we also show in the present study.

Epigenomic changes regulate fruit ripening processes in melon and other species

With our DAP-seq analysis we found a list of High Confident Targets that are putatively controlled by *CmERF024* (Table 2.2), some of them also validated in the ILs PS8.2 and VED8.2 (Figure 2.S5).

With the GO analysis we detected several significant terms related with DNA or chromatin organization (as GO:0032392, GO:0071103 or GO:0006259) (Figure 2.5) (Table 2.S10, Table 2.S11) due to the presence, among others, of two histones *H2A*, one *H3*, one *H4* and one *H2B*. These results suggest an important role of *CmERF024* in DNA and chromatin organization at the onset of fruit ripening in melon. *CmERF024* seems to be able to bind to the promoter of at least one variant of each of the histone types (with the exception of the *H1* histone), suggesting its participation in the epigenomic changes happening at the onset of ripening by directly controlling their expression. These proteins form octamers that act as the core of nucleosomes (Luger *et al*, 1997). In melon there are eleven genes encoding histones *H2A*, eight *H2B*, seven *H3* and thirteen *H4*, many of them having a similar expression profile as *CmERF024* (seven *H2A*, seven *H2B*, four *H3* and six *H4*) (Additional file 2.1), suggesting a significant role of these proteins and chromatin during climacteric ripening. Histone variants can directly impact the properties of the nucleosome, affecting transcription (Lei & Berger, 2020). Specifically, some histone variants have been studied. Histone *H2A* variant *H2A.Z* can modulate flowering time and thermosensory response in *Arabidopsis* (Kummar & Wiggem 2010; Jarillo & Piñeiro, 2015) and carotenoid biosynthesis in tomato during fruit ripening (Yang *et al*, 2021). Histone *H2B* variants are less studied, but they seem to be associated with different developmental stages (Jiang *et al*, 2020). In the case of histone *H3* variants, *H3.3* has been correlated with increased gene expression by binding at the 3' end of genes, while *H3.1* did not show this correlation, indicating different roles in coordinating the transcriptomic changes during plant development (Wollman *et al*, 2012). Also, *H3* variants are key in epigenetic reprogramming in sperm cells (Borg *et al*, 2020). All these studies agree that histone variants in plants are crucial factors for the regulation of transcriptomic and epigenomic changes that happen along plant development.

Epigenomic modifications have been proved to regulate plant development and fruit ripening. Histones can suffer post-translational modifications to modulate their effect. They can be methylated, acetylated, phosphorylated, ubiquitinated, etc. (Patel & Wang, 2013). These modifications have been reported to regulate fruit ripening in the plant model tomato. Removing H3K27 (one of the most common modifications in histones) facilitates fruit ripening by activation of ripening related genes (Li *et al*, 2020). The histone deacetylase *SIHAF1* is also important in tomato fruit ripening (Aiese Cigliano *et al*, 2013), as well as histone deacetylation (Guo *et al*, 2017). In melon, post-translational histone modifications have been associated with flower development (Lastrasse *et al*, 2017).

Another of the main epigenomic modifications is DNA methylation. In tomato, there is a general demethylation during ripening, governed, at least partially, by *SIDML2* (Liu *et al*, 2015b, Lang *et al*, 2017). In melon, this general demethylation has also been observed, governed in this case by *CmROSI* (Giordano *et al*, 2022). In other crops, general changes in methylation status of DNA have also been addressed. In strawberry, hypomethylation has also been observed during fruit ripening (Cheng *et al*, 2018), and in sweet orange the behavior is opposite, observing a global hypermethylation during ripening (Huang *et al*, 2019). Hypermethylation of specific loci causes significant changes in fruit ripening. The *cnr* phenotype in tomato, addressed before, is caused by the hypermethylation of the upstream part of the gene *SICNR* (Manning *et al*, 2006), considered a key regulator of climacteric fruit ripening in this crop.

The demethylase governing the hypomethylation in tomato, *SIDML2* is at the same time regulated by another epigenomic regulation, N⁶-Methyladenosine. This modification is made in mRNA in eukaryotes, affecting mRNA stability, splicing and nuclear export, among other processes (Shao *et al*, 2021), thus modulating plant development. This type of modification regulates *SIDML2* mRNA, increasing its stability and promoting tomato fruit ripening (Zhou *et al*, 2019).

To further confirm the effect of *CmERF024* in the regulation of chromatin structure, more experimental research need to be performed comparing the knock-out lines and the wild-type. A first step of quantification of the different histones, at expression and protein level, would help to prove our hypothesis of a histone replacement at the onset of climacteric ripening. A coupled chromatin accessibility assay, as ATAC-seq, could help

to understand these roles of histones during melon fruit ripening, expanding the knowledge about the importance of epigenomic factors in the process.

CmERF024 acts in the crosstalk of plant hormones, transcription factors and epigenomic modifications at the onset of ripening

With our results, we have demonstrated that *CmERF024* is one of the key regulators of fruit ripening in melon. Expressed at the onset of fruit ripening (around 30 DAP), this transcription factor controls the expression of different histones and DNA-related proteins. Using different natural alleles we can alter fruit ripening, and with a knock-out allele we can considerably delay fruit ripening in a climacteric variety.

With this work, we hypothesize *CmERF024* as one of the main regulators of fruit ripening acting at the switch from system 1 to system 2 of ethylene production, somehow participating in a change in the structure of chromatin allowing climacteric ripening to take place. *CmERF024* would function as a central point in the crosstalk between hormone regulation, transcription factors and epigenomic changes, three of the main factors that have been demonstrated to regulate fruit ripening in many fruit crops.

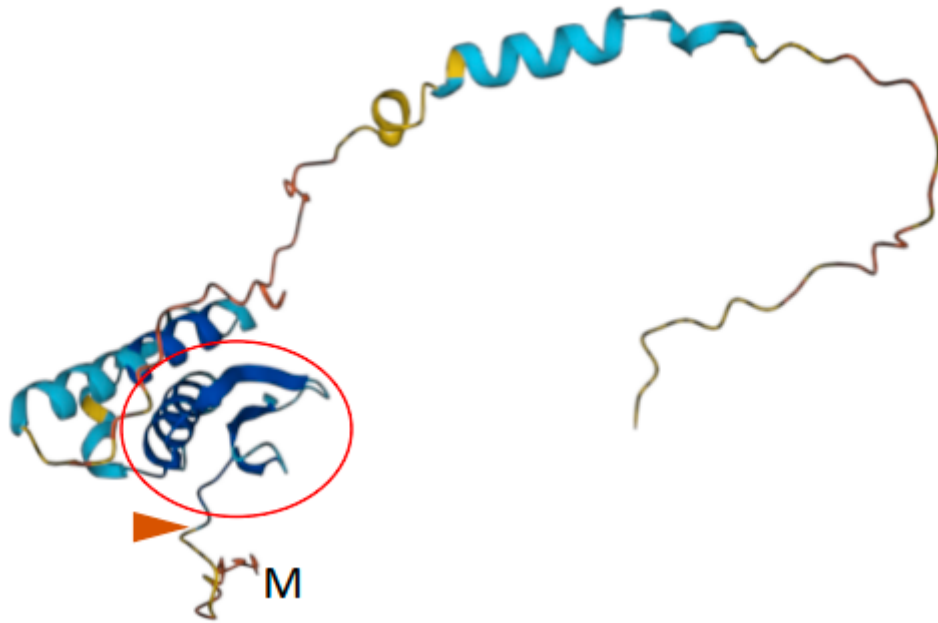


Figure 2.S3. Predicted protein structure of *CmERF024* using ‘AlphaFold’ (Jumper *et al*, 2021), indicating with a circle the conserved AP2/ERF DNA binding domain and with a triangle the position of the guide RNA for CRISPR/*Cas9* gene editing.

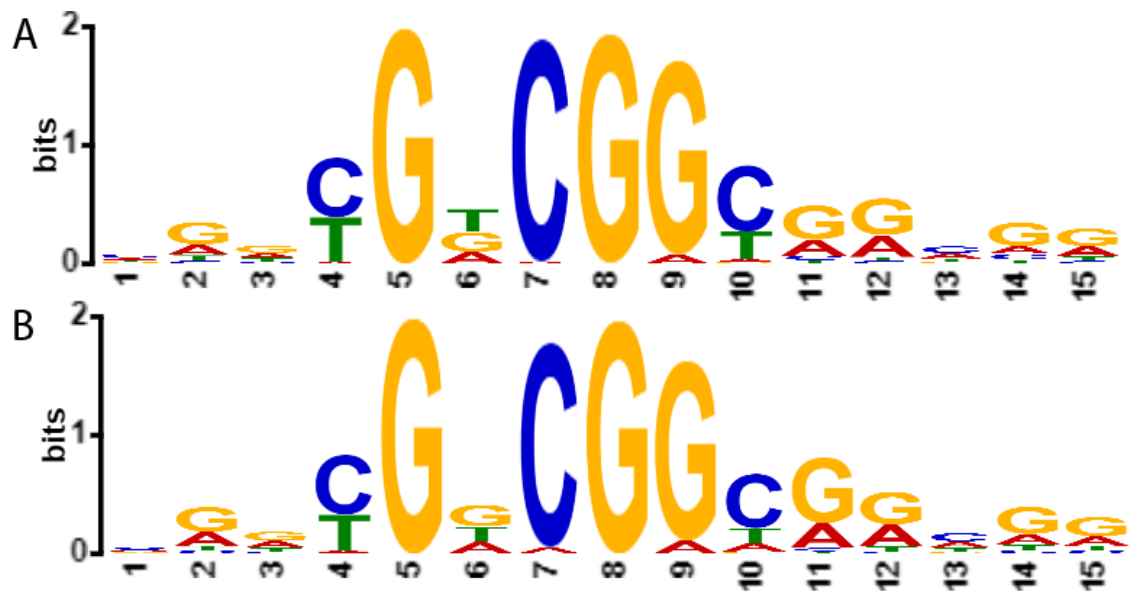


Figure 2.S4. Consensus binding motif of *CmERF024* in **A)** ‘Védrantais’ and **B)** ‘Piel de Sapo’ genome.

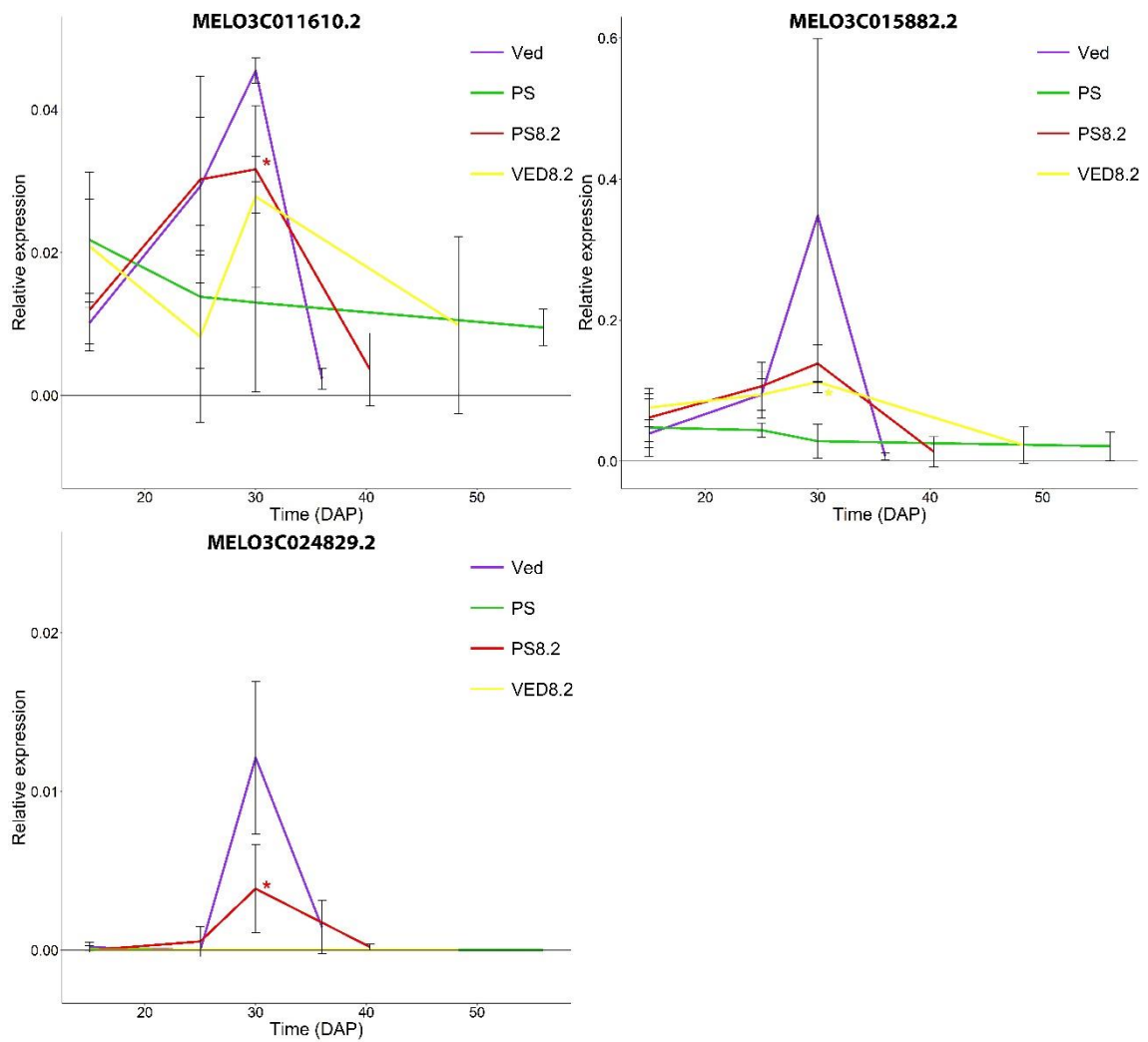


Figure 2.S5. Relative expression by qRT-PCR of three high confident targets of *CmERF024* in the parental lines ‘Védrantais’ and ‘Piel de Sapo’ and the introgression lines (ILs) PS8.2 and VED8.2 during fruit development: **A)** MELO3C011610.2, **B)** MELO3C015882.2 and **C)** MELO3C024829.2. Asterisks show significant difference between the IL and its recurrent parental line.

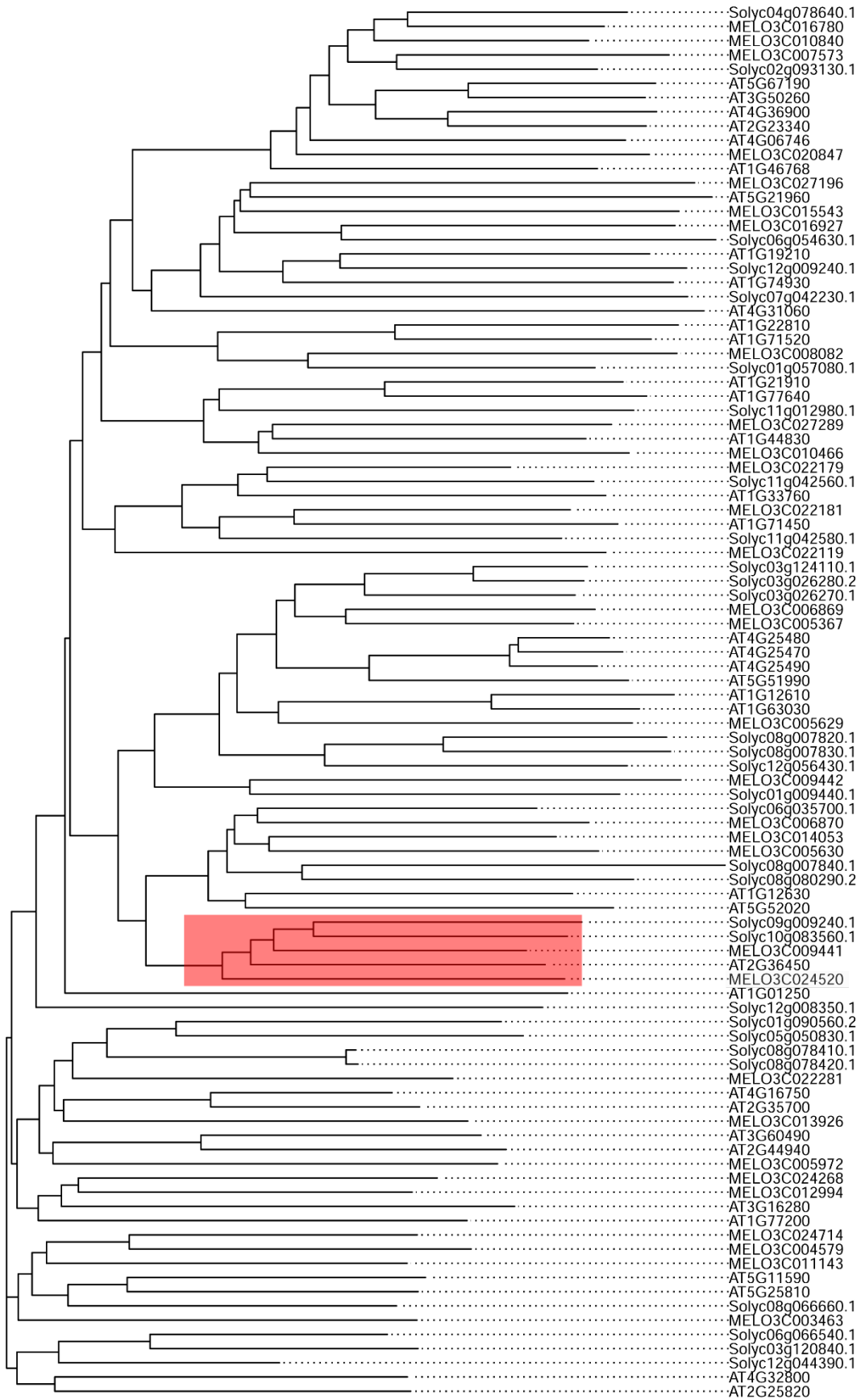


Figure 2.S6. Phylogenetic tree of the homologous gene family members of *CmERF024* (MEL03C024520) in melon, tomato and Arabidopsis. In red, the clade of *CmERF024*.

Tables**Table 2.S3.** Summary of the trimmed and uniquely aligned reads in the melon reference genome v4.0 in the DAP-seq experiment.

Sample	Genotype	Raw reads	Trimmed reads	Aligned paired reads
PS-1	PS	52843880	38229794	8542960
PS-2	PS	52981144	51745958	16485146
Ved-1	Ved	51612334	43974758	10086022
Ved-2	Ved	41605280	36771672	8902298
input_PS-1	PS	14864460	14327772	4428667
input_PS-2	PS	12106862	11885028	4226501
input_Ved-1	Ved	40130934	38496964	10627294
input_Ved-2	Ved	61628588	58044350	17666593

Table 2.S4. Summary of the alignment in the resequenced recombinant lines R14-F3, R15-F3 and R68-F3.

Sample	Raw reads	Filtered mapped reads	Average read length	Average depth	Median depth	% average coverage (>=1 read)	% average coverage (>=5 reads)
R14-F3	80293746	61,756,740	150	41.4	21.5	93.2	91.3
R15-F3	80055540	61,354,207	150	38.1	21.1	93.3	91.3
R68.F3	80211002	60,836,492	150	39.3	21.2	93.1	91

Table 2.S6. Different alleles in each position of *ETHQV8.1* using both resequencing data and SNPs markers of the resequenced families.

		Position in chromosome 8 (v4.0)																			
Line	Data	8625397	8647778	8649833	8651955	8653612	8656313	8659586	8664994	8672741	8716754	8730225	8734764	8737037	8741937	8747095	8768252	8773190	8791258	8798196	8807601
R14-F3	Resequencing	PS	PS	PS	PS	Ved	Ved	Ved	Ved	Ved	Ved	Ved	Ved	Ved	Ved	Ved	Ved	Ved	Ved	Ved	Ved
	SNPs	PS	PS	PS	PS	Ved	Ved	Ved	Ved	Ved	Ved	Ved	Ved	Ved	Ved	Ved	Ved	Ved	Ved	Ved	Ved
R68-F3	Resequencing	Ved	Ved	PS	PS	PS	PS	PS	PS	PS	PS	PS	PS	PS	PS	PS	PS	PS	PS	PS	PS
	SNPs	Ved	Ved	PS	PS	PS	PS	PS	PS	PS	PS	PS	PS	PS	PS	PS	PS	PS	PS	PS	PS
R15-F3	Resequencing	PS	PS	PS	PS	PS	PS	PS	PS	PS	PS	PS	PS	PS	PS	PS	Ved	Ved	Ved	Ved	Ved
	SNPs	PS	PS	PS	PS	PS	PS	PS	PS	PS	PS	PS	PS	PS	PS	PS	Ved	Ved	Ved	Ved	Ved

Table 2.S7. Structural variants analysis of the resequenced lines R14, R15 and R68, and PS8.2.

Chromosome	Position v4.0	Reference allele	Alternative allele	PS8.2	R14-F3	R15-F3	R68-F3
chr08	8647996	G	GAAA	0/0	0/0	0/0	1/1
chr08	8648599	T	TA	0/0	0/0	0/0	1/1
chr08	8648643	TTTC	TGTGTT	0/0	0/0	0/0	1/1
chr08	8648751	ATT	A	0/0	0/0	0/0	1/1
chr08	8648780	TCGTACCC	T	0/0	0/0	0/0	1/1
chr08	8648965	C	CA	0/0	0/0	0/0	1/1
chr08	8652531	C	CTATATATA	0/0	1/1	0/0	0/0

Digital supplementary material

Table 2.S1. List of primers used in this study for: A) genotyping with SNP markers, B) genotyping edited plants, and C) generating the guide RNA used for CRISPR/Cas9 gene editing.

Table 2.S2. Information of the RNA-seq experiment by sample. A) Sample information. B) Raw data obtained in the sequencing. C) Summary of the alignment against the reference melon genome v4.0.

Table 2.S5. Phenotypic data of the analyzed plants. A) Recombinant F2 plants in 2019. B) Recombinant selected F3 families in 2020. C) Recombinant selected F3 families in 2021. D) Parental lines and introgression lines in 2020. E) Controls and T0 knockout plants in Torre Marimon in 2022. F) Controls and T0 knockout plants in CRAG in 2022.

Table 2.S8. Binding peaks found in the DAP-seq experiments in A) ‘Piel de Sapo’ and B) ‘Védrantais’ genome.

Table 2.S9. Expression clusters obtained with WGCNA in the RNA-seq experiment.

Table 2.S10. Significant GO terms found for *CmERF024* co-expression cluster.

Table 2.S11. Significant GO terms found for the HTC gene list (Table 2).

Additional File 2.1. Raw data of the RNA-seq experiment, aligned with STAR against the reference genome v4.0.

Additional File 2.2. FASTA DNA and protein sequences of *CmERF024* in ‘Piel de Sapo’ and ‘Védrantais’.

References

- Agarwal, P. K., Gupta, K., Lopato, S., & Agarwal, P. (2017). Dehydration responsive element binding transcription factors and their applications for the engineering of stress tolerance. *Journal of Experimental Botany*, *68*(9), 2135–2148. <https://doi.org/10.1093/jxb/erx118>
- Aiese Cigliano, R., Sanseverino, W., Cremona, G., Ercolano, M. R., Conicella, C., & Consiglio, F. M. (2013). Genome-wide analysis of histone modifiers in tomato: Gaining an insight into their developmental roles. *BMC Genomics*, *14*(1), 57. <https://doi.org/10.1186/1471-2164-14-57>
- Alseekh, S., Tohge, T., Wendenberg, R., Scossa, F., Omranian, N., Li, J., Kleessen, S., Giavalisco, P., Pleban, T., Mueller-Roeber, B., Zamir, D., Nikoloski, Z., & Fernie, A. R. (2015). Identification and Mode of Inheritance of Quantitative Trait Loci for Secondary Metabolite Abundance in Tomato. *The Plant Cell*, *27*(3), 485–512. <https://doi.org/10.1105/tpc.114.132266>
- Barry, C. S., Llop-Tous, M. I., & Grierson, D. (2000). The Regulation of 1-Aminocyclopropane-1-Carboxylic Acid Synthase Gene Expression during the Transition from System-1 to System-2 Ethylene Synthesis in Tomato. *Plant Physiology*, *123*(3), 979–986. <https://doi.org/10.1104/pp.123.3.979>
- Bartlett, A., O'Malley, R. C., Huang, S. C., Galli, M., Nery, J. R., Gallavotti, A., & Ecker, J. R. (2017). Mapping genome-wide transcription factor binding sites using DAP-seq. *Nature Protocols*, *12*(8), 1659–1672. <https://doi.org/10.1038/nprot.2017.055>
- Borg, M., Jacob, Y., Susaki, D., LeBlanc, C., Buendía, D., Axelsson, E., Kawashima, T., Voigt, P., Boavida, L., Becker, J., Higashiyama, T., Martienssen, R., & Berger, F. (2020). Targeted reprogramming of H3K27me3 resets epigenetic memory in plant paternal chromatin. *Nature Cell Biology*, *22*(6), 621–629. <https://doi.org/10.1038/s41556-020-0515-y>
- Cara, B., & Giovannoni, J. J. (2008). Molecular biology of ethylene during tomato fruit development and maturation. *Plant Science*, *175*(1), 106–113. <https://doi.org/10.1016/j.plantsci.2008.03.021>
- Castelblanque L, Marfa V, Claveria E, Martinez I, Perez-Grau L, Dolcet-sanjuan R. 2008. Improving the genetic transformation efficiency of Cucumis melo subsp. melo

- ‘Piel de Sapo’ via *Agrobacterium*. In: Pitrat M, ed. *Cucurbitaceae 2008*, Proceedings of the IXth EUCARPIA meeting on genetics and breeding of Cucurbitaceae. France: INRA, 627–632.
- Chen, S., Zhou, Y., Chen, Y., & Gu, J. (2018). fastp: An ultra-fast all-in-one FASTQ preprocessor. *Bioinformatics*, 34(17), i884–i890. <https://doi.org/10.1093/bioinformatics/bty560>
- Cheng, J., Niu, Q., Zhang, B., Chen, K., Yang, R., Zhu, J.-K., Zhang, Y., & Lang, Z. (2018). Downregulation of RdDM during strawberry fruit ripening. *Genome Biology*, 19(1), 212. <https://doi.org/10.1186/s13059-018-1587-x>
- Consoli, L., Lefèvre, A., Zivy, M., de Vienne, D., & Damerval, C. (2002). QTL analysis of proteome and transcriptome variations for dissecting the genetic architecture of complex traits in maize. *Plant Molecular Biology*, 48(5), 575–581. <https://doi.org/10.1023/A:1014840810203>
- Dang, Q., Sha, H., Nie, J., Wang, Y., Yuan, Y., & Jia, D. (2021). An apple (*Malus domestica*) AP2/ERF transcription factor modulates carotenoid accumulation. *Horticulture Research*, 8, 223. <https://doi.org/10.1038/s41438-021-00694-w>
- Dobin, A., Davis, C. A., Schlesinger, F., Drenkow, J., Zaleski, C., Jha, S., Batut, P., Chaisson, M., & Gingeras, T. R. (2013). STAR: Ultrafast universal RNA-seq aligner. *Bioinformatics*, 29(1), 15–21. <https://doi.org/10.1093/bioinformatics/bts635>
- Doudna, J. A., & Charpentier, E. (2014). The new frontier of genome engineering with CRISPR-Cas9. *Science*, 346(6213), 1258096. <https://doi.org/10.1126/science.1258096>
- Doyle J (1991) DNA Protocols for Plants. In: Hewitt GM, Johnston AWB, Young JPW (eds) *Molecular Techniques in Taxonomy*. Springer Berlin Heidelberg, Berlin, Heidelberg, pp 283–293
- Eini, O., Yang, N., Pyvovarenko, T., Pillman, K., Bazanova, N., Tikhomirov, N., Eliby, S., Shirley, N., Sivasankar, S., Tingey, S., Langridge, P., Hrmova, M., & Lopato, S. (2013). Complex Regulation by *Apetala2* Domain-Containing Transcription Factors Revealed through Analysis of the Stress-Responsive *TdCor410b*

- Promoter from Durum Wheat. *PLOS ONE*, 8(3), e58713. <https://doi.org/10.1371/journal.pone.0058713>
- Feng, B., Han, Y., Xiao, Y., Kuang, J., Fan, Z., Chen, J., & Lu, W. (2016). The banana fruit Dof transcription factor MaDof23 acts as a repressor and interacts with MaERF9 in regulating ripening-related genes. *Journal of Experimental Botany*, 67(8), 2263–2275. <https://doi.org/10.1093/jxb/erw032>
- Fernandez-Pozo, N., Zheng, Y., Snyder, S. I., Nicolas, P., Shinozaki, Y., Fei, Z., Catala, C., Giovannoni, J. J., Rose, J. K. C., & Mueller, L. A. (2017). The Tomato Expression Atlas. *Bioinformatics*, 33(15), 2397–2398. <https://doi.org/10.1093/bioinformatics/btx190>
- Finkelstein, R. R., Wang, M. L., Lynch, T. J., Rao, S., & Goodman, H. M. (1998). The Arabidopsis abscisic acid response locus ABI4 encodes an APETALA 2 domain protein. *The Plant Cell*, 10(6), 1043–1054.
- Fischer, D. S., Theis, F. J., & Yosef, N. (2018). Impulse model-based differential expression analysis of time course sequencing data. *Nucleic Acids Research*, 46(20), e119. <https://doi.org/10.1093/nar/gky675>
- Fu, C.-C., Chen, H.-J., Gao, H.-Y., Wang, S.-L., Wang, N., Jin, J.-C., Lu, Y., Yu, Z.-L., Ma, Q., & Han, Y.-C. (2021). Papaya CpMADS4 and CpNAC3 co-operatively regulate ethylene signal genes CpERF9 and CpEIL5 during fruit ripening. *Postharvest Biology and Technology*, 175, 111485. <https://doi.org/10.1016/j.postharvbio.2021.111485>
- Fujimoto, S. Y., Ohta, M., Usui, A., Shinshi, H., & Ohme-Takagi, M. (2000). Arabidopsis Ethylene-Responsive Element Binding Factors Act as Transcriptional Activators or Repressors of GCC Box–Mediated Gene Expression. *The Plant Cell*, 12(3), 393–405.
- Fujisawa, M., Shima, Y., Nakagawa, H., Kitagawa, M., Kimbara, J., Nakano, T., Kasumi, T., & Ito, Y. (2014). Transcriptional Regulation of Fruit Ripening by Tomato FRUITFULL Homologs and Associated MADS Box Proteins. *The Plant Cell*, 26(1), 89–101. <https://doi.org/10.1105/tpc.113.119453>
- Galpaz, N., Gonda, I., Shem-Tov, D., Barad, O., Tzuri, G., Lev, S., Fei, Z., Xu, Y., Mao, L., Jiao, C., Harel-Beja, R., Doron-Faigenboim, A., Tzfadia, O., Bar, E., Meir, A.,

- Sa'ar, U., Fait, A., Halperin, E., Kenigswald, M., ... Katzir, N. (2018). Deciphering genetic factors that determine melon fruit-quality traits using RNA-Seq-based high-resolution QTL and eQTL mapping. *The Plant Journal*, *94*(1), 169–191. <https://doi.org/10.1111/tpj.13838>
- Gao, Y., Wei, W., Fan, Z., Zhao, X., Zhang, Y., Jing, Y., Zhu, B., Zhu, H., Shan, W., Chen, J., Grierson, D., Luo, Y., Jemrić, T., Jiang, C.-Z., & Fu, D.-Q. (2020). Re-evaluation of the nor mutation and the role of the NAC-NOR transcription factor in tomato fruit ripening. *Journal of Experimental Botany*, *71*(12), 3560–3574. <https://doi.org/10.1093/jxb/eraa131>
- Giordano, A., Santo Domingo, M., Quadrana, L., Pujol, M., Martín-Hernández, A. M., & Garcia-Mas, J. (2022). CRISPR/Cas9 gene editing uncovers the roles of CONSTITUTIVE TRIPLE RESPONSE 1 and REPRESSOR OF SILENCING 1 in melon fruit ripening and epigenetic regulation. *Journal of Experimental Botany*, *73*(12), 4022–4033. <https://doi.org/10.1093/jxb/erac148>
- Guo, J.-E., Hu, Z., Li, F., Zhang, L., Yu, X., Tang, B., & Chen, G. (2017). Silencing of histone deacetylase SIHDT3 delays fruit ripening and suppresses carotenoid accumulation in tomato. *Plant Science*, *265*, 29–38. <https://doi.org/10.1016/j.plantsci.2017.09.013>
- Guo, Z.-H., Zhang, Y.-J., Yao, J.-L., Xie, Z.-H., Zhang, Y.-Y., Zhang, S.-L., & Gu, C. (2021). The NAM/ATAF1/2/CUC2 transcription factor PpNAC.A59 enhances PpERF.A16 expression to promote ethylene biosynthesis during peach fruit ripening. *Horticulture Research*, *8*, 209. <https://doi.org/10.1038/s41438-021-00644-6>
- Hendelman, A., Zebell, S., Rodriguez-Leal, D., Dukler, N., Robitaille, G., Wu, X., Kostyun, J., Tal, L., Wang, P., Bartlett, M. E., Eshed, Y., Efroni, I., & Lippman, Z. B. (2021). Conserved pleiotropy of an ancient plant homeobox gene uncovered by cis-regulatory dissection. *Cell*, *184*(7), 1724–1739.e16. <https://doi.org/10.1016/j.cell.2021.02.001>
- Hinz, M., Wilson, I. W., Yang, J., Buerstenbinder, K., Llewellyn, D., Dennis, E. S., Sauter, M., & Dolferus, R. (2010). Arabidopsis RAP2.2: An Ethylene Response

- Transcription Factor That Is Important for Hypoxia Survival. *Plant Physiology*, 153(2), 757–772. <https://doi.org/10.1104/pp.110.155077>
- Hu, Z., Shi, X., Chen, X., Zheng, J., Zhang, A., Wang, H., & Fu, Q. (2022). Fine-mapping and identification of a candidate gene controlling seed coat color in melon (*Cucumis melo* L. var. *Chinensis* Pangalo). *Theoretical and Applied Genetics*, 135(3), 803–815. <https://doi.org/10.1007/s00122-021-03999-5>
- Huang, H., Liu, R., Niu, Q., Tang, K., Zhang, B., Zhang, H., Chen, K., Zhu, J.-K., & Lang, Z. (2019). Global increase in DNA methylation during orange fruit development and ripening. *Proceedings of the National Academy of Sciences*, 116(4), 1430–1436. <https://doi.org/10.1073/pnas.1815441116>
- Huang, J., Gao, L., Luo, S., Liu, K., Qing, D., Pan, Y., Dai, G., Deng, G., & Zhu, C. (2022). The genetic editing of GS3 via CRISPR/Cas9 accelerates the breeding of three-line hybrid rice with superior yield and grain quality. *Molecular Breeding*, 42(4), 22. <https://doi.org/10.1007/s11032-022-01290-z>
- Jarillo, J. A., & Piñeiro, M. (2015). H2A.Z mediates different aspects of chromatin function and modulates flowering responses in Arabidopsis. *The Plant Journal*, 83(1), 96–109. <https://doi.org/10.1111/tpj.12873>
- Jiang, D., Borg, M., Lorković, Z. J., Montgomery, S. A., Osakabe, A., Yelagandula, R., Axelsson, E., & Berger, F. (2020). The evolution and functional divergence of the histone H2B family in plants. *PLOS Genetics*, 16(7), e1008964. <https://doi.org/10.1371/journal.pgen.1008964>
- Jumper, J., Evans, R., Pritzel, A., Green, T., Figurnov, M., Ronneberger, O., Tunyasuvunakool, K., Bates, R., Žídek, A., Potapenko, A., Bridgland, A., Meyer, C., Kohl, S. A. A., Ballard, A. J., Cowie, A., Romera-Paredes, B., Nikolov, S., Jain, R., Adler, J., ... Hassabis, D. (2021). Highly accurate protein structure prediction with AlphaFold. *Nature*, 596(7873), 583–589. <https://doi.org/10.1038/s41586-021-03819-2>
- Karaba, A., Dixit, S., Greco, R., Aharoni, A., Trijatmiko, K. R., Marsch-Martinez, N., Krishnan, A., Nataraja, K. N., Udayakumar, M., & Pereira, A. (2007). Improvement of water use efficiency in rice by expression of HARDY, an Arabidopsis drought and salt tolerance gene. *Proceedings of the National*

Academy of Sciences, 104(39), 15270–15275.
<https://doi.org/10.1073/pnas.0707294104>

Karlova, R., Rosin, F. M., Busscher-Lange, J., Parapunova, V., Do, P. T., Fernie, A. R., Fraser, P. D., Baxter, C., Angenent, G. C., & de Maagd, R. A. (2011). Transcriptome and Metabolite Profiling Show That APETALA2a Is a Major Regulator of Tomato Fruit Ripening. *The Plant Cell*, 23(3), 923–941.
<https://doi.org/10.1105/tpc.110.081273>

Katzen, F. (2007). Gateway® recombinational cloning: A biological operating system. *Expert Opinion on Drug Discovery*, 2(4), 571–589.
<https://doi.org/10.1517/17460441.2.4.571>

Kevany, B. M., Tieman, D. M., Taylor, M. G., Cin, V. D., & Klee, H. J. (2007). Ethylene receptor degradation controls the timing of ripening in tomato fruit. *The Plant Journal*, 51(3), 458–467. <https://doi.org/10.1111/j.1365-313X.2007.03170.x>

Kim, D., Paggi, J. M., Park, C., Bennett, C., & Salzberg, S. L. (2019). Graph-based genome alignment and genotyping with HISAT2 and HISAT-genotype. *Nature Biotechnology*, 37(8), 907–915. <https://doi.org/10.1038/s41587-019-0201-4>

Kolberg, L., Raudvere, U., Kuzmin, I., Vilo, J., & Peterson, H. (2020). gprofiler2—An R package for gene list functional enrichment analysis and namespace conversion toolset g:Profiler. *F1000Research*, 9, ELIXIR-709.
<https://doi.org/10.12688/f1000research.24956.2>

Kong, Q., Gao, L., Cao, L., Liu, Y., Saba, H., Huang, Y., & Bie, Z. (2016). Assessment of Suitable Reference Genes for Quantitative Gene Expression Studies in Melon Fruits. *Frontiers in Plant Science*, 7, 1178.
<https://doi.org/10.3389/fpls.2016.01178>

Kou, X., Feng, Y., Yuan, S., Zhao, X., Wu, C., Wang, C., & Xue, Z. (2021). Different regulatory mechanisms of plant hormones in the ripening of climacteric and non-climacteric fruits: A review. *Plant Molecular Biology*, 107(6), 477–497.
<https://doi.org/10.1007/s11103-021-01199-9>

Kumar, S. V., & Wigge, P. A. (2010). H2A.Z-Containing Nucleosomes Mediate the Thermosensory Response in Arabidopsis. *Cell*, 140(1), 136–147.
<https://doi.org/10.1016/j.cell.2009.11.006>

- Lai, T., Wang, X., Ye, B., Jin, M., Chen, W., Wang, Y., Zhou, Y., Blanks, A. M., Gu, M., Zhang, P., Zhang, X., Li, C., Wang, H., Liu, Y., Gallusci, P., Tör, M., & Hong, Y. (2020). Molecular and functional characterization of the SBP-box transcription factor SPL-CNR in tomato fruit ripening and cell death. *Journal of Experimental Botany*, *71*(10), 2995–3011. <https://doi.org/10.1093/jxb/eraa067>
- Lang, Z., Wang, Y., Tang, K., Tang, D., Datsenka, T., Cheng, J., Zhang, Y., Handa, A. K., & Zhu, J.-K. (2017). Critical roles of DNA demethylation in the activation of ripening-induced genes and inhibition of ripening-repressed genes in tomato fruit. *Proceedings of the National Academy of Sciences*, *114*(22), E4511–E4519. <https://doi.org/10.1073/pnas.1705233114>
- Langfelder, P., & Horvath, S. (2008). WGCNA: An R package for weighted correlation network analysis. *BMC Bioinformatics*, *9*(1), 559. <https://doi.org/10.1186/1471-2105-9-559>
- Latrasse, D., Rodriguez-Granados, N. Y., Veluchamy, A., Mariappan, K. G., Bevilacqua, C., Crapart, N., Camps, C., Sommard, V., Raynaud, C., Dogimont, C., Boualem, A., Benhamed, M., & Bendahmane, A. (2017). The quest for epigenetic regulation underlying unisexual flower development in *Cucumis melo*. *Epigenetics & Chromatin*, *10*(1), 22. <https://doi.org/10.1186/s13072-017-0132-6>
- Lei, B., & Berger, F. (2020). H2A Variants in Arabidopsis: Versatile Regulators of Genome Activity. *Plant Communications*, *1*(1), 100015. <https://doi.org/10.1016/j.xplc.2019.100015>
- Li, R., Li, R., Li, X., Fu, D., Zhu, B., Tian, H., Luo, Y., & Zhu, H. (2018). Multiplexed CRISPR/Cas9-mediated metabolic engineering of γ -aminobutyric acid levels in *Solanum lycopersicum*. *Plant Biotechnology Journal*, *16*(2), 415–427. <https://doi.org/10.1111/pbi.12781>
- Li, S.; Zhu, B.; Pirrello, J.; Xu, C.; Zhang, B.; Bouzayen, M.; Chen, K.; Grierson, D. (2020). Roles of RIN and Ethylene in Tomato Fruit Ripening and Ripening-Associated Traits. *New Phytologist*, *226*, 460–475, doi:[10.1111/nph.16362](https://doi.org/10.1111/nph.16362).
- Li, Z., Jiang, G., Liu, X., Ding, X., Zhang, D., Wang, X., Zhou, Y., Yan, H., Li, T., Wu, K., Jiang, Y., & Duan, X. (2020). Histone demethylase SIJMJ6 promotes fruit

- ripening by removing H3K27 methylation of ripening-related genes in tomato. *New Phytologist*, 227(4), 1138–1156. <https://doi.org/10.1111/nph.16590>
- Liao, Y., Smyth, G. K., & Shi, W. (2014). featureCounts: An efficient general purpose program for assigning sequence reads to genomic features. *Bioinformatics*, 30(7), 923–930. <https://doi.org/10.1093/bioinformatics/btt656>
- Licausi, F., Kosmacz, M., Weits, D. A., Giuntoli, B., Giorgi, F. M., Voeselek, L. A. C. J., Perata, P., & van Dongen, J. T. (2011). Oxygen sensing in plants is mediated by an N-end rule pathway for protein destabilization. *Nature*, 479(7373), 419–422. <https://doi.org/10.1038/nature10536>
- Licausi, F., Ohme-Takagi, M., & Perata, P. (2013). APETALA2/Ethylene Responsive Factor (AP2/ERF) transcription factors: Mediators of stress responses and developmental programs. *The New Phytologist*, 199(3), 639–649. <https://doi.org/10.1111/nph.12291>
- Liu, B., Santo Domingo, M., Mayobre, C., Martín-Hernández, A. M., Pujol, M., & Garcia-Mas, J. (2022a). Knock-Out of CmNAC-NOR Affects Melon Climacteric Fruit Ripening. *Frontiers in Plant Science*, 13. <https://www.frontiersin.org/articles/10.3389/fpls.2022.878037>
- Liu, J., Liu, M., Jia, C., Zhang, J., Miao, H., Wang, J., Zhang, J., Wang, Z., Xu, B., Li, X., & Jin, Z. (2021). Elucidating the mechanism of MaGWD1-mediated starch degradation cooperatively regulated by MaMADS36 and MaMADS55 in banana. *Postharvest Biology and Technology*, 179, 111587. <https://doi.org/10.1016/j.postharvbio.2021.111587>
- Liu, M., Pirrello, J., Chervin, C., Roustan, J.-P., & Bouzayen, M. (2015a). Ethylene Control of Fruit Ripening: Revisiting the Complex Network of Transcriptional Regulation1. *Plant Physiology*, 169(4), 2380–2390. <https://doi.org/10.1104/pp.15.01361>
- Liu, R., How-Kit, A., Stammitti, L., Teyssier, E., Rolin, D., Mortain-Bertrand, A., Halle, S., Liu, M., Kong, J., Wu, C., Degraeve-Guibault, C., Chapman, N. H., Maucourt, M., Hodgman, T. C., Tost, J., Bouzayen, M., Hong, Y., Seymour, G. B., Giovannoni, J. J., & Gallusci, P. (2015b). A DEMETER-like DNA demethylase

- governs tomato fruit ripening. *Proceedings of the National Academy of Sciences*, 112(34), 10804–10809. <https://doi.org/10.1073/pnas.1503362112>
- Liu, X., Zhang, S., Jiang, Y., Yan, T., Fang, C., Hou, Q., Wu, S., Xie, K., An, X., & Wan, X. (2022b). Use of CRISPR/Cas9-Based Gene Editing to Simultaneously Mutate Multiple Homologous Genes Required for Pollen Development and Male Fertility in Maize. *Cells*, 11(3), 439. <https://doi.org/10.3390/cells11030439>
- Lu, J., Hou, J., Ouyang, Y., Luo, H., Zhao, J., Mao, C., Han, M., Wang, L., Xiao, J., Yang, Y., & Li, X. (2020). A direct PCR-based SNP marker-assisted selection system (D-MAS) for different crops. *Molecular Breeding*, 40(1), 9. <https://doi.org/10.1007/s11032-019-1091-3>
- Luger, K., Mäder, A. W., Richmond, R. K., Sargent, D. F., & Richmond, T. J. (1997). Crystal structure of the nucleosome core particle at 2.8 Å resolution. *Nature*, 389(6648), 251–260. <https://doi.org/10.1038/38444>
- Ma, H., Yang, T., Li, Y., Zhang, J., Wu, T., Song, T., Yao, Y., & Tian, J. (2021). The long noncoding RNA MdLNC499 bridges MdWRKY1 and MdERF109 function to regulate early-stage light-induced anthocyanin accumulation in apple fruit. *The Plant Cell*, 33(10), 3309–3330. <https://doi.org/10.1093/plcell/koab188>
- Ma, N., Feng, H., Meng, X., Li, D., Yang, D., Wu, C., & Meng, Q. (2014). Overexpression of tomato SINAC1 transcription factor alters fruit pigmentation and softening. *BMC Plant Biology*, 14, 351. <https://doi.org/10.1186/s12870-014-0351-y>
- Manning, K., Tör, M., Poole, M., Hong, Y., Thompson, A. J., King, G. J., Giovannoni, J. J., & Seymour, G. B. (2006). A naturally occurring epigenetic mutation in a gene encoding an SBP-box transcription factor inhibits tomato fruit ripening. *Nature Genetics*, 38(8), 948–952. <https://doi.org/10.1038/ng1841>
- McMurchie, E. J., McGlasson, W. B., & Eaks, I. L. (1972). Treatment of fruit with propylene gives information about the biogenesis of ethylene. *Nature*, 237(5352), 235–236. <https://doi.org/10.1038/237235a0>
- Müller, M., & Munné-Bosch, S. (2015). Ethylene Response Factors: A Key Regulatory Hub in Hormone and Stress Signaling¹. *Plant Physiology*, 169(1), 32–41. <https://doi.org/10.1104/pp.15.00677>

- Nakano, T., Suzuki, K., Fujimura, T., & Shinshi, H. (2006). Genome-Wide Analysis of the ERF Gene Family in Arabidopsis and Rice. *Plant Physiology*, *140*(2), 411–432. <https://doi.org/10.1104/pp.105.073783>
- Nakashima, K., Shinwari, Z. K., Sakuma, Y., Seki, M., Miura, S., Shinozaki, K., & Yamaguchi-Shinozaki, K. (2000). Organization and expression of two Arabidopsis DREB2 genes encoding DRE-binding proteins involved in dehydration- and high-salinity-responsive gene expression. *Plant Molecular Biology*, *42*(4), 657–665. <https://doi.org/10.1023/A:1006321900483>
- Nizan, S., Pashkovsky, K., Miller, G., Amitzur, A., Normantovich, M., Bar-Ziv, A., & Perl-Treves, R. (2020). Functional validation of Fusarium wilt and potyvirus resistance genes in melon. *Acta Horticulturae*, *1294*, 215–220. <https://doi.org/10.17660/ActaHortic.2020.1294.27>
- Pandey, G. K., Grant, J. J., Cheong, Y. H., Kim, B. G., Li, L., & Luan, S. (2005). ABR1, an APETALA2-Domain Transcription Factor That Functions as a Repressor of ABA Response in Arabidopsis. *Plant Physiology*, *139*(3), 1185–1193. <https://doi.org/10.1104/pp.105.066324>
- Patel, D. J., & Wang, Z. (2013). Readout of Epigenetic Modifications. *Annual Review of Biochemistry*, *82*(1), 81–118. <https://doi.org/10.1146/annurev-biochem-072711-165700>
- Pech, J. C., Bouzayen, M., & Latché, A. (2008). Climacteric fruit ripening: Ethylene-dependent and independent regulation of ripening pathways in melon fruit. *Plant Science*, *175*(1), 114–120. <https://doi.org/10.1016/j.plantsci.2008.01.003>
- Pereira, L., Ruggieri, V., Pérez, S., Alexiou, K. G., Fernández, M., Jahrmann, T., Pujol, M., & Garcia-Mas, J. (2018). QTL mapping of melon fruit quality traits using a high-density GBS-based genetic map. *BMC Plant Biology*, *18*(1), 324. <https://doi.org/10.1186/s12870-018-1537-5>
- Pereira, L., Santo Domingo, M., Argyris, J., Mayobre, C., Valverde, L., Martín-Hernández, A. M., Pujol, M., & Garcia-Mas, J. (2021). A novel introgression line collection to unravel the genetics of climacteric ripening and fruit quality in melon. *Scientific Reports*, *11*(1), 11364. <https://doi.org/10.1038/s41598-021-90783-6>

- Pereira, L., Santo Domingo, M., Ruggieri, V., Argyris, J., Phillips, M. A., Zhao, G., Lian, Q., Xu, Y., He, Y., Huang, S., Pujol, M., & Garcia-Mas, J. (2020). Genetic dissection of climacteric fruit ripening in a melon population segregating for ripening behavior. *Horticulture Research*, 7, 187. <https://doi.org/10.1038/s41438-020-00411-z>
- Perpiñá, G., Cebolla-Cornejo, J., Esteras, C., Monforte, A. J., & Picó, B. (2017). ‘MAK-10’: A Long Shelf-life Charentais Breeding Line Developed by Introgression of a Genomic Region from Makuwa Melon. *HortScience*, 52(11), 1633–1638. <https://doi.org/10.21273/HORTSCI12068-17>
- Pirone, R., Eduardo, I., Pacheco, I., Da Silva Linge, C., Miculan, M., Verde, I., Tartarini, S., Dondini, L., Pea, G., Bassi, D., & Rossini, L. (2013). Fine mapping and identification of a candidate gene for a major locus controlling maturity date in peach. *BMC Plant Biology*, 13(1), 166. <https://doi.org/10.1186/1471-2229-13-166>
- Quinet, M., Angosto, T., Yuste-Lisbona, F. J., Blanchard-Gros, R., Bigot, S., Martinez, J.-P., & Lutts, S. (2019). Tomato Fruit Development and Metabolism. *Frontiers in Plant Science*, 10. <https://www.frontiersin.org/articles/10.3389/fpls.2019.01554>
- R Core Team (2020). R: A language and environment for statistical computing. R Foundation for Statistical Computing, Vienna, Austria. URL <https://www.R-project.org/>.
- Ríos, P., Argyris, J., Vegas, J., Leida, C., Kenigswald, M., Tzuri, G., Troadec, C., Bendahmane, A., Katzir, N., Picó, B., Monforte, A. J., & Garcia-Mas, J. (2017). ETHQV6.3 is involved in melon climacteric fruit ripening and is encoded by a NAC domain transcription factor. *The Plant Journal*, 91(4), 671–683. <https://doi.org/10.1111/tpj.13596>
- Romero, F. M., & Gatica-Arias, A. (2019). CRISPR/Cas9: Development and Application in Rice Breeding. *Rice Science*, 26(5), 265–281. <https://doi.org/10.1016/j.rsci.2019.08.001>
- Ruggieri, V., Alexiou, K. G., Morata, J., Argyris, J., Pujol, M., Yano, R., Nonaka, S., Ezura, H., Latrasse, D., Boualem, A., Benhamed, M., Bendahmane, A., Cigliano, R. A., Sanseverino, W., Puigdomènech, P., Casacuberta, J. M., & Garcia-Mas, J.

- (2018). An improved assembly and annotation of the melon (*Cucumis melo* L.) reference genome. *Scientific Reports*, 8(1), 8088. <https://doi.org/10.1038/s41598-018-26416-2>
- Sakuma, Y., Liu, Q., Dubouzet, J. G., Abe, H., Shinozaki, K., & Yamaguchi-Shinozaki, K. (2002). DNA-Binding Specificity of the ERF/AP2 Domain of Arabidopsis DREBs, Transcription Factors Involved in Dehydration- and Cold-Inducible Gene Expression. *Biochemical and Biophysical Research Communications*, 290(3), 998–1009. <https://doi.org/10.1006/bbrc.2001.6299>
- Saladié, M., Cañizares, J., Phillips, M. A., Rodriguez-Concepcion, M., Larrigaudière, C., Gibon, Y., Stitt, M., Lunn, J. E., & Garcia-Mas, J. (2015). Comparative transcriptional profiling analysis of developing melon (*Cucumis melo* L.) fruit from climacteric and non-climacteric varieties. *BMC Genomics*, 16(1), 440. <https://doi.org/10.1186/s12864-015-1649-3>
- Santo Domingo, M., Areco, L., Mayobre, C., Valverde, L., Martín-Hernández, A. M., Pujol, M., & Garcia-Mas, J. (2022). Modulating climacteric intensity in melon through QTL stacking. *Horticulture Research*, 9, uhac131. <https://doi.org/10.1093/hr/uhac131>
- Schimpl, S., & Puchta, H. (2016). Revolutionizing plant biology: Multiple ways of genome engineering by CRISPR/Cas. *Plant Methods*, 12(1), 8. <https://doi.org/10.1186/s13007-016-0103-0>
- Shan, W., Kuang, J.-F., Lu, W.-J., & Chen, J.-Y. (2014). Banana fruit NAC transcription factor MaNAC1 is a direct target of MaICE1 and involved in cold stress through interacting with MaCBF1. *Plant, Cell & Environment*, 37(9), 2116–2127. <https://doi.org/10.1111/pce.12303>
- Shao, Y., Wong, C. E., Shen, L., & Yu, H. (2021). N6-methyladenosine modification underlies messenger RNA metabolism and plant development. *Current Opinion in Plant Biology*, 63, 102047. <https://doi.org/10.1016/j.pbi.2021.102047>
- Sun, J.-H., Luo, J.-J., Tian, L., Li, C.-L., Xing, Y., & Shen, Y.-Y. (2013). New Evidence for the Role of Ethylene in Strawberry Fruit Ripening. *Journal of Plant Growth Regulation*, 32(3), 461–470. <https://doi.org/10.1007/s00344-012-9312-6>

- Tao, Q., Niu, H., Wang, Z., Zhang, W., Wang, H., Wang, S., Zhang, X., & Li, Z. (2018). Ethylene responsive factor ERF110 mediates ethylene-regulated transcription of a sex determination-related orthologous gene in two Cucumis species. *Journal of Experimental Botany*, *69*(12), 2953–2965. <https://doi.org/10.1093/jxb/ery128>
- Vegas, J., Garcia-Mas, J., & Monforte, A. J. (2013). Interaction between QTLs induces an advance in ethylene biosynthesis during melon fruit ripening. *TAG. Theoretical and Applied Genetics. Theoretische Und Angewandte Genetik*, *126*(6), 1531–1544. <https://doi.org/10.1007/s00122-013-2071-3>
- Vrebalov, J., Ruezinsky, D., Padmanabhan, V., White, R., Medrano, D., Drake, R., Schuch, W., & Giovannoni, J. (2002). A MADS-Box Gene Necessary for Fruit Ripening at the Tomato Ripening-Inhibitor (Rin) Locus. *Science*, *296*(5566), 343–346. <https://doi.org/10.1126/science.1068181>
- Wang, J., Tian, S., Yu, Y., Ren, Y., Guo, S., Zhang, J., Li, M., Zhang, H., Gong, G., Wang, M., & Xu, Y. (2022). Natural variation in the NAC transcription factor NONRIPENING contributes to melon fruit ripening. *Journal of Integrative Plant Biology*, *n/a*(n/a). <https://doi.org/10.1111/jipb.13278>
- Wang, R., Angenent, G. C., Seymour, G., & Maagd, R. A. de. (2020). Revisiting the Role of Master Regulators in Tomato Ripening. *Trends in Plant Science*, *25*(3), 291–301. <https://doi.org/10.1016/j.tplants.2019.11.005>
- Wang, T., Zhang, H., & Zhu, H. (2019). CRISPR technology is revolutionizing the improvement of tomato and other fruit crops. *Horticulture Research*, *6*. <https://doi.org/10.1038/s41438-019-0159-x>
- Wen, J., Jiang, F., Weng, Y., Sun, M., Shi, X., Zhou, Y., Yu, L., & Wu, Z. (2019). Identification of heat-tolerance QTLs and high-temperature stress-responsive genes through conventional QTL mapping, QTL-seq and RNA-seq in tomato. *BMC Plant Biology*, *19*(1), 398. <https://doi.org/10.1186/s12870-019-2008-3>
- Wessler, S. R. (2005). Homing into the origin of the AP2 DNA binding domain. *Trends in Plant Science*, *10*(2), 54–56. <https://doi.org/10.1016/j.tplants.2004.12.007>
- Wollmann, H., Holec, S., Alden, K., Clarke, N. D., Jacques, P.-É., & Berger, F. (2012). Dynamic Deposition of Histone Variant H3.3 Accompanies Developmental

- Remodeling of the Arabidopsis Transcriptome. *PLOS Genetics*, 8(5), e1002658. <https://doi.org/10.1371/journal.pgen.1002658>
- Xiao, Y., Chen, J., Kuang, J., Shan, W., Xie, H., Jiang, Y., & Lu, W. (2013). Banana ethylene response factors are involved in fruit ripening through their interactions with ethylene biosynthesis genes. *Journal of Experimental Botany*, 64(8), 2499–2510. <https://doi.org/10.1093/jxb/ert108>
- Yang, X., Zhang, X., Yang, Y., Zhang, H., Zhu, W., & Nie, W.-F. (2021). The histone variant Sl_H2A.Z regulates carotenoid biosynthesis and gene expression during tomato fruit ripening. *Horticulture Research*, 8(1), 1–17. <https://doi.org/10.1038/s41438-021-00520-3>
- Yano, R.; Ariizumi, T.; Nonaka, S.; Kawazu, Y.; Zhong, S.; Mueller, L.; Giovannoni, J.J.; Rose, J.K.C.; Ezura, H. Comparative Genomics of Muskmelon Reveals a Potential Role for Retrotransposons in the Modification of Gene Expression. *Commun Biol* 2020, 3, 1–13, doi:10.1038/s42003-020-01172-0.
- Yu, C.-P., Lin, J.-J., & Li, W.-H. (2016). Positional distribution of transcription factor binding sites in Arabidopsis thaliana. *Scientific Reports*, 6(1), 25164. <https://doi.org/10.1038/srep25164>
- Yu, Z.-X., Li, J.-X., Yang, C.-Q., Hu, W.-L., Wang, L.-J., & Chen, X.-Y. (2012). The Jasmonate-Responsive AP2/ERF Transcription Factors AaERF1 and AaERF2 Positively Regulate Artemisinin Biosynthesis in Artemisia annua L. *Molecular Plant*, 5(2), 353–365. <https://doi.org/10.1093/mp/ssr087>
- Yue, P., Lu, Q., Liu, Z., Lv, T., Li, X., Bu, H., Liu, W., Xu, Y., Yuan, H., & Wang, A. (2020). Auxin-activated MdARF5 induces the expression of ethylene biosynthetic genes to initiate apple fruit ripening. *New Phytologist*, 226(6), 1781–1795. <https://doi.org/10.1111/nph.16500>
- Zhai, Y., Fan, Z., Cui, Y., Gu, X., Chen, S., & Ma, H. (2022). APETALA2/ethylene responsive factor in fruit ripening: Roles, interactions and expression regulation. *Frontiers in Plant Science*, 13. <https://www.frontiersin.org/articles/10.3389/fpls.2022.979348>
- Zhang, J., Xu, H., Wang, N., Jiang, S., Fang, H., Zhang, Z., Yang, G., Wang, Y., Su, M., Xu, L., & Chen, X. (2018). The ethylene response factor MdERF1B regulates

- anthocyanin and proanthocyanidin biosynthesis in apple. *Plant Molecular Biology*, 98(3), 205–218. <https://doi.org/10.1007/s11103-018-0770-5>
- Zhang, Z., Zhang, H., Quan, R., Wang, X.-C., & Huang, R. (2009). Transcriptional Regulation of the Ethylene Response Factor LeERF2 in the Expression of Ethylene Biosynthesis Genes Controls Ethylene Production in Tomato and Tobacco. *Plant Physiology*, 150(1), 365–377. <https://doi.org/10.1104/pp.109.135830>
- Zhou, H., Zhao, L., Yang, Q., Amar, M. H., Ogotu, C., Peng, Q., Liao, L., Zhang, J., & Han, Y. (2020a). Identification of EIL and ERF Genes Related to Fruit Ripening in Peach. *International Journal of Molecular Sciences*, 21(8), 2846. <https://doi.org/10.3390/ijms21082846>
- Zhou, L., Tian, S., & Qin, G. (2019). RNA methylomes reveal the m6A-mediated regulation of DNA demethylase gene SIDML2 in tomato fruit ripening. *Genome Biology*, 20(1), 156. <https://doi.org/10.1186/s13059-019-1771-7>
- Zhou, M., Guo, S., Tian, S., Zhang, J., Ren, Y., Gong, G., Li, C., Zhang, H., & Xu, Y. (2020b). Overexpression of the Watermelon Ethylene Response Factor CIERF069 in Transgenic Tomato Resulted in Delayed Fruit Ripening. *Horticultural Plant Journal*, 6(4), 247–256. <https://doi.org/10.1016/j.hpj.2020.05.004>
- Zhu, M., Chen, G., Zhang, J., Zhang, Y., Xie, Q., Zhao, Z., Pan, Y., & Hu, Z. (2014). The abiotic stress-responsive NAC-type transcription factor SINAC4 regulates salt and drought tolerance and stress-related genes in tomato (*Solanum lycopersicum*). *Plant Cell Reports*, 33(11), 1851–1863. <https://doi.org/10.1007/s00299-014-1662-z>

Chapter 3

Epistatic interaction among QTLs modulates fruit ripening
in both climacteric and non-climacteric genetic
backgrounds

Background

Quantitative traits are known to be controlled by several interacting QTLs. The availability of different introgression line populations sharing genetic background allows the mendelization of QTLs and their stacking through marker assisted selection, thus minimizing the effect of the genetic background. The previous characterization of two ripening-related QTLs in the ‘Piel de Sapo’ non-climacteric background, *ETHQB3.5* and *ETHQV6.3*, and one QTL in the ‘Védrantais’ climacteric background, *MAK10*, provides powerful material that we can apply in studying the effect of *ETHQV8.1* in both genetic backgrounds. The stacking of the different fruit ripening QTLs in both genetic backgrounds allows us to study the role of the QTLs, as well as their interactions, in modulating fruit ripening.

Results

In both IL populations, *ETHQV8.1* interacts epistatically with the other QTLs to modulate fruit ripening, affecting both ethylene production and related traits. In the ‘Piel de Sapo’ non-climacteric background, *ETHQB3.5*, *ETHQV6.3* and *ETHQV8.1* promoted a climacteric behavior by themselves at different levels, also displaying two-by-two interactions to modulate fruit ripening covering a wide range of behaviors. These QTLs presented specific roles during ripening. *ETHQB3.5* accelerated the ethylene peak, while *ETHQV6.1* advanced the ethylene production. In the case of *ETHQV8.1*, it was enhancing the effect of the other two ripening-related QTLs. In the ‘Védrantais’ climacteric background, *ETHQV8.1* was also interacting epistatically with *MAK10.1*, covering also a wide range of ripening behavior in this genetic background. While *ETHQV8.1* was delaying and decreasing the ethylene peak, *MAK10.1* was totally disrupting its shape with drastic effects in fruit quality.

Conclusions

Although ripening behavior in melon is a complex quantitative trait, we demonstrated that a few major QTLs interacting epistatically can modulate it, covering a wide range of behaviors. In both genetic backgrounds, we were able to develop lines with extreme opposite behaviors: a very early and harsh climacteric line from the non-climacteric ‘Piel de Sapo’, and a very late and smooth climacteric line from the climacteric ‘Védrantais’.

Chapter 3.1

Modulating climacteric intensity in melon through QTL
stacking

Modulating climacteric intensity in melon through QTL stacking

Miguel Santo Domingo¹, Lorena Areco¹, Carlos Mayobre¹, Laura Valverde¹, Ana Montserrat Martín-Hernández^{1,2}, Marta Pujol^{1,2*}, Jordi Garcia-Mas^{1,2*}

¹Centre for Research in Agricultural Genomics (CRAG) CSIC-IRTA-UAB-UB, Edifici CRAG, Campus UAB, 08193 Bellaterra, Barcelona, Spain

²Institut de Recerca i Tecnologia Agoralimentàries (IRTA), Edifici CRAG, Campus UAB, 08193 Bellaterra, Barcelona, Spain

***Corresponding authors**

Miguel Santo Domingo, miguel.santodomingo@cragenomica.es

Lorena Areco, lorena.areco@cragenomica.es

Carlos Mayobre, carlos.mayobre@cragenomica.es

Laura Valverde, laura.valverde@cragenomica.es

Ana Montserrat Martín-Hernández, montse.martin@irta.cat

Jordi Garcia-Mas, jordi.garcia@irta.cat

Marta Pujol, marta.pujol@irta.cat

***Corresponding authors**

Jordi Garcia-Mas, jordi.garcia@irta.cat Phone: +34 935636600

Marta Pujol, marta.pujol@irta.cat Phone: +34 935636600

Horticulture Research, Volume 9, 2022, uhac131, <https://doi.org/10.1093/hr/uhac131>

Abstract

Fruit ripening is one of the main processes affecting fruit quality and shelf-life. In melon there are both climacteric and non-climacteric genotypes, making it a suitable species to study fruit ripening. In the current study, in order to fine tune ripening, we have pyramided three climacteric QTLs in the non-climacteric genotype “Piel de Sapo”: *ETHQB3.5*, *ETHQV6.3* and *ETHQV8.1*. The results showed that the three QTLs interact epistatically, affecting ethylene production and ripening-related traits such as aroma profile. Each individual QTL has a specific role in the ethylene production profile. *ETHQB3.5* accelerates the ethylene peak, *ETHQV6.3* advances the ethylene production and *ETHQV8.1* enhances the effect of the other two QTLs. Regarding aroma, the three QTLs independently activated the production of esters changing the aroma profile of the fruits, with no significant effects in fruit firmness, soluble solid content and fruit size. Understanding the interaction and the effect of different ripening QTLs offers a powerful knowledge for candidate gene identification as well as for melon breeding programs, where fruit ripening is one of the main objectives.

Keywords

Fruit ripening, ethylene, melon, QTL, breeding.

Running head

QTL stacking allows to fine-tune ripening in melon fruits.

Introduction

Fruit development is one of the most important and energy-consuming processes during plant development. Ripening is the last step of this process, producing several biochemical and physiological changes in the fruit and making it attractive for animal and human consumption. Moreover, ripening has a significant role in plant breeding as it has a major effect in fruit shelf-life and fruit quality. During this process, fruits undergo several changes, such as softening due to cell wall degradation or accumulation of pigments (Seymour *et al*, 2002; Prassana *et al*, 2007; Giovannoni, 2007). These changes happen in both climacteric and non-climacteric fruits. The difference between both types is the presence of a peak in ethylene production coupled to an increase in the respiration rate in the climacteric ones, or its absence in the non-climacteric (Giovannoni, 2004). The classical model organism to study fruit ripening has generally been tomato, due to the availability of several mutants with delayed or failed climacteric ripening (Giovannoni, 2007); but, as tomato is a climacteric fruit, there is much less information about non-climacteric ripening.

Melon (*Cucumis melo* L.) has emerged as an interesting model to study fruit ripening, as it has both climacteric and non-climacteric varieties within the same species (Ezura & Owino, 2008). In melon fruits, some ripening traits are dependent on ethylene, as aroma production or abscission layer formation, and other traits are independent, as carotenoid synthesis, sugar accumulation or, partially, flesh softening (Périn *et al*, 20002). Also, the availability of different mapping populations, such as Recombinant Inbred Lines (RILs) (Périn *et al*, 2002; Pereira *et al*, 2018) or Introgression Lines (ILs) (Eduardo *et al*, 2005; Pereira *et al*, 2021), together with sequenced genome (Garcia-Mas *et al*, 2012), makes melon a suitable model for studying both climacteric and non-climacteric fruit ripening.

The availability of IL populations makes possible to mendelize and study QTLs minimizing the effect of the genetic background. These populations have been used as genetic resources for several crops, as tomato (Bernacchi *et al*, 2008), strawberry (Urrutia *et al*, 2017) or peach (Serra *et al*, 2016). In melon, they have been widely used to study different traits, including ripening (Eduardo *et al*, 2005; Pereira *et al*, 2021; Castro *et al*, 2019; Perpiñá *et al*, 2019). In previous studies, two IL populations were used to dissect climacteric ripening in a non-climacteric background. In an IL population with non-climacteric genetic background of Piel de Sapo (PS) and the non-climacteric Songwan Charmi (SC) as donor parent, two QTLs were found triggering a climacteric response

(Moreno *et al*, 2008; Vegas *et al*, 2013). Located in chromosome 3 and 6, they were named *ETHQB3.5* and *ETHQV6.3*, respectively. Besides, in an IL population with the same recurrent parent PS as genetic background, and Védrantais (Ved, climacteric) as donor parent, another major QTL was found, located in chromosome 8 and named *ETHQV8.1* (Pereira *et al*, 2020).

The effect of these QTLs has been previously studied. *ETHQB3.5* was found to provoke the production of a peak of ethylene, compared to PS and SC (Moreno *et al*, 2008; Vegas *et al*, 2013). *ETHQB3.5* is located within the interval 26,000,631 – 28,759,416 bp in chromosome 3 (melon genome v3.6.1) (Pereira, 2018), but the causal gene is still unknown. *ETHQV6.3*, encoded by a *NAC* transcription factor (*MELO3C016540.2*), is also capable of producing a climacteric response in PS, and increase and advance the ethylene production when both *ETHQB3.5* and *ETHQV6.3* alleles from SC are present in PS (Vegas *et al*, 2013). In a climacteric background, *MELO3C016540.2* mutants showed a delayed production of ethylene (Ríos *et al*, 2017). *ETHQV8.1*, located in the interval 9,603,217 – 9,757,373 bp in chromosome 8 (melon genome v3.6.1), has been also studied in both climacteric and non-climacteric genetic backgrounds. In a non-climacteric background, introgressing the climacteric allele produces a climacteric response, and in a climacteric background, introgressing the non-climacteric allele produces a delay and a decrease in ethylene production (Pereira *et al*, 2020). However, we do not know the relationship between these three QTLs when they are combined in the same line and the consequences for melon ripening process and fruit quality.

The aim of this work is to study the effect of three QTLs, *ETHQB3.5*, *ETHQV6.3* and *ETHQV8.1*, in the non-climacteric background of PS and their possible interactions, to further modulate the climacteric response and associated traits happening during melon fruit ripening.

Results

Fruit ripening behavior and fruit quality of the parental lines

The three parental lines used in this study had different fruit ripening behavior (Figure 3.1.1). Piel de Sapo (PS) is a Spanish variety, belonging to *melo* subspecies and *inodorous* group. It produced a low amount of ethylene, insufficient to trigger the climacteric

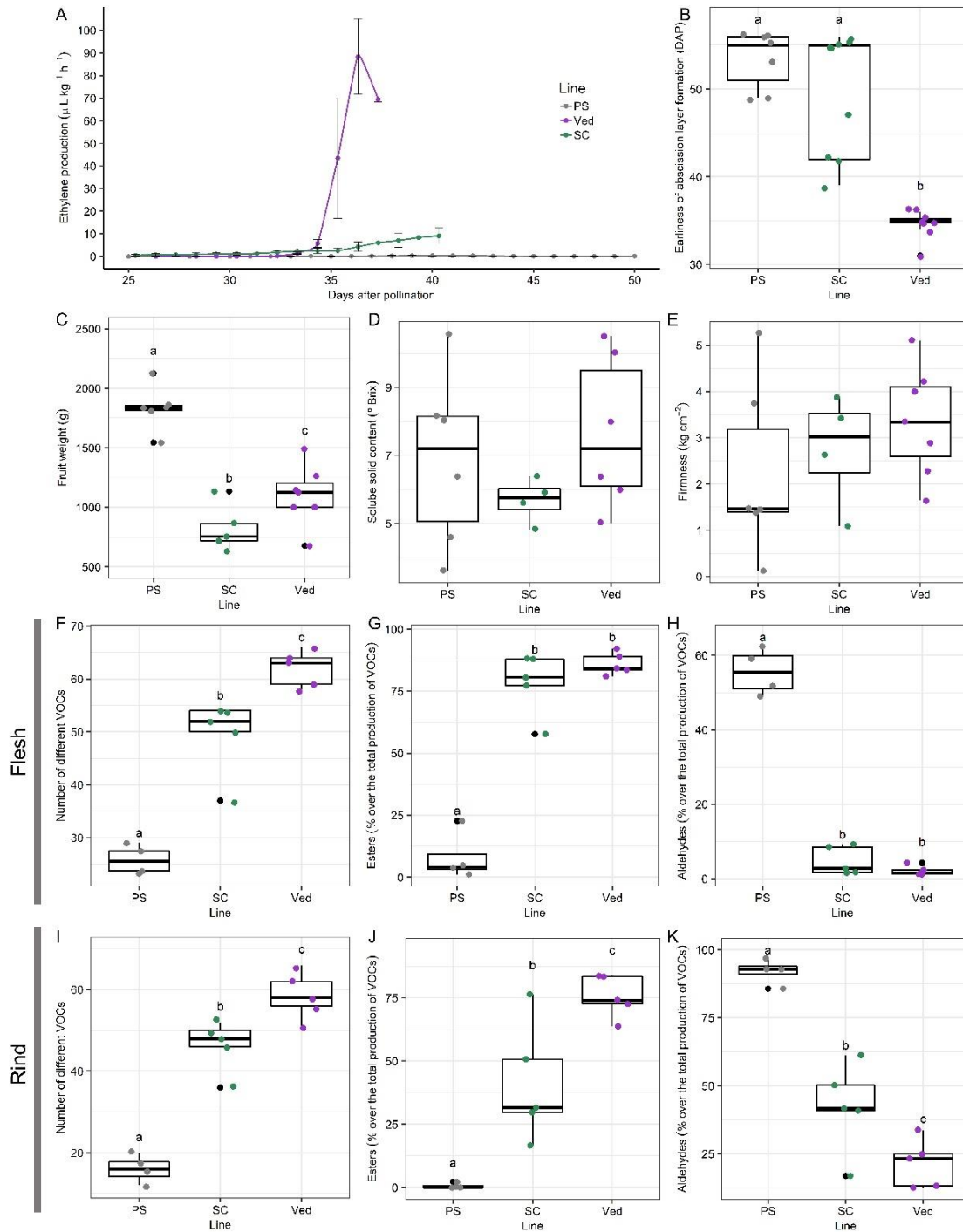


Figure 3.1.1. Phenotypic evaluation of the three parental lines PS, SC and Ved used in the study, showing: **A)** ethylene production (ETH), **B)** earliness of abscission layer formation (EALF), **C)** fruit weight (FW), **D)** soluble solid content (SSC), **E)** flesh firmness (FIR), **F)** diversity of VOCs in flesh, **G)** percentage of esters over the total amount of VOCs in flesh, **H)** percentage of aldehydes over the total amount of VOCs in flesh, **I)** diversity of VOCs in rind, **J)** percentage of esters over the total amount of VOCs in rind, **K)** percentage of aldehydes over the total amount of VOCs in rind. Letters represent significant difference between groups (p-value < 0.05).

response. We considered PS as a classical non-climacteric cultivar (Pereira *et al*, 2020). Songwan Charmi (SC) is a Korean accession belonging to the *agrestis* subspecies,

considered non-climacteric, but presenting some phenotypes associated with the climacteric response, as the production of aroma. It also produced ethylene during ripening, although in much less quantity if compared to climacteric types. Védraçais (Ved) is a French variety, from the *melo* subspecies as PS, and the *cantaloupensis* group. It had a typical climacteric fruit ripening behavior, with a sharp ethylene peak and noticeable related climacteric traits as abscission layer formation at 35 days after pollination (DAP) (Figure 3.1.1A, B).

Regarding fruit quality phenotypes, PS produced significantly bigger fruits compared to SC and Ved. Also, SC had the smallest fruits of the three parental lines (Figure 3.1.1C). We did not observe significant differences among the three parental lines in soluble solid content nor firmness of the flesh (Figure 3.1.1D, E; Table 3.1.S1).

When we studied the aroma profile, the three lines behaved differently. In flesh tissue, Ved accumulated the biggest amount of total volatile organic compounds (VOCs) followed by SC, and PS was the one accumulating the least amount of VOCs, being the differences significant ($p < 0.05$) among the three genotypes (Table 3.1.S2A). In rind tissue, both PS and SC accumulated low amount of VOCs, and Ved significantly ($p < 0.05$) accumulated more VOCs than the other two genotypes (Table 3.1.S2B). Looking at the number of different compounds produced by each line, Ved was also producing the most diverse aroma profile in both tissues, with around 60 different VOCs, followed by SC with 50 and PS with less than 30 different VOCs in flesh and less than 20 different compounds in rind tissue (Figure 3.1.1F, I; Table 3.1.S2). PS had a non-climacteric aroma profile, being aldehydes the major component in both rind and flesh tissues (92% and 55% of total amount of volatile compounds, respectively) with a lesser accumulation of esters (Figure 3.1.1G, H, J, K) (Table 3.1.S3). Ved had a major component of esters in both rind and flesh (75.5% and 86%, respectively) and a minor component of aldehydes, although the total production of aldehydes was similar to PS in flesh and significantly bigger in rind ($p < 0.05$) (Figure 3.1.1G, H, J, K; Table 3.1.S3). In the case of SC, it had a different VOCs profile depending on the tissue. Regarding flesh tissue, although the total amount of produced VOCs is half the one found in Ved, it had a similar profile with a major component of esters (78%) (Figure 3.1.1G, H; Table 3.1.S3A, B). When focusing into the rind tissue, the production of VOCs was also reduced compared to Ved, and the profile also changed, with an intermediate behavior between Ved and PS with a mean of 40% of VOCs being esters and 40% aldehydes (Figure 3.1.1J, K; Table 3.1.S3C, D).

Regarding other minor compounds, SC was the only line producing alkanes and furans in the rind, while PS produced furans in the flesh and phenols in rind (Table 3.1.S3).

In a deeper analysis, when looking into the compounds that are most related to melon aroma such as (E,Z)-2,6-Nonadienal, Nonanal, (Z)-6-Nonenal, Ethyl acetate, Ethyl 2-methylbutanoate and Ethyl butanoate (Table 3.1.S4A) (Mayobre *et al*, 2021), although SC is more similar to Ved than to PS regarding aroma profile, it produces more melon and cucumber-like aromas, while Ved produces more floral and fruity ones (Table 3.1.S4B, C). Otherwise, PS has a general low production of these VOCs, both in flesh and rind tissues (Table 3.1.S4B, C).

Pyramiding ILs with 2 and 3 QTLs

We developed a collection of ILs in the PS background with homozygous introgressions covering one, two or three QTLs related with climacteric ripening, coming from two different parental lines (SC for *ETHQB3.5* and *ETHQV6.3*, and Ved for *ETHQV8.1*) (Figure 3.1.2) in two generations. The ILs developed in previous studies were renamed consistently with the new developed ILs (Table 3.1.1).

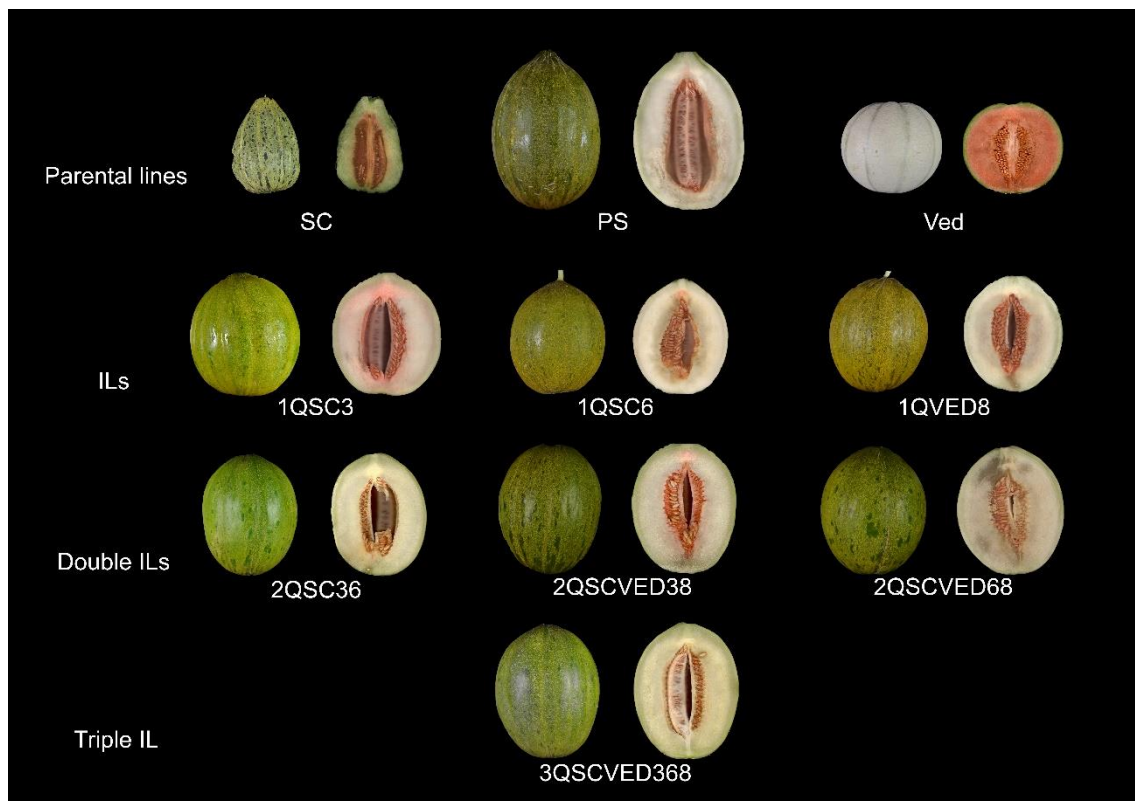


Figure 3.1.2. External and internal visualization of the fruits of the lines used in this study, including the parental lines. IL = Introgression Line, SC = Songwan Charmi, PS = Piel de Sapo, Ved = Védraçais.

Table 3.1.1. Melon lines used in this work. SC = Songwan Charmi, VED = Védraçais.

Melon line ¹ name	QTL (allele-code)	Previous line name	Reference
1QSC3	SC- <i>ETHQB3.5</i>	8M35	Moreno <i>et al</i> 2008 (17) Vegas <i>et al</i> 2013 (18)
1QSC6	SC- <i>ETHQV6.3</i>	8M40	Vegas <i>et al</i> 2013 (18)
1QVED8	VED- <i>ETHQV8.1</i>	VED8.2	Pereira <i>et al</i> 2020 (19)
2QSC36	SC- <i>ETHQB3.5</i> SC- <i>ETHQV6.3</i>	8M31	Vegas <i>et al</i> 2013 (18)
2QSCVED38	SC- <i>ETHQB3.5</i> VED- <i>ETHQV8.1</i>	-	This work
2QSCVED68	SC- <i>ETHQV6.3</i> VED- <i>ETHQV8.1</i>	-	This work
3QSCVED368	SC- <i>ETHQB3.5</i> SC- <i>ETHQV6.3</i> VED- <i>ETHQV8.1</i>	-	This work

¹The genetic background of all the lines is Piel de Sapo (PS)

Fruit ripening behavior of the developed ILs

The main goal of this study was to dissect the ripening behavior of the developed ILs to understand the role of each QTL and their interactions.

Regarding the climacteric symptoms earliness of aroma production (EARO), earliness of abscission layer formation (EALF) and harvest date (HAR), a Principal Component Analysis showed that only one component explained 98% of the variation (Figure 3.1.S2). EALF is the trait which covariates more with this component, so, we analyzed this trait as representative of the three main climacteric symptoms. After model selection, we selected the multiple linear model with the single effects and the three double interactions as the best fitting model ($R^2 = 0.86$). Taking as reference PS, with the non-climacteric alleles for the three QTLs, the linear model showed a significant predicted advance in the symptoms for *ETHQB3.5*, *ETHQV6.3* and *ETHQV8.1* (Figure 3.1.3; Table 3.1.2). Also, all the double interactions were predicted as significant (Figure 3.1.3; Table 3.1.2). As seen in the model, the three double interaction effects are significantly “less than additive”, noticed in the different signs of the three main effects compared to the three interaction effects. The model predicts a minor advance in EALF when introgressing more than one QTL than the expected by the addition of the main effects of these QTLs (Table 3.1.2; Figure 3.1.S3).

Table 3.1.2. Multiple linear model used to analyze the earliness of abscission layer formation (EALF) in the ILs. $R^2 = 0.86$.

Coefficients:	Effect	Estimate	Std. Error	t value	Pr(> t)	Significance
PS	Intercept	53.16	0.97	54.715	< 2e-16	***
<i>ETHQB3.5-SC</i>	Main	-17.29	1.20	-14.397	< 2e-16	***
<i>ETHQV6.3-SC</i>	Main	-16.78	1.18	-14.17	< 2e-16	***
<i>ETHQV8.1-VED</i>	Main	-8.73	1.20	-7.272	6.19E-10	***
<i>ETHQV6.3-SC:ETHQV8.1-VED</i>	Interaction	3.16	1.35	2.343	0.022226	*
<i>ETHQB3.5-SC:ETHQV8.1-VED</i>	Interaction	5.17	1.35	3.835	0.000289	***
<i>ETHQB3.5-SC:ETHQV6.3-SC</i>	Interaction	8.59	1.34	6.415	1.95E-08	***

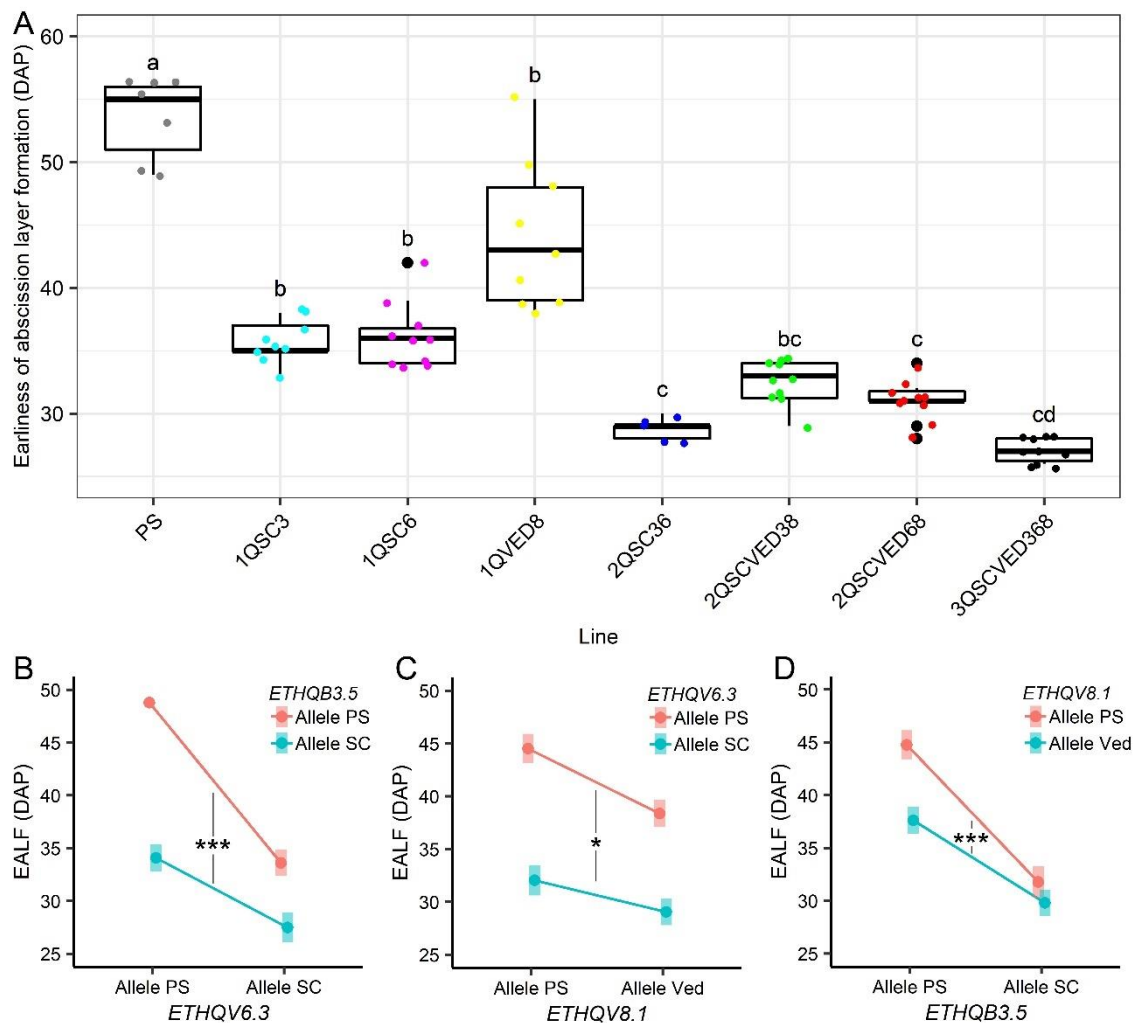


Figure 3.1.3. **A**) Representation of the phenotype Earliness of abscission layer formation (EALF) in the ILs. Significance based on t-test p-value < 0.05. **B**), **C**), and **D**) Interaction plots showing the two-by-two interactions of the three studied QTLs. Significance is calculated through a multiple linear model.

Regarding the semi-quantitative ripening-related level of abscission (ABS), it shows a statistically significant interaction between *ETHQB3.5* and *ETHQV6.3* (p-value = 0.005).

While in PS the abscission level is low, when introgressing one of the QTLs coming from SC most of the melons presented complete abscission from the plant. On the other hand, when introgressing the Ved allele from *ETHQV8.1* the level of abscission increased but not as much as for SC alleles in chromosome 3 or 6 (Figure 3.1.S4).

The ethylene production of each of the ILs developed is presented in Figure 3.1.4A.

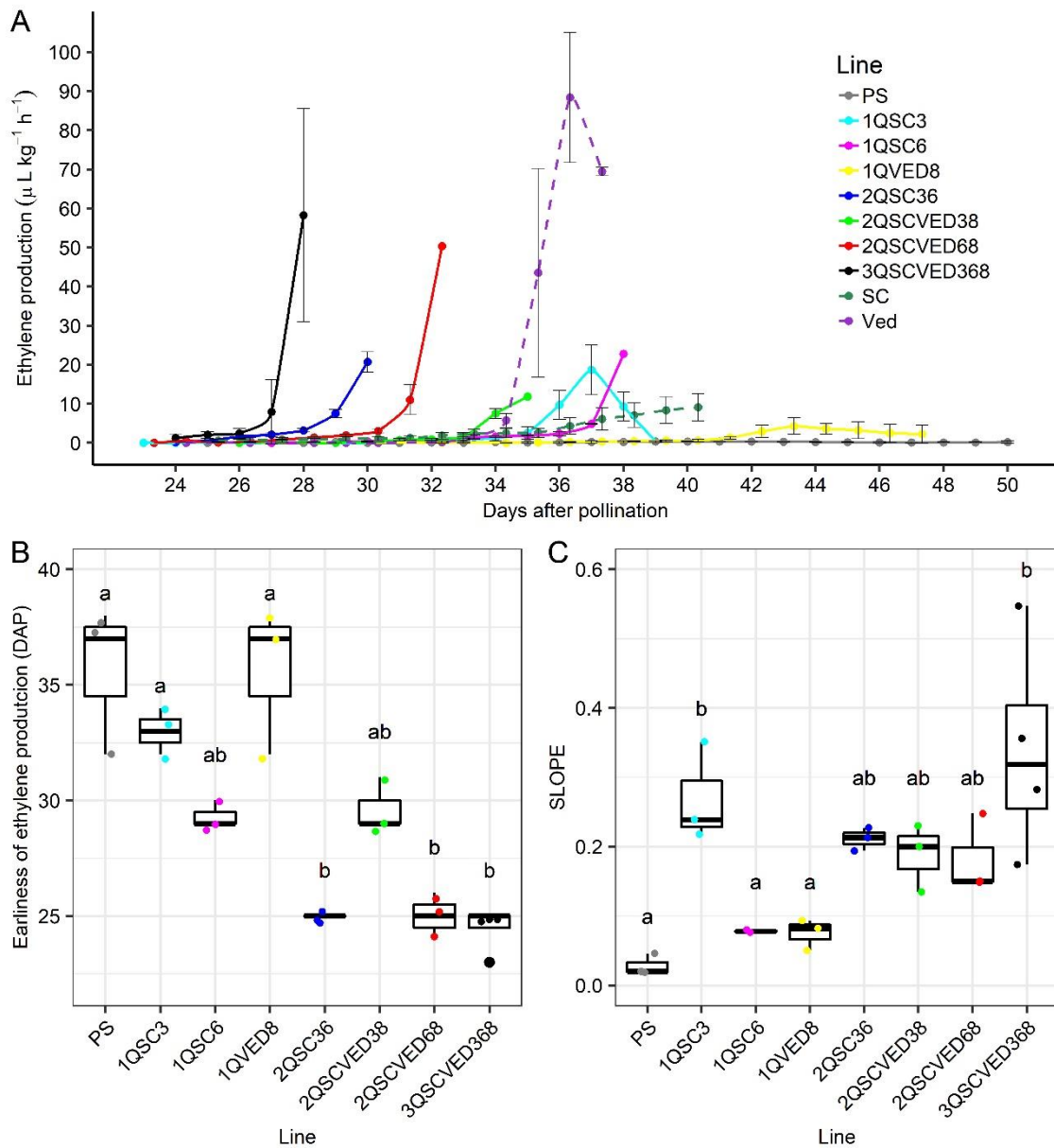


Figure 3.1.4. A) Ethylene production (ETH) of the ILs during fruit ripening, and in dashed lines, the two donor parents Ved and SC. B) earliness of ethylene production (DAPE) and C) slope of the log10 transformed data in the exponential part of the peak (SLOPE). Significance fixed at p-value < 0.05.

With the single introgression of any of the QTLs, PS turned climacteric, but in different degrees. While *ETHQB3.5* and *ETHQV6.3* provoked an important peak of ethylene

production around 36-37 DAP, *ETHQV8.1* only triggered a flat peak of ethylene production around 43-45 DAP. In the double ILs, we observed a diverse degree of climacteric, from an early one in 2QSC36 to a late one in 2QSCVED38. Also, we can observe that when pyramiding more than one QTL, an earlier climacteric response and a higher production of ethylene was induced. With the triple IL 3QSCVED368 we observed the sum of both effects, earlier and higher production, being the line with the highest climacteric behavior. While Ved had its ethylene production peak at 36 DAP (Figure 3.1.1), 3QSCVED368 had it at 28 DAP, one week earlier.

When we analyzed ethylene production related traits, we saw that for earliness of ethylene production and the peak of this production, a significant effect of *ETHQV6.3* was detected, and the interaction between the two QTLs *ETHQV8.1* and *ETHQV6.3* and the triple one was also significant (Figure 3.1.4B; Table 3.1.S5A, B). Concerning the SLOPE, which is related with the sharpness of the peak explaining how quick the ethylene production increases, the model predicted a significant effect of *ETHQB3.5* narrowing the peak, and also an interaction between *ETHQV6.3* and *ETHQV8.1* when they were together (Figure 3.1.4C; Table 3.1.S5C). For ethylene production related traits, our data suggest that *ETHQV6.3* has a significant effect for the earliness of the peak, and *ETHQB3.5* for its sharpness. On the other hand, although *ETHQV8.1* does not have a significant effect on its own, it enhanced the effect of the other two QTLs.

Aroma production and fruit quality of the developed ILs

Another important trait for fruit quality in melon is the volatile compounds composition, as their combination shapes the aroma profile of the fruit. The introgression of the climacteric ripening QTLs produced a significant increase in the total amount of volatiles production, compared to PS, in both fruit flesh and rind (Figure 3.1.5; Table 3.1.S2A, B). Analyzing the different compounds, we can observe that, although there was variability within each line, the most important effect was due to the accumulation of esters (mainly acetic acid esters) in fruit flesh and rind, and the accumulation of aldehydes (mainly benzaldehyde) in the rind (Figure 3.1.S5). In PS, there was little production of esters in

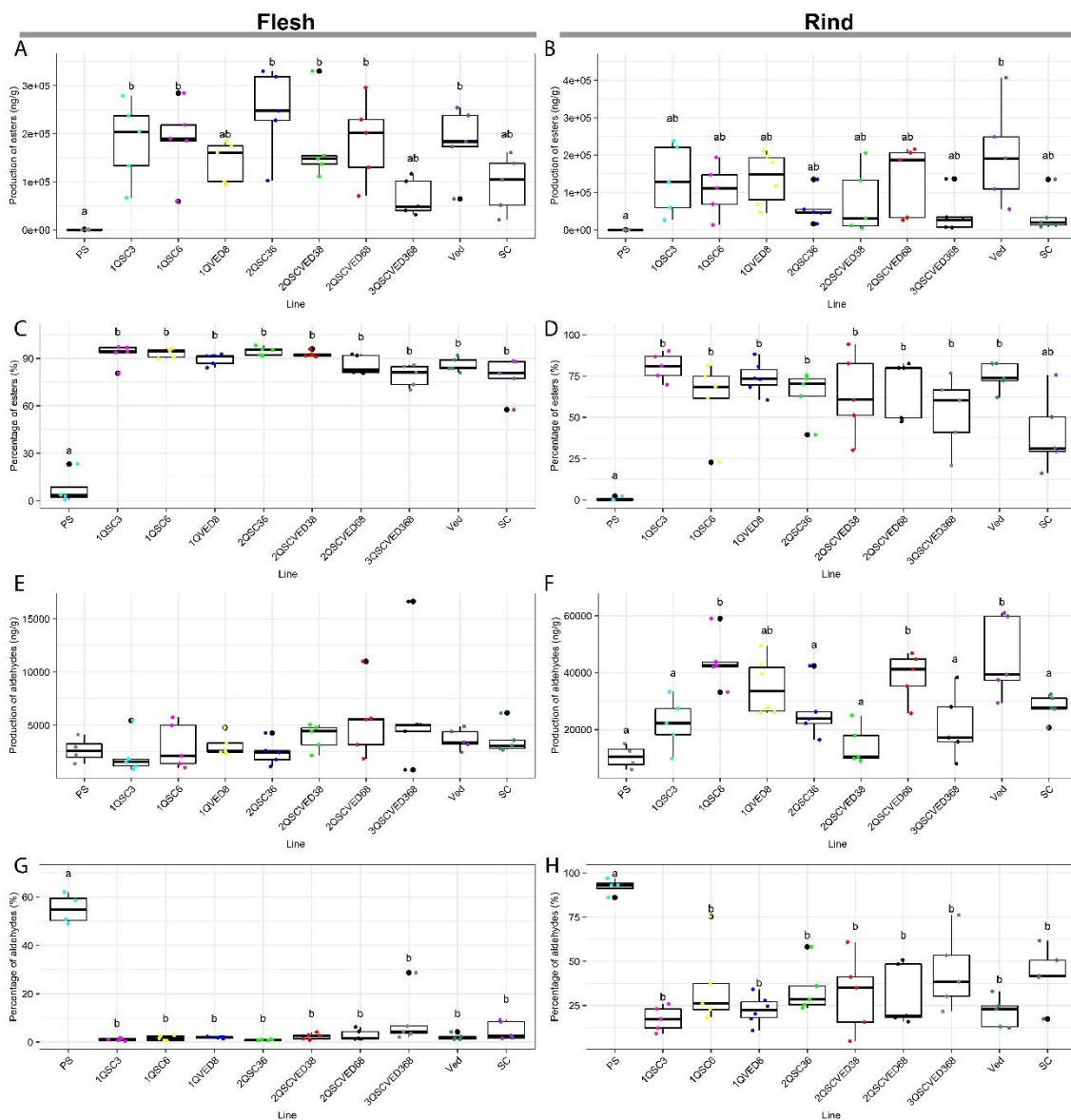


Figure 3.1.5. Production of esters and aldehydes, showing both total relative production respect to the internal standard (3-hexanone) and percentage over the total VOCs. **A), C), E)** and **G)** in flesh tissue, and **B), D), F)** and **H)** in rind tissue

both rind and flesh, but when we introgressed the QTLs, the fruits significantly accumulated a bigger quantity of esters in flesh, even reaching the levels of esters production in Ved (Table 3.1.S3A; Figure 3.1.5A). There was also an increase of ester production in rind, although generally, the reached levels were not higher than Ved (Table 3.1.S3C; Figure 3.1.5B). In both rind and flesh, the accumulation of esters became the main component of the aroma profile in the introgression lines (more than 75% and 50% of total volatiles in flesh and rind, respectively), similar to the climacteric cultivar Ved and significantly higher than in PS in all the pyramided lines (Table 3.1.S3B, D; Figure 3.1.5C, D). Regarding the aldehydes (the second group in importance in melon fruit

aroma profile), the total amount was very variable. In flesh, there was not a significant increase in any of the lines, even in the other parents Ved and SC (Table 3.1.S3A; Figure 3.1.5E). In rind tissue, although we did observe a significant increase in some lines, the behavior was very variable without a clear trend (Table 3.1.S3C; Figure 3.1.5F). However, looking at the percentage of aldehydes we did observe a significant trend. While in PS the aldehydes were the main contributor to the aroma profile in both rind and flesh (more than 90% and 50% respectively), in the introgression lines the percentage was significantly lower in both tissues probably due to the high percentage of esters (Table 3.1.S3B, D; Figure 3.1.5G, H). If we look at the other analyzed compounds, we can observe that when we introgressed the climacteric QTLs, the lines lost the capacity of accumulating furans in fruit flesh (Table 3.1.S3A). We can also observe a bigger accumulation of alcohols when introgressing *ETHQV8.1*, approaching the levels of SC and Ved in flesh and rind (Table 3.1.S3A, C). Also, when introgressing the QTLs, the fruits produced more terpenes, especially the lines with *ETHQB3.5*, but not reaching the levels of Ved (Table 3.1.S3A, C).

Moreover, we studied the association of all the VOCs with individual QTLs, considering the large variability within genotypes. Using linear models, we selected the additive model to see the individual association of each single QTL with the compounds, and then selected the models which explained more than 40% of the variance (adjusted $R^2 > 0.4$), indicating a major genetic control of the trait by the QTLs individually. In the case of rind, two compounds met this condition: eucalyptol and benzeneacetaldehyde (Table 3.1.S6). Both were associated significantly with *ETHQB3.5*, and highly associated with *ETHQV6.3* in the case of benzenacetaldehyde, and with *ETHQV8.1* in the case of eucalyptol (Table 3.1.S6A, B). When focusing on the flesh, four compounds were associated with the QTLs. Eucalyptol appeared also associated with *ETHQV8.1* and *ETHQB3.5* in flesh, and phenylethyl alcohol with *ETHQV8.1* and *ETHQV6.3* (Table 3.1.S6C, D). Moreover, another compound, 1-octen-3-ol was highly associated with *ETHQV8.1* (Table 3.1.S6F). All of these compounds increased their production with the donor parent allele. Interestingly, the last compound highly associated with one QTL was propanoic acid, 2-methyl-, ethyl ester, one of the compounds described as main contributor of melon aroma (Table 3.1.S4A). We detected a highly significant association ($p < 0.01$) of this compound with *ETHQV8.1*, increasing its production when introgressing the donor allele (Table 3.1.S6E).

Regarding the analysis of the main contributors to the melon aroma (Table 3.1.S4A), we can observe different behaviors. Although SC produced the cucumber-like aroma compound 2-6 nonadienal in rind, none of the ILs recovered this phenotype, while we observed non-significant increase of its production in flesh in most of the ILs (Table 3.1.S2A). Regarding the melon-like aroma compounds nonanal and 6-nonenal, we detected a significant increase of nonanal in flesh in the line 3QSCVED368 ($p < 0.05$), and non-significant increase in other introgression lines, such as 1QSC6 and 2QSC36, when compared to PS (Table 3.1.S2A). The major effect was observed in the floral and fruity aroma compounds. By introgressing the QTLs, we could mostly recover the phenotype of Ved in both rind and flesh for those compounds. Individually, there was an increase in the production of ethyl acetate, and butanoic acid ethyl ester in 1QVED8, producing bigger amounts than Ved, but we did not observe this trend in other lines carrying *ETHQV8.1*. In these compounds, the lesser effect was observed when introgressing *ETHQB3.5*, being 1QSC3, 2QSC36, 2QSCVED38 and 3QSCVED368 similar to PS (Table 3.1.S2A, B). For the other compounds, although there was an increase in the ILs compared to PS, we did not observe significant changes or trends (Table 3.1.S2).

For the fruit quality traits, there was no significant effect of either of the QTLs, and we did not observe significant differences among the lines compared to PS for fruit weight, sugar content or firmness (Figure 3.1.S6). However, we detected a trend of smaller fruits for any of the introgressed QTLs (Figure 3.1.S6A).

Discussion

In this study, we present the pyramiding of three QTLs involved in climacteric ripening coming from two different populations sharing the non-climacteric recurrent parental line PS. While *ETHQB3.5* and *ETHQV6.1* come from an IL population with the non-climacteric donor parent Songwan Charmi PI 161375 (Eduardo *et al*, 2005; Argyris *et al*, 2015), *ETHQV8.1* comes from an IL population with the climacteric Ved as the donor parent (Pereira *et al*, 2020). This pyramiding strategy has been used in different crops and with several traits, such as improving yield under stress conditions or blast resistance in rice (Sandhu *et al*, 2019; Ortega *et al*, 2016), fungi resistance in pea (Lavaud *et al*, 2016) or insect resistance in soybean (Ortega *et al*, 2016). Similar strategies, but with a single donor parent, have been used to improve yield in different crops, as cucumber (Robbins

et al., 2008) or tomato (Gur & Zamir, 2015). In the case of melon, there have been studies of pyramided QTLs to improve resistance to gummy stem blight (Zhang *et al.*, 2017) and to advance ripening (Vegas *et al.*, 2013). In all of these studies, the use of ILs with combinations of different QTLs has proved as a powerful tool to uncover their effect in diverse phenotypes, as well as their interactions. However, pyramiding genes involved in fruit quality or ripening has not been yet fully implemented in cultivated crops (Wang *et al.*, 2020). With the genomic tools available in melon, such as the reference genome and more than one thousand accessions resequenced (Garcia-Mas *et al.*, 2012; Zhao *et al.*, 2019), molecular markers can be easily obtained and used for shortening the process of pyramiding QTLs by MAS.

QTLs interact to modulate the climacteric ripening behavior in melon fruits

To date, most of the work about climacteric ripening has been done in tomato fruits. Several mutants with delayed ripening have been used to characterize genes controlling climacteric response (Giovannoni, 2007; Vrebalov *et al.*, 2002; Manning *et al.*, 2006). However, inducing early climacteric ripening in a non-climacteric background, as we present in this work, has not been addressed.

Although the effects of the three QTLs here described have been studied separately, this is the first time that they are combined and analyzed in the same experiment. The three QTLs produce a climacteric response in PS independently, with production of ethylene and related climacteric symptoms. *ETHQV8.1* was the weakest QTL, provoking a lower and delayed ethylene peak (Figure 3.1.4A). *ETHQB3.5* caused a fast production of the ethylene peak (Figure 3.1.4C), and *ETHQV6.3* significantly advanced both the ethylene production and the peak intensity (Figure 3.1.4B). When observing the climacteric symptoms, the analysis showed a significant effect when introgressing *ETHQV6.3*, *ETHQB3.5* or *ETHQV8.1* (Table 3.1.2), being the effect bigger for the first two QTLs. This bigger effect of the QTLs coming from SC was previously observed (Vegas *et al.*, 2013; Pereira *et al.*, 2020) and *ETHQV8.1* has been reported to be unstable, provoking a mild climacteric behavior depending on the environmental conditions (Pereira *et al.*, 2020). When combining two of the QTLs in the same line, we observed a statistical interaction in the three combinations, bringing out a potential interaction among the causal genes. The general trend of these QTLs is a “less than additive” effect, being this model significant for the three double interactions, predicting a lighter effect when

introgressing two QTLs that the expected if it was additive (Table 3.1.2; Figure 3.1.S3). As melons are reported to start ripening at around 30 DAP, coinciding with the starting of sucrose accumulation (Saladié *et al*, 2015), maybe the mathematically estimated additive value is too early, during the fruit growth stage. Melons carrying two or three of the QTLs should ripe before 20 DAP when the fruit is still under development and probably it is not ready for ripening. Thus, linear models seem an appropriate tool for this type of experiment, as they can detect statistical interactions among variables, in this case QTLs, and have been used previously for this kind of studies (Lavaud *et al*, 2016; Gur & Zamir, 2015). After model selection, the most suitable model was the one with the three double interactions that explains 88.55% of the variance, evidencing also that there is no need to include the triple interaction to predict the ripening behavior of the population. This significance of all the interactions may be indicating that the phenotype is due to the interactions between the different alleles of those QTLs.

When we looked individually to each of the QTLs, we observed a clear effect of them in the ethylene production profile. *ETHQV6.3* advanced the ethylene production, as well as the ethylene peak. This result matches previous studies showing that *TILLING* mutants of *MELO3C016540.2* in a climacteric background delay the production of ethylene but not the amount or the shape of the peak (Ríos *et al*, 2017). In the case of *ETHQB3.5* and *ETHQV8.1*, although the causal genes are not yet known, our results could help in their identification. Our results suggest that the role of *ETHQB3.5* is to narrow the ethylene peak, decreasing the days from the start of the ethylene production to the maximum production. In a recent study, two candidate genes have been suggested in the *ETHQB3.5* interval: *MELO3C011432.2*, a WRKY family transcription factor, and *MELO3C011365.2*, related with signal transduction (Oren *et al*, 2022). *ETHQV8.1*, although it has a weaker effect compared to the other two QTLs, has an important role in enhancing the response in combination with both of them. Three candidate genes have been suggested in the region of this QTL: *MELO3C024516.2*, *MELO3C024518.2* and *MELO3C024520.2*, encoding a demethylase, a negative regulator of ethylene signal transduction and an ethylene responsive transcription factor, respectively (Pereira *et al*, 2020). All three of them may play a role in fruit ripening, and our work can contribute to understand the specific function of *ETHQV8.1*.

Our results suggested an important role of the genetic background, since *ETHQB3.5* and *ETHQV6.3*, both carrying SC alleles, behave differently when introgressed in PS. This

effect reveals the complex architecture of ripening in melon, as it has been reported before in other crops (Wang *et al*, 2020). Moreover, when introgressing two (2QSCVED68) or three (3QSCVED368) QTLs in PS, we can obtain a line that is even more climacteric than Ved, which is known to be a typical climacteric *cantaloupe* type. This finding suggests that there are some key genes governing the climacteric response, and combining their natural variation, we can convert a non-climacteric variety with long shelf life into an early maturation and aromatic melon line.

By combining these three QTLs we can obtain melons with different degrees of climacteric response. As ethylene production is one of the main traits affecting fruit shelf life, here we have implemented a tool to control its production with only three major QTLs that can potentially be fine-tuned using other minor QTLs found in previous studies (Pereira *et al*, 2020). This approach could be used to develop new melon cultivars with different degrees of shelf life in both directions. We could develop aromatic climacteric varieties from a non-climacteric variety as shown in this study; and from a climacteric cultivar as Ved, pyramiding ILs with delayed ripening (Pereira *et al*, 2021; Perpiñá *et al*, 2017), we could develop long shelf-life climacteric varieties.

The aroma profile can be modified in an *inodorus* melon

Piel de Sapo (PS), the recurrent parent of the ILs, belongs to the *inodorous* group, the term meaning “no aroma” in Latin. As a non-climacteric variety, PS is characterized by a mild or even undetectable aroma profile. In this study, we introgressed different QTLs in the PS background triggering a climacteric response during ripening, and all of them induced accumulation of ester compounds and a meaningful change in the aroma profile of the fruit. Regarding the aroma profile, we cannot differentiate the pyramided lines when smelling them, as all of them are climacteric and produce a similar aroma. The analysis of melon fruits by GC-MS showed that for the climacteric lines, the main contributor to the aroma profile are esters (Mayobre *et al*, 2021; Obando-Ulloa *et al*, 2008), while the non-climacteric PS does not produce esters, being aldehydes the main contributors to the aroma profile. The line 3QSCVED368, the earliest climacteric line, had a lower production of esters than the other lines, suggesting that this effect may be due to its quick ripening and fruit abscission, preventing the accumulation of esters. Alcohol acyl-transferases, the enzymes driving esters biosynthesis, have been reported to be expressed later than 30 DAP in melon (Yahyaoui *et al*, 2002), later than the harvest

date of 3QSCVED368, probably leading to a minor accumulation of esters in this line compared to the other ILs. We also detected changes in the composition of the aroma in the pyramided lines. The introgression of *ETHQV8.1* from Ved enhances the production of fruity and floral aromas, and the introgression of *ETHQB3.5* does not produce a strong effect in the main contributors to melon aroma (Table 3.1.S4). Therefore, even if *ETHQV8.1* has not the highest impact in ethylene production, it seems to affect key VOCs implicated in melon aroma.

Our results suggest a potential use of different QTLs to shape the aroma profile in melon. Although we observed a high variation regarding VOCs accumulation in both rind and flesh tissues, some compounds seemed to be associated with a particular QTL, making it possible to fine-tune the melon aroma by pyramiding different QTLs. Moreover, we demonstrated that it is possible to introduce aroma in an *inodorous* cultivar by introgressing any of the three QTLs, suggesting that the control of aroma production depends mainly on ethylene production.

Minor effect in fruit quality caused by the introgressions

Our results showed that there were not significant differences between PS and the pyramided lines related to fruit quality traits as weight, soluble solid content and firmness. However, there was a trend showing a decrease in fruit weight in all the ILs. A relationship between ripening and fruit size has been reported in tomato (Wang *et al*, 2020) and melon (Chatzpoulou *et al*, 2020). However, the ILs here reported contain large regions with many genes, making it possible that the effect on fruit size may be the result of other genes present inside the introgression. In the case of fruit firmness, although the softening of the fruit is partially regulated by ethylene (Pech *et al*, 2008), we did not detect any significant effect.

The results of this study demonstrate the possibility of pyramiding different QTLs in the same genetic background to shape and fine-tune the ripening process in melon fruits. With only three QTLs, we can obtain a line with an extreme climacteric behavior in the non-climacteric cultivar Piel de Sapo background. In addition, we can modify the aroma profile of the ripe fruit using these QTLs. The combination of these three major QTLs represents a powerful tool to modify and fine-tune climacteric fruit ripening in melon breeding programs.

Materials and methods

Plant material

The starting lines are part of two different IL populations, both with the same genetic background, the Spanish commercial variety Piel de Sapo (PS) from the *inodorous* group. Three of the initial lines belong to a previously described and characterized IL population (Eduardo *et al*, 2005; Vegas *et al*, 2013), using the Korean variety Songwan Charmi (SC, accession number PI 161375) as the donor parent. These three lines are 1QSC3 (previously known as 8M35), 1QSC6 (previously named 8M40) and 2QSC36 (known as 8M31), carrying the QTLs *ETHQB3.5*, *ETHQV6.3* and both, respectively. The second IL population used in this study, with the same PS genetic background and the French variety Védraçais (Ved) as the donor parent, is still under construction. The line used in this study 1QVED8 was previously described as VED8.2, carrying the QTL *ETHQV8.1* (Pereira *et al*, 2020). For a more understandable and consistent naming, the initial lines were renamed. All lines are described in Table 3.1.1.

Breeding scheme

The pyramided ILs with double and triple introgressions were developed by crosses and Marker Assisted Selection (Figure 3.1.S1). To construct the double ILs 2QSCVED38 and 2QSCVED68, two single ILs were first crossed and then self-pollinated. 192 F₂ plants of each cross were genotyped with flanking markers selecting two individual plants containing the two introgressions in homozygosity, which were self-pollinated to obtain the progeny for phenotyping. For the triple IL, the already developed double introgression line 2QSC36 was crossed with IL 1QVED8, and then self-pollinated. 384 F₂ individuals were genotyped and two plants carrying the three QTLs in homozygosity were selected, which were self-pollinated to obtain the progeny for phenotyping. With this scheme, 7 lines with all the possible homozygous combinations of the three QTLs were developed in two generations, and another generation was needed to multiply the seeds.

DNA extraction and genotyping

DNA extractions were performed from young leaves using two different protocols depending on the use of the DNA: for quick genotyping and short-term storage, alkaline-

Chapter 3: QTL interactions

lysis extraction was used (Lu *et al*, 2020), and for genotyping and long-term storage, a CTAB protocol (Doyle, 1991) with some modifications was used (Pereira *et al*, 2018). The genotyping was performed using two similar SNP genotyping systems: KASPar SNP Genotyping System (KBiosciences, Herts, UK), and PACE2.0 SNP Genotyping System (3CR Bioscience, Essex, UK). Primers for both systems were designed following the genotyping system instructions (Table 3.1.S7). Two of the QTLs were genotyped using flanking markers (*ETHQB3.5* and *ETHQV8.1*). The other QTL (*ETHQV6.3*) was genotyped using a marker into the causal gene, *MELO3C016540.2* (Ríos *et al*, 2017).

Growing conditions

Seedlings were planted in fertipots and maintained under controlled conditions in an indoor greenhouse facility (CRAG, Barcelona) during approximately three weeks for genotyping purposes. After this period, selected plants were grown randomized in a greenhouse in Caldes de Montbui (Barcelona). For the development of the new lines, two generations were obtained in the same year during 2018 and 2019, and the phenotyping was performed during summer 2020. Plants were pruned weekly and pollinations were executed manually, allowing developing only one fruit per plant. The harvest point was determined based on the presence of abscission layer, as this is a trait highly associated with ethylene production. Harvest date was fixed at: a) abscission date when the fruit abscised; b) five days after the appearance of the abscission layer; c) 56 days after pollination (DAP) when fruits were non-climacteric and did not form abscission layer, considering them fully ripe at that point. Ten plants were grown per genotype, and more than seven fruits were evaluated, depending on the fruit set of each genotype.

Phenotyping

Ripening-related traits were evaluated as qualitative (production of aroma (ARO)), semi-quantitative (abscission (ABS)) or quantitative (rest of traits) (Table 3.1.3). Traits were divided in three different categories: fruit quality (fruit weight (FW), soluble solid content (SSC) and firmness (FIR)), fruit ripening-related (aroma production (ARO), earliness of aroma production (EARO), earliness of abscission layer formation (EALF), level of abscission (ABS) and harvest date (HAR)) and ethylene-related (ethylene production (ETH), earliness of ethylene production (DAPE), earliness of the ethylene peak (DAPP) and the slope of the peak measuring the log₁₀ transformed data in the exponential part of

the peak (SLOPE)). ARO and ABS were inspected daily from 20 days after pollination (DAP) until the appearance of the symptom. ABS was recorded using an index from 0, no abscission layer formation; 1, subtle and/or partial abscission layer; 2, almost complete abscission layer with obvious scar; and 3, total abscission layer formation generally with fruit abscission.

Table 3.1.3. Traits evaluated in the experiment.

Category	Trait (units)	Code
Fruit quality	Fruit weight (g)	FW
	Soluble solid content (°Brix)	SSC
	Flesh firmness (kg cm ⁻²)	FIR
Fruit ripening	Earliness of aroma production (DAP*)	EARO
	Aroma production	ARO
	Earliness of abscission layer formation (DAP*)	EALF
	Level of abscission	ABS
	Harvest date (DAP*)	HAR
Ethylene production	Ethylene production (μL kg ⁻¹ h ⁻¹)	ETH
	Earliness of ethylene production (DAP*)	DAPE
	Earliness of the ethylene peak (DAP*)	DAPP
	Slope of the peak	SLOPE

*DAP Days after pollination

The firmness of fruit flesh was measured at harvest using a penetrometer (Fruit TestTM, Wagner Instruments), in at least three regions of the fruit (distal, proximal and median), and the mean value was registered. Total soluble solids content was estimated in flesh juice by measuring the Brix index with a refractometer (AtagoTM). Fruits were weighed at harvest.

Ethylene production

Ethylene production in attached melon fruits was measured using gas chromatography – mass spectrometry (GC-MS) as previously described (Pereira *et al*, 2017). In summary, melon fruits were covered with a sealed plastic bag, and then filled with atmospheric air. After one hour, gas sample was withdrawn using a syringe and introduced in a vial for later GC-MS analysis.

The ethylene production was monitored from 25 DAP until harvest. For the ILs and climacteric parental line Ved, the atmosphere of the chamber containing the fruit was measured every other day while ethylene was undetectable and every day after ethylene detection. For non-climacteric parental lines PS and SC, the atmosphere of the chamber was examined at least every three days. Three or four fruits were analyzed per line.

Chapter 3: QTL interactions

To better characterize the ethylene peak, four traits were defined: earliness of ethylene production (DAPE), representing the first day when ethylene was detectable, earliness of the ethylene peak (DAPP), and the slope of the ethylene peak, using the slope of the logarithm-transformed measurement of ethylene in the linear part (SLOPE) (Table 3.1.3).

Aroma profiling

The aroma profiling of the rind and the flesh tissue of melon fruits was analyzed at harvest with GC-MS as previously described (Mayobre *et al.*, 2021). In summary, 2 g of grinded frozen tissue were added to a vial, with 7 ml of saturated NaCl solution and 3-hexanone as internal standard. Tubes were stored at 4 °C in the dark for no longer than a week, until gas chromatograph (GC) mass spectrometer (MS) analysis was performed. Then, the vials were analyzed with GC-MS using Solid Phase Micro Extraction (SPME) with a 7890A GC coupled to a 5975C MS and a GC PAL 80 autosampler (Agilent Technologies®, Santa Clara, CA). With the GC-MS data obtained, volatile organic compounds (VOCs) were identified by comparison of their mass spectra with the NIST 11 library and by their Kovats retention index. The relative content of each compound was estimated by comparison to the 3-hexanone internal standard peak area.

Statistical analyses

All the statistical analyses and graphical representations were obtained using the software R v3.5.3 with the RStudio v1.0.143 interface (R Core Team, 2020).

To compute the analyses, the data should not contain any missing data. To include non-climacteric fruits in the analyses, EARO and EALF were imputed as the harvest day value when not present.

The PCAs were performed using R package “factoextra”. The multiple linear models were performed with the function “lm”, using as factor the correspondent allele of each QTL. Model selection was performed under Akaike Information Criterion. ANOVA and pairwise t-test were performed using R package “rstats” with Holm correction. In general, significance was fixed at p-value < 0.05.

Author contributions

J.G.-M. and M.P. conceived and designed the research. M.S.D., LA, LV and CM performed the experiments. AMM-H contributed to the management of the plant material. M.S.D. analyzed the data and wrote the original draft. M.P. and J.G.-M. reviewed and edited the manuscript. All authors read and approved the manuscript.

Supplementary material

Figures

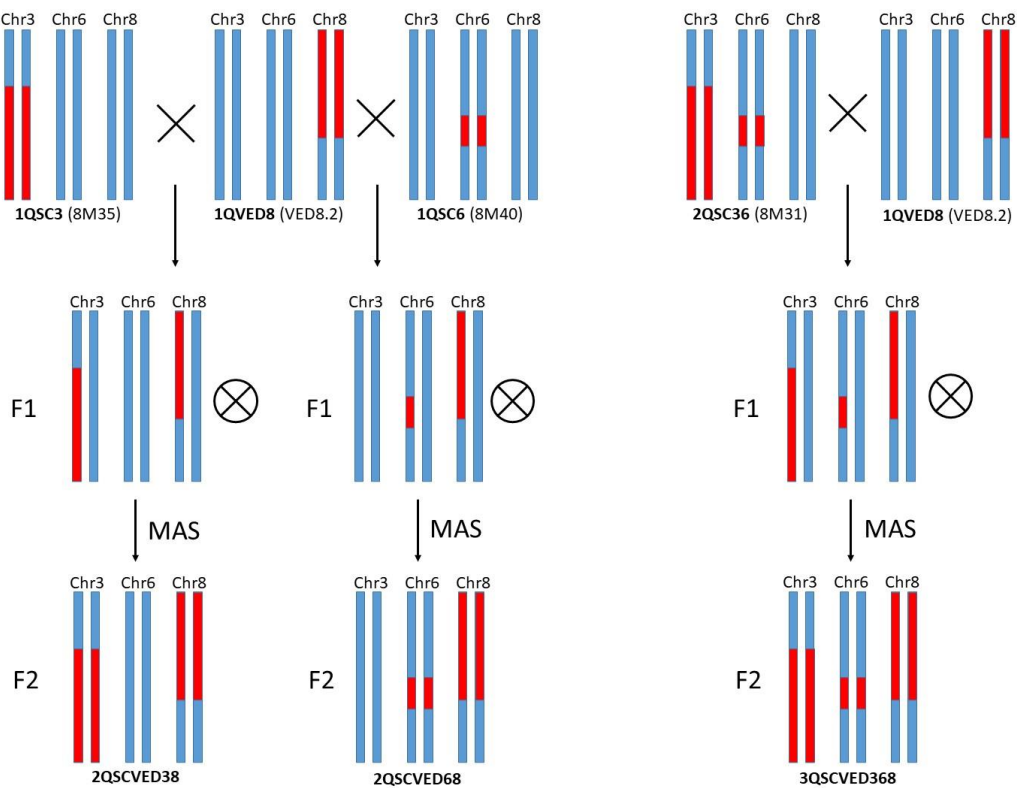


Figure 3.1.S1 . Representation of the breeding scheme followed to develop the double and triple ILs from the initial lines 1QSC3, 1QSC6, 1QVED8 and 2QSC36. Marker Assisted Selection (MAS) was performed in F2 seedlings with markers linked to the target QTLs.

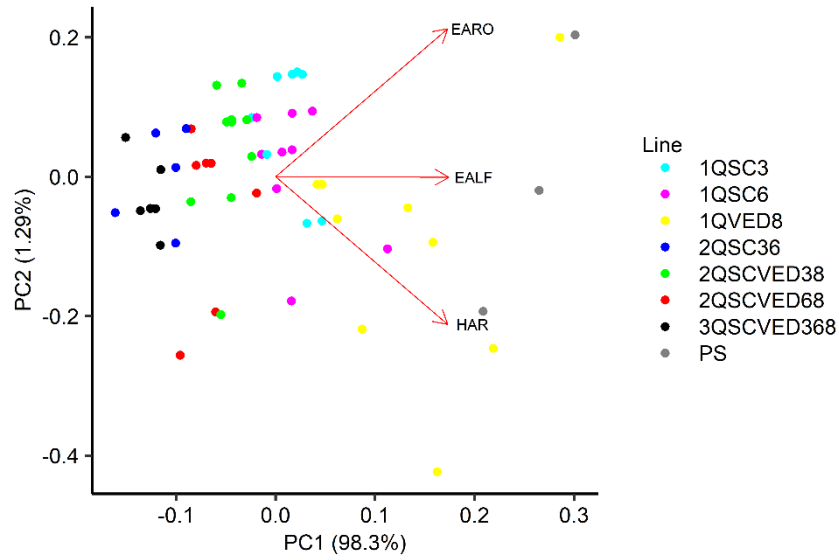


Figure 3.1.S2. Principal Component Analysis of the three main climacteric symptoms in the population, showing their effects in first two Principal Components. EARO = Earliness of aroma production, EALF = Earliness of abscission layer formation and HAR = Harvest date

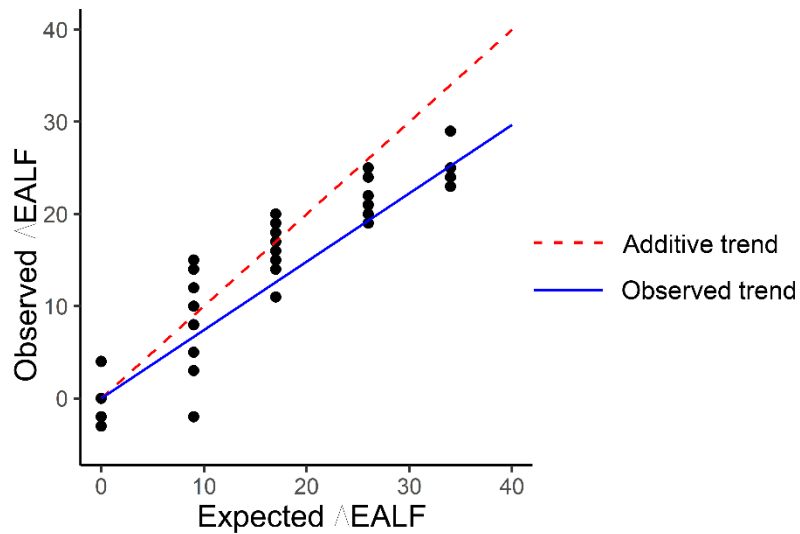


Figure 3.1.S3. General “less than additive” trend observed in the population for the earliness of abscission layer formation (EALF), being the observed phenotype lesser than the expected additive one.

Chapter 3: QTL interactions

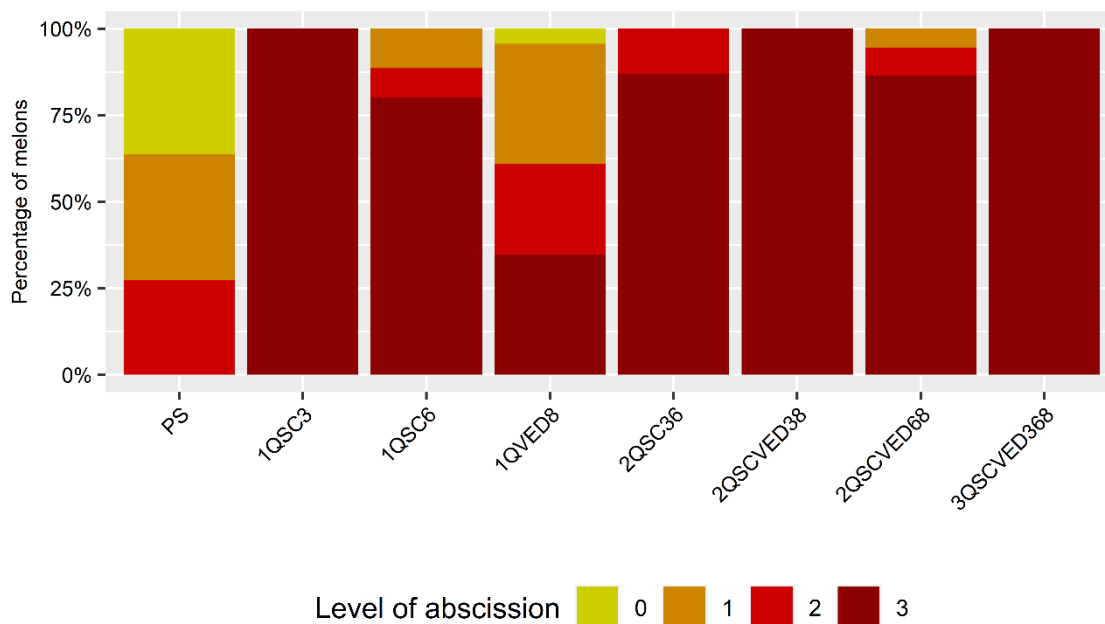


Figure 3.1.S4. Phenotype evaluation of the level of abscission (ABS), showing the percentage of melons presenting each of the considered levels.

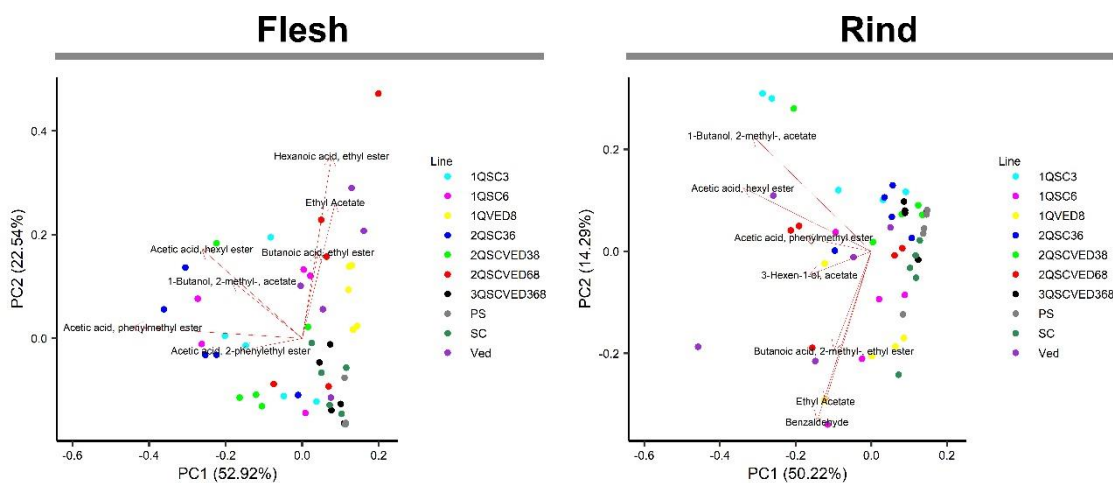


Figure 3.1.S5. Principal component analysis for the aroma profile of the population in rind and flesh, showing the top Volatile Organic Compounds (VOCs) affecting the observed variation in the population

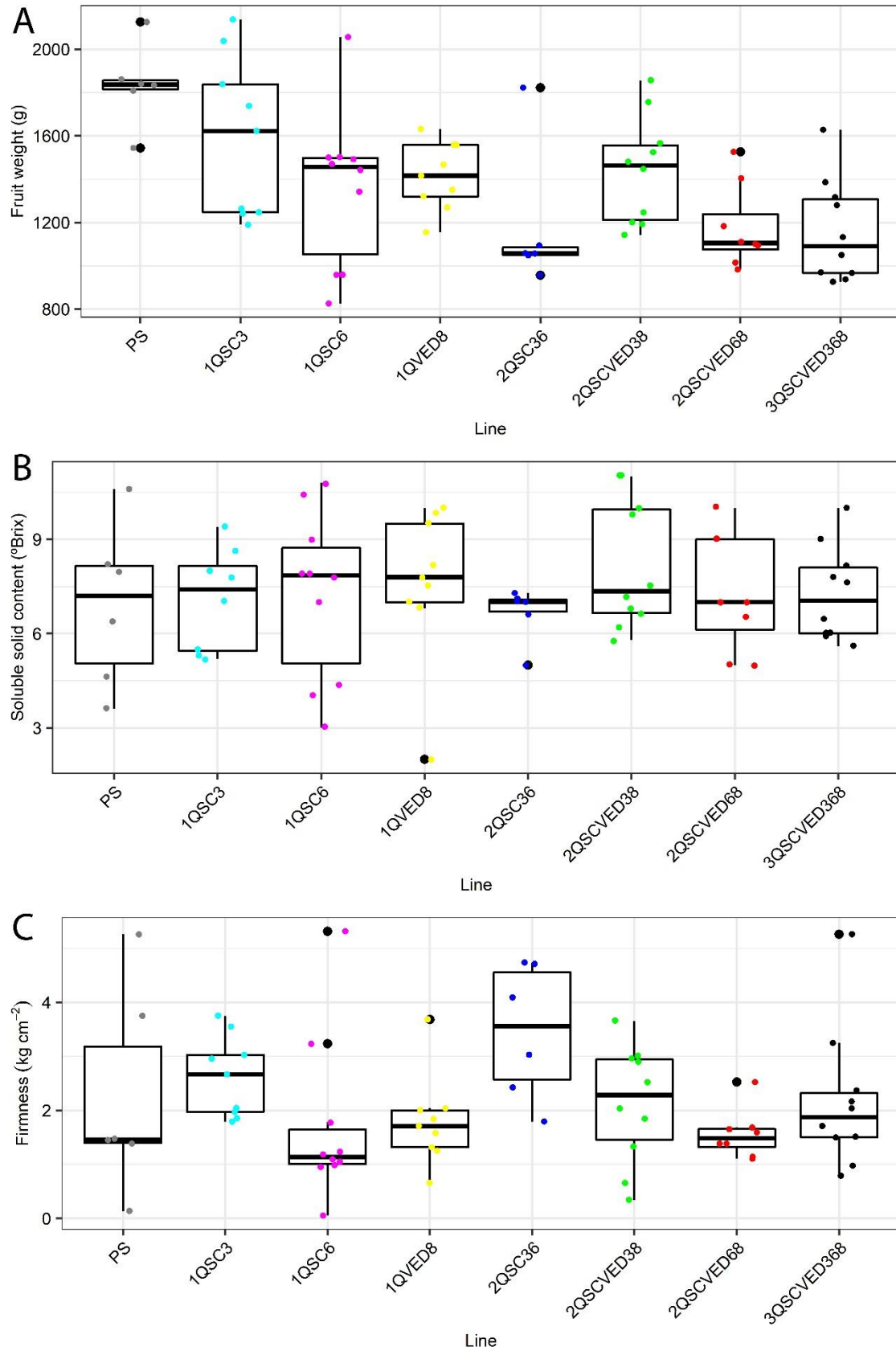


Figure 3.1.S6. Phenotypic evaluation of **A)** fruit weight, **B)** soluble solid content and **C)** firmness in the population analyzed in the study.

Chapter 3: QTL interactions

Tables

Table 3.1.S1. Phenotypes of the lines used in this study, along with the parental lines.

Line	FW		SSC		FIR		EARO		EALF		HAR		DAPE		DAPP		Slope	
	Mean	SD	Mean	SD	Mean	SD	Mean	SD	Mean	SD	Mean	SD	Mean	SD	Mean	SD	Mean	SD
PS	1835.33	184.79	6.90	2.57	2.13	1.79	52.33	4.41	53.17	3.43	55.33	1.03	35.67	3.21	41.00	1.73	0.03	0.02
SC	820.00	194.55	5.68	0.67	2.62	1.16	38.63	4.87	42.67	4.04	50.22	7.01	24.67	0.58	40.00	1.00	0.06	0.01
Ved	1100.29	251.19	7.65	2.24	3.19	1.13	34.63	1.69	34.63	1.60	36.13	0.83	33.00	1.73	36.33	0.58	0.67	0.10
1QSC3	1590.67	369.32	7.10	1.62	2.49	0.71	36.78	1.72	35.67	1.73	38.11	2.26	33.00	1.00	37.67	1.53	0.27	0.07
1QSC6	1354.60	360.37	7.22	2.66	1.60	1.43	35.89	1.27	36.20	2.62	39.00	3.20	29.33	0.58	36.00	2.65	0.08	0.00
1QVED8	1413.78	155.31	7.62	2.42	1.70	0.79	42.89	5.60	44.22	5.80	47.89	5.53	35.67	3.21	43.67	4.16	0.08	0.02
2QSC36	1172.33	321.58	6.67	0.85	3.29	1.18	28.00	1.67	28.00	2.10	30.17	1.47	25.00	0.00	30.00	1.00	0.21	0.02
2QSCVED38	1440.80	245.63	8.19	2.03	2.02	1.03	32.70	1.89	32.50	1.72	34.40	0.97	29.67	1.15			0.19	0.05
2QSCVED68	1176.75	190.67	7.31	1.87	1.48	0.42	30.30	1.89	31.00	1.63	33.60	1.90	25.00	1.00	31.67	0.58	0.18	0.06
3QSCVED368	1159.20	235.58	7.26	1.50	2.05	1.24	26.80	0.79	27.10	0.88	29.10	1.52	24.50	1.00	28.50	1.73	0.27	0.09

Digital supplementary material

Table 3.1.S2. Production of each analyzed compound (ng/g), total production (ng/g) and number of different compounds produced in each line in **A**) flesh tissue and **B**) rind tissue.

Table 3.1.S3. Quantity (**A, C**) and percentage (**B, D**) of volatile compounds found in flesh tissue (**A,B**) and rind tissue (**C,D**) in each of the lines , divided by class

Table 3.1.S4. Compounds related to melon aroma, and their single effect (**A**), and their production in flesh tissue (**B**) and rind tissue (**C**).

Table 3.1.S5. Linear model for the phenotype DAPE (**A**), DAPP (**B**) and SLOPE (**C**), showing single effects and interaction between QTLs

Table 3.1.S6. Linear model for the production of benzeacetaldehyde in rind (**A**), eucalyptol in flesh (**B**), phenylethyl alcohol in flesh (**C**), propanoic acid, 2-methyl-, ethyl ester in flesh (**D**) and 1-octen-3-ol in flesh (**E**), showing single effects of the QTLs.

Table 3.1.S7. Primers used to genotype the three QTLs.

References

- Argyris, J. M., Pujol, M., Martín-Hernández, A. M., and Garcia-Mas, J. (2015). Combined use of genetic and genomics resources to understand virus resistance and fruit quality traits in melon. *Physiologia Plantarum* 155, 4–11. doi:<https://doi.org/10.1111/ppl.12323>.
- Bernacchi, D., *et al* (1998). Advanced backcross QTL analysis of tomato. II. Evaluation of near-isogenic lines carrying single-donor introgressions for desirable wild QTL-alleles derived from *Lycopersicon hirsutum* and *L. pimpinellifolium*. *Theor Appl Genet* 97, 170–180. doi:[10.1007/s001220050882](https://doi.org/10.1007/s001220050882).
- Castro, G., Perpiñá, G., Monforte, A. J., Picó, B., and Esteras, C. (2019). New melon introgression lines in a Piel de Sapo genetic background with desirable agronomical traits from dudaim melons. *Euphytica* 215, 169. doi:[10.1007/s10681-019-2479-1](https://doi.org/10.1007/s10681-019-2479-1).
- Chatzopoulou, F., *et al* (2020). Silencing of ascorbate oxidase results in reduced growth, altered ascorbic acid levels and ripening pattern in melon fruit. *Plant Physiology and Biochemistry* 156, 291–303. doi:[10.1016/j.plaphy.2020.08.040](https://doi.org/10.1016/j.plaphy.2020.08.040).
- Doyle J (1991) DNA Protocols for Plants. In: Hewitt GM, Johnston AWB, Young JPW (eds) *Molecular Techniques in Taxonomy*. Springer Berlin Heidelberg, Berlin, Heidelberg, pp 283–293
- Eduardo, I., Arús, P., and Monforte, A. J. (2005). Development of a genomic library of near isogenic lines (NILs) in melon (*Cucumis melo* L.) from the exotic accession PI161375. *Theor Appl Genet* 112, 139–148. doi:[10.1007/s00122-005-0116-y](https://doi.org/10.1007/s00122-005-0116-y).
- Ezura, H., and Owino, W. O. (2008). Melon, an alternative model plant for elucidating fruit ripening. *Plant Science* 175, 121–129. doi:[10.1016/j.plantsci.2008.02.004](https://doi.org/10.1016/j.plantsci.2008.02.004).
- Garcia-Mas, J., *et al* (2012) The genome of melon (*Cucumis melo* L.). *Proc Natl Acad Sci U S A* 109:11872–7. doi: 10.1073/pnas.1205415109
- Giovannoni, J. J. (2004). Genetic Regulation of Fruit Development and Ripening. *THE PLANT CELL ONLINE* 16, S170–S180. doi:[10.1105/tpc.019158](https://doi.org/10.1105/tpc.019158).
- Giovannoni, J. J. (2007). Fruit ripening mutants yield insights into ripening control. *Current Opinion in Plant Biology* 10, 283–289. doi:[10.1016/j.pbi.2007.04.008](https://doi.org/10.1016/j.pbi.2007.04.008).

- Guan, H., *et al* (2019). Feature of blast resistant near-isogenic lines using an elite maintainer line II-32B by marker-assisted selection. *J Plant Pathol* 101, 491–501. doi:[10.1007/s42161-018-00222-1](https://doi.org/10.1007/s42161-018-00222-1).
- Gur, A., and Zamir, D. (2015). Mendelizing all Components of a Pyramid of Three Yield QTL in Tomato. *Frontiers in Plant Science* 6, 1096. doi:[10.3389/fpls.2015.01096](https://doi.org/10.3389/fpls.2015.01096).
- Lavaud, C., *et al* (2016). Single and multiple resistance QTL delay symptom appearance and slow down root colonization by *Aphanomyces euteiches* in pea near isogenic lines. *BMC Plant Biology* 16, 166. doi:[10.1186/s12870-016-0822-4](https://doi.org/10.1186/s12870-016-0822-4).
- Lu, J., *et al* (2020). A direct PCR-based SNP marker-assisted selection system (D-MAS) for different crops. *Mol Breeding* 40, 9. doi:[10.1007/s11032-019-1091-3](https://doi.org/10.1007/s11032-019-1091-3).
- Manning, K., *et al* (2006). A naturally occurring epigenetic mutation in a gene encoding an SBP-box transcription factor inhibits tomato fruit ripening. *Nature Genetics* 38, 948–952. doi: 10.1038/ng1841
- Mayobre, C., *et al* (2021). Genetic dissection of aroma biosynthesis in melon and its relationship with climacteric ripening. *Food Chemistry* 353, 129484. doi:[10.1016/j.foodchem.2021.129484](https://doi.org/10.1016/j.foodchem.2021.129484).
- Moreno, E., *et al* (2008). Candidate genes and QTLs for fruit ripening and softening in melon. *Theor Appl Genet* 116, 589–602. doi: 10.1007/s00122-007-0694-y
- Obando-Ulloa, J. M., *et al* (2008). Climacteric or non-climacteric behavior in melon fruit: 1. Aroma volatiles. *Postharvest Biology and Technology* 49, 27–37. doi:[10.1016/j.postharvbio.2007.11.004](https://doi.org/10.1016/j.postharvbio.2007.11.004).
- Oren, E., *et al* (2022). QTL mapping and genomic analyses of earliness and fruit ripening traits in a melon Recombinant Inbred Lines population supported by de novo assembly of their parental genomes. *Horticulture Research*, uhab081. doi:[10.1093/hr/uhab081](https://doi.org/10.1093/hr/uhab081).
- Ortega, M. A., All, J. N., Boerma, H. R., and Parrott, W. A. (2016). Pyramids of QTLs enhance host-plant resistance and Bt-mediated resistance to leaf-chewing insects in soybean. *Theor Appl Genet* 129, 703–715. doi:[10.1007/s00122-015-2658-y](https://doi.org/10.1007/s00122-015-2658-y).
- Pech, J. C., Bouzayen, M., and Latché, A. (2008). Climacteric fruit ripening: Ethylene-dependent and independent regulation of ripening pathways in melon fruit. *Plant Science* 175, 114–120. doi:[10.1016/j.plantsci.2008.01.003](https://doi.org/10.1016/j.plantsci.2008.01.003).

- Pereira, L. (2018). Genetic dissection of fruit quality and ripening traits in melon. PhD thesis, Universitat Autònoma de Barcelona, Barcelona.
- Pereira, L., *et al* (2018). QTL mapping of melon fruit quality traits using a high-density GBS-based genetic map. *BMC Plant Biology* 18, 324. doi:[10.1186/s12870-018-1537-5](https://doi.org/10.1186/s12870-018-1537-5).
- Pereira, L., *et al* (2020). Genetic dissection of climacteric fruit ripening in a melon population segregating for ripening behavior. *Horticulture Research* 7, 1–18. doi:[10.1038/s41438-020-00411-z](https://doi.org/10.1038/s41438-020-00411-z).
- Pereira, L., *et al* (2021). A novel introgression line collection to unravel the genetics of climacteric ripening and fruit quality in melon. *Sci Rep* 11, 11364. doi:[10.1038/s41598-021-90783-6](https://doi.org/10.1038/s41598-021-90783-6).
- Pereira, L., Pujol, M., Garcia-Mas, J., and Phillips, M. A. (2017). Non-invasive quantification of ethylene in attached fruit headspace at 1 p.p.b. by gas chromatography–mass spectrometry. *The Plant Journal* 91, 172–183. doi:[10.1111/tpj.13545](https://doi.org/10.1111/tpj.13545).
- Périn, C., *et al* (2002). A reference map of *Cucumis melo* based on two recombinant inbred line populations. *Theor Appl Genet* 104, 1017–1034. doi:[10.1007/s00122-002-0864-x](https://doi.org/10.1007/s00122-002-0864-x).
- Perpiñá, G., Cebolla-Cornejo, J., Esteras, C., Monforte, A. J., and Picó, B. (2017). ‘MAK-10’: A Long Shelf-life Charentais Breeding Line Developed by Introgression of a Genomic Region from Makuwa Melon. *HortScience* 52, 1633–1638. doi:[10.21273/HORTSCI12068-17](https://doi.org/10.21273/HORTSCI12068-17).
- Prasanna, V., Prabha, T. N., and Tharanathan, R. N. (2007). Fruit ripening phenomena—an overview. *Critical Reviews in Food Science and Nutrition* 47, 1–19. doi:10.1080/10408390600976841
- R Core Team (2020). R: A language and environment for statistical computing. R Foundation for Statistical Computing, Vienna, Austria. URL <https://www.R-project.org/>.
- Ríos, P., *et al* (2017). ETHQV6.3 is involved in melon climacteric fruit ripening and is encoded by a NAC domain transcription factor. *The Plant Journal* 91, 671–683. doi:[10.1111/tpj.13596](https://doi.org/10.1111/tpj.13596).

- Robbins, M. D., Casler, M. D., and Staub, J. E. (2008). Pyramiding QTL for multiple lateral branching in cucumber using inbred backcross lines. *Mol Breeding* 22, 131–139. doi:[10.1007/s11032-008-9162-x](https://doi.org/10.1007/s11032-008-9162-x).
- Saladié, M., *et al* Comparative transcriptional profiling analysis of developing melon (*Cucumis melo* L.) fruit from climacteric and non-climacteric varieties. *BMC Genomics* 16, 440 (2015). doi: 10.1186/s12864-015-1649-3
- Sandhu, N., *et al* (2019). Marker Assisted Breeding to Develop Multiple Stress Tolerant Varieties for Flood and Drought Prone Areas. *Rice* 12, 8. doi: 10.1186/s12284-019-0269-y
- Serra, O., *et al* (2016). Marker-assisted introgression (MAI) of almond genes into the peach background: a fast method to mine and integrate novel variation from exotic sources in long intergeneration species. *Tree Genetics & Genomes* 12, 96. doi:[10.1007/s11295-016-1056-1](https://doi.org/10.1007/s11295-016-1056-1).
- Seymour, G. B., Manning, K., Eriksson, E. M., Popovich, A. H., and King, G. J. (2002). Genetic identification and genomic organization of factors affecting fruit texture. *Journal of Experimental Botany* 53, 2065–2071. doi:[10.1093/jxb/erf087](https://doi.org/10.1093/jxb/erf087).
- Urrutia, M., Rambla, J. L., Alexiou, K. G., Granell, A., and Monfort, A. (2017). Genetic analysis of the wild strawberry (*Fragaria vesca*) volatile composition. *Plant Physiology and Biochemistry* 121, 99–117. doi:[10.1016/j.plaphy.2017.10.015](https://doi.org/10.1016/j.plaphy.2017.10.015).
- Vegas, J., Garcia-Mas, J., and Monforte, A. J. (2013). Interaction between QTLs induces an advance in ethylene biosynthesis during melon fruit ripening. *Theor Appl Genet* 126, 1531–1544. doi:[10.1007/s00122-013-2071-3](https://doi.org/10.1007/s00122-013-2071-3).
- Vrebalov, J., *et al* (2002). A MADS-Box Gene Necessary for Fruit Ripening at the Tomato Ripening-Inhibitor (Rin) Locus. *Science* 296, 343–346. doi:[10.1126/science.1068181](https://doi.org/10.1126/science.1068181).
- Wang, R., *et al*(2020). The rin, nor and Cnr spontaneous mutations inhibit tomato fruit ripening in additive and epistatic manners. *Plant Science* 294, 110436. doi:[10.1016/j.plantsci.2020.110436](https://doi.org/10.1016/j.plantsci.2020.110436).
- Yahyaoui, F. E. L., *et al* (2002). Molecular and biochemical characteristics of a gene encoding an alcohol acyl-transferase involved in the generation of aroma volatile

esters during melon ripening. *European Journal of Biochemistry* 269, 2359–2366. doi:<https://doi.org/10.1046/j.1432-1033.2002.02892.x>.

Zhang, N., *et al* (2017). Development of a muskmelon cultivar with improved resistance to gummy stem blight and desired agronomic traits using gene pyramiding. *Czech J. Genet. Plant Breed.* 53, 23–29. doi:[10.17221/84/2016-CJGPB](https://doi.org/10.17221/84/2016-CJGPB).

Zhao, G., *et al* (2019). A comprehensive genome variation map of melon identifies multiple domestication events and loci influencing agronomic traits. *Nat Genet* 51, 1607–1615. doi:[10.1038/s41588-019-0522-8](https://doi.org/10.1038/s41588-019-0522-8).

Chapter 3.2

Pyramiding four ripening-related QTLs in the elite melon variety ‘Védrantais’ to slow down climacteric ripening

Pyramiding four ripening-related QTLs in the elite melon variety ‘Védrantais’ to slow down climacteric ripening

Miguel Santo Domingo¹, Luis Reig¹, Marta Pujol^{1,2}, Jordi Garcia-Mas^{1,2}

¹Centre for Research in Agricultural Genomics (CRAG) CSIC-IRTA-UAB-UB, Edifici CRAG, Campus UAB, 08193 Bellaterra, Barcelona, Spain

²Institut de Recerca i Tecnologia Agoralimentàries (IRTA), Edifici CRAG, Campus UAB, 08193 Bellaterra, Barcelona, Spain

Abstract

Fruit ripening is an essential process for seed dispersal, and it has significant effects in fruit shelf-life and quality. While tomato is the model plant to study this process, melon has the advantage of having both climacteric and non-climacteric varieties within the same species. In melon climacteric ripening, a peak of ethylene during ripening leads to some physiological changes affecting fruit quality, as aroma production or flesh softening. In non-climacteric melon ripening, with the absence of the ethylene peak, these physiological changes are milder, improving consumers' perception of fruit quality. In this study, we pyramided four already characterized QTLs affecting climacteric ripening, *ETHQB3.5*, *ETHQV6.3*, *ETHQV8.1* and *MAK10.1*, in the genetic background of the climacteric variety 'Védraçais', with the goal of generating slow ripening lines. Preliminary results of the project with *ETHQV8.1* and *MAK10.1* suggest the possibility of remarkably smoothing and delaying the ethylene peak, improving fruit shelf-life. Both analyzed QTLs epistatically controlled fruit ripening by shaping the ethylene peak, although their effects were different. While *ETHQV8.1* reduced and delayed the ethylene peak without major changes in fruit quality, *MAK10.1* had a great effect in the ethylene peak. The total disruption of the shape of the peak provoked drastic changes in fruit quality perception, mainly affecting fruit firmness and aroma production. With these results, we present an effective approach to modulate fruit ripening and quality, but we also present the drawbacks of using some QTLs for plant breeding, also pointing out the importance of identifying the causal genes in order to search for natural allelic variability or inducing new ones.

Keywords

Fruit ripening, ethylene, melon, QTL stacking, fruit quality.

Introduction

Fruit development is an essential process in the life cycle of fruity plants, as fruits contain the seeds and allow them to develop. Fruit ripening is the last stage of fruit development, where fruits become attractive for animals, including humans. Thus, ripening process has a high economic importance but also a high ecological impact due to its effect on fruit loss and the generation of organic waste.

Melon (*Cucumis melo* L.) is a highly interesting crop for fruit ripening studies, due to its wide spectrum of fruit ripening behavior in the same species. There are climacteric varieties, where there is a peak of autocatalytic ethylene production and respiration during ripening, and non-climacteric varieties, without a peak of autocatalytic ethylene production nor increased respiration rate. In this species, some changes happening during fruit ripening are dependent on ethylene as the production of aroma, and other changes are independent of the hormone as the accumulation of sugars, both traits highly appreciated by consumers (Pech *et al*, 2008).

Improving these complex traits has been one of the major goals in melon plant breeding, and several mapping populations have been developed to identify the regions controlling them. One type of mapping populations are Introgression Line (IL) populations, where the whole collection shares the genetic background of the recurrent parent, but each line has one introgression from the donor parent, ideally covering the whole genome considering all the lines (Eshed & Zamir, 1995). This mapping strategy has been used several times in melon with different parents, detecting QTLs for several ripening-related traits (Zarid *et al*, 2021; Pereira *et al*, 2021; Perpiñá *et al*, 2021; Eduardo *et al*, 2007; Obando-Ulloa *et al*, 2008). ILs have been also used in tomato to study some ripening-related traits (Dariva *et al*, 2021). In melon, some major QTLs for ripening have been previously reported using ILs. *ETHQB3.5* and *ETHQV6.3* were firstly mapped in an IL population with 'Piel de Sapo' (PS) as recurrent parent, and 'Songwan Charmi' (SC, PI 161375) as donor parent (Eduardo *et al*, 2005; Vegas *et al*, 2013). Later, *ETHQV6.3* was validated in a climacteric background, and the causal gene, *CmNAC-NOR*, was identified (Ríos *et al*, 2017). This QTL was also mapped in other IL populations, with different parental lines (Pereira *et al*, 2021; Santo Domingo *et al*, 2022). *CmNAC-NOR* has been recently re-validated using CRISPR/Cas9 gene editing in different backgrounds (Wang *et al*, 2022; Liu *et al*, 2022), revealing new roles on seed and fruit development. In the case of *ETHQB3.5*, the causal gene has not been identified yet although epistatic effects

have been observed when combined with *ETHQV6.3* and *ETHQV8.1* in a non-climacteric background (Santo Domingo *et al*, 2022). Another interesting ripening-related QTL is *MAK10.1*. It was first reported in an IL population in the 'Védrantais' (Ved) genetic background with introgressions of 'Ginseng Makuwa' PI 420176 (Mak) (Perpiñá *et al*, 2016; Perpiñá *et al*, 2017), and it was later characterized for its aroma profile (Perpiñá *et al*, 2021). The fourth major QTL described in melon, *ETHQV8.1*, was firstly mapped in a Recombinant Inbred Line (RIL) population funded by PS and Ved, affecting ethylene production and all ripening-related traits (Pereira *et al*, 2020). It was then validated in reciprocal IL populations with the same parents (Pereira *et al*, 2021; Santo Domingo *et al*, accepted), emerging as the main QTL controlling climacteric ripening between these two varieties.

IL populations allow to pyramid different QTLs in the same genetic background, making possible to study epistatic effects and minimizing the effect of the background. This strategy has been performed in different crops for several traits. It has been used to study biotic stress resistance in pea, rice, and soybean (Sandhu *et al*, 2019; Guan *et al*, 2019; Lavaud *et al*, 2016; Ortega *et al*, 2016), and also yield related traits in tomato and cucumber (Gur & Zamir, 2015; Robbins *et al*, 2008). In melon, this strategy has been previously used to study fruit ripening in the non-climacteric background PS (Vegas *et al*, 2013; Santo Domingo *et al*, 2022). In those studies, the QTLs *ETHQB3.5*, *ETHQV6.3* and *ETHQV8.1* have been reported to interact epistatically, being their effect in ripening a non-linear combination of their single effects. Delaying and/or smoothing the climacteric behavior of melon has not been addressed yet using this approach, but it can be a powerful tool in melon breeding to increase fruit shelf-life and reduce food waste.

The single effects of these QTLs have been validated, with the exception of *ETHQB3.5*, in the Ved background, all of them delaying climacteric ripening with different degrees, but no interaction studies have been performed. Pyramiding and analyzing together *ETHQB3.5*, *ETHQV6.3*, *ETHQV8.1* and *MAK10.1* can bring to light new interactions in the climacteric 'Védrantais' background, helping to understand climacteric ripening process and to fine-tune it, allowing future developments of interesting new alleles of the causal genes with potential applications in melon breeding programs to develop long shelf-life varieties.

Materials and methods

Plant material

To develop a new collection of ILs with four QTLs pyramided in a climacteric genetic background, two different IL populations were used, both sharing the same recurrent parent ‘Védrantais’, a French climacteric cultivar with a climacteric behavior, but two different donors. The first population had ‘Piel de Sapo’ as the donor parent (Pereira *et al*, 2021). PS is a Spanish cultivar with non-climacteric behavior, and three ILs belong to this population: 1QPS3, 1QPS6 and 1QPS8, previously known as PS3.2, PS6.1 and PS8.2, respectively (Table 3.2.1). The second population had ‘Ginseng Makuwa’ as donor parent (Perpiñá *et al*, 2016). Mak has a climacteric behavior, but not as strong as Ved. One IL comes from this second population: 1QMAK10, previously known as MAK_10.1 (Table 3.2.1).

Table 3.2.1. Summary of the ILs used or developed in the present study. All lines share the genetic background of ‘Védrantais’.

Line	QTL	Previous name	Reference
1QPS3	PS-ETHQB3.5	PS3.2	Pereira <i>et al</i> , 2021
1QPS6	PS-ETHQV6.3	PS6.1	Pereira <i>et al</i> , 2021
1QPS8	PS-ETHQV8.1	PS8.2	Pereira <i>et al</i> , 2021
1QMAK10	Mak-MAK10.1	MAK_10-1	Perpiñá <i>et al</i> , 2016
2QPS3.6	PS-ETHQB3.5 + PS-ETHQV6.3		This work
2QPS3.8	PS-ETHQB3.5 + PS-ETHQV8.1		This work
2QPSMAK3.10	PS-ETHQB3.5 + Mak-MAK10.1		This work
2QPS6.8	PS-ETHQV6.3 + PS-ETHQV8.1		This work
2QPSMAK6.10	PS-ETHQV6.3 + Mak-MAK10.1		This work
2QPSMAK8.10	PS-ETHQV8.1 + Mak-MAK10.1		This work
3QPS3.6.8	PS-ETHQB3.5 + PS-ETHQV6.3 + PS-ETHQV8.1		This work
3QPSMAK3.6.10	PS-ETHQB3.5 + PS-ETHQV6.3 + Mak-MAK10.1		This work
3QPSMAK3.8.10	PS-ETHQB3.5 + PS-ETHQV8.1 + Mak-MAK10.1		This work
3QPSMAK6.8.10	PS-ETHQV6.3 + PS-ETHQV8.1 + Mak-MAK10.1		This work
4QPSMAK3.6.8.10	PS-ETHQB3.5 + PS-ETHQV6.3 + PS-ETHQV8.1 + Mak-MAK10.1		This work

1QPS6, 1QPS8 and 1QMAK10 carried QTLs delaying climacteric ripening. 1QPS3 did not have an effect in climacteric ripening, but it carried in its introgression the region of

Chapter 3: QTL interactions

a previously known QTL *ETHQB3.5* found in another population involved in climacteric ripening (Vegas *et al*, 2013).

Breeding scheme

To develop the pyramided lines, Marker Assisted Selection (MAS) was used to select homozygous introgressions in the F₂ populations (Figure 3.2.1). To develop the double ILs, two ILs were crossed in spring 2020, and the F₁ was self-pollinated to obtain the F₂ and select the homozygous plants for the two respective introgressions. For the development of the triple ILs, two double ILs sharing one of the introgressions were crossed and then self-pollinated in spring 2021. Plants with two homozygous introgressions (plus the one that was already homozygous in the F₁) were selected, carrying three homozygous introgressions. For the quadruple IL (under development), two triple ILs were crossed in summer 2022, sharing two of the introgressions. In the F₂, the remaining two introgressions will be genotyped by the end of 2022, and the plants carrying the four introgressions in homozygosity will be selected. So, the entire population for the experiment will be developed in 6 generations and finished by 2023.

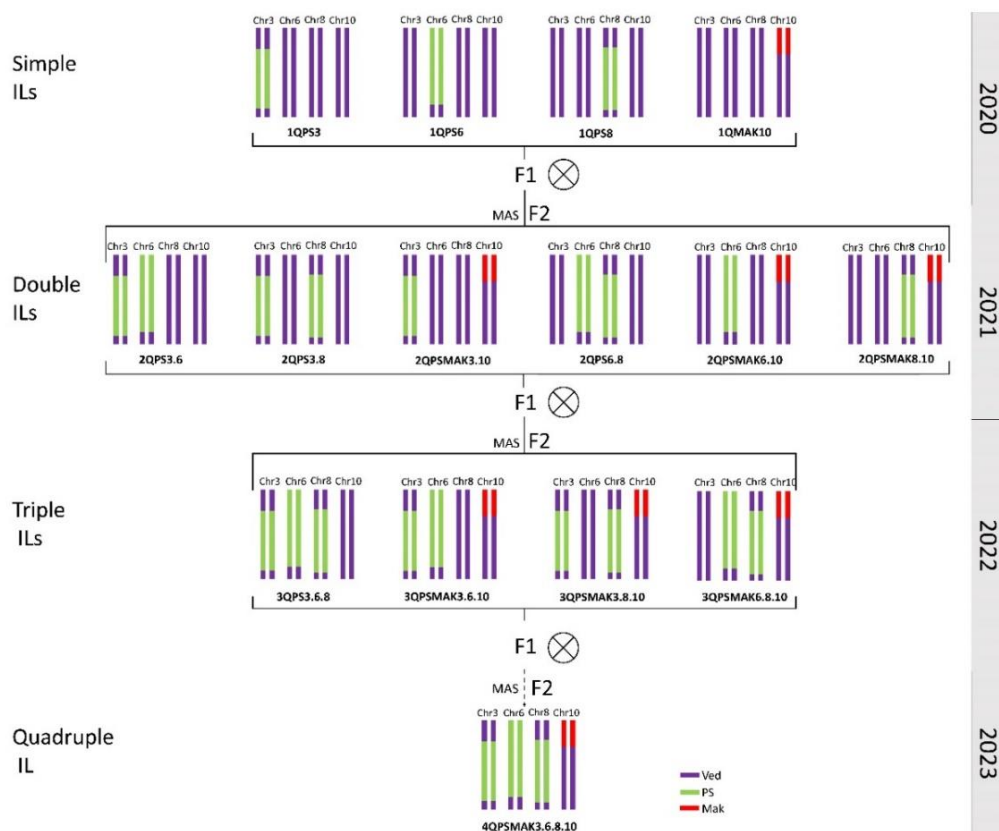


Figure 3.2.1. Graphic representation of the breeding scheme followed to develop the IL population.

DNA extraction and genotyping

The DNA for genotyping and selection of plants was extracted from seedlings using an alkaline-lysis extraction protocol (Lu *et al*, 2020). In summary, grinded leaf tissue was treated with NaOH and then neutralized with Tris-HCl. The extracted DNA was genotyped using SNPs markers, with PACE2.0 system (3CR Bioscience, Essex, UK) based on an allele-specific PCR performed in a LightCycler480 (Roche). Primers used for this PCR were designed by the 3CR Bioscience free design service (Table 3.2.S1). In the case of the introgressions in chromosome 3, 8 and 10, two flanking markers for the QTL were used. In the case of the introgression in chromosome 6, the marker used was inside the causal gene MELO3C016540.2 (Ríos *et al*, 2017).

Growing conditions

Seedlings were grown under controlled conditions in a greenhouse (CRAG, Barcelona) for three weeks in organic pots. After genotyping and selection, they were transferred to coconut fiber sacks and grown under greenhouse conditions in Caldes de Montbui (Barcelona). For the development of the multiple ILs, two generations were obtained per year, and for the phenotyping experiment, one generation was grown per year during spring-summer season. Plants were hand-pollinated until one fruit per plant was set and pruned twice per week.

During the development of the lines, they were harvested once the abscission layer was formed, considering seeds fully developed at that point. For the phenotyping experiment, the harvest point was fixed based in three considerations: (i) when the fruit fully abscised from the plant, (ii) 5 days after the abscission layer detection if the fruit did not abscise, or (iii) at 56 days after pollination (DAP) when the fruit did not form abscission layer in the case of PS.

Phenotyping

Melon fruits were phenotyped regarding their ripening behavior and fruit quality as previously described, with some modifications (Pereira *et al*, 2020). In the case of ripening behavior, five traits were phenotyped: production of aroma (EARO), change of color of the rind (ECC), abscission layer formation (EALF), abscission level (ABS) and harvest date (HAR). ABS was treated as semi-quantitative, in a range from 0 (no abscission layer formation) to 3 (complete abscission from the plant). Related with ripening, also some ethylene traits were analyzed: maximum ethylene production (ETH), earliness of ethylene production (DAPE) and earliness of the ethylene peak (DAPP). In

the case of fruit quality traits, three traits were measured: fruit weight (FW), soluble solid content (SSC) and flesh firmness (FIR) (Table 3.2.2). Also, two more characteristics were annotated considering fruit quality: the type of aroma and the color of the rind after ripening. For the ethylene production measurements, four fruits were evaluated per genotype, while more than nine fruits were analyzed per genotype for the rest of traits.

Table 3.2.2. Phenotypes evaluated in the present study.

Category	Trait (units)	Code
Fruit quality	Fruit weight (g)	FW
	Soluble solid content (°Brix)	SSC
	Flesh firmness (kg cm ⁻²)	FIR
	Type of aroma	
	Color of the rind when ripe	
Fruit ripening	Earliness of aroma production (DAP*)	EARO
	Earliness of abscission layer formation (DAP*)	EALF
	Earliness of the change of color (DAP*)	ECC
	Level of abscission	ABS
	Harvest date (DAP*)	HAR
Ethylene production	Ethylene production (μL kg ⁻¹ h ⁻¹)	ETH
	Earliness of ethylene production (DAP*)	DAPE
	Earliness of the ethylene peak (DAP*)	DAPP

*DAP Days after pollination

For FW, fruits were weighted at harvest. SSC was measured using a refractometer (Atago TM) from fresh flesh juice. FIR was measured using a penetrometer (Fruit TestTM, Wagner Instruments) at harvest.

Ethylene production

Ethylene production was monitored *in vine* in four fruits per genotype, starting from 25 DAP until harvest. Gas chromatography – mass spectrometry (GC-MS) was used, as previously described (Pereira *et al*, 2017). In summary, fruits were covered hermetically with polyethylene bags and filled with air. After one hour, a sample of the atmosphere of the bag was withdrawn using a syringe and introduced in a 10 mL GC-MS vial. Then, the vials were analyzed in a GC-MS (Agilent 7890A). The production of ethylene was measured every other day until it was detected, and then it was measured daily until harvest.

Statistical analyses

For statistical analyses, ripening related traits were imputed as the harvest date when they were not observed.

All analyses and representations were performed using R v4.1.1 with RStudio interface (R Core Team, 2020). Plots were made with “ggplot2” package, and linear models were performed using function “lm” using the different alleles of the QTLs as factors. Model selection was performed using Akaike Information Criterion. ANOVA and t-tests were done using “rstats” package. The significance level was considered as p-value < 0.05.

Results

Development of the pyramided introgression lines

The construction of the pyramided lines started by crossing the two single ILs 1QPS8 and 1QMAK10 in summer 2020 (Figure 3.2.1). Then, by self-pollinating the F1, we obtained the F2 population where we selected the two QTLs in homozygosity in 2021. From 384 F2 seedlings, we obtained 11 double IL plants 2QPSMAK8.10 (Table 3.2.S2).

These double IL (2QPSMAK8.10) and the single ILs 1QPS8 and 1QMAK10 were then crossed with the two remaining single ILs 1QPS3 and 1QPS6. In 2022, from the F2 of these different crosses we selected by MAS the triple ILs 3QPSMAK3.8.10 and 3QPSMAK6.8.10 and the double ILs 2QPS3.8, 2QPS6.8, 2QPSMAK3.10 and 2QPSMAK6.10 (Table 3.2.S2). We crossed these ILs to obtain the remaining triple and quadruple ILs in 2023 (Table 3.2.S2).

The development of the IL population for the experiment, with four stacked QTLs with all the combinations, was done in 6 generations during 3 years. Another year is needed for the phenotyping experiment.

The parental lines covered a wide range of ripening behavior

During summer 2021, we characterized the three parental lines of the entire population: Ved, Mak and PS. Ved is the common recurrent parent for all the ILs, as they share most of the genome from this cultivar. Ved is considered an elite climacteric cultivar, appreciated for its flavor. It produced round small melons, very aromatic and sweet. PS is also considered an elite cultivar, but it is non-climacteric, with the lack of sweet aroma that characterize climacteric melons. Mak is a Japanese cultivar producing sweet small melons, with a similar SSC as Ved, and a mild climacteric behavior (Perpiñá *et al*, 2016).

Comparing the three of them, we could detect significant differences regarding FW, but not FIR or SSC. Ved produced medium size melons of around 1 kg, while PS melons were double their size, and Mak half their size, approximately (Figure 3.2.2A; Table

3.2.S3). We could not observe statistical differences between the three cultivars for FIR and SSC (Figure 3.2.2B,C; Table 3.2.S3).

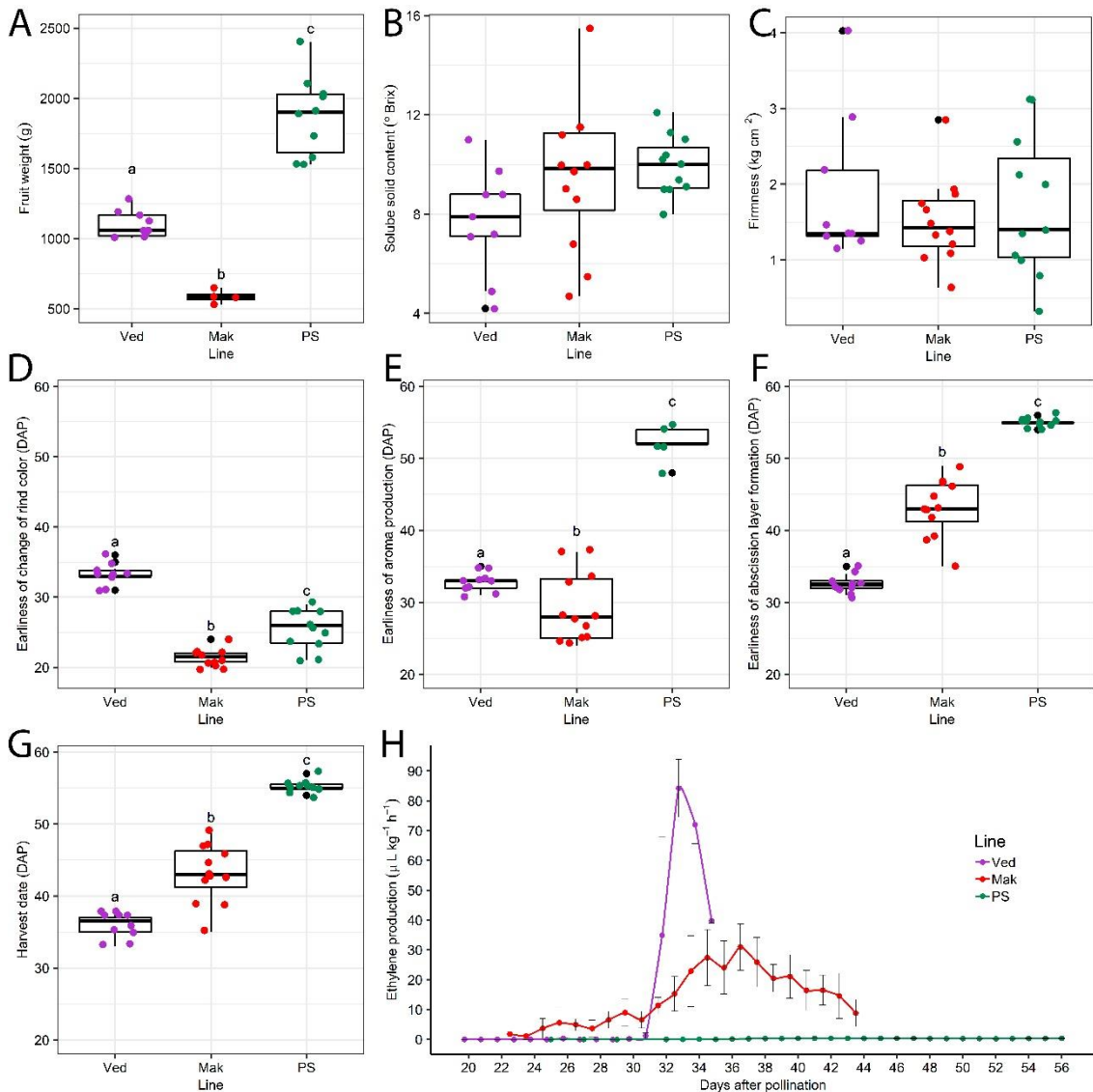


Figure 3.2.2 Phenotypes of the parental lines ‘Védrantais’ (Ved), ‘Ginseng makuwa’ (Mak) and ‘Piel de Sapo’ (PS). **A)** Fruit weight (g), **B)** Soluble solid content (°Brix), **C)** Flesh firmness (kg cm⁻²), **D)** First day of rind color change (DAP), **E)** First day of aroma production (DAP), **F)** First day of abscission layer formation (DAP), **G)** Harvest date (DAP), and **H)** Ethylene production profile from 20 DAP until harvest (μL kg⁻¹ h⁻¹). DAP = Days after pollination. Lower case letters indicate significantly different groups and black points represent outliers.

Also related with fruit quality is the change of color of the rind during ripening. Ved turned orange quickly during climacteric ripening, while Mak turned yellow slowly and PS also presented some yellowing in parts of the rind during ripening (Figure 3.2.2D; Figure 3.2.3). It is interesting to note that the color change in Ved was related with climacteric ripening, as it was produced at the same time as the ethylene peak, while in PS and Mak the change to yellow was ethylene independent, since it was observed long

before ethylene production in Mak and PS did not produce ethylene at all (Figure 3.2.2D; Table 3.2.S3).

When we focused on ripening traits, we detected significant differences for all the traits. Apart from the differences on the already mentioned change of color in the rind, we also perceived differences in aroma production (Figure 3.2.2E; Table 3.2.S3). In both Ved and Mak, aroma was coupled to the ethylene production, and in contrast, PS did not produce aroma or produce a slight aroma 15 days later than the other two. The abscission layer was formed also differently in the three cultivars (Figure 3.2.2F; Table 3.2.S3). In Ved, the abscission layer was developed during the ethylene peak, while PS and Mak did not form an abscission layer. The harvest date followed the same trend, because it depends on the abscission layer formation in our protocol. Ved was harvested at around 35 DAP, after climacteric ethylene production (Figure 3.2.2G,H; Table 3.2.S3), while PS was harvested at 56 DAP as it did not have climacteric response. In the case of Mak, although it produced ethylene and it is considered climacteric, we harvested it later than Ved, at around 45 DAP, when melons presented extreme softening considering them fully ripe at that point (Figure 3.3.2G; Table 3.2.S3).

The ethylene production profile was different also among the three cultivars (Figure 3.2.2H). Ved presented a typical climacteric ethylene peak, with a sharp increase in ethylene production at the onset of ripening producing the physiological changes related with climacteric. Meanwhile, PS produced the typical non-climacteric profile, with a very low ethylene production all along fruit ripening ($< 0.5 \mu\text{L kg}^{-1} \text{h}^{-1}$), with no detectable peak. Mak, considered climacteric, produced a medium amount of ethylene during ripening with a wide peak few days after Ved, and in this cultivar the ethylene production triggered some of the typical climacteric responses, as the aroma production, but not others as the abscission layer formation.

Fruit quality drastically changed by introgressing *MAK10.1*

While the rest of the ILs were under development, we performed a preliminary phenotyping of the already developed lines 1QPS8, 1QMAK10 and 2QPSMAK8.10, together with the above-mentioned parental lines in 2021 (Figure 3.2.3).

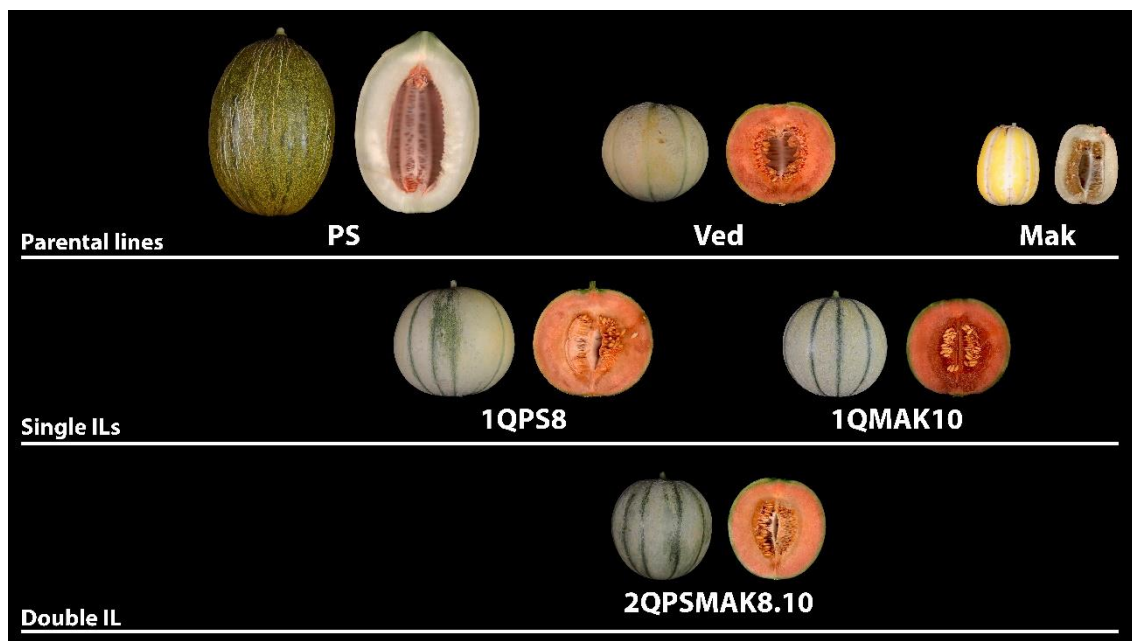


Figure 3.2.3. External and internal appearance of the six lines characterized in 2021.

The introgressions of the QTLs were not affecting FW or SSC (Figure 3.2.4A,B, Table 3.2.S3), but we detected significant changes in fruit firmness (Figure 3.2.4C, Table 3.2.S3). When introgressing the QTL from PS in chromosome 8 we increased the firmness of the flesh, a trait partially dependent on ethylene (Pech *et al*, 2008). But the bigger effect was observed when introgressing the QTL from Mak in chromosome 10. The lines carrying this introgression presented an extremely hard fruit flesh, obtaining the maximum possible values with the penetrometer. Also, we could observe an epistatic interaction between the two QTLs, being *MAK10.1* dominant over *ETHQV8.1*. (Figure 3.2.4C, Figure 3.2.5A, Table 3.2.S3, Table 3.2.S4A).

Also, the change of color of the rind was different in the lines. While Ved and 1QPS8 turned orange when ripe, 1QMAK10 and 2QPSMAK8.10 did not turn yellow or orange, but they had some light green regions in the rind (Figure 3.2.3).

The detected aroma was also different. While Ved and 1QPS8 had sweet fruity aroma when harvested, the lines carrying the Mak allele in chromosome 10 did not smell sweet, and the aroma was much milder, indicating a dominant epistatic effect of *MAK10.1* over *ETHQV8.1*.

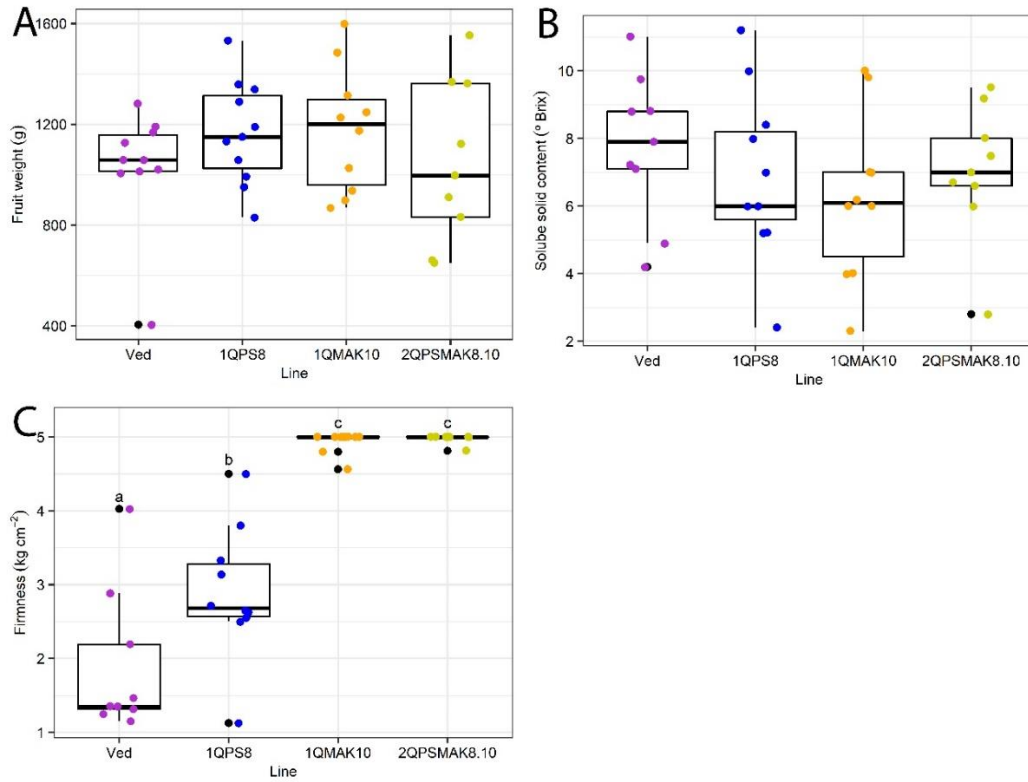


Figure 3.2.4. Fruit quality related phenotypes of the parental line Ved and the evaluated ILs at harvest. **A)** Fruit weight (g), **B)** Soluble solid content (°Brix), and **C)** Flesh firmness (kg cm⁻²). Lower case letters indicate significantly different groups and black points represent outliers.

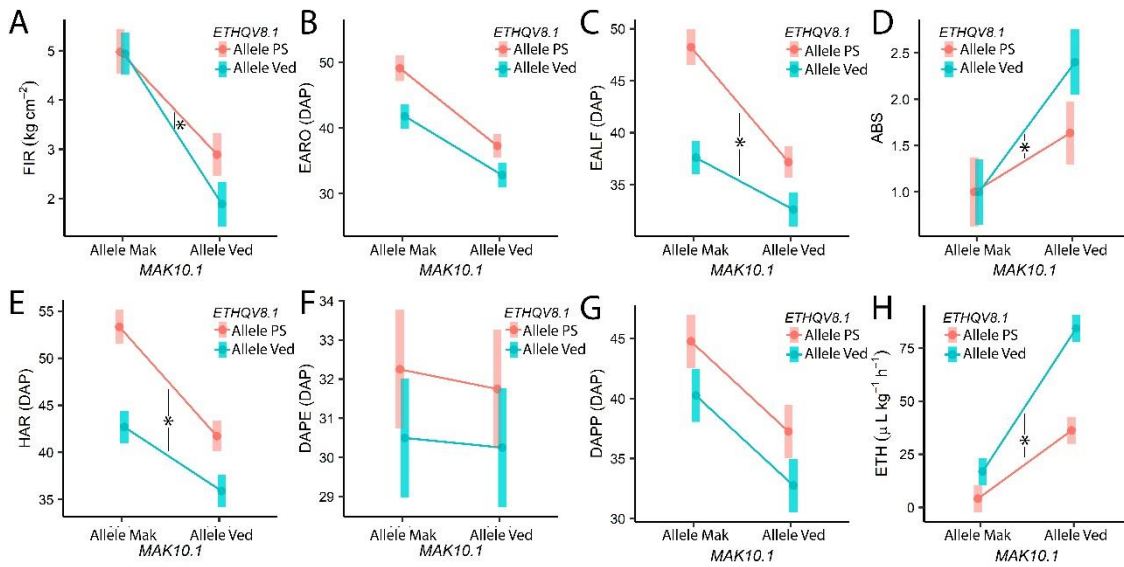


Figure 3.2.5. Interaction plots showing the interactions between ETHQV8.1 and MAK10.1 for **A)** firmness (FIR), **B)** earliness of aroma production (EARO), **C)** earliness of abscission layer formation (EALF), **D)** abscission level (ABS), **E)** harvest date (HAR), **F)** earliness of ethylene production (DAPE), **G)** earliness of the ethylene peak (DAPP), and **H)** maximum ethylene production (ETH). Asterisks indicate significant interactions.

Climacteric ripening is affected by the interaction of *ETHQV8.1* and *MAK10.1*

We detected differences regarding all the ripening-related traits after phenotyping the ripening behavior of the developed ILs (Figure 3.2.6).

Although the type of detected aroma was different, we considered that the first day of aroma detection was dependent on ethylene (Pech *et al*, 2008), and so, on climacteric ripening. In Ved, the aroma started earlier than in the ILs, being the double IL the latest line to produce aroma (Figure 3.2.6A; Table 3.2.S3).

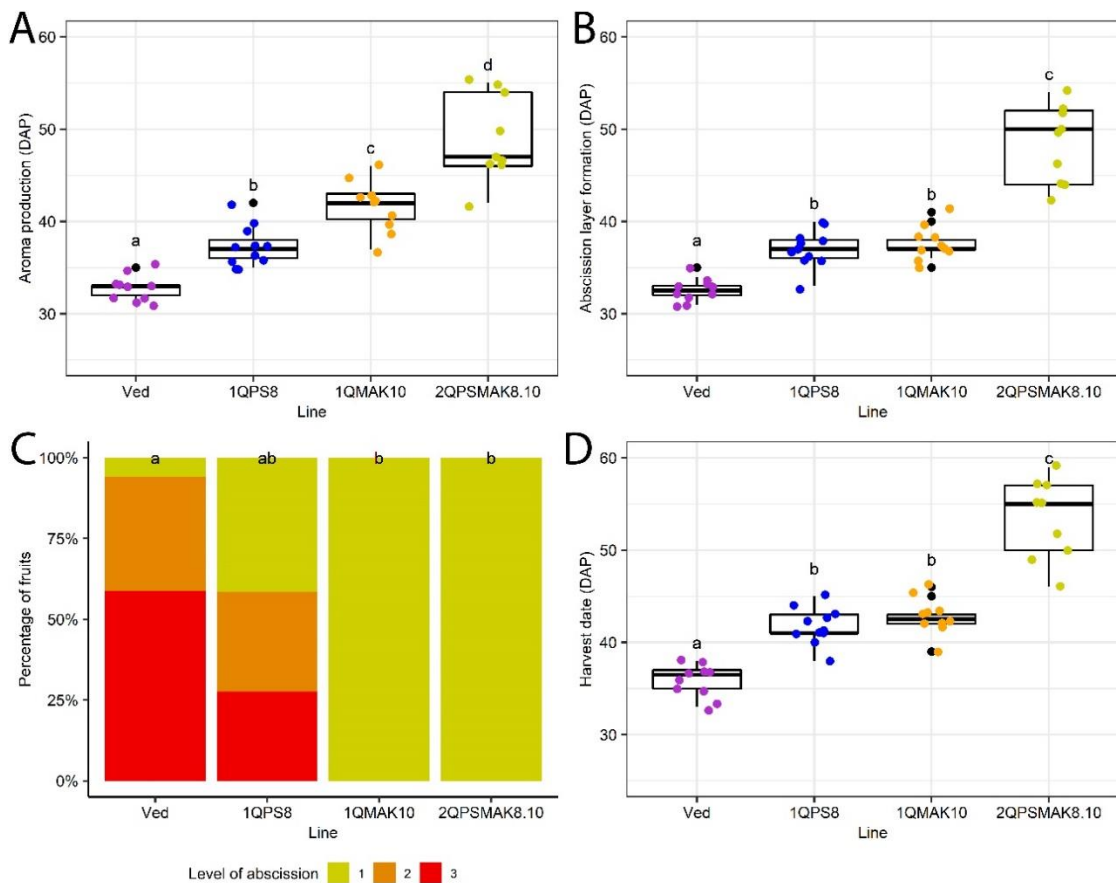


Figure 3.2.6. Ripening related phenotypes of the parental line Ved and the evaluated ILs 1QPS8, 1QMAK10 and 2QPSMAK8.10. **A)** First day of aroma production (DAP), **B)** First day of abscission layer formation (DAP), **C)** Percentage of fruits per line with a certain level of abscission layer formation at harvest (abscission level: 1 (yellow), 2 (orange), 3 (red)) and **D)** Harvest date (DAP). DAP = Days after pollination. Lower case letters indicate significantly different groups. In **A)**, **B)** and **D)**, black points represent outliers.

The same behavior was observed in the other ripening traits, with a general delay on ripening for all the ILs compared to Ved. The abscission layer was formed at the same time in 1QPS8 and 1QMAK10 (Figure 3.2.6B; Table 3.2.S3), but its development was different. While in Ved most of the fruits abscised completely from the plant, this behavior was milder in 1QPS8, with partial abscission layer formation. On the other hand,

when having the Mak allele in chromosome 10 (1QMAK10, 2QPSMAK8.10), the abscission layer development was completely stopped after its appearance, keeping it in an initial step with no progress (Figure 3.2.6C; Table 3.2.S3). In the case of the harvest date, the behavior was similar as the abscission layer formation: it was delayed when introgressing one QTL, and even more delayed when having the two QTLs, having a similar harvest date in 2QPSMAK8.10 and PS (Figure 3.2.6D; Figure 3.2.1G; Table 3.2.S3).

To investigate the interaction between the two QTLs we used linear modeling with the single effects and the interaction between the two QTLs (Table 3.2.S4). Except from EARO (Table 3.2.S4B), we detect significant interaction effects for the other three traits, manifesting that the effects of the QTLs are due to their interaction (Table 3.2.S4C-E). In the case of EALF and HAR, when introgressing both QTLs, the delay was even bigger than the expected without interaction (Table 3.2.S4C,D; Figure 3.2.5B-E), having a “more than additive” effect. In the case of ABS, we observed a dominant epistasis of the QTL in chromosome 10 over the one in chromosome 8, because, as seen in the model, the interaction effect offsets the effect of *ETHQV8.1* (Figure 3.2.6C; Figure 3.3.5D; Table 3.2.S4E).

MAK10.1 disrupts the ethylene peak dominantly over *ETHQV8.1*

To better characterize the ripening behavior of the lines, we measured the ethylene production of the fruits during ripening (Figure 3.2.7).

Analyzing the ethylene profile of the four lines with linear models, we could detect a significant effect of *ETHQV8.1* in delaying the starting date of ethylene production and decreasing the peak (Figure 3.2.7A-C; Table 3.2.S4F-H), but still maintaining the shape of the peak similar to Ved. No interaction was detected in the starting date of ethylene production or the day of the peak (Figure 3.2.5F,G)

The most interesting effect was detected in the two ILs carrying *MAK10.1*, 1QMAK10 and 2QPSMAK8.10. In both lines, the shape of the peak was totally disrupted, having an increase in the ethylene at the beginning and then it was maintained flat until harvest (Figure 3.2.7A). 1QMAK10 had the plateau of ethylene production at a moderate level (around 13 $\mu\text{L kg}^{-1} \text{h}^{-1}$), and 2QPSMAK8.10 had the plateau at a much lower level (around 3 $\mu\text{L kg}^{-1} \text{h}^{-1}$), manifesting also an interaction between the two QTLs in the case of maximum ethylene production (Figure 3.2.5H; Figure 3.2.7C; Table 3.2.S4H) but a

dominance of *MAK10.1* over *ETHQV8.1* in the case the disruption of the ethylene production profile.

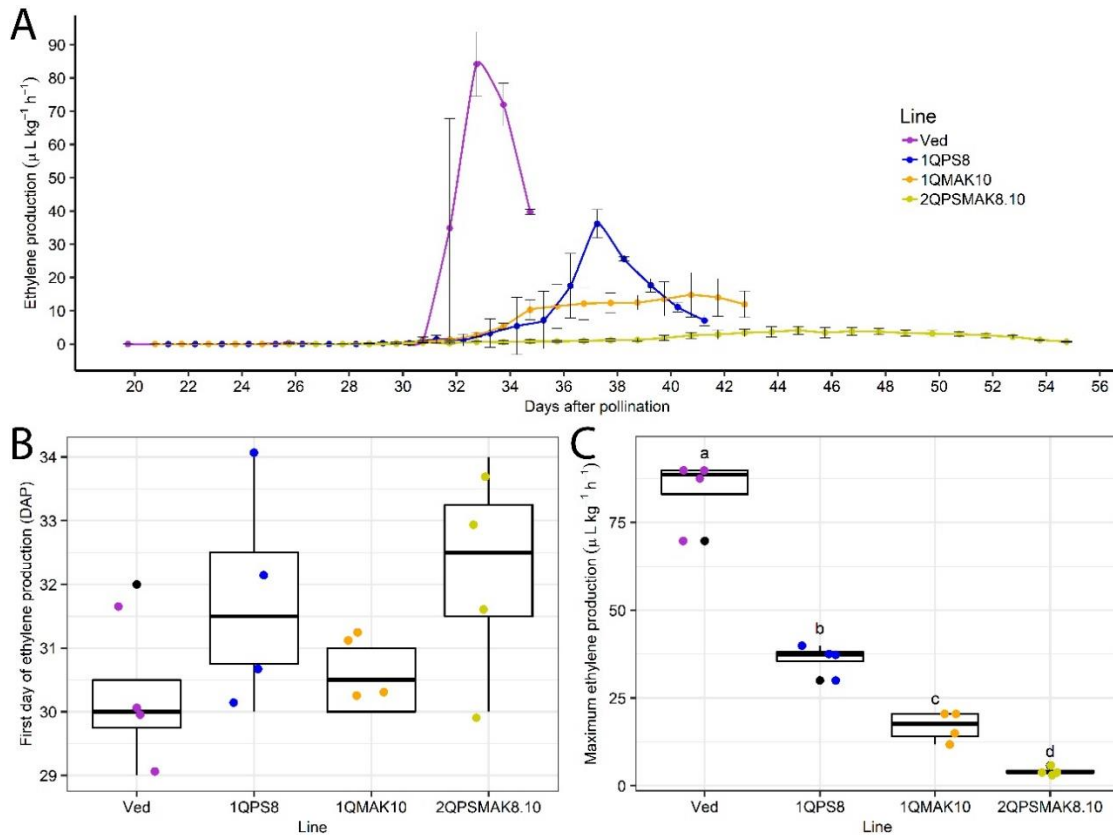


Figure 3.2.7. Ethylene related phenotypes of the parental line Ved and the evaluated ILs 1QPS8, 1QMAK10 and 2QPSMAK8.10. **A)** Ethylene production from 20 DAP until harvest ($\mu\text{L kg}^{-1} \text{h}^{-1}$), **B)** First day of detected ethylene production (DAP), and **C)** Maximum detected ethylene production ($\mu\text{L kg}^{-1} \text{h}^{-1}$). DAP = Days after pollination. In B) and C), lower case letters indicate significantly different groups and black points represent outliers.

Discussion

QTLs *MAK10.1* and *ETHQV8.1* interact to determine fruit ripening behavior in melon

In this work we present a part of an ongoing project, where we try to understand the genetic bases of climacteric fruit ripening in melon, as well as develop a tool to improve fruit shelf-life through marker assisted selection for plant breeding.

We have already analyzed two of the four QTLs that are being pyramided in the climacteric background ‘Védrantais’, detecting a significant interaction between both, shaping climacteric fruit ripening. The interactions between QTLs to tune different traits have been reported before for many species. In rice, epistatic effects have been detected for plant height (Fu *et al*, 2022) or grain chalkiness (Misra *et al*, 2021). In soybean, interaction effects have been also reported for iron deficiency (Assefa *et al*, 2020) or water

use efficiency (Bazzler *et al*, 2020). In fleshy fruits, tomato has been extensively studied, and many traits have been reported to be controlled under epistasis, as fruit morphology (Vazquez *et al*, 2022), mineral content (Capel *et al*, 2017) or yield (Gur & Zamir, 2015). Moreover, some studies had found epistatic effects affecting climacteric behavior in tomato (Wang *et al*, 2020) and melon (Vegas *et al*, 2013; Santo Domingo *et al*, 2022).

Due to epistasis, it may seem difficult to control the phenotypic performance of some important traits in agriculture, as yield, fruit quality or fruit ripening behavior. Understanding the single effects of the QTLs in the same genetic background and their interactions can help to dissect the genetic architecture of these complex traits. Here we only present the work performed with two QTLs, but the future work with four QTLs will provide powerful knowledge to be applied in melon breeding programs, where increasing fruit shelf-life without impairing organoleptic quality is one of the main goals. Also, our studies can help to identify the causal genes of these traits, helping to understand how the QTLs interact and opening new ways for new plant breeding tools as gene editing, allowing the development of new beneficial alleles and fine-tune these quantitative traits.

Putative use of *ETHQV8.1*, *ETHQV6.3*, *ETHQB3.5* and *MAK10.1* in plant breeding

We have been working with two different QTLs coming from different parental lines. In the case of *ETHQV8.1*, coming from PS, we observed a delay in ripening and a decrease and delay in ethylene production (Figure 3.2.7), but we did not observe a decay in fruit quality. Fruits were sweet with a sweet aroma, with a slight increase in firmness (Figure 3.2.4C). A similar effect was reported for *ETHQV6.3*, although there is not ethylene profiling described for 1QPS6 (Pereira *et al*, 2021). In the case of *ETHQB3.5*, we are trying to find out if it has some epistatic effect when combined with other QTLs, since 1QPS3 has not been reported to have an effect in fruit ripening by itself (Pereira *et al*, 2021). These 3 QTLs coming from PS do not seem to have important effects in fruit quality, but they delay fruit ripening, so they can be suitable candidates for melon breeding by improving the shelf life of existing cultivars.

On the contrary, *MAK10.1* seems to be different. Although the effect in ethylene production and ripening was remarkably interesting, it had also negative effects in fruit quality (Figure 3.2.4; Figure 3.2.7). Fruits containing this QTL remained hard when ripe (Figure 3.2.4C), with an unpleasant texture. The worst effect was related with the aroma. Ved is characterized by a sweet and fruity aroma with a major component of esters in its aroma profile (Mayobre *et al*, 2021), making it attractive for consumption. After

introgressing *MAK10.1*, although there was production of aroma, it was unpleasant and completely different to Ved aroma. The effect of this QTL in both firmness and aroma was characterized before (Perpiñá *et al*, 2016). They also reported a reduction in the content of key esters in the aroma profile of MAK_7-2, an IL carrying also the Mak allele in *MAK10.1*, explaining the reduction and change of aroma observed in 1QMAK10 and 2QPSMAK8.10 (Perpiñá *et al*, 2021). This effect was not observed in 1QPS8, but it was in 2QPSMAK8.10, evidencing the dominance of *MAK10.1* over *ETHQV8.1*. On the other hand, *MAK10.1* is a large QTL, covering more than 2 Mbp in the beginning of chromosome 10, so the harmful and beneficial effects of the QTL may be caused by different genes inside the introgression. In that case, a fine mapping of the QTL could help to separate the causal genes and benefit only from the delay in ripening without the undesirable effects in fruit quality.

A balance between fruit ripening and quality should be maintained

The study of the complete set of combinations with the four QTLs will allow us to understand the epistatic effects among them in a climacteric genetic background, and figure out which QTLs or combination is suitable for melon breeding. In the case of *MAK10.1*, it seems an interesting candidate, because of its big effect in the ethylene profiling, but the loss in fruit quality makes this Mak allele unsuitable for breeding. It is important for plant breeding that there is a balance between the positive and negative effects of the QTLs that are used. We can observe a positive balance in 1QPS8, with a delay in ripening, and consequently in fruit shelf-life, which has been reported before (Pereira *et al*, 2020; Pereira *et al*, 2021). The same scenario has been reported in 1QPS6 (Pereira *et al*, 2021). For 1QMAK10, although we have developed a line with a smooth climacteric behavior, its negative effect in fruit aroma and flesh firmness discard its use in plant breeding at the moment.

In this kind of genomic studies with marker assisted introgression, usually two alleles are characterized, one of each parental line of the population. The detrimental effect of one of these alleles does not mean the discard of the QTL for breeding purposes, as other natural or induced alleles may better balance the positives and negatives effects, as it has been reported for *ETHQV6.3*. In the case of this QTL, different effects have been reported when different natural alleles were studied. In a PS background, the introgression of ‘Songwan Charmi’ allele provoked a climacteric behavior at 35 DAP (Santo Domingo *et al*, 2022), while the introgression of a Ved allele led to an unstable climacteric behavior

at 45 DAP (Santo Domingo *et al*, accepted). Moreover, CRISPR/*Cas9* induced alleles of *ETHQV6.3* in a Ved background showed different effects depending on the edit, from a delay in ethylene production to a total loss of climacteric behavior for the knock-out allele, with the consequent loss in fruit quality (Liu *et al*, 2022). These different behaviors reveal the importance of searching for different alleles when an interesting QTL is characterized, to find the perfect balance between its effects. Also, the identification of candidate genes is an interesting approach to develop new alleles and fine-tune the desired phenotypes using gene editing. This approach has been previously used to improve some fruit traits in tomato, such as yield (Li *et al*, 2022) or locule number (Wang *et al*, 2021b).

Conclusion

Here we present an ongoing project of pyramiding four QTLs in the climacteric variety ‘Védrantais’ with the final purpose of developing a slow-ripening line with minimal losses in fruit quality. Although the population is not finished, a preliminary experiment showed an epistatic control of this trait by *ETHQV8.1* and *MAK10.1*, producing a significantly slow-ripening line with detrimental effects in fruit quality due to *MAK10.1*. These results point out the relevance of QTL x QTL interactions shaping ripening behavior, and the importance of finding a balance between the positive and negative effects of the different introgressed alleles.

Supplementary material**Table 3.2.S2.** Summary of the Marker Assisted Selection (MAS) results for the construction of the entire IL population.

Year	Parents	F2 seedlings	Selected plants	Final IL
2021	1QPS8	384	11	2QPSMAK8.10
	1QMAK10			
	1QPS3	384	5	3QPSMAK3.8.10
	2QPSMAK8.10			
	1QPS6	384	4	3QPSMAK6.8.10
	2QPSMAK8.10			
	1QPS3	96	1	2QPS3.6
	1QPS6			
2022	1QPS3	96	3	2QPS3.8
	1QPS8			
	1QPS6	96	3	2QPS6.8
	1QPS8			
	1QPS3	96	4	2QPSMAK3.10
	1QMAK10			
	1QPS6	96	3	2QPSMAK6.10
	1QMAK10			
	3QPSMAK3.8.10	*	*	4QPSMAK3.6.8.10
	3QPSMAK6.8.10			
2023*	2QPS3.10	*	*	3QPSMAK3.6.10
	2QPS6.10			
	2QPS3.8	*	*	3QPS3.6.8
	2QPS6.8			

*F2 seeds for MAS are already developed and will be selected in the near future.

Digital supplementary material

Table 3.2.S1. Markers used for Marker Assisted Selection, with the respective primers design for PACE2.0 genotyping system.

Table 3.2.S3. Mean and standard deviation (SD) of the different analyzed phenotypes in the parental lines and the introgression lines.

Table 3.2.S4. Multiple linear model for the analyzed phenotypes

References

- Assefa, T.; Zhang, J.; Chowda-Reddy, R.V.; Moran Lauter, A.N.; Singh, A.; O'Rourke, J.A.; Graham, M.A.; Singh, A.K. Deconstructing the Genetic Architecture of Iron Deficiency Chlorosis in Soybean Using Genome-Wide Approaches. *BMC Plant Biology* **2020**, *20*, 42, doi:[10.1186/s12870-020-2237-5](https://doi.org/10.1186/s12870-020-2237-5).
- Bazzer, S.K.; Kaler, A.S.; Ray, J.D.; Smith, J.R.; Fritschi, F.B.; Purcell, L.C. Identification of Quantitative Trait Loci for Carbon Isotope Ratio ($\Delta^{13}C$) in a Recombinant Inbred Population of Soybean. *Theor Appl Genet* **2020**, *133*, 2141–2155, doi:[10.1007/s00122-020-03586-0](https://doi.org/10.1007/s00122-020-03586-0).
- Capel, C.; Yuste-Lisbona, F.J.; López-Casado, G.; Angosto, T.; Heredia, A.; Cuartero, J.; Fernández-Muñoz, R.; Lozano, R.; Capel, J. QTL Mapping of Fruit Mineral Contents Provides New Chances for Molecular Breeding of Tomato Nutritional Traits. *Theor Appl Genet* **2017**, *130*, 903–913, doi:[10.1007/s00122-017-2859-7](https://doi.org/10.1007/s00122-017-2859-7).
- Dariva, F.D.; Pessoa, H.P.; Copati, M.G.F.; de Almeida, G.Q.; de Castro Filho, M.N.; Picoli, E.A. de T.; da Cunha, F.F.; Nick, C. Yield and Fruit Quality Attributes of Selected Tomato Introgression Lines Subjected to Long-Term Deficit Irrigation. *Scientia Horticulturae* **2021**, *289*, 110426, doi:[10.1016/j.scienta.2021.110426](https://doi.org/10.1016/j.scienta.2021.110426).
- Eduardo, I.; Arús, P.; Monforte, A.J. Development of a Genomic Library of near Isogenic Lines (NILs) in Melon (*Cucumis Melo L.*) from the Exotic Accession PI161375. *Theor Appl Genet* **2005**, *112*, 139–148, doi:[10.1007/s00122-005-0116-y](https://doi.org/10.1007/s00122-005-0116-y).
- Eduardo, I.; Arús, P.; Monforte, A.J.; Obando, J.; Fernández-Trujillo, J.P.; Martínez, J.A.; Alarcón, A.L.; Álvarez, J.M.; Knaap, E. van der Estimating the Genetic Architecture of Fruit Quality Traits in Melon Using a Genomic Library of Near Isogenic Lines. *Journal of the American Society for Horticultural Science* **2007**, *132*, 80–89, doi:[10.21273/JASHS.132.1.80](https://doi.org/10.21273/JASHS.132.1.80).
- Eshed, Y.; Zamir, D. An Introgression Line Population of *Lycopersicon Pennellii* in the Cultivated Tomato Enables the Identification and Fine Mapping of Yield-Associated QTL. *Genetics* **1995**, *141*, 1147–1162, doi:[10.1093/genetics/141.3.1147](https://doi.org/10.1093/genetics/141.3.1147).
- Fu, Y.; Zhao, H.; Huang, J.; Zhu, H.; Luan, X.; Bu, S.; Liu, Z.; Wang, X.; Peng, Z.; Meng, L.; *et al* Dynamic Analysis of QTLs on Plant Height with Single Segment

- Substitution Lines in Rice. *Sci Rep* **2022**, *12*, 5465, doi:[10.1038/s41598-022-09536-8](https://doi.org/10.1038/s41598-022-09536-8).
- Guan, H.; Hou, X.; Jiang, Y.; Srivastava, V.; Mao, D.; Pan, R.; Chen, M.; Zhou, Y.; Wang, Z.; Chen, Z. Feature of Blast Resistant Near-Isogenic Lines Using an Elite Maintainer Line II-32B by Marker-Assisted Selection. *J Plant Pathol* **2019**, *101*, 491–501, doi:[10.1007/s42161-018-00222-1](https://doi.org/10.1007/s42161-018-00222-1).
- Gur, A.; Zamir, D. Mendelizing All Components of a Pyramid of Three Yield QTL in Tomato. *Frontiers in Plant Science* **2015**, *6*.
- Lavaud, C.; Baviere, M.; Le Roy, G.; Hervé, M.R.; Moussart, A.; Delourme, R.; Pilet-Nayel, M.-L. Single and Multiple Resistance QTL Delay Symptom Appearance and Slow down Root Colonization by *Aphanomyces Euteiches* in Pea near Isogenic Lines. *BMC Plant Biology* **2016**, *16*, 166, doi:[10.1186/s12870-016-0822-4](https://doi.org/10.1186/s12870-016-0822-4).
- Li, Q.; Feng, Q.; Snouffer, A.; Zhang, B.; Rodríguez, G.R.; van der Knaap, E. Increasing Fruit Weight by Editing a Cis-Regulatory Element in Tomato KLUH Promoter Using CRISPR/Cas9. *Frontiers in Plant Science* **2022**, *13*.
- Liu, B.; Santo Domingo, M.; Mayobre, C.; Martín-Hernández, A.M.; Pujol, M.; Garcia-Mas, J. Knock-Out of CmNAC-NOR Affects Melon Climacteric Fruit Ripening. *Frontiers in Plant Science* **2022**, *13*.
- Lu, J.; Hou, J.; Ouyang, Y.; Luo, H.; Zhao, J.; Mao, C.; Han, M.; Wang, L.; Xiao, J.; Yang, Y.; *et al* A Direct PCR-Based SNP Marker-Assisted Selection System (D-MAS) for Different Crops. *Mol Breeding* **2020**, *40*, 9, doi:[10.1007/s11032-019-1091-3](https://doi.org/10.1007/s11032-019-1091-3).
- Mayobre, C.; Pereira, L.; Eltahiri, A.; Bar, E.; Lewinsohn, E.; Garcia-Mas, J.; Pujol, M. Genetic Dissection of Aroma Biosynthesis in Melon and Its Relationship with Climacteric Ripening. *Food Chemistry* **2021**, *353*, 129484, doi:[10.1016/j.foodchem.2021.129484](https://doi.org/10.1016/j.foodchem.2021.129484).
- Misra, G.; Badoni, S.; Parween, S.; Singh, R.K.; Leung, H.; Ladejobi, O.; Mott, R.; Sreenivasulu, N. Genome-Wide Association Coupled Gene to Gene Interaction Studies Unveil Novel Epistatic Targets among Major Effect Loci Impacting Rice

- Grain Chalkiness. *Plant Biotechnology Journal* **2021**, *19*, 910–925, doi:[10.1111/pbi.13516](https://doi.org/10.1111/pbi.13516).
- Obando-Ulloa, J.M.; Moreno, E.; García-Mas, J.; Nicolai, B.; Lammertyn, J.; Monforte, A.J.; Fernández-Trujillo, J.P. Climacteric or Non-Climacteric Behavior in Melon Fruit: 1. Aroma Volatiles. *Postharvest Biology and Technology* **2008**, *49*, 27–37, doi:[10.1016/j.postharvbio.2007.11.004](https://doi.org/10.1016/j.postharvbio.2007.11.004).
- Ortega, M.A.; All, J.N.; Boerma, H.R.; Parrott, W.A. Pyramids of QTLs Enhance Host–Plant Resistance and Bt-Mediated Resistance to Leaf-Chewing Insects in Soybean. *Theor Appl Genet* **2016**, *129*, 703–715, doi:[10.1007/s00122-015-2658-y](https://doi.org/10.1007/s00122-015-2658-y).
- Pech, J.C.; Bouzayen, M.; Latché, A. Climacteric Fruit Ripening: Ethylene-Dependent and Independent Regulation of Ripening Pathways in Melon Fruit. *Plant Science* **2008**, *175*, 114–120, doi:[10.1016/j.plantsci.2008.01.003](https://doi.org/10.1016/j.plantsci.2008.01.003).
- Pereira, L.; Pujol, M.; Garcia-Mas, J.; Phillips, M.A. Non-Invasive Quantification of Ethylene in Attached Fruit Headspace at 1 p.p.b. by Gas Chromatography–Mass Spectrometry. *The Plant Journal* **2017**, *91*, 172–183, doi:[10.1111/tpj.13545](https://doi.org/10.1111/tpj.13545).
- Pereira, L.; Santo Domingo, M.; Argyris, J.; Mayobre, C.; Valverde, L.; Martín-Hernández, A.M.; Pujol, M.; Garcia-Mas, J. A Novel Introgression Line Collection to Unravel the Genetics of Climacteric Ripening and Fruit Quality in Melon. *Sci Rep* **2021**, *11*, 11364, doi:[10.1038/s41598-021-90783-6](https://doi.org/10.1038/s41598-021-90783-6).
- Pereira, L.; Santo Domingo, M.; Ruggieri, V.; Argyris, J.; Phillips, M.A.; Zhao, G.; Lian, Q.; Xu, Y.; He, Y.; Huang, S.; *et al* Genetic Dissection of Climacteric Fruit Ripening in a Melon Population Segregating for Ripening Behavior. *Horticulture Research* **2020**, *7*, 187, doi:[10.1038/s41438-020-00411-z](https://doi.org/10.1038/s41438-020-00411-z).
- Perpiñá, G.; Cebolla-Cornejo, J.; Esteras, C.; Monforte, A.J.; Picó, B. ‘MAK-10’: A Long Shelf-Life Charentais Breeding Line Developed by Introgression of a Genomic Region from Makuwa Melon. *HortScience* **2017**, *52*, 1633–1638, doi:[10.21273/HORTSCI12068-17](https://doi.org/10.21273/HORTSCI12068-17).
- Perpiñá, G.; Esteras, C.; Gibon, Y.; Monforte, A.J.; Picó, B. A New Genomic Library of Melon Introgression Lines in a Cantaloupe Genetic Background for Dissecting

- Desirable Agronomical Traits. *BMC Plant Biology* **2016**, *16*, 154, doi:[10.1186/s12870-016-0842-0](https://doi.org/10.1186/s12870-016-0842-0).
- Perpiñá, G.; Roselló, S.; Esteras, C.; Beltrán, J.; Monforte, A.J.; Cebolla-Cornejo, J.; Picó, B. Analysis of Aroma-Related Volatile Compounds Affected by ‘Ginsen Makuwa’ Genomic Regions Introgressed in ‘Vedrantais’ Melon Background. *Scientia Horticulturae* **2021**, *276*, 109664, doi:[10.1016/j.scienta.2020.109664](https://doi.org/10.1016/j.scienta.2020.109664).
- R Core Team. R: A language and environment for statistical computing. R Foundation for Statistical Computing **2020**, Vienna, Austria. URL <https://www.R-project.org/>.
- Ríos, P.; Argyris, J.; Vegas, J.; Leida, C.; Kenigswald, M.; Tzuri, G.; Troadec, C.; Bendahmane, A.; Katzir, N.; Picó, B.; *et al* ETHQV6.3 Is Involved in Melon Climacteric Fruit Ripening and Is Encoded by a NAC Domain Transcription Factor. *The Plant Journal* **2017**, *91*, 671–683, doi:[10.1111/tpj.13596](https://doi.org/10.1111/tpj.13596).
- Robbins, M.D.; Casler, M.D.; Staub, J.E. Pyramiding QTL for Multiple Lateral Branching in Cucumber Using Inbred Backcross Lines. *Mol Breeding* **2008**, *22*, 131–139, doi:[10.1007/s11032-008-9162-x](https://doi.org/10.1007/s11032-008-9162-x).
- Sandhu, N.; Dixit, S.; Swamy, B.P.M.; Raman, A.; Kumar, S.; Singh, S.P.; Yadaw, R.B.; Singh, O.N.; Reddy, J.N.; Anandan, A.; *et al* Marker Assisted Breeding to Develop Multiple Stress Tolerant Varieties for Flood and Drought Prone Areas. *Rice* **2019**, *12*, 8, doi:[10.1186/s12284-019-0269-y](https://doi.org/10.1186/s12284-019-0269-y).
- Santo Domingo, M.S.; Areco, L.; Mayobre, C.; Valverde, L.; Martín-Hernández, A.M.; Pujol, M.; Garcia-Mas, J. Modulating Climacteric Intensity in Melon through QTL Stacking. *Horticulture Research* **2022**, uhac131, doi:[10.1093/hr/uhac131](https://doi.org/10.1093/hr/uhac131).
- Vazquez, D.V.; Pereira da Costa, J.H.; Godoy, F.N.I.; Cambiaso, V.; Rodríguez, G.R. Genetic Basis of the Lobedness Degree in Tomato Fruit Morphology. *Plant Science* **2022**, *319*, 111258, doi:[10.1016/j.plantsci.2022.111258](https://doi.org/10.1016/j.plantsci.2022.111258).
- Vegas, J.; Garcia-Mas, J.; Monforte, A.J. Interaction between QTLs Induces an Advance in Ethylene Biosynthesis during Melon Fruit Ripening. *Theor Appl Genet* **2013**, *126*, 1531–1544, doi:[10.1007/s00122-013-2071-3](https://doi.org/10.1007/s00122-013-2071-3).

Chapter 3: QTL interactions

Wang, J.; Tian, S.; Yu, Y.; Ren, Y.; Guo, S.; Zhang, J.; Li, M.; Zhang, H.; Gong, G.; Wang, M.; *et al* Natural Variation in the NAC Transcription Factor NONRIPENING Contributes to Melon Fruit Ripening. *Journal of Integrative Plant Biology* **2022**, *n/a*, doi:[10.1111/jipb.13278](https://doi.org/10.1111/jipb.13278).

Wang, R.; Lammers, M.; Tikunov, Y.; Bovy, A.G.; Angenent, G.C.; de Maagd, R.A. The Rin, nor and Cnr Spontaneous Mutations Inhibit Tomato Fruit Ripening in Additive and Epistatic Manners. *Plant Science* **2020**, *294*, 110436, doi:[10.1016/j.plantsci.2020.110436](https://doi.org/10.1016/j.plantsci.2020.110436).

Wang, X.; Aguirre, L.; Rodríguez-Leal, D.; Hendelman, A.; Benoit, M.; Lippman, Z.B. Dissecting Cis-Regulatory Control of Quantitative Trait Variation in a Plant Stem Cell Circuit. *Nat. Plants* **2021**, *7*, 419–427, doi:[10.1038/s41477-021-00898-x](https://doi.org/10.1038/s41477-021-00898-x).

Zarid, M.; García-Carpintero, V.; Esteras, C.; Esteva, J.; Bueso, M.C.; Cañizares, J.; Picó, M.B.; Monforte, A.J.; Fernández-Trujillo, J.P. Transcriptomic Analysis of a Near-Isogenic Line of Melon with High Fruit Flesh Firmness during Ripening. *Journal of the Science of Food and Agriculture* **2021**, *101*, 754–777, doi:[10.1002/jsfa.10688](https://doi.org/10.1002/jsfa.10688).

Chapter 4

Cross-talk among ethylene production, respiration and primary metabolism shapes ripening behavior in melon

Cross-talk among ethylene production, respiration and primary metabolism shapes ripening behavior in melon

Miguel Santo Domingo¹, Igor Florez-Sarasa^{1,2} Leonardo Perez de Souza³, Laura Valverde¹, Alisdair R. Fernie³, Marta Pujol^{1,2}, Jordi Garcia-Mas^{1,2}

¹Centre for Research in Agricultural Genomics (CRAG) CSIC-IRTA-UAB-UB, Edifici CRAG, Campus UAB, 08193 Bellaterra, Barcelona, Spain

²Institut de Recerca i Tecnologia Agoralimentàries (IRTA), Edifici CRAG, Campus UAB, 08193 Bellaterra, Barcelona, Spain

³Max-Planck-Institute of Molecular Plant Physiology, Am Mühlenberg 1, 14476 Potsdam-Golm

Abstract

Fruit ripening is an essential process in crop plants, considered the last stage of fruit development. When seeds are developed, fruits suffer a set of physiological changes that make them attractive for animals, in order to promote seed dispersal. This process is controlled at several layers, involving hormones, metabolites, transcription factors and other components. Depending on the profile of ethylene production and respiration rates during ripening, fruits can be divided in climacteric and non-climacteric. In climacteric fruits, ethylene is the hormone governing the control of fruit ripening and also considered to affect cellular respiration, while in non-climacteric fruits, ABA is the main controller. In both types of ripening, several metabolic and physiological changes take place. In melon, there are both climacteric and non-climacteric varieties, presenting an advantage for comparative ripening studies with respect to other species. During two seasons, ethylene production and respiration rates were measured in four genotypes with differences in their ripening behavior caused by the introgression of the QTL *ETHQV8.1*. In climacteric lines (Ved, PS8.2 and VED8.2), an increase in respiration rate took place before the start of ethylene production, in contrast to the non-climacteric variety (PS), where no ethylene nor respiration peaks were observed. After determining primary metabolite profiles, changes in particular amino acids and organic acids mainly related to TCA cycle were observed according to the climacteric behavior of the different lines studied. All these results suggest a temporal line where respiration alterations were followed by differences in ethylene production, organic and amino acid profiles, which lead to profound changes in several primary metabolites. Finally, the present work denotes the potential of using metabolic profiling in combination with introgressing ripening-related alleles or gene editing for melon breeding strategies oriented to increase healthy-related metabolites as well as for studies aimed at better understand the fruit ripening process.

Introduction

Melon is a fruit crop member of the *Cucurbitaceae* family mainly consumed as a dessert, which production has been increasing steadily during the last 30 years (FAOSTAT, 2020). With a wide variability in fruit traits, each variety has a distinct metabolic profile (Bernillon *et al*, 2013; Saladié *et al*, 2015), although the profiles are highly dependent on the environment. These metabolic profiles make each variety unique for their organoleptic characteristics, having an impact on the consumer preferences.

Another important trait for the producer and the consumer is fruit shelf-life, heavily influenced by the ripening behavior. In general, fruits are classified as climacteric or non-climacteric depending on the process governing fruit ripening. Climacteric fruit ripening is dependent on the plant hormone ethylene and tomato has been used as the model plant (Alexander *et al*, 2002), while in non-climacteric fruit ripening the physiological changes are dependent on other hormones, as ABA, being strawberry the model plant for this process (Given *et al*, 1988). In climacteric fruits, ethylene production during ripening is coupled to an increase in the respiration rate (Biale *et al*, 1954), although this relationship is not so clear in melon (Schellie & Saltveit, 1993). This increase in the respiration capacity of fruits would lead to the physiological changes happening during fruit ripening, as the production of aroma or the accumulation/degradation of pigments (Golding *et al*, 1999; Trincherro *et al*, 1999).

Fruit ripening has profound effects on several metabolic pathways thus changing fruit metabolite contents. Free amino acids change their concentration during fruit ripening, as well as organic acids (Perez *et al*, 1992; Ackerman *et al*, 1992; Osorio *et al*, 2011). Sugars accumulation, mainly fructose, sucrose and glucose, is also altered during ripening which affects fruits taste, with its consequent importance for human and animal consumption. In tomato, both glucose and fructose accumulate during ripening, but sucrose changes are cultivar-dependent (Osorio *et al*, 2011; Carrari *et al*, 2006). In the case of strawberry, these three sugars accumulate during ripening (Jia *et al*, 2013). Osorio *et al* (2011) found that sugar accumulation is altered in tomato *nor* mutants, but not in tomato *rin* mutants. Other metabolites, as alanine or glutamate, were also modified in these mutants, indicating an important interdependence between primary metabolism and ethylene-induced ripening.

In melon, both climacteric and non-climacteric varieties coexist in the same species. Some metabolic studies have been performed in different varieties with different climacteric behavior (Saladié *et al*, 2015), suggesting differences in carotenoids accumulation during fruit development and ripening, but similar sugar accumulation profiles, although the accumulation of other primary metabolites was not evaluated. Other studies have focused on the spatial and developmental changes in metabolic profiles of particular melon varieties (Biais *et al*, 2009; Moing *et al*, 2011; Tang *et al*, 2010). However, the direct effects of altering fruit ripening in melon respiration and primary metabolism have not been, to our knowledge, studied yet.

In previous studies, we have developed different melon populations to understand fruit ripening and other fruit associated traits. We constructed a Recombinant Inbred Lines (RIL) population (Pereira *et al*, 2018) and two reciprocal Introgression Lines (IL) populations (Pereira *et al*, 2021; Santo Domingo *et al*, accepted) by using as parental lines “Piel de Sapo” (PS), a non-climacteric Spanish cultivar, and “Védrantias” (Ved), a climacteric French cultivar. Using the RIL population, we mapped a major QTL affecting fruit ripening in chromosome 8, *ETHQV8.1* (Pereira *et al*, 2020). On the other hand, we obtained two lines from the IL populations (PS8.2 and VED8.2) with introgressions containing *ETHQV8.1* and we observed a modified ripening behavior when compared to their respective parental lines (Ved and PS). Our aim in the present study is to study the effect of altering fruit ripening on ethylene production, respiration rate and primary metabolism by using the mentioned ILs (PS8.2 and VED8.2), in order to shed light on the relationships among ethylene synthesis and primary metabolism during melon fruit ripening.

Materials and methods

Plant material

Four genotypes were used in this experiment: the parental lines Ved and PS and two introgression lines, PS8.2 and VED8.2 (Pereira *et al*, 2021; Santo Domingo *et al*, accepted). PS8.2 has Ved as the recurrent parent and PS as the donor parent, while VED8.2 has PS as the recurrent parent and Ved as the donor parent. Both ILs have a single introgression in chromosome 8 containing *ETHQV8.1* and have been previously characterized for fruit ripening (Pereira *et al*, 2020; Pereira *et al*, 2021; Santo Domingo *et al*, 2022; Santo Domingo *et al*, accepted).

Growth conditions and sampling

Seeds were germinated in Petri dishes, and then sown in organic pots at CRAG (Barcelona, Spain). After three weeks, plants were transferred to sacks filled with coconut fiber in Caldes de Montbui (Barcelona, Spain). When growing, plants were pruned twice a week, and, when flowering, they were hand pollinated. Only one fruit per plant was allowed in order to optimize fruit development and ripening.

The experiment was performed in two different seasons: 2020 and 2021. In 2020, 4 time-points were analyzed: 15, 25, 30 days after pollination (DAP) and harvest date; and in 2021, two more time-points were added: 28 and 35 DAP. Harvest date was fixed as: i) the day the fruit abscised from the plant; ii) 5 days after the abscission layer formation if the fruit did not abscise from the plant; iii) at 56 DAP when the fruit did not form abscission layer. Melons were harvested at each time-point and several samples were taken from similar central region of the fruit flesh, some were used for respiration measurements while the rest were frozen in liquid nitrogen and conserved at -80 °C.

Ethylene measurements

Ethylene production of melon fruits was measured *in planta* as described before (Pereira *et al.*, 2017). Briefly, fruits were covered with a plastic bag and the bag was then filled with air. After one hour, samples of the internal atmosphere were taken with a syringe for a later analysis by gas chromatography- mass spectrometry (GC-MS). Three biological replicates of each line were monitored in 2020, and four replicates in 2021. PS8.2 was not characterized in 2020. Sampling was performed from 25 DAP until harvest. When ethylene was not detected, samples were taken every other day, and when ethylene was detected, they were taken every day.

Respiration measurements

Fresh flesh samples of 0.5-cm width were incubated in respiration buffer (30 mM MES pH 6.2, 0.2 mM CaCl₂) for 20 minutes in the dark to avoid high wounding-induced respiration. Oxygen consumption was measured using a liquid-phase oxygen electrode (Rank Brothers) with respiration buffer at a constant temperature of 25°C. Thereafter, samples were weighted fresh and dried in an oven at 65°C for at least two days to obtain dry weights. Three to five biological replicates (each corresponding to different melon fruits) were measured per genotype at each time-point.

Metabolic profiling

Freeze-dried 10 mg flesh samples were extracted, derivatized and analyzed by gas chromatography coupled to time-of-flight mass spectrophotometer (GC-TOF-MS) as previously described (Lisec *et al*, 2016). The GC-TOF-MS system was of an Agilent 6890N chromatograph and a LECO Pegasus II TOF-MS.

To identify metabolites, elution times and mass spectra were compared to databases (Kopka *et al*, 2005; Schauer *et al*, 2005). Probabilistic Quotient Normalization (PQN) method was used for normalization, using pool of representative samples as QC (Dieterle *et al*, 2006). Three to six biological replicates were measured of each genotype at each time-point.

Statistical analysis

All statistical analyses were performed using R (R Core team, 2022). For Principal Component Analysis (PCA), package “rstats” was used. Clustering was performed using “maSigPro” package, and correlations were performed using package “heatmaply”. For correlations, z-score normalized median values were used, to avoid the significant effects of outliers.

Results

ETHQV8.1 affects ripening behavior in the introgression lines VED8.2 and PS8.2

For this study, we used two ILs, VED8.2 and PS8.2, developed in two reciprocal IL populations funded by the parental lines Ved and PS (Pereira *et al*, 2020; Santo Domingo *et al*, accepted) with their introgressions covering *ETHQV8.1*, a QTL affecting climacteric ripening. These ILs, along with the parental lines, were characterized for different ripening-related phenotypes, showing a delay in ripening in PS8.2 compared with Ved, and an advance in VED8.2 when compared with PS (Figure 4.1).

During two seasons (2020 and 2021), we measured the ethylene production during ripening of the fruits (PS8.2 was missing in 2020), and the respiration rate of the same lines in several stages of fruit development (Figure 4.1).

Ved produced a sharp peak of ethylene during climacteric ripening, while PS did not produce ethylene during ripening (although we detected a minor peak around 56 DAP in 2020) (Fig 4.1A, B). In these two parental lines, we also detected differences regarding the respiration rate (Fig 4.1C, D). While in PS the oxygen consumption remained low

during all the development of the fruits, Ved respiration increased at 30 DAP, before the ethylene production started.

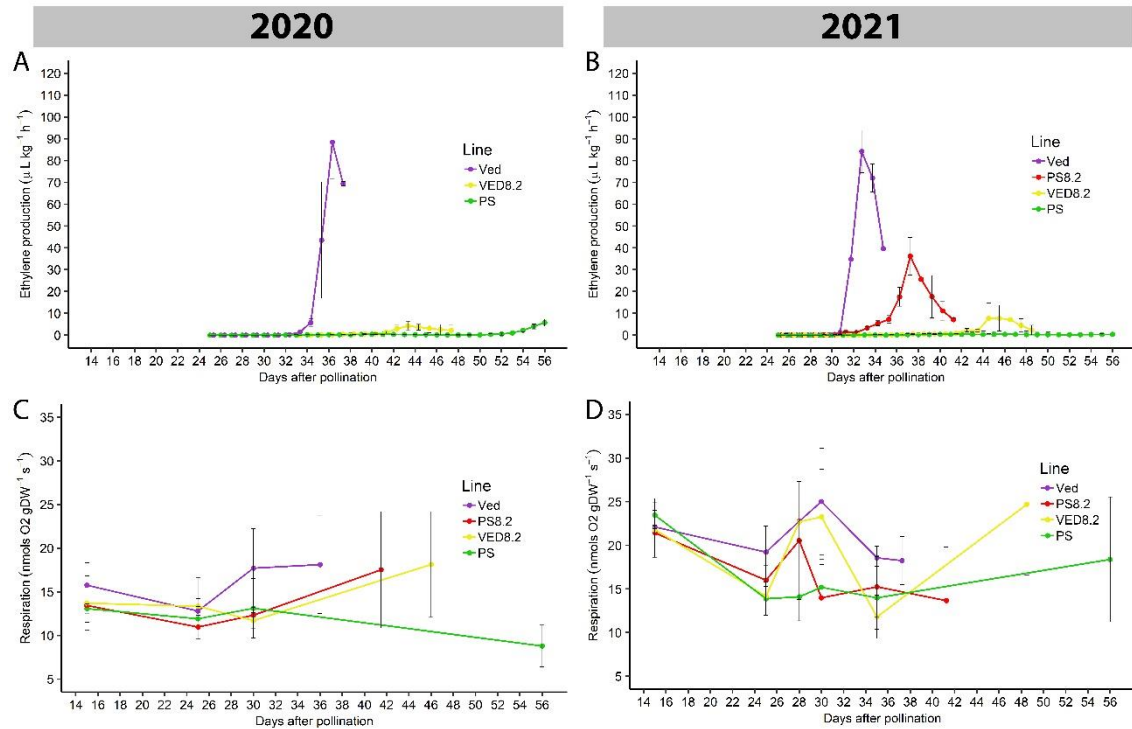


Figure 4.6. Mean ethylene production (A, B) and respiration rate (C, D) of the four analyzed genotypes (Ved, PS, PS8.2 and VED8.2) during fruit development and ripening, measured in summer 2020 and 2021. Error bars represent standard deviation of three to five biological replicates.

Introgressing the PS allele of *ETHQV8.1* in Ved background (PS8.2), caused a 5-days delay of the ethylene peak and half decrease in the maximum ethylene production compared to Ved (Fig 4.1B). On the other hand, introgressing the Ved allele of *ETHQV8.1* in the PS background (VED8.2) induced a climacteric ripening, although with a low peak of ethylene production around 45 DAP (Fig 4.1 A, B). The cellular respiration was also altered in both ILs in comparison to their corresponding background parents. Despite the high variability observed in respiration among biological replicates and years, PS8.2 displayed a reduced oxygen consumption at 30 DAP as compared to Ved (Fig 4.1C, D). On the contrary, VED8.2 displayed an increase of oxygen consumption when compared to PS, although variable between both years. In summer 2020, the increase in respiration in VED8.2 was observed only at harvest (Fig 4.1C). In 2021, we could observe two respiration peaks in VED8.2, one at harvest (similar to the one detected in 2020) and another around 30 DAP, thus coinciding with the respiration peak observed in Ved and never present in PS (Fig 4.1D).

When comparing ethylene production and respiration rate an interesting and clear behavior is observed regarding their sequential timing: the rise in oxygen consumption always precedes that of ethylene production in all lines displaying a climacteric behavior.

Modifications of ripening behavior have an effect in melon primary metabolism

To deepen our knowledge about the metabolic effect of *ETHQV8.1* in melon, we determined primary metabolite profiles of the fruit flesh in all four lines at both years. We could detect 45 different metabolites in 2020 samples, while 49 were detected in 2021, most of them shared in the two years. As the behavior of most of the shared metabolites was consistent during both seasons (Table 4.S1), we focused on 2021 samples for the general analysis, as more time points were available.

We firstly performed a PCA (Figure 4.2) to have an overview of the general behavior of the lines and detected interesting trends. When representing PC1 (explaining 26.72% of the variance) and PC2 (explaining 16.17% of the variance), we could see a similar clustering between Ved and PS8.2 during fruit development, but a different ripening behavior. While at the harvest point they clustered together, PS8.2 was harvested 5 days later than Ved due to its delay in climacteric ripening (Figure 4.1). PS8.2 samples at 35 DAP were clustered close to Ved samples at 30 DAP, while Ved samples at 35 DAP (harvest) were clustered together with PS8.2 samples at 40 DAP (harvest). These observations indicate a similar ripening behavior of both lines regarding primary metabolism, but PS8.2 displaying a delay of 5 days as compared to Ved. In the PS background we only detected differences at harvest, but not at earlier stages of development where PS and VED8.2 clustered together. Although variability at harvest (45 DAP for VED8.2 and 56 DAP for PS) is substantially higher in VED8.2 than in the other lines, we could observe a trend of VED8.2 clustering close to the climacteric lines in Ved background, while PS did not, suggesting a general change of primary metabolism behavior when turning PS climacteric.

PC2 explained the variation between the three climacteric lines and PS at harvest, and the top metabolites affecting this PC are methionine, serine, citrate, threonine, maltotriose, adenine and fumarate (Table 4.S2, Table 4.S3). Of them, we did not see differences between PS and VED8.2 in methionine, serine, maltotriose and threonine, indicating that these metabolites are affected more by the genetic background than by the ripening behavior, as PC2 also separates Ved and PS background all along fruit development. So,

citrate, adenine and fumarate are the main metabolites leading the different clustering we observed at the harvest point in the four lines.

These results indicated that *ETHQV8.1*, apart from having an effect in ethylene production and respiration, had also effects in primary metabolism, indicating the narrow relationships existing among these processes.

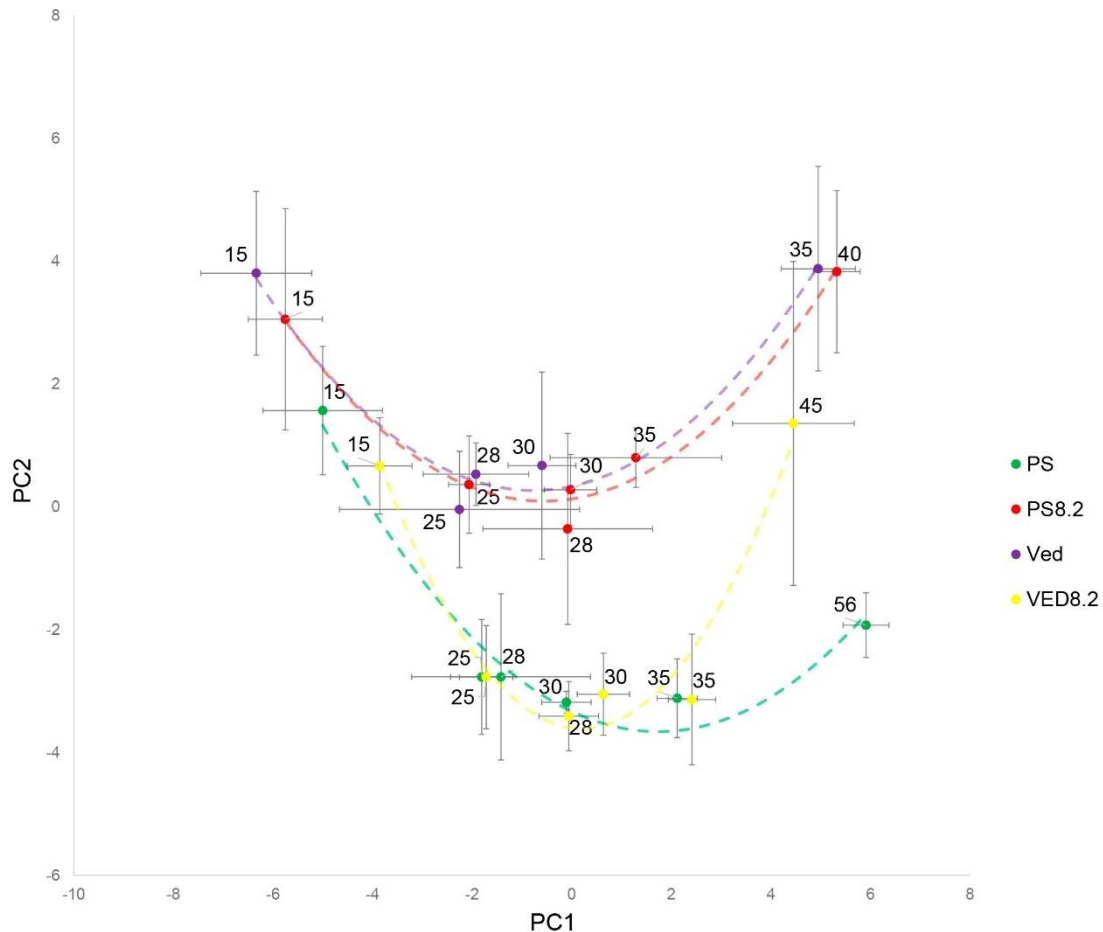


Figure 4.7. PCA of the metabolic profiling of the flesh samples of the analyzed genotypes in season 2021. PC1 and PC2 are represented, showing 26.7% and 16.2% of the variance, respectively. Points represent means, and error bars represent standard deviation from the mean in both PC.

ETHQV8.1 is able to control the abundance of amino acids and organic acids

For a deeper analysis, we focused on the different profiles of the metabolites' abundance, detecting different behaviors (Figure 4.3, Figure 4.4, Figure 4.5, Figure 4.S1, Table 4.S2). Some of them were accumulated at the end of the fruit development, as sucrose, while others were consumed during the growth of the fruit, as glucose and fructose. Also, some were genetic background-specific, as glutamate, more abundant in the Ved background, or methionine, more abundant in the PS background. Due to the different behaviors of

several metabolites along the ripening process, we decided to cluster them for shared behaviors.

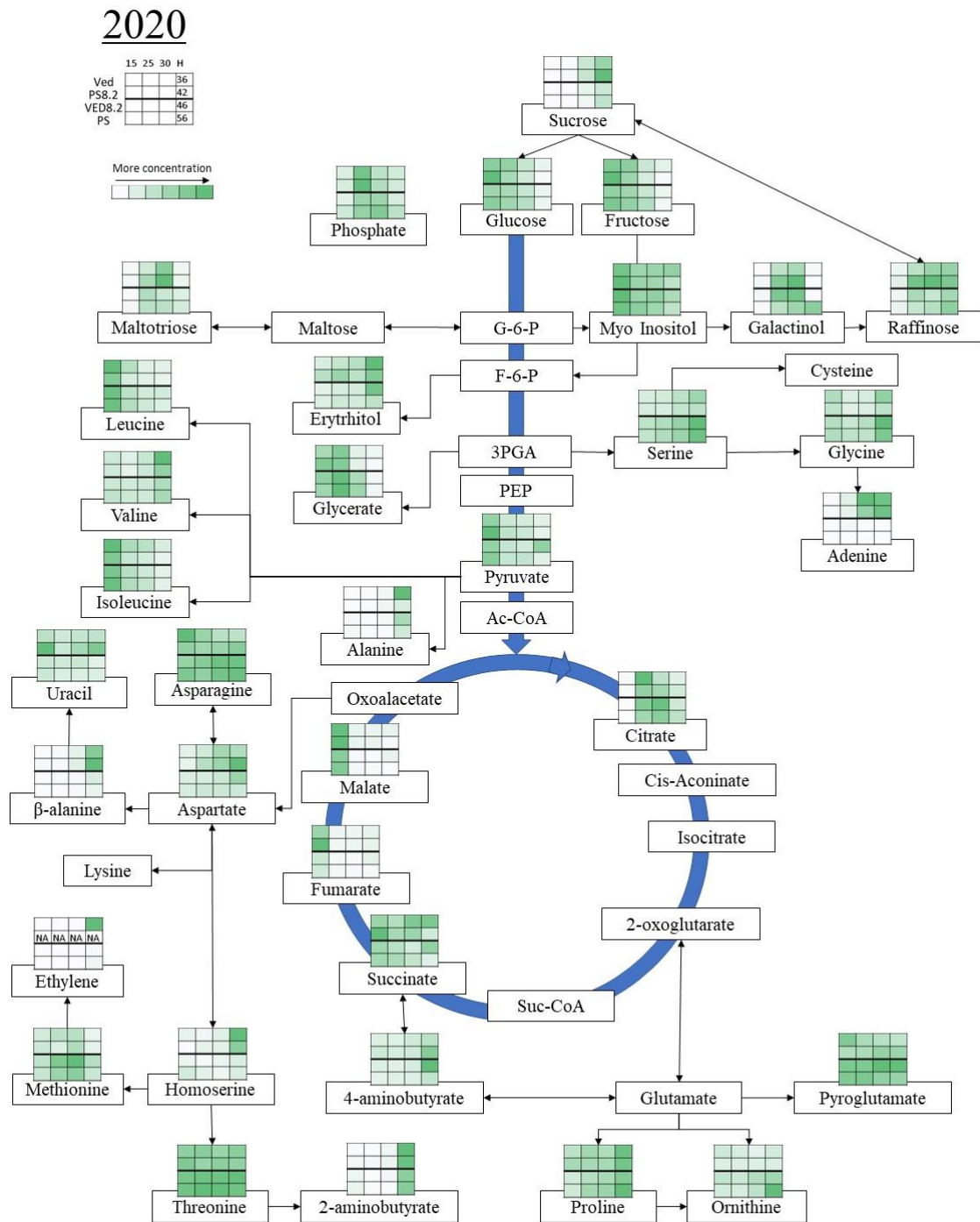


Figure 4.8. Summary of the relative abundance of the primary metabolites during the fruit development of the four analyzed lines in 2020.

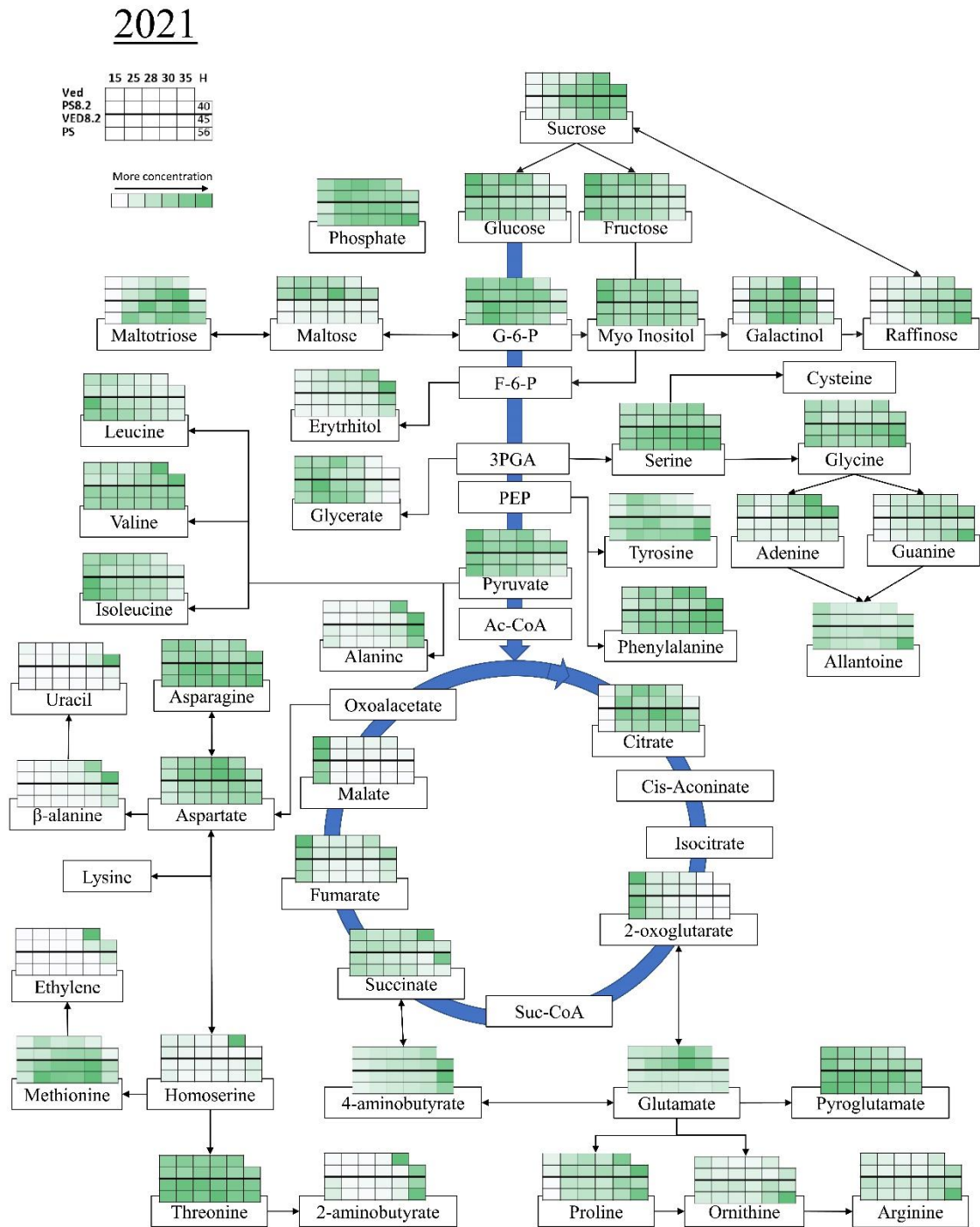


Figure 4.4. Summary of the relative abundance of the primary metabolites during the fruit development of the four analyzed lines in 2021.

Clustering was performed with 2021 data, due to the high correlation between both seasons and the higher availability of data in 2021 season. After clustering, we detected 25 significantly different abundant metabolites between the four genotypes, which were grouped in 9 clusters (Figure 4.S2, Table 4.S4). To select the most interesting clusters,

we considered that: i) PS8.2 had to behave as Ved at harvest, but delayed; and ii) VED8.2 had to behave differently than PS at later stages of development. Four clusters met these two requirements: Clusters 3, 4, 6 and 9.

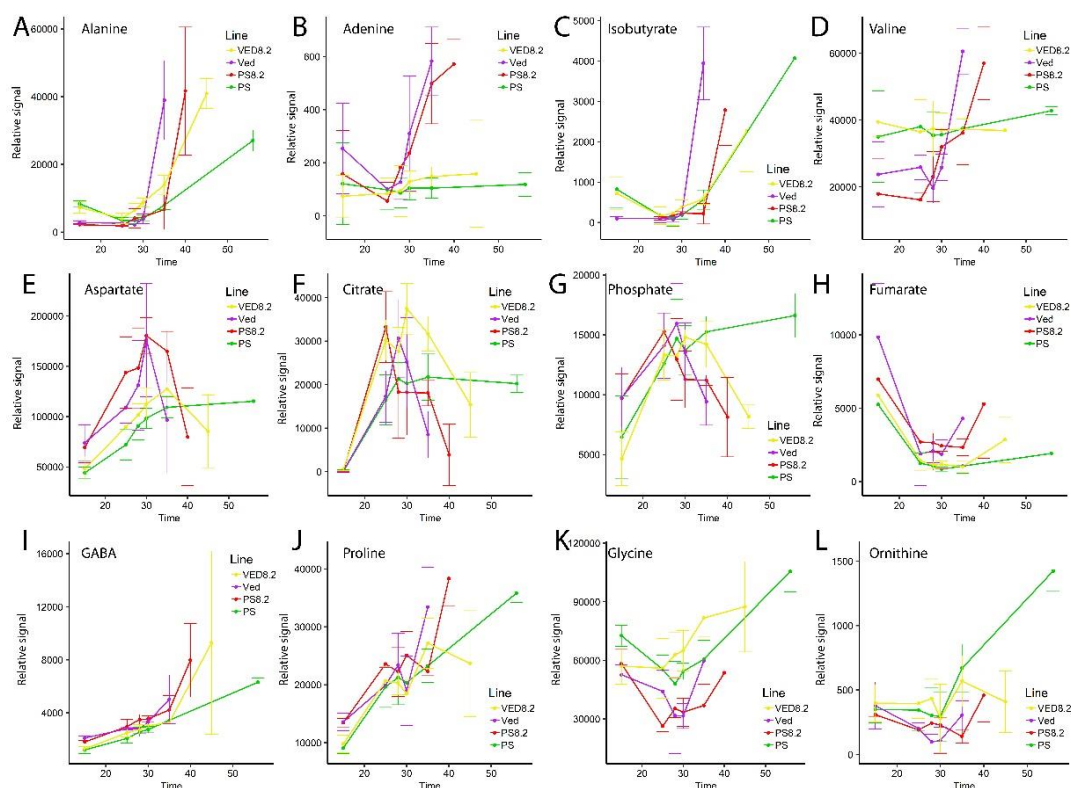


Figure 4.9. Abundance profile of the metabolites considered as most related with ripening after the analysis of the general metabolic profile of the four genotypes during fruit development. Shown profiles correspond to 2021 season. Error bars represent standard deviation. Three to six replicates were analyzed for each genotype at each time-point.

In cluster 3, containing alanine, isobutyrate, beta-alanine, adenine and valine, the metabolites were more abundant at harvest, starting their accumulation at 30 DAP (Figure 4.5A-D). In this cluster there was one organic acid (isobutyrate), one nucleobase (adenine) and three amino acids, two of them proteinogenic (alanine and valine). Also, adenine was considered an important metabolite in the PCA.

In cluster 4, containing citrate (also considered important in the PCA) and phosphate, both metabolites were more abundant at the end of the growing of the fruit, and decreased drastically their abundance at harvest in the climacteric lines, but not in PS (Figure 4.5F, G). Citrate is an organic acid participating in the TCA cycle, central respiratory pathway, while phosphate could be related to energy metabolism as well.

In cluster 6, containing GABA and proline, both metabolites were increasing steadily during the development, with a higher increase at harvest in the climacteric lines, and steadier in PS, especially regarding GABA (Figure 4.5I, J). Both amino acids can be produced from glutamate, presenting a side branch of the TCA cycle.

In cluster 9, containing glycine and ornithine, both metabolites were more abundant during fruit growth and then at harvest, especially in PS (Figure 4.5K, L). Both are amino acids, ornithine being a precursor of polyamines produced in the same pathway as proline, and glycine could be produced in a side branch of glycolysis or as part of photorespiration.

We also considered two other metabolites due to their profiles: aspartate and fumarate (Figure 4.5E, H). Aspartate is an amino acid, and its abundance increased during fruit growth and decreased during climacteric ripening, but not during non-climacteric ripening in PS (Figure 4.5E). Fumarate is an organic acid present in the TCA cycle that was found as a top metabolite affecting clustering in the PCA. Abundant at 15 DAP, it decreased during fruit development, presenting an increase during ripening, more evident in the climacteric lines (Figure 4.5H)

In summary, of the nearly 50 metabolites detected by GC-MS, twelve of them were considered related to climacteric fruit ripening due to their abundance profile in the four analyzed lines through the development of the fruits (Figure 4.5). Among them, there are several amino acids, both proteinogenic and non-proteinogenic, suggesting a role of these type of metabolites in the regulation of ripening. Also, some organic acids present in the TCA cycle, and phosphate, were considered as related with climacteric ripening, indicating the direct relationship between respiratory/energy metabolism and fruit ripening. Moreover, the presence of ornithine and proline in this set of metabolites suggests a role of polyamines in fruit ripening.

Gene expression and amino acids profiles are correlated in the parental lines

In order to deepen into the analysis of the primary metabolism in the parental lines PS and Ved, we analyzed the metabolic profile of these two lines together with gene expression data coming from an RNA-seq analysis (Chapter 2). We used the primary metabolism dataset of 2020, with four time-points, as it was the same season and time-points that we used for the RNA-seq experiment in the parental lines PS and Ved (Chapter 2).

First we clustered the differently abundant metabolites of the parental lines in 2020, which yielded 9 clusters of metabolites with similar behaviors along ripening (Figure 4.S3, Table 4.S5). Also, we clustered the differentially expressed genes (DEGs) obtained with the RNA-seq experiment, finishing with 24 expression clusters (Figure 2.S2, Table 2.S9). After z-score normalization of all the data, we did a correlation analysis using both the metabolite clusters (Met-#) and the transcriptome clusters (RNA-#) (Figure 4.6).

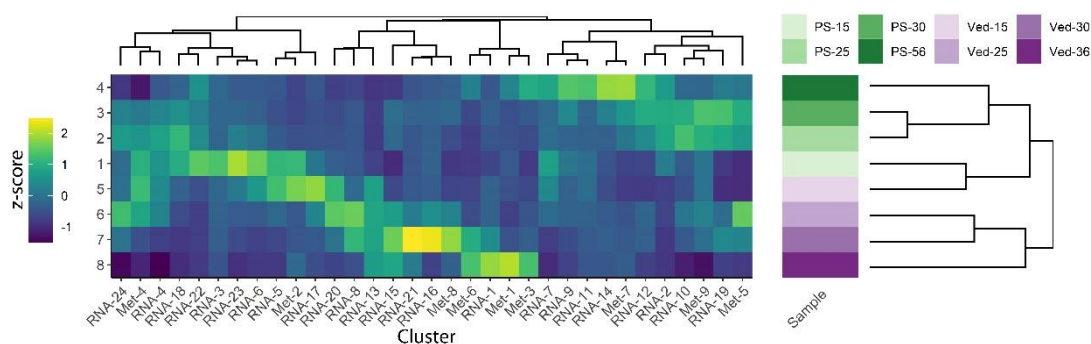


Figure 10. Correlation heatmap of the clusters obtained in the RNA-seq data analysis and the metabolic profiling data of the two parental lines PS and Ved in 2020 season.

Focusing on the differences in fruit ripening, we obtained high correlation between clusters Met-1, Met-3 and Met-6 of the metabolic profiling and cluster RNA-1 of the RNA-seq data. These clusters contain the metabolites with high relative abundance at harvest in Ved, as alanine, valine, glycine, adenine or GABA, also considered important metabolites for fruit ripening in our previous analysis (Figure 4.5). After a GO analysis of the RNA-1 cluster (containing 3,691 DEGs), we obtained some interesting significant terms, as purine biosynthesis related terms (GO:0009168, GO:0009127, GO:0072522, GO:0006164), that together with the increase of adenine could point to a significant role of this metabolite during climacteric ripening. Another interesting set of terms are the ones related with protein catabolism (GO:0030163, GO:0006508, GO:0010498, GO:1903050), that together with the increase of free amino acids, could indicate a role of protein degradation in climacteric fruit ripening. Also, these three clusters of metabolites had a high negative correlation with clusters RNA-4 and RNA-24 of DEGs, although no interesting GO terms were found related with them.

Another interesting metabolite cluster is Met-7, containing, among others, ornithine, a metabolite studied as important in the previous analysis. This cluster has a high correlation with cluster RNA-14 of RNA-seq, but only one GO term was found in the

enrichment analysis: GO:0098588, annotated as “bounding membrane of organelle”, with no relationship with ornithine, in principle.

The last cluster we investigated was cluster Met-8 (containing aspartate and glutamate), correlated with clusters RNA-21 and RNA-16 of the RNA-seq experiment, which we merged into one cluster, containing *CmERF024*, the causal gene of *ETHQV8.1* (Chapter 2). In the enrichment analysis we detected GO terms related with DNA replication and chromatin organization, but no one directly associated with the production of these two amino acids.

Zooming in each cluster, we could find some interesting genes related with their respective metabolites, mainly with proteinogenic amino acids.

In cluster RNA-1, we found some genes of the alanine biosynthetic pathway, as alanine-glyoxylate aminotransferases (*MELO3C017571.2.1* or *MELO3C015151.2.1*). We could also find genes related with the biosynthesis of the other amino acids, as serine hydroxymethyltransferases (*MELO3C018308.2.1* or *MELO3C019443.2.1*) related with glycine or branched-chain-amino-acid aminotransferase (*MELO3C030975.2.1* and *MELO3C010776.2.1*) with valine. Also, two genes related with proline metabolism were found, proline dehydrogenase (*MELO3C022076.2.1*) and pyrroline-5-carboxylate reductase (*MELO3C019039.2.1*).

In the other clusters we could not find genes directly related with the biosynthesis or degradation pathways of their respective metabolites, but as their abundance is controlled by different complex pathways, they could be regulated by other mechanisms.

Discussion

Ethylene production and respiration are not simultaneous during climacteric ripening in melon

In previous works, *ETHQV8.1* had been reported to affect climacteric ripening. In the Ved climacteric background, the non-climacteric allele of the QTL affected the amount of ethylene production, as well as delayed the climacteric symptoms for about 5 days (Pereira *et al*, 2020; Pereira *et al*, 2021). In the PS non-climacteric background, the introgression of the Ved allele produced a climacteric response, with ethylene production and an advance of the climacteric symptoms (Santo Domingo *et al*, 2022; Santo Domingo *et al*, accepted).

Climacteric ripening, apart from having an effect in ethylene production during ripening, is classically characterized by an increase in the respiration rate of fruits such as tomato (Andrews *et al*, 1995; Colombié *et al*, 2017) or avocado (Bennett *et al*, 1987). In melon, the relationship between the respiratory rise and climacteric ripening is not so clear and has been attributed to an artifact due to the detachment of the fruit from the plant (Schellie & Salvteit, 1993). In this work, we have analyzed fruit samples the same day they were harvested, minimizing the possible effect of the detachment of the fruit from the plant. Despite the high variability observed, differences in the respiration profiles of the four tested lines are evident. Ved, a classical cantaloupe climacteric variety, had an increase in oxygen consumption before ripening started, while PS did not show this increase. Interestingly, we could observe a decreased response of respiration in the IL with Ved background (PS8.2) as well as a stimulation of respiration in the IL with PS background (VED8.2). These observations confirm the tight and gradual relationship between respiration and climacteric response in melon, as previously observed for other fruits (Hewitt & Dingra, 2020).

Nevertheless, an interesting observation arise when ethylene and respiration peaks are compared (Figure 4.1). The differences in days between both peaks in the climacteric lines clearly shows that both processes are not simultaneous and suggests that an increase in respiration is probably necessary for the peak of ethylene production. Decreased synthesis of ethylene coincided with a reduced respiration peak in PS8.2 as compared to Ved, thus suggesting a quantitative relationship between respiration and ethylene synthesis in the climacteric genetic background. However, VED8.2 displayed a high increase in respiration rate meanwhile ethylene production was minor (as compared to Ved background lines), thus denoting that ethylene synthesis is probably not only dependent on respiratory metabolism but also on the genetic background. Notably, our oxygen consumption measurements are directly linked to the ATP-coupled and -uncoupled respiratory pathways of the mitochondrial electron transport chain (cytochrome and alternative oxidase), while most of the existing literature on fruit respiration is based on CO₂ production measurements, mostly linked to the TCA cycle activity and the pentose phosphate pathway (Del-Saz & Ribas-Carbo, 2018). Based on CO₂ production, papaya, avocado and banana displayed the ethylene peak before the increase in respiration rate, while in other species, as tomato and pear, the respiration rate

increases before ethylene (Hewitt & Dingra, 2020), as observed here in our O₂ consumption measurements.

Primary metabolism changes are associated with ripening in melon fruits

In our analysis, we found that several metabolites were associated with the different degrees of climacteric ripening present in our four melon lines, mainly amino acids and organic acids of the TCA cycle. However, sugars, mainly sucrose, seemed to be dependent on the genetic background of the line, but independent on the climacteric behavior (Table 4.S2). Furthermore, the two other main sugars, fructose and glucose, presented a similar profile in the four lines. This ethylene-independent sugar accumulation behavior is in agreement with what was previously described (Pech *et al*, 2008; Saladié *et al*, 2015).

Focusing on the specific metabolites associated with ripening, we detected the major differences at harvest, when most of them were more abundant, as the proteinogenic amino acids alanine, valine, proline, and glycine. This general increase in free amino acid abundance at the end of ripening has been previously reported in tomato (Sorrequieta *et al*, 2010), although in tomato glutamate was the main amino acid. In the non-climacteric strawberry, an accumulation of free amino acids also happens at the end of fruit development (Reis *et al*, 2020). It has been suggested that a higher protein degradation activity during ripening may be the cause for the increase in free amino acid abundance (Sorrequieta *et al*, 2010), consistent with our gene expression results where we found an enrichment in protein degradation GO terms.

Analyzing these amino acids one by one, we could not find a reported relationship of alanine or glycine and fruit ripening, while in our melon data it seems quite clear (Figure 4.5A, K). Regarding valine, its increase during climacteric ripening has been reported previously in the climacteric fruit banana (Alsmairat *et al*, 2018). In melon, valine is known to be the precursor of some volatile compounds present in the aroma profile of climacteric fruits (Gonda *et al*, 2010), maybe explaining the increase in valine in our climacteric lines at harvest. In the case of PS and VED8.2 we did not detect an increase in the amount of valine, so the aroma in these melons could be produced from other precursors, also explaining the different aroma profile between Ved and VED8.2 (Mayobre *et al*, 2021; Santo Domingo *et al*, 2022). In the case of proline, it has been

associated with ripening in the non-climacteric grape (Stines *et al*, 1999), where they describe an accumulation at the end of fruit development.

Several TCA cycle metabolites were also modified depending on fruit ripening (Figure 4.3, Figure 4.4). Both citrate and fumarate levels presented nearly opposite profiles and they depend on the ripening behavior of the melons. In the case of fumarate, we observed an increase in its abundance during the later stages of ripening, being this increase higher in climacteric melons, while citrate levels decreased at harvest in climacteric melons but not in PS. The observed variation in the levels of these important TCA cycle intermediates could be originated by the altered respiratory flux observed in the different studied lines. In tomato, citric acid level also decreases at later stages of climacteric ripening, presenting a milder decrease in *rin* and *nor* ripening mutants (Osorio *et al*, 2020). Moreover, a decrease in fumarate levels during fruit development and an increase at the end of ripening was also described, similar to our results in melon (Table 4.S2, Figure 4.5). The same report also found a smaller increase of fumarate in the ripening mutants, consistently with our results in the diverse levels of climacteric intensity in our lines, where PS, the non-climacteric variety, barely increases in fumarate abundance at harvest. In the non-climacteric fruit model strawberry, citrate has a similar profile as PS, increasing during the development and without a decrease at later stages of ripening (Zhang *et al*, 2011). Fumarate in strawberry has a similar profile as tomato ripening mutants and non-climacteric melon, with a decrease during fruit growth and a minor increase at later stages of ripening, compared to the bigger increase in wild-type tomato and climacteric melons in our study. Comparing both fruit models and considering our results, fumarate and citrate seem to be associated with the type of ripening and the intensity of the climacteric response. Moreover, the climacteric behavior of citrate has also been observed in other fruits, as mango (Aung *et al*, 2022) or peach (Lombardo *et al*, 2011), and milder changes have been also reported in non-climacteric grape and pepper during ripening (Leng *et al*, 2021; Osorio *et al*, 2012) (Figure 4.S4). In summary, the balance between citrate and fumarate may have a key role in fruit ripening and could be also used as an indicator of the intensity of the climacteric behavior. In agreement, citrate and malate (directly interconvertible with fumarate) have been highlighted as key players in the regulation of fruit development and ripening (Batista-Silva *et al*, 2018).

Phosphoric acid had an abundance profile similar to citrate, increasing in PS at the end of ripening, but strongly decreasing in the climacteric Ved, PS8.2 and VED8.2. Although

phosphate is present in many chemical reactions, the decrease in phosphate abundance may be due to its use in protein phosphorylation, a process that has been related with fruit ripening in tomato (Xie *et al*, 2021). The phosphorylation and dephosphorylation of proteins alter their activity. It may be one of the processes controlling the physiological changes happening during climacteric fruit ripening in melon, acting together with the transcriptional changes observed in our RNA-seq analysis and the epigenomic changes that have been reported previously in melon (Giordano *et al*, 2022).

Another set of important metabolites in fruit ripening, both in climacteric and non-climacteric types, are polyamines (Gao *et al*, 2021). These metabolites (mainly putrescine, spermine and spermidine) are synthesized from arginine via ornithine (Figure 4.3, Figure 4.4). In our study, we detected a significant increase in these two metabolites in PS at later stages of ripening, while this increase was not present in the climacteric lines. In tomato, elevated levels of polyamines have been associated with a longer shelf-life and lower levels of ethylene (Pandey *et al*, 2015). This behavior has also been observed in peach (Torrighiani *et al*, 2012). This relationship is caused because both polyamines and ethylene have a common substrate, S-adenosyl-L-methionine, so there is an apparent competition between both pathways during ripening. In our results, a higher quantity of both arginine and ornithine could lead to a displace of the chemical reactions to the formation of polyamines, though inhibiting the production of ethylene.

Metabolic profiling could be used in plant breeding to improve human health benefits

In the present study, we show that the amounts of particular fruit metabolites can be modified by using ILs in melon. This approach has been widely used in other crops for modifying their nutritional content, as in tomato (Schauer *et al*, 2006; Nunes-Nesi *et al*, 2019). Also, other mapping populations have been used to find QTLs related with different metabolites in eggplant or wheat (Sulli *et al*, 2021; Hill *et al*, 2015). The low association we detected between metabolites' abundance and the expression of their biosynthetic genes' points out the importance of directly studying metabolite profiles to improve crops nutritional value.

In our work, we have been able to increase the abundance of certain metabolites by introgressing the Ved allele of *ETHQV8.1* in PS background, as alanine, erythritol, and γ -aminobutyrate (GABA) (Figure 4.5, Figure 4.S1, Table 4.S2). GABA is a non-proteinogenic amino acid that can be used as a supplement with different benefits for

human health. Indeed, the first CRISPR-edited crop to enter the market was a GABA-enriched tomato, produced in Japan (Nonaka *et al*, 2017; Waltz, 2021). In our experiment, we detected a higher concentration of GABA in the climacteric lines, pointing to an association between climacteric ripening and GABA accumulation. Also, the slower the climacteric ripening was, the higher the concentration of GABA (Figure 4.5J). With this knowledge we could develop slow-ripening climacteric melons to increase the concentration of GABA and improve their benefits for human health.

In conclusion, ethylene synthesis and particular changes in primary metabolism are closely interconnected and associated with ripening behavior in melon. Respiration changes among the different lines occur at the onset of ripening, while ethylene production together with organic and amino acid differences take place all along ripening, although metabolite changes became more evident at harvest point when fruit ripening is complete. This temporal distribution of the processes suggests a structure of the ripening process in melon, starting with an increase in respiration that would lead to a higher ethylene production during climacteric ripening with the consequent changes in the metabolic profile, but more evidence is needed to identify the specific role of each process in fruit ripening.

Supplementary material

Figures

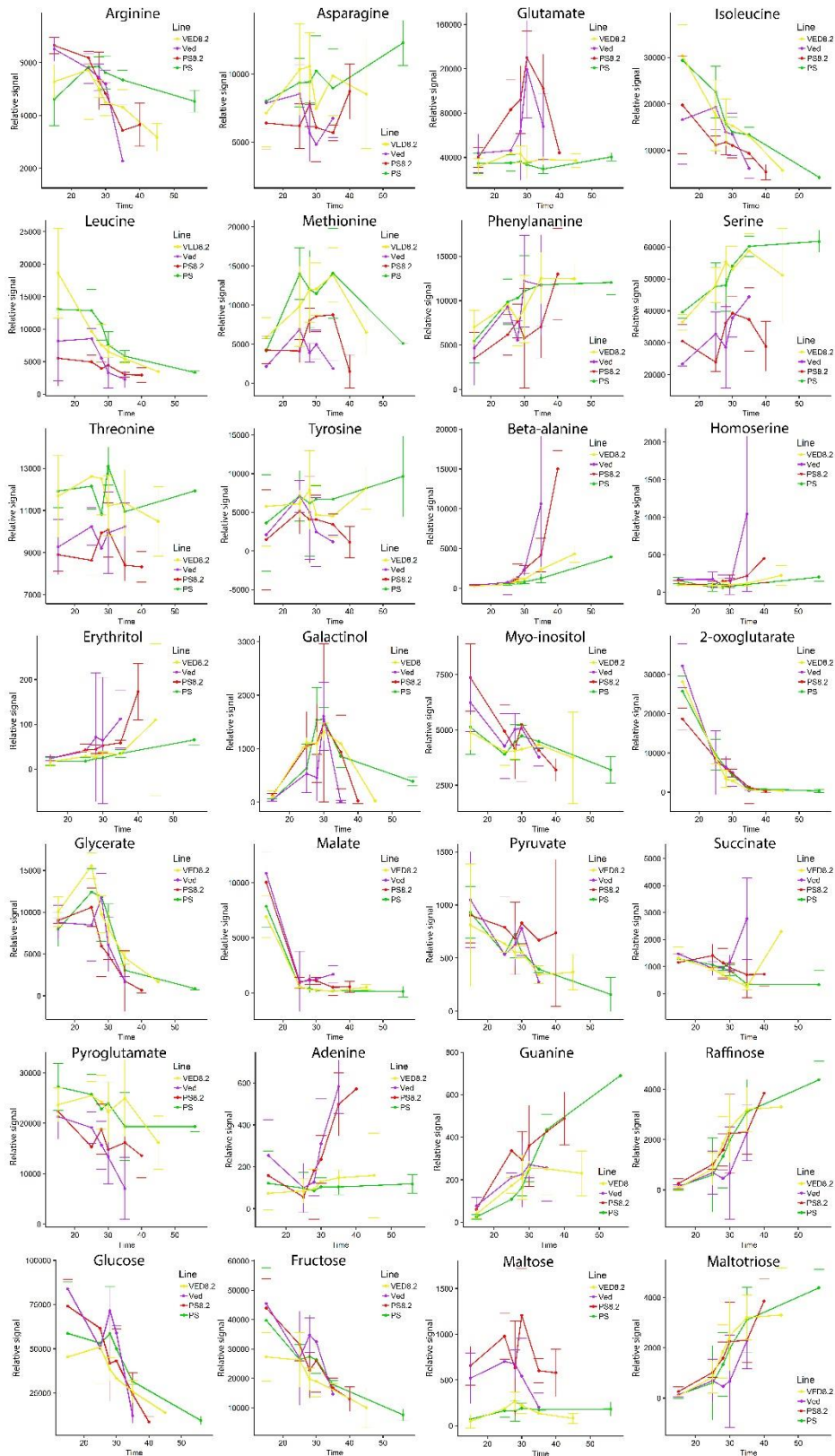


Figure 4.S1. Abundance profile of the metabolites not considered as related with ripening in 2021. Error bars represent standard deviation of three to six replicates.

Chapter 4: metabolic profiling

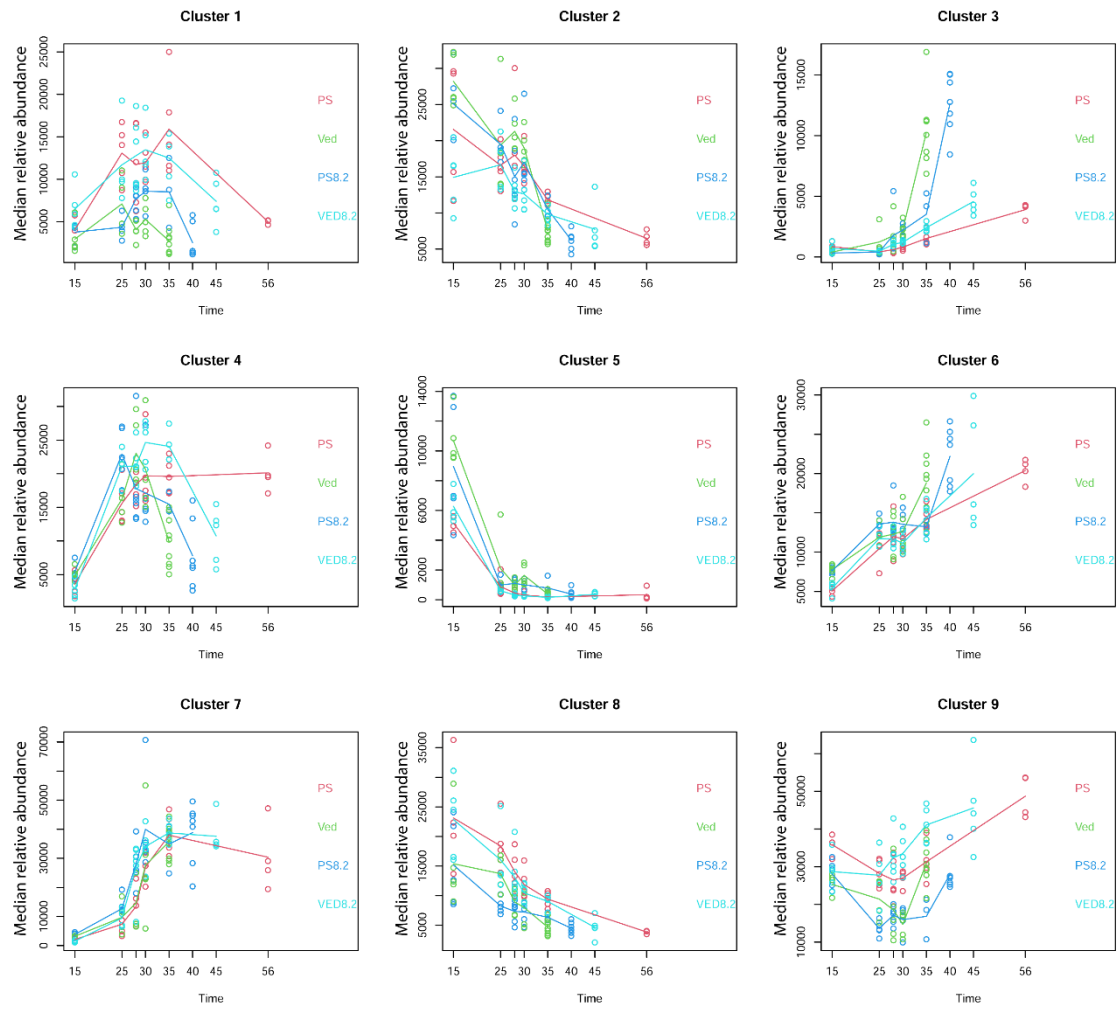


Figure 4.S2. Clusters of metabolite profiles in the four lines in 2021.

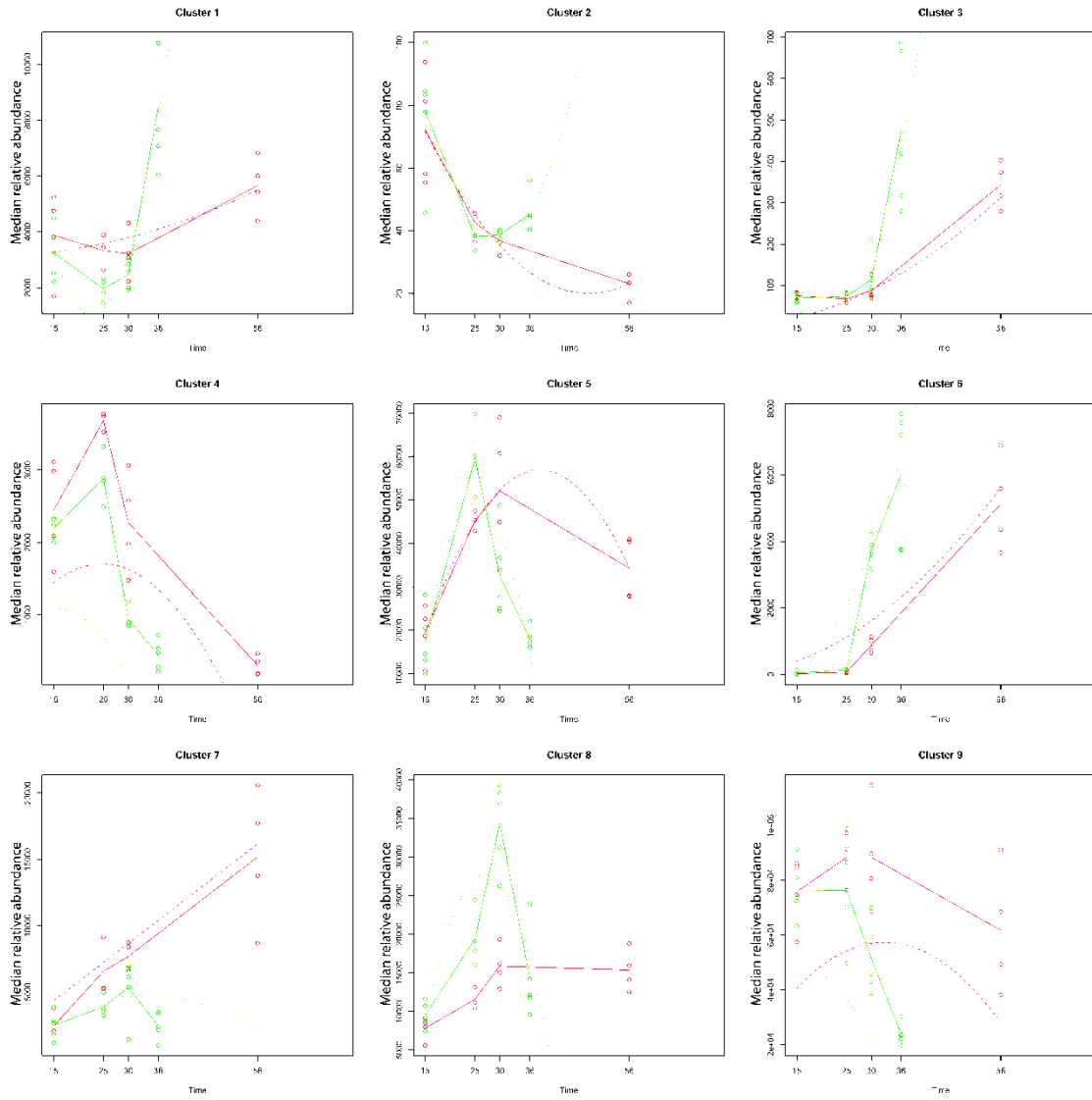


Figure 4.S3. Clusters of metabolite profiles in the parental lines PS and Ved in 2020.

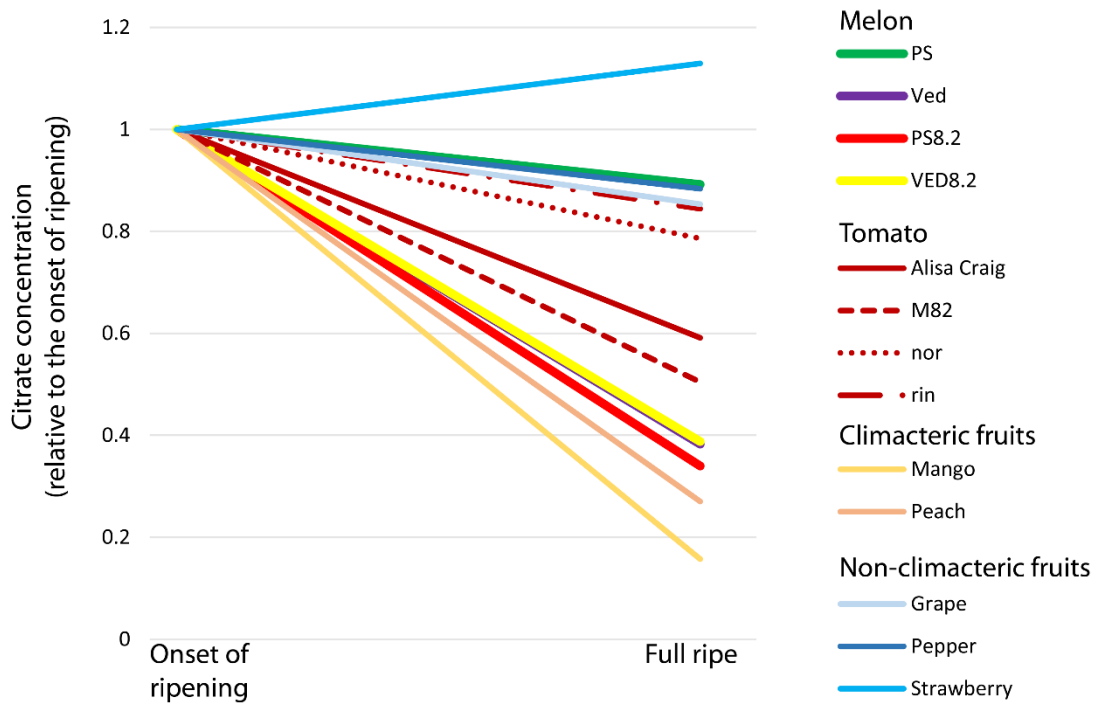


Figure 4.S4. Summary of the citric acid behavior from the onset of ripening to fully ripe fruits in different crops.

Tables**Table 4.S1.** Pearman's correlation between the metabolite profiles in 2020 and 2021.

Metabolite	R2
trans-4-hydroxyproline	-0.399
Nicotinic acid	0.281
Glycerol	0.385
Aspartate	0.403
Pyruvate	0.47
Uracil	0.51
Succinate	0.554
Urea	0.567
Pyroglutamate	0.57
Asparagine	0.575
Raffinose	0.593
Phosphate	0.684
Maltotriose	0.723
Myoinositol	0.734
Leucine	0.741
Fumarate	0.769
Erythritol	0.777
Alanine	0.797
Sucrose	0.803
Phenylalanine	0.809
Adenine	0.822
Glutamate	0.828
Valine	0.831
Isoleucine	0.84
Threonine	0.843
Citrate	0.849
Glycine	0.865
Galactinol	0.867
Ornithine	0.87
Methionine	0.875
Fructose	0.877
Serine	0.88
Glucose	0.899
Proline	0.906
GABA	0.916
Glycerate	0.941
2-oxoglutarate	0.942
Homoserine	0.951
Isobutyrate	0.972
Malate	0.993

Table 4.S4. Differently abundant metabolites in season 2021, classified by cluster. An R2 of 0.6 was used for clustering.

Metabolite	Cluster
Serine	1
Methionine	1
Fructose	2
Glucose	2
Arginine	2
Alanine	3
Isobutyrate	3
Valine	3
Beta-alanine	3
Adenine	3
Phosphate	4
Citrate	4
Malate	5
Fumarate	5
trans-4-hydroxyproline	5
Xylose	5
2-oxoglutarate	5
GABA	6
Proline	6
Sucrose	7
Guanine	7
Leucine	8
Isoleucine	8
Glycine	9
Ornithine	9

Table 4.S5. Differently abundant metabolites between the parents PS and Ved in season 2020, classified by cluster. An R2 of 0.6 was used for clustering.

Metabolite	Cluster
Alanine	1
Valine	1
Glycine	1
S-methylcysteine	1
Malate	2
Myo inositol	2
Fumaric_acid	2
GABA	3
Isobutyrate	3
Proline	3
Trans-4-hydroxyproline	3
Fructose	4
Glucose	4
Glycerate	4
Citric_acid	5
Phosphate	5
Sucrose	6
Adenine	6
Serine	7
Ornithine	7
Galactinol	7
Aspartate	8
Glutamate	8
Methionine	9
Pyroglutamate	9

Digital supplementary material

Table 4.S2. Mean values and standard deviation of the relative abundance of each detected metabolite after PQN normalization during **A)** 2020 season and **B)** 2021 season.

Table 4.S3. PCA loadings of all the analyzed metabolites in 2021.

References

- Ackermann, Joerg.; Fischer, Monica.; Amado, Renato. Changes in Sugars, Acids, and Amino Acids during Ripening and Storage of Apples (Cv. Glockenapfel). *J. Agric. Food Chem.* **1992**, *40*, 1131–1134, doi:[10.1021/jf00019a008](https://doi.org/10.1021/jf00019a008).
- Alexander, L.; Grierson, D. Ethylene Biosynthesis and Action in Tomato: A Model for Climacteric Fruit Ripening. *Journal of Experimental Botany* **2002**, *53*, 2039–2055, doi:[10.1093/jxb/erf072](https://doi.org/10.1093/jxb/erf072).
- Alsmairat, N.; Engelgau, P.; Beaudry, R. Changes in Free Amino Acid Content in the Flesh and Peel of ‘Cavendish’ Banana Fruit as Related to Branched-Chain Ester Production, Ripening, and Senescence. *Journal of the American Society for Horticultural Science* **2018**, *143*, 370–380, doi:[10.21273/JASHS04476-18](https://doi.org/10.21273/JASHS04476-18).
- Andrews, J. The Climacteric Respiration Rise in Attached and Detached Tomato Fruit. *Postharvest Biology and Technology* **1995**, *6*, 287–292, doi:[10.1016/0925-5214\(95\)00013-V](https://doi.org/10.1016/0925-5214(95)00013-V).
- Aung, Y.L.; Lorjaroenphon, Y.; Rumpagaporn, P.; Sittipod, S.; Jirapakkul, W.; Na Jom, K. Integrative Metabolomics–Flavoromics Approach to Assess Metabolic Shifts during Ripening of Mango (*Mangifera Indica* L.) Cultivar Nam Dok Mai Si Thong. *Chemical and Biological Technologies in Agriculture* **2022**, *9*, 25, doi:[10.1186/s40538-022-00289-0](https://doi.org/10.1186/s40538-022-00289-0).
- Batista-Silva, W.; Nascimento, V.L.; Medeiros, D.B.; Nunes-Nesi, A.; Ribeiro, D.M.; Zsögön, A.; Araújo, W.L. Modifications in Organic Acid Profiles During Fruit Development and Ripening: Correlation or Causation? *Frontiers in Plant Science* **2018**, *9*.
- Bennett, A.B.; Smith, G.M.; Nichols, B.G. Regulation of Climacteric Respiration in Ripening Avocado Fruit 1. *Plant Physiol* **1987**, *83*, 973–976.
- Bernillon, S.; Biais, B.; Deborde, C.; Maucourt, M.; Cabasson, C.; Gibon, Y.; Hansen, T.H.; Husted, S.; de Vos, R.C.H.; Mumm, R.; *et al* Metabolomic and Elemental Profiling of Melon Fruit Quality as Affected by Genotype and Environment. *Metabolomics* **2013**, *9*, 57–77, doi:[10.1007/s11306-012-0429-1](https://doi.org/10.1007/s11306-012-0429-1).
- Biais, B.; Allwood, J.W.; Deborde, C.; Xu, Y.; Maucourt, M.; Beauvoit, B.; Dunn, W.B.; Jacob, D.; Goodacre, R.; Rolin, D.; *et al* ¹H NMR, GC–EI–TOFMS, and

- Data Set Correlation for Fruit Metabolomics: Application to Spatial Metabolite Analysis in Melon. *Anal. Chem.* **2009**, *81*, 2884–2894, doi:[10.1021/ac9001996](https://doi.org/10.1021/ac9001996).
- Biale, J.B.; Young, R.E.; Olmstead, A.J. Fruit Respiration and Ethylene Production. 1. *Plant Physiol* **1954**, *29*, 168–174.
- Carrari, F.; Baxter, C.; Usadel, B.; Urbanczyk-Wochniak, E.; Zanon, M.-I.; Nunes-Nesi, A.; Nikiforova, V.; Centero, D.; Ratzka, A.; Pauly, M.; *et al* Integrated Analysis of Metabolite and Transcript Levels Reveals the Metabolic Shifts That Underlie Tomato Fruit Development and Highlight Regulatory Aspects of Metabolic Network Behavior. *Plant Physiology* **2006**, *142*, 1380–1396, doi:[10.1104/pp.106.088534](https://doi.org/10.1104/pp.106.088534).
- Colombié, S.; Beauvoit, B.; Nazaret, C.; Bénard, C.; Vercambre, G.; Le Gall, S.; Biais, B.; Cabasson, C.; Maucourt, M.; Bernillon, S.; *et al* Respiration Climacteric in Tomato Fruits Elucidated by Constraint-Based Modelling. *New Phytologist* **2017**, *213*, 1726–1739, doi:[10.1111/nph.14301](https://doi.org/10.1111/nph.14301).
- Del-Saz, N.F.; Ribas-Carbo, M. Ecophysiology of Plant Respiration. In *Annual Plant Reviews online*; John Wiley & Sons, Ltd, 2018; pp. 269–292 ISBN 978-1-119-31299-4.
- Dieterle, F.; Ross, A.; Schlotterbeck, G.; Senn, H. Probabilistic Quotient Normalization as Robust Method to Account for Dilution of Complex Biological Mixtures. Application in 1H NMR Metabonomics. *Anal. Chem.* **2006**, *78*, 4281–4290, doi:[10.1021/ac051632c](https://doi.org/10.1021/ac051632c).
- FAOSTAT, 2020. <https://www.fao.org/faostat/es/#data/QV/visualize>
- Gao, F.; Mei, X.; Li, Y.; Guo, J.; Shen, Y. Update on the Roles of Polyamines in Fleshy Fruit Ripening, Senescence, and Quality. *Frontiers in Plant Science* **2021**, *12*.
- Giordano, A.; Santo Domingo, M.; Quadrana, L.; Pujol, M.; Martín-Hernández, A.M.; Garcia-Mas, J. CRISPR/Cas9 Gene Editing Uncovers the Roles of CONSTITUTIVE TRIPLE RESPONSE 1 and REPRESSOR OF SILENCING 1 in Melon Fruit Ripening and Epigenetic Regulation. *Journal of Experimental Botany* **2022**, *73*, 4022–4033, doi:[10.1093/jxb/erac148](https://doi.org/10.1093/jxb/erac148).

- Given, N.K.; Venis, M.A.; Gierson, D. Hormonal Regulation of Ripening in the Strawberry, a Non-Climacteric Fruit. *Planta* **1988**, *174*, 402–406, doi:[10.1007/BF00959527](https://doi.org/10.1007/BF00959527).
- Golding, J.B.; Shearer, D.; McGlasson, W.B.; Wyllie, S.G. Relationships between Respiration, Ethylene, and Aroma Production in Ripening Banana. *J. Agric. Food Chem.* **1999**, *47*, 1646–1651, doi:[10.1021/jf980906c](https://doi.org/10.1021/jf980906c).
- Gonda, I.; Bar, E.; Portnoy, V.; Lev, S.; Burger, J.; Schaffer, A.A.; Tadmor, Y.; Gepstein, S.; Giovannoni, J.J.; Katzir, N.; *et al* Branched-Chain and Aromatic Amino Acid Catabolism into Aroma Volatiles in Cucumis Melo L. Fruit. *J Exp Bot* **2010**, *61*, 1111–1123, doi:[10.1093/jxb/erp390](https://doi.org/10.1093/jxb/erp390).
- Hewitt, S.; Dhingra, A. Beyond Ethylene: New Insights Regarding the Role of Alternative Oxidase in the Respiratory Climacteric. *Frontiers in Plant Science* **2020**, *11*.
- Hill, C.B.; Taylor, J.D.; Edwards, J.; Mather, D.; Langridge, P.; Bacic, A.; Roessner, U. Detection of QTL for Metabolic and Agronomic Traits in Wheat with Adjustments for Variation at Genetic Loci That Affect Plant Phenology. *Plant Science* **2015**, *233*, 143–154, doi:[10.1016/j.plantsci.2015.01.008](https://doi.org/10.1016/j.plantsci.2015.01.008).
- Jia, H.; Wang, Y.; Sun, M.; Li, B.; Han, Y.; Zhao, Y.; Li, X.; Ding, N.; Li, C.; Ji, W.; *et al* Sucrose Functions as a Signal Involved in the Regulation of Strawberry Fruit Development and Ripening. *New Phytologist* **2013**, *198*, 453–465, doi:[10.1111/nph.12176](https://doi.org/10.1111/nph.12176).
- Kopka, J.; Schauer, N.; Krueger, S.; Birkemeyer, C.; Usadel, B.; Bergmüller, E.; Dörmann, P.; Weckwerth, W.; Gibon, Y.; Stitt, M.; *et al* GMD@CSB.DB: The Golm Metabolome Database. *Bioinformatics* **2005**, *21*, 1635–1638, doi:[10.1093/bioinformatics/bti236](https://doi.org/10.1093/bioinformatics/bti236).
- Leng, F.; Duan, S.; Song, S.; Zhao, L.; Xu, W.; Zhang, C.; Ma, C.; Wang, L.; Wang, S. Comparative Metabolic Profiling of Grape Pulp during the Growth Process Reveals Systematic Influences under Root Restriction. *Metabolites* **2021**, *11*, 377, doi:[10.3390/metabo11060377](https://doi.org/10.3390/metabo11060377).

- Lisec, J.; Schauer, N.; Kopka, J.; Willmitzer, L.; Fernie, A.R. Gas Chromatography Mass Spectrometry–Based Metabolite Profiling in Plants. *Nat Protoc* **2006**, *1*, 387–396, doi:[10.1038/nprot.2006.59](https://doi.org/10.1038/nprot.2006.59).
- Lombardo, V.A.; Osorio, S.; Borsani, J.; Lauxmann, M.A.; Bustamante, C.A.; Budde, C.O.; Andreo, C.S.; Lara, M.V.; Fernie, A.R.; Drincovich, M.F. Metabolic Profiling during Peach Fruit Development and Ripening Reveals the Metabolic Networks That Underpin Each Developmental Stage1[C][W]. *Plant Physiol* **2011**, *157*, 1696–1710, doi:[10.1104/pp.111.186064](https://doi.org/10.1104/pp.111.186064).
- Mayobre, C.; Pereira, L.; Eltahiri, A.; Bar, E.; Lewinsohn, E.; Garcia-Mas, J.; Pujol, M. Genetic Dissection of Aroma Biosynthesis in Melon and Its Relationship with Climacteric Ripening. *Food Chemistry* **2021**, *353*, 129484, doi:[10.1016/j.foodchem.2021.129484](https://doi.org/10.1016/j.foodchem.2021.129484).
- Moing, A.; Aharoni, A.; Biais, B.; Rogachev, I.; Meir, S.; Brodsky, L.; Allwood, J.W.; Erban, A.; Dunn, W.B.; Kay, L.; *et al* Extensive Metabolic Cross-Talk in Melon Fruit Revealed by Spatial and Developmental Combinatorial Metabolomics. *New Phytologist* **2011**, *190*, 683–696, doi:[10.1111/j.1469-8137.2010.03626.x](https://doi.org/10.1111/j.1469-8137.2010.03626.x).
- Nonaka, S.; Arai, C.; Takayama, M.; Matsukura, C.; Ezura, H. Efficient Increase of γ -Aminobutyric Acid (GABA) Content in Tomato Fruits by Targeted Mutagenesis. *Sci Rep* **2017**, *7*, 7057, doi:[10.1038/s41598-017-06400-y](https://doi.org/10.1038/s41598-017-06400-y).
- Nunes-Nesi, A.; Alseekh, S.; de Oliveira Silva, F.M.; Omranian, N.; Lichtenstein, G.; Mirnezhad, M.; González, R.R.R.; Sabio Y Garcia, J.; Conte, M.; Leiss, K.A.; *et al* Identification and Characterization of Metabolite Quantitative Trait Loci in Tomato Leaves and Comparison with Those Reported for Fruits and Seeds. *Metabolomics* **2019**, *15*, 46, doi:[10.1007/s11306-019-1503-8](https://doi.org/10.1007/s11306-019-1503-8).
- Osorio, S.; Alba, R.; Damasceno, C.M.B.; Lopez-Casado, G.; Lohse, M.; Zanor, M.I.; Tohge, T.; Usadel, B.; Rose, J.K.C.; Fei, Z.; *et al* Systems Biology of Tomato Fruit Development: Combined Transcript, Protein, and Metabolite Analysis of Tomato Transcription Factor (nor, Rin) and Ethylene Receptor (Nr) Mutants Reveals Novel Regulatory Interactions. *Plant Physiology* **2011**, *157*, 405–425, doi:[10.1104/pp.111.175463](https://doi.org/10.1104/pp.111.175463).

- Osorio, S.; Alba, R.; Nikoloski, Z.; Kochevenko, A.; Fernie, A.R.; Giovannoni, J.J. Integrative Comparative Analyses of Transcript and Metabolite Profiles from Pepper and Tomato Ripening and Development Stages Uncovers Species-Specific Patterns of Network Regulatory Behavior. *Plant Physiology* **2012**, *159*, 1713–1729, doi:[10.1104/pp.112.199711](https://doi.org/10.1104/pp.112.199711).
- Osorio, S.; Carneiro, R.T.; Lytovchenko, A.; McQuinn, R.; Sørensen, I.; Vallarino, J.G.; Giovannoni, J.J.; Fernie, A.R.; Rose, J.K.C. Genetic and Metabolic Effects of Ripening Mutations and Vine Detachment on Tomato Fruit Quality. *Plant Biotechnology Journal* **2020**, *18*, 106–118, doi:[10.1111/pbi.13176](https://doi.org/10.1111/pbi.13176).
- Pandey, R.; Gupta, A.; Chowdhary, A.; Pal, R.K.; Rajam, M.V. Over-Expression of Mouse Ornithine Decarboxylase Gene under the Control of Fruit-Specific Promoter Enhances Fruit Quality in Tomato. *Plant Mol Biol* **2015**, *87*, 249–260, doi:[10.1007/s11103-014-0273-y](https://doi.org/10.1007/s11103-014-0273-y).
- Pech, J.C.; Bouzayen, M.; Latché, A. Climacteric Fruit Ripening: Ethylene-Dependent and Independent Regulation of Ripening Pathways in Melon Fruit. *Plant Science* **2008**, *175*, 114–120, doi:[10.1016/j.plantsci.2008.01.003](https://doi.org/10.1016/j.plantsci.2008.01.003).
- Pereira, L.; Pujol, M.; Garcia-Mas, J.; Phillips, M.A. Non-Invasive Quantification of Ethylene in Attached Fruit Headspace at 1 p.p.b. by Gas Chromatography–Mass Spectrometry. *The Plant Journal* **2017**, *91*, 172–183, doi:[10.1111/tpj.13545](https://doi.org/10.1111/tpj.13545).
- Pereira, L.; Ruggieri, V.; Pérez, S.; Alexiou, K.G.; Fernández, M.; Jahrmann, T.; Pujol, M.; Garcia-Mas, J. QTL Mapping of Melon Fruit Quality Traits Using a High-Density GBS-Based Genetic Map. *BMC Plant Biology* **2018**, *18*, 324, doi:[10.1186/s12870-018-1537-5](https://doi.org/10.1186/s12870-018-1537-5).
- Pereira, L.; Santo Domingo, M.; Argyris, J.; Mayobre, C.; Valverde, L.; Martín-Hernández, A.M.; Pujol, M.; Garcia-Mas, J. A Novel Introgression Line Collection to Unravel the Genetics of Climacteric Ripening and Fruit Quality in Melon. *Sci Rep* **2021**, *11*, 11364, doi:[10.1038/s41598-021-90783-6](https://doi.org/10.1038/s41598-021-90783-6).
- Pereira, L.; Santo Domingo, M.; Ruggieri, V.; Argyris, J.; Phillips, M.A.; Zhao, G.; Lian, Q.; Xu, Y.; He, Y.; Huang, S.; *et al* Genetic Dissection of Climacteric Fruit Ripening in a Melon Population Segregating for Ripening Behavior. *Hortic Res* **2020**, *7*, 1–18, doi:[10.1038/s41438-020-00411-z](https://doi.org/10.1038/s41438-020-00411-z).

- Perez, A.G.; Rios, J.J.; Sanz, Carlos.; Olias, J.M. Aroma Components and Free Amino Acids in Strawberry Variety Chandler during Ripening. *J. Agric. Food Chem.* **1992**, *40*, 2232–2235, doi:[10.1021/jf00023a036](https://doi.org/10.1021/jf00023a036).
- R Core Team . R: A language and environment for statistical computing. R Foundation for Statistical Computing, **2022**, Vienna, Austria. URL <https://www.R-project.org/>.
- Reis, L.; Forney, C.F.; Jordan, M.; Munro Pennell, K.; Fillmore, S.; Schemberger, M.O.; Ayub, R.A. Metabolic Profile of Strawberry Fruit Ripened on the Plant Following Treatment With an Ethylene Elicitor or Inhibitor. *Front Plant Sci* **2020**, *11*, 995, doi:[10.3389/fpls.2020.00995](https://doi.org/10.3389/fpls.2020.00995).
- Saladié, M.; Cañizares, J.; Phillips, M.A.; Rodriguez-Concepcion, M.; Larrigaudière, C.; Gibon, Y.; Stitt, M.; Lunn, J.E.; Garcia-Mas, J. Comparative Transcriptional Profiling Analysis of Developing Melon (*Cucumis Melo* L.) Fruit from Climacteric and Non-Climacteric Varieties. *BMC Genomics* **2015**, *16*, 440, doi:[10.1186/s12864-015-1649-3](https://doi.org/10.1186/s12864-015-1649-3).
- Schauer, N.; Semel, Y.; Roessner, U.; Gur, A.; Balbo, I.; Carrari, F.; Pleban, T.; Perez-Melis, A.; Bruedigam, C.; Kopka, J.; *et al* Comprehensive Metabolic Profiling and Phenotyping of Interspecific Introgression Lines for Tomato Improvement. *Nat Biotechnol* **2006**, *24*, 447–454, doi:[10.1038/nbt1192](https://doi.org/10.1038/nbt1192).
- Schauer, N.; Steinhauser, D.; Strelkov, S.; Schomburg, D.; Allison, G.; Moritz, T.; Lundgren, K.; Roessner-Tunali, U.; Forbes, M.G.; Willmitzer, L.; *et al* GC–MS Libraries for the Rapid Identification of Metabolites in Complex Biological Samples. *FEBS Letters* **2005**, *579*, 1332–1337, doi:[10.1016/j.febslet.2005.01.029](https://doi.org/10.1016/j.febslet.2005.01.029).
- Shellie, K.C.; Saltveit, M.E. The Lack of a Respiratory Rise in Muskmelon Fruit Ripening on the Plant Challenges the Definition of Climacteric Behaviour. *Journal of Experimental Botany* **1993**, *44*, 1403–1406.
- Sorrequieta, A.; Ferraro, G.; Boggio, S.B.; Valle, E.M. Free Amino Acid Production during Tomato Fruit Ripening: A Focus on l-Glutamate. *Amino Acids* **2010**, *38*, 1523–1532, doi:[10.1007/s00726-009-0373-1](https://doi.org/10.1007/s00726-009-0373-1).

- Stines, A.P.; Naylor, D.J.; Høj, P.B.; van Heeswijck, R. Proline Accumulation in Developing Grapevine Fruit Occurs Independently of Changes in the Levels of Δ 1-Pyrroline-5-Carboxylate Synthetase mRNA or Protein. *Plant Physiol* **1999**, *120*, 923.
- Sulli, M.; Barchi, L.; Toppino, L.; Diretto, G.; Sala, T.; Lanteri, S.; Rotino, G.L.; Giuliano, G. An Eggplant Recombinant Inbred Population Allows the Discovery of Metabolic QTLs Controlling Fruit Nutritional Quality. *Frontiers in Plant Science* **2021**, *12*.
- Tang, M.; Bie, Z.; Wu, M.; Yi, H.; Feng, J. Changes in Organic Acids and Acid Metabolism Enzymes in Melon Fruit during Development. *Scientia Horticulturae* **2010**, *123*, 360–365, doi:[10.1016/j.scienta.2009.11.001](https://doi.org/10.1016/j.scienta.2009.11.001).
- Torrigiani, P.; Bressanin, D.; Ruiz, K.B.; Tadiello, A.; Trainotti, L.; Bonghi, C.; Ziosi, V.; Costa, G. Spermidine Application to Young Developing Peach Fruits Leads to a Slowing down of Ripening by Impairing Ripening-Related Ethylene and Auxin Metabolism and Signaling. *Physiol Plant* **2012**, *146*, 86–98, doi:[10.1111/j.1399-3054.2012.01612.x](https://doi.org/10.1111/j.1399-3054.2012.01612.x).
- Trincherro, G.D.; Sozzi, G.O.; Cerri, A.M.; Vilella, F.; Frascina, A.A. Ripening-Related Changes in Ethylene Production, Respiration Rate and Cell-Wall Enzyme Activity in Goldenberry (*Physalis Peruviana* L.), a Solanaceous Species. *Postharvest Biology and Technology* **1999**, *16*, 139–145, doi:[10.1016/S0925-5214\(99\)00011-3](https://doi.org/10.1016/S0925-5214(99)00011-3).
- Waltz, E. GABA-Enriched Tomato Is First CRISPR-Edited Food to Enter Market. *Nature Biotechnology* **2021**, *40*, 9–11, doi:[10.1038/d41587-021-00026-2](https://doi.org/10.1038/d41587-021-00026-2).
- Wen, J.; Jiang, F.; Weng, Y.; Sun, M.; Shi, X.; Zhou, Y.; Yu, L.; Wu, Z. Identification of Heat-Tolerance QTLs and High-Temperature Stress-Responsive Genes through Conventional QTL Mapping, QTL-Seq and RNA-Seq in Tomato. *BMC Plant Biol* **2019**, *19*, 398, doi:[10.1186/s12870-019-2008-3](https://doi.org/10.1186/s12870-019-2008-3).
- Xie, Q.; Tian, Y.; Hu, Z.; Zhang, L.; Tang, B.; Wang, Y.; Li, J.; Chen, G. Novel Translational and Phosphorylation Modification Regulation Mechanisms of Tomato (*Solanum Lycopersicum*) Fruit Ripening Revealed by Integrative

Proteomics and Phosphoproteomics. *Int J Mol Sci* **2021**, *22*, 11782,
doi:[10.3390/ijms222111782](https://doi.org/10.3390/ijms222111782).

Zhang, J.; Wang, X.; Yu, O.; Tang, J.; Gu, X.; Wan, X.; Fang, C. Metabolic Profiling of Strawberry (*Fragaria×ananassa* Duch.) during Fruit Development and Maturation. *Journal of Experimental Botany* **2011**, *62*, 1103–1118,
doi:[10.1093/jxb/erq343](https://doi.org/10.1093/jxb/erq343).

General discussion

Introgression lines are powerful resources for genetic studies

During this thesis, two reciprocal IL populations have been developed and characterized. These two populations have been a powerful starting point for this work, allowing a set of genetic studies. This kind of populations have been widely used before in melon to study different traits (Eduardo *et al*, 2005; Perpiñá *et al*, 2017; Díaz *et al*, 2014), and also in other important crops as tomato (Barrantes *et al*, 2016) or strawberry (Urrutia *et al*, 2015). From the beginning, IL populations have allowed to genetically study different important traits in crops, as well as provide prebreeding plant material for introducing beneficial alleles in related species or varieties. Using marker assisted introgression, several resistances have been introgressed in elite varieties (Sundarman *et al*, 2008; Varshney *et al*, 2014), together with other favorable QTLs to improve yield (Bouchez *et al*, 2002; Muthusamy *et al*, 2014), proving this strategy profitable in plant breeding. Our reciprocal IL populations, obtained from two elite commercial varieties ‘Védraçais’ and ‘Piel de Sapo’, are of high value to understand the genetics behind fruit quality and ripening, as discussed in the next paragraphs, and also as donors of target QTLs for melon breeding programs.

The presence of mendelized QTLs in these lines, without the potential interactions with other *loci* in the genome, has allowed the validation of several QTLs, as the main QTL in this work, *ETHQV8.1*, or other known QTLs, as *ETHQV6.3*. Also, the validation of known major genes, as the *loci* controlling flesh and rind color, proved the robustness of this type of populations (Chapter 1).

Another advantage of these populations is their potential to fine map QTLs. Minimizing the effect of the genetic background, the different analyzed phenotypes are manifested more uniformly allowing a more sensitive analysis of the region of the QTL, which is important for complex traits as fruit ripening. In three generations, analyzing recombinant homozygous F3 families, *ETHQV8.1* has been narrowed down to a 3.6 Kbp region containing a single annotated gene, *CmERF024* (Chapter 2). This high resolution in the QTL mapping of quantitative traits due to the use of ILs, allows the identification of candidate genes in a fast and cheap way, as seen before in melon (Ríos *et al*, 2017), but also in other crops as rice and tomato (Xie *et al*, 2014; Hovav *et al*, 2007). A similar approach could be used to dissect the genetic architecture of other traits, as fruit morphology and other fruit quality traits, with high segregation observed in both IL populations.

General discussion

The third advantage of the IL populations applied in this thesis is their application in QTL x QTL interaction studies (Vegas *et al*, 2013, Gur & Zamir, 2015). Same as discussed above, the isolation of the QTLs from the background noise facilitates the detection of their single effects, as well as their interactions. Apart from the characterization of the genetic interactions between QTLs, these stacking experiments also help to unravel the specific roles of each QTL shaping the studied traits. Following previous work, where the interaction between *ETHQB3.5* and *ETHQV6.3* was already discussed (Vegas *et al*, 2013), the addition of *ETHQV8.1* has helped to understand the specific function of each QTL and create a highly climacteric line in a non-climacteric background (Chapter 3). Using a similar approach but in a climacteric background, by pyramiding two QTLs, *MAK10.1* and *ETHQV8.1*, a long shelf-life line has been developed, although fruit quality was compromised and further studies should be performed to minimize these undesirable side effects.

Transcription factors as key regulators of fruit ripening

As reported in tomato, transcription factors play significant roles in fruit ripening (Wang *et al*, 2020). In melon, apart from the already described *CmNAC-Nor*, the present work describes another key regulator of this process, *CmERF024* (Chapter 2).

Fruit ripening in melon is characterized by a transcriptomic shift happening in climacteric varieties, but not in non-climacteric ones, at later stages of ripening (Chapter 2, Figure 2.S1). This shift in the transcriptome is orchestrated by transcription factors together with other processes, as epigenomic changes. *CmERF024* seems to act just before this shift, participating in the transition between the transcriptional states of fruit development and climacteric fruit ripening, apparently controlling some epigenomic changes (Chapter 2). These attributes make *CmERF024* an interesting target for further studies regarding the integration of different layers of fruit ripening regulation, as it seems to be in the center of the transcriptional, epigenetic and hormonal control of this process, and having effects not only in fruit ripening, but also in fruit metabolism and nutritional content of melon fruits (Chapter 4).

Apart from *CmERF024*, *CmNAC-Nor* transcription factor has also been studied in this work, although not as deeply. The fact that they are the first validated genes in the ripening process manifests the importance of transcription factors in the control of fruit ripening in melon, as it has been reported in the model fruit crops tomato (Wang *et al*, 2020) and strawberry (Aharoni *et al*, 2001; Medina-Puche *et al*, 2015). Transcription factors have

the ability to modulate the activity of a high number of genes, explaining their key role in processes characterized by a significant shift in the transcriptomic state of the cells, as fruit ripening.

Another mechanism that our results suggest as involved in melon fruit ripening is DNA accessibility. Same as transcription factors, epigenomic changes have genome-wide effects. Modifying the activity of genes controlling epigenomic changes (as *CmERF024*), we can generate a huge impact in plant performance. In our case, just modulating the expression of *CmERF024* we can cover a wide range of fruit ripening behaviors, apparently by changing DNA accessibility and structure.

QTL x QTL interactions control quantitative traits, as fruit ripening

Due to the multigenic control of quantitative traits, predicting the phenotype of a certain genotype can be a hard task. Interactions between genomic regions, more than single effects, should be considered when developing prediction models for plant performance.

This problem has been addressed more extensively in tomato than in other crops regarding the control of quantitative traits. Interactions between different gene families determine fruit morphology (Snouffer *et al*, 2020), and interactions between QTLs are known to control yield (Gur & Zamir, 2015). More recently, plant architecture has been reported to be controlled by *MADS-box* transcription factors with epistatic effects (Soyk *et al*, 2017; Wang *et al*, 2021b).

In melon, the epistatic control of fruit ripening was addressed before in a non-climacteric background (Vegas *et al*, 2013), a work that has been extended in the present PhD thesis by adding another QTL to the study (Chapter 3.1). All this information can help to understand how fruit ripening is shaped by a small number of major QTLs, making it more predictable for breeders. However, a QTL stacking project in a *cantaloup* melon type to delay climacteric fruit ripening has not been addressed yet. Some preliminary results in the present work anticipate the possibility of developing long shelf-life cantaloups with this breeding approach, although not all QTLs may be suitable for this purpose until candidate genes or narrowed intervals are obtained (Chapter 3.2).

Our use of introgression lines has an advantage over other genetic approaches. Mendelizing complex quantitative traits allows the study of this polygenic traits as oligogenic, making the study more affordable technically. On the other hand, with this approach we can only study two alleles of a limited number of QTLs, losing allelic

General discussion

diversity and disregarding other interactions with other QTLs that are fixed in our population.

The same approach could be used to stack different QTLs affecting fruit shape using ILs with the same recurrent parent, study their interactions, and, similar to ripening behavior, predict the fruit morphology when certain alleles are present, always considering the limitations in allelic diversity of our populations.

The combination of classical and new breeding techniques as a robust tool in plant breeding

During this PhD thesis, both molecular breeding techniques and new generation breeding technologies have been used to dissect and understand fruit ripening in melon.

In a first step, marker assisted selection (MAS) was used to develop two IL populations that facilitated later work. A fine mapping, performed also with MAS, allowed the discovery of the main candidate gene for *ETHQV8.1*, *CmERF024*, which was later validated with CRISPR/*Cas9* gene editing. This combination of molecular breeding (MAS) and new breeding techniques (gene editing) has allowed the detection and validation of a master regulator of fruit ripening, also suggesting the epigenomic control of this process with the DAP-seq results. The relevance of this discovery comes from two sides. On one hand, the description of the gene function helps plant scientist to better understand the fruit ripening process, one of the main phases of plant life cycle. On the other hand, the generation of a knock-out mutant that delays ripening without compromising fruit quality has potential application in plant breeding for the development of novel long shelf-life varieties.

Another application of gene editing in plants is the generation of new alleles. Using mapping populations, a few number of alleles can be characterized, and, if the causal gene is identified, new alleles of wild or exotic accessions can be detected and used for introgression. However, in both cases the allelic variability is limited to the accessions available. Gene editing, especially CRISPR/*Cas9* due to its easily adaptable nature, opens the possibility to generate new allelic variability within the target genes.

The different effects of different alleles are well-known in melon when studying fruit ripening. The first cloned causal gene, *CmNAC-Nor*, has been intensively studied with natural and induced alleles. In the climacteric genetic background ‘Védrantais’, the natural allele of ‘Piel de sapo’ causes a delay of 4 days in ripening (Chapter 1), while an

induced -3 bp mutation delays it around one week (Liu *et al*, 2022a). Also, an induced knock-out allele completely prevents climacteric ripening (Liu *et al*, 2022a). In the non-climacteric ‘Piel de Sapo’ there are also different effects depending on the allele. The ‘Védrantais’ allele provokes a climacteric response around 48 days after fruit set (Chapter 1), while the ‘Songwan Charmi’ allele around 38 days (Chapter 3). This example perfectly illustrates the importance of exploring allelic diversity when studying an interesting gene or QTL, because with different natural or induced alleles we can modulate its effect to select the most beneficial one for our purpose.

Same as in this work, CRISPR/*Cas* gene editing has been used in melon to validate candidate genes. Apart from the above mentioned example of *CmNAC-Nor*, other two genes have been edited to study their effects, *CmROS1* and *CmCTR1-like* (Giordano *et al*, 2022). These two genes are located nearby *ETHQV8.1* (182.2 Kbp region before the fine-mapping), and both have an effect in melon fruit ripening. In the case of *CmROS1* (a demethylase), the knock-out mutant changed the methylation state of the fruit, inducing an earlier ripening. On the other hand, *CmCTR1-like*, which is a negative regulator of ethylene signal transduction, also induced an earlier ripening, as expected. The identification of *CmERF024* as the causal gene of *ETHQV8.1* (Chapter 2), together with the reported effects of *CmROS1* and *CmCTR1-like*, suggests this region in chromosome 8 is crucial in the control of fruit ripening.

The identification of a list of genes affecting the same process is the first step for multiplex gene editing. With this multiplex approach, the causal genes could be edited simultaneously boosting the single effects of the different generated alleles. This approach has been applied in corn, generating genetic variability in several gene families known to control yield in order to increase it (Lorenzo *et al*, 2022) and in tomato it has been used to generate a wide range of allelic variability in the cis-regulatory sequences to modulate locule number (Wang *et al*, 2021b). Knowing the epistatic effects of these genes, as we have done in Chapter 3, helps in the genetic prediction of new phenotypes, making it easier to select the genes and the most interesting edits.

The knowledge generated during this work, identifying the causal gene of *ETHQV8.1* and proving the epistatic control of fruit ripening, is adding a meaningful insight into the genetic regulation of this trait and opening up the incorporation of new breeding techniques to the traditional breeding programs.

General references

- Adams-Phillips, L.; Barry, C.; Giovannoni, J. Signal Transduction Systems Regulating Fruit Ripening. *Trends in Plant Science* **2004**, *9*, 331–338, doi:[10.1016/j.tplants.2004.05.004](https://doi.org/10.1016/j.tplants.2004.05.004).
- Aharoni, A.; De Vos, C.H.R.; Wein, M.; Sun, Z.; Greco, R.; Kroon, A.; Mol, J.N.M.; O'Connell, A.P. The Strawberry FaMYB1 Transcription Factor Suppresses Anthocyanin and Flavonol Accumulation in Transgenic Tobacco. *The Plant*
- Aiese Cigliano, R.; Sanseverino, W.; Cremona, G.; Ercolano, M.R.; Conicella, C.; Consiglio, F.M. Genome-Wide Analysis of Histone Modifiers in Tomato: Gaining an Insight into Their Developmental Roles. *BMC Genomics* **2013**, *14*, 57, doi:[10.1186/1471-2164-14-57](https://doi.org/10.1186/1471-2164-14-57).
- Alseekh, S.; Bermudez, L.; de Haro, L.A.; Fernie, A.R.; Carrari, F. Crop Metabolomics: From Diagnostics to Assisted Breeding. *Metabolomics* **2018**, *14*, 148, doi:[10.1007/s11306-018-1446-5](https://doi.org/10.1007/s11306-018-1446-5).
- Argyris, J.M.; Ruiz-Herrera, A.; Madriz-Masis, P.; Sanseverino, W.; Morata, J.; Pujol, M.; Ramos-Onsins, S.E.; Garcia-Mas, J. Use of Targeted SNP Selection for an Improved Anchoring of the Melon (*Cucumis Melo* L.) Scaffold Genome Assembly. *BMC Genomics* **2015**, *16*, 4, doi:[10.1186/s12864-014-1196-3](https://doi.org/10.1186/s12864-014-1196-3).
- Arumuganathan, K.; Earle, E.D. Nuclear DNA Content of Some Important Plant Species. *Plant Mol Biol Rep* **1991**, *9*, 208–218, doi:[10.1007/BF02672069](https://doi.org/10.1007/BF02672069).
- Ayub, R.; Guis, M.; Amor, M.B.; Gillot, L.; Roustan, J.-P.; Latche, A.; Bouzayen, M.; Pech, J.-C. Expression Of ACC Oxidase Antisense Gene Inhibits Ripening of Cantaloupe Tnelon Fruits. **1996**, *14*, 5.
- Bai, C.; Twyman, R.M.; Farré, G.; Sanahuja, G.; Christou, P.; Capell, T.; Zhu, C. A Golden Era—pro-Vitamin A Enhancement in Diverse Crops. *In Vitro Cell.Dev.Biol.-Plant* **2011**, *47*, 205–221, doi:[10.1007/s11627-011-9363-6](https://doi.org/10.1007/s11627-011-9363-6).
- Bai, Q.; Huang, Y.; Shen, Y. The Physiological and Molecular Mechanism of Abscisic Acid in Regulation of Fleshy Fruit Ripening. *Frontiers in Plant Science* **2021**, *11*.
- Barrantes, W.; López-Casado, G.; García-Martínez, S.; Alonso, A.; Rubio, F.; Ruiz, J.J.; Fernández-Muñoz, R.; Granell, A.; Monforte, A.J. Exploring New Alleles

General references

- Involved in Tomato Fruit Quality in an Introgression Line Library of *Solanum Pimpinellifolium*. *Frontiers in Plant Science* **2016**, 7.
- Barrero, J.M.; Cavanagh, C.; Verbyla, K.L.; Tibbits, J.F.G.; Verbyla, A.P.; Huang, B.E.; Rosewarne, G.M.; Stephen, S.; Wang, P.; Whan, A.; *et al* Transcriptomic Analysis of Wheat Near-Isogenic Lines Identifies PM19-A1 and A2 as Candidates for a Major Dormancy QTL. *Genome Biology* **2015**, 16, 93, doi:[10.1186/s13059-015-0665-6](https://doi.org/10.1186/s13059-015-0665-6).
- Barry, C.S.; Blume, B.; Bouzayen, M.; Cooper, W.; Hamilton, A.J.; Grierson, D. Differential Expression of the 1-Aminocyclopropane-1-Carboxylate Oxidase Gene Family of Tomato. *Plant J* **1996**, 9, 525–535, doi:[10.1046/j.1365-313x.1996.09040525.x](https://doi.org/10.1046/j.1365-313x.1996.09040525.x).
- Barry, C.S.; Giovannoni, J.J. Ripening in the Tomato Green-Ripe Mutant Is Inhibited by Ectopic Expression of a Protein That Disrupts Ethylene Signaling. *Proceedings of the National Academy of Sciences* **2006**, 103, 7923–7928, doi:[10.1073/pnas.0602319103](https://doi.org/10.1073/pnas.0602319103).
- Barry, C.S.; Llop-Tous, M.I.; Grierson, D. The Regulation of 1-Aminocyclopropane-1-Carboxylic Acid Synthase Gene Expression during the Transition from System-1 to System-2 Ethylene Synthesis in Tomato1. *Plant Physiology* **2000**, 123, 979–986, doi:[10.1104/pp.123.3.979](https://doi.org/10.1104/pp.123.3.979).
- Baudracco-Arnas, S.; Pitrat, M. A Genetic Map of Melon (*Cucumis Melo* L.) with RFLP, RAPD, Isozyme, Disease Resistance and Morphological Markers. *Theoret. Appl. Genetics* **1996**, 93, 57–64, doi:[10.1007/BF00225727](https://doi.org/10.1007/BF00225727).
- Belfanti, E.; Silfverberg-Dilworth, E.; Tartarini, S.; Patocchi, A.; Barbieri, M.; Zhu, J.; Vinatzer, B.A.; Gianfranceschi, L.; Gessler, C.; Sansavini, S. The HcrVf2 Gene from a Wild Apple Confers Scab Resistance to a Transgenic Cultivated Variety. *Proceedings of the National Academy of Sciences* **2004**, 101, 886–890, doi:[10.1073/pnas.0304808101](https://doi.org/10.1073/pnas.0304808101).
- Bevan, M.W.; Flavell, R.B.; Chilton, M.-D. A Chimaeric Antibiotic Resistance Gene as a Selectable Marker for Plant Cell Transformation. *Nature* **1983**, 304, 184–187, doi:[10.1038/304184a0](https://doi.org/10.1038/304184a0).

- Bineau, E.; Diouf, I.; Carretero, Y.; Duboscq, R.; Bitton, F.; Djari, A.; Zouine, M.; Causse, M. Genetic Diversity of Tomato Response to Heat Stress at the QTL and Transcriptome Levels. *The Plant Journal* **2021**, *107*, 1213–1227, doi:[10.1111/tpj.15379](https://doi.org/10.1111/tpj.15379).
- Bleecker, A.B.; Kende, H. Ethylene: A Gaseous Signal Molecule in Plants. *Annual Review of Cell and Developmental Biology* **2000**, *16*, 1–18, doi:[10.1146/annurev.cellbio.16.1.1](https://doi.org/10.1146/annurev.cellbio.16.1.1).
- Bouchez, A.; Hospital, F.; Causse, M.; Gallais, A.; Charcosset, A. Marker-Assisted Introgression of Favorable Alleles at Quantitative Trait Loci Between Maize Elite Lines. *Genetics* **2002**, *162*, 1945–1959, doi:[10.1093/genetics/162.4.1945](https://doi.org/10.1093/genetics/162.4.1945).
- Brady, C.J. Fruit Ripening. *Annual Review of Plant Physiology* **1987**, *38*, 155–178, doi:[10.1146/annurev.pp.38.060187.001103](https://doi.org/10.1146/annurev.pp.38.060187.001103).
- Breitel, D.A.; Chappell-Maor, L.; Meir, S.; Panizel, I.; Puig, C.P.; Hao, Y.; Yifhar, T.; Yasuor, H.; Zouine, M.; Bouzayen, M.; *et al* AUXIN RESPONSE FACTOR 2 Intersects Hormonal Signals in the Regulation of Tomato Fruit Ripening. *PLOS Genetics* **2016**, *12*, e1005903, doi:[10.1371/journal.pgen.1005903](https://doi.org/10.1371/journal.pgen.1005903).
- Buchholzer, M.; Frommer, W.B. An Increasing Number of Countries Regulate Genome Editing in Crops. *New Phytologist* **2022**, *n/a*, doi:[10.1111/nph.18333](https://doi.org/10.1111/nph.18333).
- Castanera, R.; Ruggieri, V.; Pujol, M.; Garcia-Mas, J.; Casacuberta, J.M. An Improved Melon Reference Genome With Single-Molecule Sequencing Uncovers a Recent Burst of Transposable Elements With Potential Impact on Genes. *Frontiers in Plant Science* **2020**, *10*.
- Castro, G.; Perpiñá, G.; Monforte, A.J.; Picó, B.; Esteras, C. New Melon Introgression Lines in a Piel de Sapo Genetic Background with Desirable Agronomical Traits from Dudaim Melons. *Euphytica* **2019**, *215*, 169, doi:[10.1007/s10681-019-2479-1](https://doi.org/10.1007/s10681-019-2479-1).
- Chang, C.-W.; Wang, Y.-H.; Tung, C.-W. Genome-Wide Single Nucleotide Polymorphism Discovery and the Construction of a High-Density Genetic Map for Melon (*Cucumis Melo* L.) Using Genotyping-by-Sequencing. *Frontiers in Plant Science* **2017**, *8*.

General references

- Chao, Q.; Rothenberg, M.; Solano, R.; Roman, G.; Terzaghi, W.; Ecker†, J.R. Activation of the Ethylene Gas Response Pathway in Arabidopsis by the Nuclear Protein ETHYLENE-INSENSITIVE3 and Related Proteins. *Cell* **1997**, *89*, 1133–1144, doi:[10.1016/S0092-8674\(00\)80300-1](https://doi.org/10.1016/S0092-8674(00)80300-1).
- Chaudhuri, A.; Halder, K.; Datta, A. Classification of CRISPR/Cas System and Its Application in Tomato Breeding. *Theor Appl Genet* **2022**, *135*, 367–387, doi:[10.1007/s00122-021-03984-y](https://doi.org/10.1007/s00122-021-03984-y).
- Chen, Y.; Rofidal, V.; Hem, S.; Gil, J.; Nosarzewska, J.; Berger, N.; Demolombe, V.; Bouzayen, M.; Azhar, B.J.; Shakeel, S.N.; *et al* Targeted Proteomics Allows Quantification of Ethylene Receptors and Reveals SIETR3 Accumulation in Never-Ripe Tomatoes. *Frontiers in Plant Science* **2019**, *10*.
- Cheng, J.; Niu, Q.; Zhang, B.; Chen, K.; Yang, R.; Zhu, J.-K.; Zhang, Y.; Lang, Z. Downregulation of RdDM during Strawberry Fruit Ripening. *Genome Biol* **2018**, *19*, 212, doi:[10.1186/s13059-018-1587-x](https://doi.org/10.1186/s13059-018-1587-x).
- Dai, D.; Zeng, S.; Wang, L.; Li, J.; Ji, P.; Liu, H.; Sheng, Y. Identification of Fruit Firmness QTL Ff2.1 by SLAF-BSA and QTL Mapping in Melon. *Euphytica* **2022**, *218*, 52, doi:[10.1007/s10681-022-02999-w](https://doi.org/10.1007/s10681-022-02999-w).
- Danin-Poleg, Y.; Tadmor, Y.; Tzuri, G.; Reis, N.; Hirschberg, J.; Katzir, N. Construction of a Genetic Map of Melon with Molecular Markers and Horticultural Traits, and Localization of Genes Associated with ZYMV Resistance. *Euphytica* **2002**, *125*, 373–384, doi:[10.1023/A:1016021926815](https://doi.org/10.1023/A:1016021926815).
- Delfino, P.; Zenoni, S.; Imanifard, Z.; Tornielli, G.B.; Bellin, D. Selection of Candidate Genes Controlling Veraison Time in Grapevine through Integration of Meta-QTL and Transcriptomic Data. *BMC Genomics* **2019**, *20*, 739, doi:[10.1186/s12864-019-6124-0](https://doi.org/10.1186/s12864-019-6124-0).
- Díaz, A.; Zarouri, B.; Fergany, M.; Eduardo, I.; Álvarez, J.M.; Picó, B.; Monforte, A.J. Mapping and Introgression of QTL Involved in Fruit Shape Transgressive Segregation into ‘Piel de Sapo’ Melon (*Cucumis Melo* L.). *PLOS ONE* **2014**, *9*, e104188, doi:[10.1371/journal.pone.0104188](https://doi.org/10.1371/journal.pone.0104188).
- Doudna, J.A.; Charpentier, E. The New Frontier of Genome Engineering with CRISPR-Cas9. *Science* **2014**, *346*, 1258096, doi:[10.1126/science.1258096](https://doi.org/10.1126/science.1258096).

- Duan, X.; Jiang, C.; Zhao, Y.; Gao, G.; Li, M.; Qi, H. Transcriptome and Metabolomics Analysis Revealed That CmWRKY49 Regulating CmPSY1 Promotes β -Carotene Accumulation in Orange Fleshed Oriental Melon. *Horticultural Plant Journal* **2022**, doi:[10.1016/j.hpj.2022.07.005](https://doi.org/10.1016/j.hpj.2022.07.005).
- Durán-Soria, S.; Pott, D.M.; Osorio, S.; Vallarino, J.G. Sugar Signaling During Fruit Ripening. *Frontiers in Plant Science* **2020**, *11*.
- Eduardo, I.; Arús, P.; Monforte, A.J. Development of a Genomic Library of near Isogenic Lines (NILs) in Melon (*Cucumis Melo* L.) from the Exotic Accession PI161375. *Theor Appl Genet* **2005**, *112*, 139–148, doi:[10.1007/s00122-005-0116-y](https://doi.org/10.1007/s00122-005-0116-y).
- Endl, J.; Achigan-Dako, E.G.; Pandey, A.K.; Monforte, A.J.; Pico, B.; Schaefer, H. Repeated Domestication of Melon (*Cucumis Melo*) in Africa and Asia and a New Close Relative from India. *American Journal of Botany* **2018**, *105*, 1662–1671, doi:[10.1002/ajb2.1172](https://doi.org/10.1002/ajb2.1172).
- Essafi, A.; Díaz-Pendón, J.A.; Moriones, E.; Monforte, A.J.; Garcia-Mas, J.; Martín-Hernández, A.M. Dissection of the Oligogenic Resistance to Cucumber Mosaic Virus in the Melon Accession PI 161375. *Theor Appl Genet* **2009**, *118*, 275–284, doi:[10.1007/s00122-008-0897-x](https://doi.org/10.1007/s00122-008-0897-x).
- Ezura, H.; Owino, W.O. Melon, an Alternative Model Plant for Elucidating Fruit Ripening. *Plant Science* **2008**, *175*, 121–129, doi:[10.1016/j.plantsci.2008.02.004](https://doi.org/10.1016/j.plantsci.2008.02.004).
- FAOSTAT, 2020. <https://www.fao.org/faostat/es/#data/QV/visualize>
- Fujisawa, M.; Shima, Y.; Nakagawa, H.; Kitagawa, M.; Kimbara, J.; Nakano, T.; Kasumi, T.; Ito, Y. Transcriptional Regulation of Fruit Ripening by Tomato FRUITFULL Homologs and Associated MADS Box Proteins. *The Plant Cell* **2014**, *26*, 89–101, doi:[10.1105/tpc.113.119453](https://doi.org/10.1105/tpc.113.119453).
- Gagne, J.M.; Smalle, J.; Gingerich, D.J.; Walker, J.M.; Yoo, S.-D.; Yanagisawa, S.; Vierstra, R.D. Arabidopsis EIN3-Binding F-Box 1 and 2 Form Ubiquitin-Protein Ligases That Repress Ethylene Action and Promote Growth by Directing EIN3 Degradation. *Proceedings of the National Academy of Sciences* **2004**, *101*, 6803–6808, doi:[10.1073/pnas.0401698101](https://doi.org/10.1073/pnas.0401698101).

General references

- Gao, F.; Mei, X.; Li, Y.; Guo, J.; Shen, Y. Update on the Roles of Polyamines in Fleshy Fruit Ripening, Senescence, and Quality. *Frontiers in Plant Science* **2021**, *12*.
- Gao, Y.; Wei, W.; Zhao, X.; Tan, X.; Fan, Z.; Zhang, Y.; Jing, Y.; Meng, L.; Zhu, B.; Zhu, H.; *et al* A NAC Transcription Factor, NOR-Like1, Is a New Positive Regulator of Tomato Fruit Ripening. *Horticulture Research* **2018**, *5*, 75, doi:[10.1038/s41438-018-0111-5](https://doi.org/10.1038/s41438-018-0111-5).
- Gao, Y.; Zhu, N.; Zhu, X.; Wu, M.; Jiang, C.-Z.; Grierson, D.; Luo, Y.; Shen, W.; Zhong, S.; Fu, D.-Q.; *et al* Diversity and Redundancy of the Ripening Regulatory Networks Revealed by the FruitENCODE and the New CRISPR/Cas9 CNR and NOR Mutants. *Horticulture Research* **2019**, *6*, 39, doi:[10.1038/s41438-019-0122-x](https://doi.org/10.1038/s41438-019-0122-x).
- Garbowicz, K.; Liu, Z.; Alseekh, S.; Tieman, D.; Taylor, M.; Kuhalskaya, A.; Ofner, I.; Zamir, D.; Klee, H.J.; Fernie, A.R.; *et al* Quantitative Trait Loci Analysis Identifies a Prominent Gene Involved in the Production of Fatty Acid-Derived Flavor Volatiles in Tomato. *Molecular Plant* **2018**, *11*, 1147–1165, doi:[10.1016/j.molp.2018.06.003](https://doi.org/10.1016/j.molp.2018.06.003).
- Garcia-Mas, J.; Benjak, A.; Sanseverino, W.; Bourgeois, M.; Mir, G.; González, V.M.; Hénaff, E.; Câmara, F.; Cozzuto, L.; Lowy, E.; *et al* The Genome of Melon (*Cucumis Melo* L.). *Proceedings of the National Academy of Sciences* **2012**, *109*, 11872–11877, doi:[10.1073/pnas.1205415109](https://doi.org/10.1073/pnas.1205415109).
- Gillaspy, G.; Ben-David, H.; Gruissem, W. Fruits: A Developmental Perspective. *Plant Cell* **1993**, *5*, 1439–1451.
- Giner, A.; Pascual, L.; Bourgeois, M.; Gyetvai, G.; Rios, P.; Picó, B.; Troadec, C.; Bendahmane, A.; Garcia-Mas, J.; Martín-Hernández, A.M. A Mutation in the Melon Vacuolar Protein Sorting 41prevents Systemic Infection of Cucumber Mosaic Virus. *Sci Rep* **2017**, *7*, 10471, doi:[10.1038/s41598-017-10783-3](https://doi.org/10.1038/s41598-017-10783-3).
- Giordano, A.; Santo Domingo, M.; Quadrana, L.; Pujol, M.; Martín-Hernández, A.M.; Garcia-Mas, J. CRISPR/Cas9 Gene Editing Uncovers the Roles of CONSTITUTIVE TRIPLE RESPONSE 1 and REPRESSOR OF SILENCING 1 in Melon Fruit Ripening and Epigenetic Regulation. *Journal of Experimental Botany* **2022**, *73*, 4022–4033, doi:[10.1093/jxb/erac148](https://doi.org/10.1093/jxb/erac148).

- Goulao, L.F.; Oliveira, C.M. Cell Wall Modifications during Fruit Ripening: When a Fruit Is Not the Fruit. *Trends in Food Science & Technology* **2008**, *19*, 4–25, doi:[10.1016/j.tifs.2007.07.002](https://doi.org/10.1016/j.tifs.2007.07.002).
- Gu, T.; Jia, S.; Huang, X.; Wang, L.; Fu, W.; Huo, G.; Gan, L.; Ding, J.; Li, Y. Transcriptome and Hormone Analyses Provide Insights into Hormonal Regulation in Strawberry Ripening. *Planta* **2019**, *250*, 145–162, doi:[10.1007/s00425-019-03155-w](https://doi.org/10.1007/s00425-019-03155-w).
- Guo, J.; Wang, S.; Yu, X.; Dong, R.; Li, Y.; Mei, X.; Shen, Y. Polyamines Regulate Strawberry Fruit Ripening by Abscisic Acid, Auxin, and Ethylene. *Plant Physiology* **2018**, *177*, 339–351, doi:[10.1104/pp.18.00245](https://doi.org/10.1104/pp.18.00245).
- Guo, J.-E.; Hu, Z.; Li, F.; Zhang, L.; Yu, X.; Tang, B.; Chen, G. Silencing of Histone Deacetylase SIHDT3 Delays Fruit Ripening and Suppresses Carotenoid Accumulation in Tomato. *Plant Science* **2017**, *265*, 29–38, doi:[10.1016/j.plantsci.2017.09.013](https://doi.org/10.1016/j.plantsci.2017.09.013).
- Gupta, A.; Pandey, R.; Sinha, R.; Chowdhary, A.; Pal, R.K.; Rajam, M.V. Improvement of Post-Harvest Fruit Characteristics in Tomato by Fruit-Specific over-Expression of Oat Arginine Decarboxylase Gene. *Plant Growth Regul* **2019**, *88*, 61–71, doi:[10.1007/s10725-019-00488-0](https://doi.org/10.1007/s10725-019-00488-0).
- Gur, A.; Zamir, D. Mendelizing All Components of a Pyramid of Three Yield QTL in Tomato. *Frontiers in Plant Science* **2015**, *6*.
- Hajheidari, M.; Eivazi, A.; Buchanan, B.B.; Wong, J.H.; Majidi, I.; Salekdeh, G.H. Proteomics Uncovers a Role for Redox in Drought Tolerance in Wheat. *J. Proteome Res.* **2007**, *6*, 1451–1460, doi:[10.1021/pr060570j](https://doi.org/10.1021/pr060570j).
- Hao, Y.; Hu, G.; Breitel, D.; Liu, M.; Mila, I.; Frasse, P.; Fu, Y.; Aharoni, A.; Bouzayen, M.; Zouine, M. Auxin Response Factor SlARF2 Is an Essential Component of the Regulatory Mechanism Controlling Fruit Ripening in Tomato. *PLOS Genetics* **2015**, *11*, e1005649, doi:[10.1371/journal.pgen.1005649](https://doi.org/10.1371/journal.pgen.1005649).
- Harel-Beja, R.; Tzuri, G.; Portnoy, V.; Lotan-Pompan, M.; Lev, S.; Cohen, S.; Dai, N.; Yeselson, L.; Meir, A.; Libhaber, S.E.; *et al* A Genetic Map of Melon Highly Enriched with Fruit Quality QTLs and EST Markers, Including Sugar and

General references

- Carotenoid Metabolism Genes. *Theor Appl Genet* **2010**, *121*, 511–533, doi:[10.1007/s00122-010-1327-4](https://doi.org/10.1007/s00122-010-1327-4).
- Higashi, K.; Hosoya, K.; Ezura, H. Histological Analysis of Fruit Development between Two Melon (*Cucumis Melo* L. *Reticulatus*) Genotypes Setting a Different Size of Fruit. *Journal of Experimental Botany* **1999**, *50*, 1593–1597, doi:[10.1093/jxb/50.339.1593](https://doi.org/10.1093/jxb/50.339.1593).
- Hovav, R.; Chehanovsky, N.; Moy, M.; Jetter, R.; Schaffer, A.A. The Identification of a Gene (Cwp1), Silenced during Solanum Evolution, Which Causes Cuticle Microfissuring and Dehydration When Expressed in Tomato Fruit. *The Plant Journal* **2007**, *52*, 627–639, doi:[10.1111/j.1365-3113X.2007.03265.x](https://doi.org/10.1111/j.1365-3113X.2007.03265.x).
- Huang, S.; Sawaki, T.; Takahashi, A.; Mizuno, S.; Takezawa, K.; Matsumura, A.; Yokotsuka, M.; Hirasawa, Y.; Sonoda, M.; Nakagawa, H.; *et al* Melon EIN3-like Transcription Factors (CmEIL1 and CmEIL2) Are Positive Regulators of an Ethylene- and Ripening-Induced 1-Aminocyclopropane-1-Carboxylic Acid Oxidase Gene (CM-ACO1). *Plant Science* **2010**, *178*, 251–257, doi:[10.1016/j.plantsci.2010.01.005](https://doi.org/10.1016/j.plantsci.2010.01.005).
- ISAAA (2017). Global Status of Commercialized Biotech/GM Crops in 2017: Biotech Crop Adoption Surges as Economic Benefits Accumulate in 22 Years. ISAAA Brief No. 53. ISAAA: Ithaca, NY
- Jia, H.; Jiu, S.; Zhang, C.; Wang, C.; Tariq, P.; Liu, Z.; Wang, B.; Cui, L.; Fang, J. Abscisic Acid and Sucrose Regulate Tomato and Strawberry Fruit Ripening through the Abscisic Acid-Stress-Ripening Transcription Factor. *Plant Biotechnology Journal* **2016**, *14*, 2045–2065, doi:[10.1111/pbi.12563](https://doi.org/10.1111/pbi.12563).
- Jia, H.; Wang, Y.; Sun, M.; Li, B.; Han, Y.; Zhao, Y.; Li, X.; Ding, N.; Li, C.; Ji, W.; *et al* Sucrose Functions as a Signal Involved in the Regulation of Strawberry Fruit Development and Ripening. *New Phytologist* **2013**, *198*, 453–465, doi:[10.1111/nph.12176](https://doi.org/10.1111/nph.12176).
- Jia, H.-F.; Chai, Y.-M.; Li, C.-L.; Lu, D.; Luo, J.-J.; Qin, L.; Shen, Y.-Y. Abscisic Acid Plays an Important Role in the Regulation of Strawberry Fruit Ripening. *Plant Physiology* **2011**, *157*, 188–199, doi:[10.1104/pp.111.177311](https://doi.org/10.1104/pp.111.177311).

- Jiang, Y.; Joyce, D.C. ABA Effects on Ethylene Production, PAL Activity, Anthocyanin and Phenolic Contents of Strawberry Fruit. *Plant Growth Regulation* **2003**, *39*, 171–174, doi:[10.1023/A:1022539901044](https://doi.org/10.1023/A:1022539901044).
- Jiménez-Ruiz, J.; Leyva-Pérez, M. de la O.; Schilirò, E.; Barroso, J.B.; Bombarely, A.; Mueller, L.; Mercado-Blanco, J.; Luque, F. Transcriptomic Analysis of *Olea Europaea* L. Roots during the *Verticillium Dahliae* Early Infection Process. *The Plant Genome* **2017**, *10*, plantgenome2016.07.0060, doi:[10.3835/plantgenome2016.07.0060](https://doi.org/10.3835/plantgenome2016.07.0060).
- Jones, B.; Frasse, P.; Olmos, E.; Zegzouti, H.; Li, Z.G.; Latché, A.; Pech, J.C.; Bouzayen, M. Down-Regulation of DR12, an Auxin-Response-Factor Homolog, in the Tomato Results in a Pleiotropic Phenotype Including Dark Green and Blotchy Ripening Fruit. *The Plant Journal* **2002**, *32*, 603–613, doi:[10.1046/j.1365-313X.2002.01450.x](https://doi.org/10.1046/j.1365-313X.2002.01450.x).
- Kende, H. Ethylene Biosynthesis. *Annual Review of Plant Physiology and Plant Molecular Biology* **1993**, *44*, 283–307, doi:[10.1146/annurev.pp.44.060193.001435](https://doi.org/10.1146/annurev.pp.44.060193.001435).
- Kerr, E. Never Ripe-2 (Nr-2) a Slow Ripening Mutant Resembling Nr an Gr. *TGC Reports* **1982**, *32*, 33.
- Khalil, A.M. The Genome Editing Revolution: Review. *Journal of Genetic Engineering and Biotechnology* **2020**, *18*, 68, doi:[10.1186/s43141-020-00078-y](https://doi.org/10.1186/s43141-020-00078-y).
- Kim, J.-M.; To, T.K.; Matsui, A.; Tanoi, K.; Kobayashi, N.I.; Matsuda, F.; Habu, Y.; Ogawa, D.; Sakamoto, T.; Matsunaga, S.; *et al* Acetate-Mediated Novel Survival Strategy against Drought in Plants. *Nature Plants* **2017**, *3*, 1–7, doi:[10.1038/nplants.2017.97](https://doi.org/10.1038/nplants.2017.97).
- Klee, H.J. Ethylene Signal Transduction. Moving beyond Arabidopsis. *Plant Physiology* **2004**, *135*, 660–667, doi:[10.1104/pp.104.040998](https://doi.org/10.1104/pp.104.040998).
- Koch, M.S.; Ward, J.M.; Levine, S.L.; Baum, J.A.; Vicini, J.L.; Hammond, B.G. The Food and Environmental Safety of Bt Crops. *Frontiers in Plant Science* **2015**, *6*.
- Koehler, G.; Wilson, R.C.; Goodpaster, J.V.; Sønsteby, A.; Lai, X.; Witzmann, F.A.; You, J.-S.; Rohloff, J.; Randall, S.K.; Alsheikh, M. Proteomic Study of Low-

General references

- Temperature Responses in Strawberry Cultivars (*Fragaria* × *Ananassa*) That Differ in Cold Tolerance. *Plant Physiology* **2012**, *159*, 1787–1805, doi:[10.1104/pp.112.198267](https://doi.org/10.1104/pp.112.198267).
- Kou, X.; Yang, S.; Chai, L.; Wu, C.; Zhou, J.; Liu, Y.; Xue, Z. Abscisic Acid and Fruit Ripening: Multifaceted Analysis of the Effect of Abscisic Acid on Fleshy Fruit Ripening. *Scientia Horticulturae* **2021**, *281*, 109999, doi:[10.1016/j.scienta.2021.109999](https://doi.org/10.1016/j.scienta.2021.109999).
- Kramer, M.G.; Redenbaugh, K. Commercialization of a Tomato with an Antisense Polygalacturonase Gene: The FLAVR SAVR™ Tomato Story. *Euphytica* **1994**, *79*, 293–297, doi:[10.1007/BF00022530](https://doi.org/10.1007/BF00022530).
- Kumar, R.; Tamboli, V.; Sharma, R.; Sreelakshmi, Y. NAC-NOR Mutations in Tomato Penjar Accessions Attenuate Multiple Metabolic Processes and Prolong the Fruit Shelf Life. *Food Chemistry* **2018**, *259*, 234–244, doi:[10.1016/j.foodchem.2018.03.135](https://doi.org/10.1016/j.foodchem.2018.03.135).
- Lang, Z.; Wang, Y.; Tang, K.; Tang, D.; Datsenka, T.; Cheng, J.; Zhang, Y.; Handa, A.K.; Zhu, J.-K. Critical Roles of DNA Demethylation in the Activation of Ripening-Induced Genes and Inhibition of Ripening-Repressed Genes in Tomato Fruit. *Proceedings of the National Academy of Sciences* **2017**, *114*, E4511–E4519, doi:[10.1073/pnas.1705233114](https://doi.org/10.1073/pnas.1705233114).
- Lashbrook, C.C.; Tieman, D.M.; Klee, H.J. Differential Regulation of the Tomato ETR Gene Family throughout Plant Development. *The Plant Journal* **1998**, *15*, 243–252, doi:[10.1046/j.1365-313X.1998.00202.x](https://doi.org/10.1046/j.1365-313X.1998.00202.x).
- Li, C.; Hou, X.; Qi, N.; Liu, H.; Li, Y.; Huang, D.; Wang, C.; Liao, W. Insight into Ripening-Associated Transcription Factors in Tomato: A Review. *Scientia Horticulturae* **2021**, *288*, 110363, doi:[10.1016/j.scienta.2021.110363](https://doi.org/10.1016/j.scienta.2021.110363).
- Li, M.; Li, D.; Feng, F.; Zhang, S.; Ma, F.; Cheng, L. Proteomic Analysis Reveals Dynamic Regulation of Fruit Development and Sugar and Acid Accumulation in Apple. *Journal of Experimental Botany* **2016**, *67*, 5145–5157, doi:[10.1093/jxb/erw277](https://doi.org/10.1093/jxb/erw277).

- Li, N.; Parsons, B.L.; Liu, D.; Mattoo, A.K. Accumulation of Wound-Inducible ACC Synthase Transcript in Tomato Fruit Is Inhibited by Salicylic Acid and Polyamines. *Plant Mol Biol* **1992**, *18*, 477–487, doi:[10.1007/BF00040664](https://doi.org/10.1007/BF00040664).
- Li, T.; Liu, B.; Spalding, M.H.; Weeks, D.P.; Yang, B. High-Efficiency TALEN-Based Gene Editing Produces Disease-Resistant Rice. *Nat Biotechnol* **2012**, *30*, 390–392, doi:[10.1038/nbt.2199](https://doi.org/10.1038/nbt.2199).
- Li, Y.; Fan, C.; Xing, Y.; Jiang, Y.; Luo, L.; Sun, L.; Shao, D.; Xu, C.; Li, X.; Xiao, J.; *et al* Natural Variation in GS5 Plays an Important Role in Regulating Grain Size and Yield in Rice. *Nat Genet* **2011**, *43*, 1266–1269, doi:[10.1038/ng.977](https://doi.org/10.1038/ng.977).
- Li, Z.; Jiang, G.; Liu, X.; Ding, X.; Zhang, D.; Wang, X.; Zhou, Y.; Yan, H.; Li, T.; Wu, K.; *et al* Histone Demethylase SIJMJ6 Promotes Fruit Ripening by Removing H3K27 Methylation of Ripening-Related Genes in Tomato. *New Phytologist* **2020**, *227*, 1138–1156, doi:[10.1111/nph.16590](https://doi.org/10.1111/nph.16590).
- Liao, X.; Li, M.; Liu, B.; Yan, M.; Yu, X.; Zi, H.; Liu, R.; Yamamuro, C. Interlinked Regulatory Loops of ABA Catabolism and Biosynthesis Coordinate Fruit Growth and Ripening in Woodland Strawberry. *Proceedings of the National Academy of Sciences* **2018**, *115*, E11542–E11550, doi:[10.1073/pnas.1812575115](https://doi.org/10.1073/pnas.1812575115).
- Liu, B.; Santo Domingo, M.; Mayobre, C.; Martín-Hernández, A.M.; Pujol, M.; Garcia-Mas, J. Knock-Out of CmNAC-NOR Affects Melon Climacteric Fruit Ripening. *Frontiers in Plant Science* **2022a**, *13*.
- Liu, M.; Gomes, B.L.; Mila, I.; Purgatto, E.; Peres, L.E.P.; Frasse, P.; Maza, E.; Zouine, M.; Roustan, J.-P.; Bouzayan, M.; *et al* Comprehensive Profiling of Ethylene Response Factor Expression Identifies Ripening-Associated ERF Genes and Their Link to Key Regulators of Fruit Ripening in Tomato. *Plant Physiology* **2016**, *170*, 1732–1744, doi:[10.1104/pp.15.01859](https://doi.org/10.1104/pp.15.01859).
- Liu, R.; How-Kit, A.; Stammitti, L.; Teyssier, E.; Rolin, D.; Mortain-Bertrand, A.; Halle, S.; Liu, M.; Kong, J.; Wu, C.; *et al* A DEMETER-like DNA Demethylase Governs Tomato Fruit Ripening. *Proceedings of the National Academy of Sciences* **2015**, *112*, 10804–10809, doi:[10.1073/pnas.1503362112](https://doi.org/10.1073/pnas.1503362112).
- Liu, Y.; Zhu, L.; Yang, M.; Xie, X.; Sun, P.; Fang, C.; Zhao, J. R2R3-MYB Transcription Factor FaMYB5 Is Involved in Citric Acid Metabolism in Strawberry Fruits.

General references

- Journal of Plant Physiology* **2022b**, 277, 153789, doi:[10.1016/j.jplph.2022.153789](https://doi.org/10.1016/j.jplph.2022.153789).
- Lorenzo, C.D.; Debray, K.; Herwegh, D.; Develtere, W.; Impens, L.; Schaumont, D.; Vandeputte, W.; Aesaert, S.; Coussens, G.; De Boe, Y.; *et al* BREEDIT: A Multiplex Genome Editing Strategy to Improve Complex Quantitative Traits in Maize. *The Plant Cell* **2022**, koac243, doi:[10.1093/plcell/koac243](https://doi.org/10.1093/plcell/koac243).
- Lü, P.; Yu, S.; Zhu, N.; Chen, Y.-R.; Zhou, B.; Pan, Y.; Tzeng, D.; Fabi, J.P.; Argyris, J.; Garcia-Mas, J.; *et al* Genome Encode Analyses Reveal the Basis of Convergent Evolution of Fleshy Fruit Ripening. *Nature Plants* **2018**, 4, 784–791, doi:[10.1038/s41477-018-0249-z](https://doi.org/10.1038/s41477-018-0249-z).
- Luo, J.; Peng, F.; Zhang, S.; Xiao, Y.; Zhang, Y. The Protein Kinase FaSnRK1 α Regulates Sucrose Accumulation in Strawberry Fruits. *Plant Physiology and Biochemistry* **2020a**, 151, 369–377, doi:[10.1016/j.plaphy.2020.03.044](https://doi.org/10.1016/j.plaphy.2020.03.044).
- Luo, Y.; Ge, C.; Ling, Y.; Mo, F.; Yang, M.; Jiang, L.; Chen, Q.; Lin, Y.; Sun, B.; Zhang, Y.; *et al* ABA and Sucrose Co-Regulate Strawberry Fruit Ripening and Show Inhibition of Glycolysis. *Mol Genet Genomics* **2020b**, 295, 421–438, doi:[10.1007/s00438-019-01629-w](https://doi.org/10.1007/s00438-019-01629-w).
- Luo, Y.; Lin, Y.; Mo, F.; Ge, C.; Jiang, L.; Zhang, Y.; Chen, Q.; Sun, B.; Wang, Y.; Wang, X.; *et al* Sucrose Promotes Strawberry Fruit Ripening and Affects Ripening-Related Processes. *International Journal of Genomics* **2019**, 2019, e9203057, doi:[10.1155/2019/9203057](https://doi.org/10.1155/2019/9203057).
- Maeder, M.L.; Thibodeau-Beganny, S.; Osiak, A.; Wright, D.A.; Anthony, R.M.; Eichinger, M.; Jiang, T.; Foley, J.E.; Winfrey, R.J.; Townsend, J.A.; *et al* Rapid “Open-Source” Engineering of Customized Zinc-Finger Nucleases for Highly Efficient Gene Modification. *Molecular Cell* **2008**, 31, 294–301, doi:[10.1016/j.molcel.2008.06.016](https://doi.org/10.1016/j.molcel.2008.06.016).
- Manning, K.; Tör, M.; Poole, M.; Hong, Y.; Thompson, A.J.; King, G.J.; Giovannoni, J.J.; Seymour, G.B. A Naturally Occurring Epigenetic Mutation in a Gene Encoding an SBP-Box Transcription Factor Inhibits Tomato Fruit Ripening. *Nat Genet* **2006**, 38, 948–952, doi:[10.1038/ng1841](https://doi.org/10.1038/ng1841).

- Martínez-Madrid, M.C.; Flores, F.; Romojaro, F. Behaviour of Abscisic Acid and Polyamines in Antisense ACC Oxidase Melon (*Cucumis Melo*) during Ripening. *Functional Plant Biol.* **2002**, *29*, 865–872, doi:[10.1071/pp01164](https://doi.org/10.1071/pp01164).
- Martín-Pizarro, C.; Vallarino, J.G.; Osorio, S.; Meco, V.; Urrutia, M.; Pillet, J.; Casañal, A.; Merchante, C.; Amaya, I.; Willmitzer, L.; *et al* The NAC Transcription Factor FaRIF Controls Fruit Ripening in Strawberry. *The Plant Cell* **2021**, *33*, 1574–1593, doi:[10.1093/plcell/koab070](https://doi.org/10.1093/plcell/koab070).
- Mayobre, C.; Pereira, L.; Eltahiri, A.; Bar, E.; Lewinsohn, E.; Garcia-Mas, J.; Pujol, M. Genetic Dissection of Aroma Biosynthesis in Melon and Its Relationship with Climacteric Ripening. *Food Chemistry* **2021**, *353*, 129484, doi:[10.1016/j.foodchem.2021.129484](https://doi.org/10.1016/j.foodchem.2021.129484).
- Medina-Puche, L.; Molina-Hidalgo, F.J.; Boersma, M.; Schuurink, R.C.; López-Vidriero, I.; Solano, R.; Franco-Zorrilla, J.-M.; Caballero, J.L.; Blanco-Portales, R.; Muñoz-Blanco, J. An R2R3-MYB Transcription Factor Regulates Eugenol Production in Ripe Strawberry Fruit Receptacles. *Plant Physiology* **2015**, *168*, 598–614, doi:[10.1104/pp.114.252908](https://doi.org/10.1104/pp.114.252908).
- Ministerio de Agricultura, Ganadería y Pesca. (2021). *Melón y sandía. Balance campaña 2020 y perspectivas 2021*. https://www.mapa.gob.es/es/ganaderia/estadisticas/balancefinaldecampana2020melonysandia_tcm30-561109.pdf
- Moghissi, A.A.; Pei, S.; Liu, Y. Golden Rice: Scientific, Regulatory and Public Information Processes of a Genetically Modified Organism. *Critical Reviews in Biotechnology* **2016**, *36*, 535–541, doi:[10.3109/07388551.2014.993586](https://doi.org/10.3109/07388551.2014.993586).
- Mohan, C.; Satish, L.; Muthubharathi, B.C.; Selvarajan, D.; Easterling, M.; Yau, Y.-Y. CRISPR-Cas Technology: A Genome-Editing Powerhouse for Molecular Plant Breeding. In *Biotechnological Innovations for Environmental Bioremediation*; Arora, S., Kumar, A., Ogita, S., Yau, Y.-Y., Eds.; Springer Nature: Singapore, **2022**; pp. 803–879 ISBN 9789811690013.
- Mojica, F.J.M.; Díez-Villaseñor, C.; García-Martínez, J.; Almendros, C.Y. 2009 Short Motif Sequences Determine the Targets of the Prokaryotic CRISPR Defence System. *Microbiology* **2022**, *155*, 733–740, doi:[10.1099/mic.0.023960-0](https://doi.org/10.1099/mic.0.023960-0).

General references

- Mojica, F.J.M.; Díez-Villaseñor, C.; García-Martínez, J.; Soria, E. Intervening Sequences of Regularly Spaced Prokaryotic Repeats Derive from Foreign Genetic Elements. *J Mol Evol* **2005**, *60*, 174–182, doi:[10.1007/s00239-004-0046-3](https://doi.org/10.1007/s00239-004-0046-3).
- Moreno, E.; Obando, J.M.; Dos-Santos, N.; Fernández-Trujillo, J.P.; Monforte, A.J.; Garcia-Mas, J. Candidate Genes and QTLs for Fruit Ripening and Softening in Melon. *Theor Appl Genet* **2008**, *116*, 589–602, doi:[10.1007/s00122-007-0694-y](https://doi.org/10.1007/s00122-007-0694-y).
- Mu, Q.; Li, X.; Luo, J.; Pan, Q.; Li, Y.; Gu, T. Characterization of Expansin Genes and Their Transcriptional Regulation by Histone Modifications in Strawberry. *Planta* **2021**, *254*, 21, doi:[10.1007/s00425-021-03665-6](https://doi.org/10.1007/s00425-021-03665-6).
- Muthusamy, V.; Hossain, F.; Thirunavukkarasu, N.; Choudhary, M.; Saha, S.; Bhat, J.S.; Prasanna, B.M.; Gupta, H.S. Development of β -Carotene Rich Maize Hybrids through Marker-Assisted Introgression of β -Carotene Hydroxylase Allele. *PLOS ONE* **2014**, *9*, e113583, doi:[10.1371/journal.pone.0113583](https://doi.org/10.1371/journal.pone.0113583).
- Nath, P.; Bouzayen, M.; Mattoo, A.K.; Pech, J. *claude Fruit Ripening: Physiology, Signalling and Genomics*; CABI, 2014; ISBN 978-1-84593-962-5.
- Neuhausen, S.L. Evaluation of Restriction Fragment Length Polymorphism in Cucumis Melo. *Theoret. Appl. Genetics* **1992**, *83*, 379–384, doi:[10.1007/BF00224286](https://doi.org/10.1007/BF00224286).
- Nicolia, A.; Proux-Wéra, E.; Åhman, I.; Onkokesung, N.; Andersson, M.; Andreasson, E.; Zhu, L.-H. Targeted Gene Mutation in Tetraploid Potato through Transient TALEN Expression in Protoplasts. *Journal of Biotechnology* **2015**, *204*, 17–24, doi:[10.1016/j.jbiotec.2015.03.021](https://doi.org/10.1016/j.jbiotec.2015.03.021).
- Nielsen, L.J.; Stuart, P.; Pičmanová, M.; Rasmussen, S.; Olsen, C.E.; Harholt, J.; Møller, B.L.; Bjarnholt, N. Dhurrin Metabolism in the Developing Grain of Sorghum Bicolor (L.) Moench Investigated by Metabolite Profiling and Novel Clustering Analyses of Time-Resolved Transcriptomic Data. *BMC Genomics* **2016**, *17*, 1021, doi:[10.1186/s12864-016-3360-4](https://doi.org/10.1186/s12864-016-3360-4).
- Nimmakayala, P.; Tomason, Y.R.; Abburi, V.L.; Alvarado, A.; Saminathan, T.; Vajja, V.G.; Salazar, G.; Panicker, G.K.; Levi, A.; Wechter, W.P.; *et al* Genome-Wide Differentiation of Various Melon Horticultural Groups for Use in GWAS for Fruit Firmness and Construction of a High Resolution Genetic Map. *Frontiers in Plant Science* **2016**, *7*.

- Nonaka, S.; Arai, C.; Takayama, M.; Matsukura, C.; Ezura, H. Efficient Increase of γ -Aminobutyric Acid (GABA) Content in Tomato Fruits by Targeted Mutagenesis. *Sci Rep* **2017**, *7*, 7057, doi:[10.1038/s41598-017-06400-y](https://doi.org/10.1038/s41598-017-06400-y).
- Obando-Ulloa, J.M.; Eduardo, I.; Monforte, A.J.; Fernández-Trujillo, J.P. Identification of QTLs Related to Sugar and Organic Acid Composition in Melon Using Near-Isogenic Lines. *Scientia Horticulturae* **2009**, *121*, 425–433, doi:[10.1016/j.scienta.2009.02.023](https://doi.org/10.1016/j.scienta.2009.02.023).
- Oetiker, J.H.; Olson, D.C.; Shiu, O.Y.; Yang, S.F. Differential Induction of Seven 1-Aminocyclopropane-1-Carboxylate Synthase Genes by Elicitor in Suspension Cultures of Tomato (*Lycopersicon Esculentum*). *Plant Mol Biol* **1997**, *34*, 275–286, doi:[10.1023/a:1005800511372](https://doi.org/10.1023/a:1005800511372).
- Olson, D.C.; Oetiker, J.H.; Yang, S.F. Analysis of LE-ACS3, a 1-Aminocyclopropane-1-Carboxylic Acid Synthase Gene Expressed during Flooding in the Roots of Tomato Plants. *J Biol Chem* **1995**, *270*, 14056–14061, doi:[10.1074/jbc.270.23.14056](https://doi.org/10.1074/jbc.270.23.14056).
- Osorio, S.; Carneiro, R.T.; Lytovchenko, A.; McQuinn, R.; Sørensen, I.; Vallarino, J.G.; Giovannoni, J.J.; Fernie, A.R.; Rose, J.K.C. Genetic and Metabolic Effects of Ripening Mutations and Vine Detachment on Tomato Fruit Quality. *Plant Biotechnology Journal* **2020**, *18*, 106–118, doi:[10.1111/pbi.13176](https://doi.org/10.1111/pbi.13176).
- Payton, S.; Fray, R.G.; Brown, S.; Grierson, D. Ethylene Receptor Expression Is Regulated during Fruit Ripening, Flower Senescence and Abscission. *Plant Mol Biol* **1996**, *31*, 1227–1231, doi:[10.1007/BF00040839](https://doi.org/10.1007/BF00040839).
- Pech, J.C.; Bouzayen, M.; Latché, A. Climacteric Fruit Ripening: Ethylene-Dependent and Independent Regulation of Ripening Pathways in Melon Fruit. *Plant Science* **2008**, *175*, 114–120, doi:[10.1016/j.plantsci.2008.01.003](https://doi.org/10.1016/j.plantsci.2008.01.003).
- Pereira, L.; Ruggieri, V.; Pérez, S.; Alexiou, K.G.; Fernández, M.; Jahrmann, T.; Pujol, M.; Garcia-Mas, J. QTL Mapping of Melon Fruit Quality Traits Using a High-Density GBS-Based Genetic Map. *BMC Plant Biology* **2018**, *18*, 324, doi:[10.1186/s12870-018-1537-5](https://doi.org/10.1186/s12870-018-1537-5).
- Pereira, L.; Santo Domingo, M.; Ruggieri, V.; Argyris, J.; Phillips, M.A.; Zhao, G.; Lian, Q.; Xu, Y.; He, Y.; Huang, S.; *et al* Genetic Dissection of Climacteric Fruit

General references

- Ripening in a Melon Population Segregating for Ripening Behavior. *Horticulture Research* **2020**, 7, 187, doi:[10.1038/s41438-020-00411-z](https://doi.org/10.1038/s41438-020-00411-z).
- Perpiñá, G.; Cebolla-Cornejo, J.; Esteras, C.; Monforte, A.J.; Picó, B. ‘MAK-10’: A Long Shelf-Life Charentais Breeding Line Developed by Introgression of a Genomic Region from Makuwa Melon. *HortScience* **2017**, 52, 1633–1638, doi:[10.21273/HORTSCI12068-17](https://doi.org/10.21273/HORTSCI12068-17).
- Perpiñá, G.; Esteras, C.; Gibon, Y.; Monforte, A.J.; Picó, B. A New Genomic Library of Melon Introgression Lines in a Cantaloupe Genetic Background for Dissecting Desirable Agronomical Traits. *BMC Plant Biology* **2016**, 16, 154, doi:[10.1186/s12870-016-0842-0](https://doi.org/10.1186/s12870-016-0842-0).
- Pillet, J.; Folta, K.M. Pigments in Strawberry. In *Pigments in Fruits and Vegetables: Genomics and Dietetics*; Chen, C., Ed.; Springer: New York, NY, 2015; pp. 205–216 ISBN 978-1-4939-2356-4.
- Pratt, H.K.; Goeschl, J.D.; Martin, F.W. Fruit Growth and Development, Ripening, and the Role of Ethylene in the ‘Honey Dew’ Muskmelon1. *Journal of the American Society for Horticultural Science* **1977**, 102, 203–210, doi:[10.21273/JASHS.102.2.203](https://doi.org/10.21273/JASHS.102.2.203).
- Prieto, J.; Redondo, P.; Padró, D.; Arnould, S.; Epinat, J.-C.; Pâques, F.; Blanco, F.J.; Montoya, G. The C-Terminal Loop of the Homing Endonuclease I-CreI Is Essential for Site Recognition, DNA Binding and Cleavage. *Nucleic Acids Research* **2007**, 35, 3262–3271, doi:[10.1093/nar/gkm183](https://doi.org/10.1093/nar/gkm183).
- Puchta, H.; Dujon, B.; Hohn, B. Two Different but Related Mechanisms Are Used in Plants for the Repair of Genomic Double-Strand Breaks by Homologous Recombination. *Proceedings of the National Academy of Sciences* **1996**, 93, 5055–5060, doi:[10.1073/pnas.93.10.5055](https://doi.org/10.1073/pnas.93.10.5055).
- Qin, G.; Zhu, Z.; Wang, W.; Cai, J.; Chen, Y.; Li, L.; Tian, S. A Tomato Vacuolar Invertase Inhibitor Mediates Sucrose Metabolism and Influences Fruit Ripening. *Plant Physiology* **2016**, 172, 1596–1611, doi:[10.1104/pp.16.01269](https://doi.org/10.1104/pp.16.01269).
- Renner, S.S.; Schaefer, H. Phylogeny and Evolution of the Cucurbitaceae. In *Genetics and Genomics of Cucurbitaceae*; Grumet, R., Katzir, N., Garcia-Mas, J., Eds.;

- Plant Genetics and Genomics: Crops and Models; Springer International Publishing: Cham, 2017; pp. 13–23 ISBN 978-3-319-49332-9.
- Rick, C. New Mutants. *Rep. Tomato Genet. Coop.* **1956**, *6*, 22–23.
- Ríos, P.; Argyris, J.; Vegas, J.; Leida, C.; Kenigswald, M.; Tzuri, G.; Troadec, C.; Bendahmane, A.; Katzir, N.; Picó, B.; *et al* ETHQV6.3 Is Involved in Melon Climacteric Fruit Ripening and Is Encoded by a NAC Domain Transcription Factor. *The Plant Journal* **2017**, *91*, 671–683, doi:[10.1111/tpj.13596](https://doi.org/10.1111/tpj.13596).
- Robinson, R. Ripening Inhibitor: A Gene with Multiple Effects on Ripening. *Rep Tomato Genet Coop* **1968**.
- Ruggieri, V.; Alexiou, K.G.; Morata, J.; Argyris, J.; Pujol, M.; Yano, R.; Nonaka, S.; Ezura, H.; Latrasse, D.; Boualem, A.; *et al* An Improved Assembly and Annotation of the Melon (*Cucumis Melo* L.) Reference Genome. *Sci Rep* **2018**, *8*, 8088, doi:[10.1038/s41598-018-26416-2](https://doi.org/10.1038/s41598-018-26416-2).
- Sayre, R.; Beeching, J.R.; Cahoon, E.B.; Egesi, C.; Fauquet, C.; Fellman, J.; Fregene, M.; Gruissem, W.; Mallowa, S.; Manary, M.; *et al* The BioCassava Plus Program: Biofortification of Cassava for Sub-Saharan Africa. *Annual Review of Plant Biology* **2011**, *62*, 251–272, doi:[10.1146/annurev-arplant-042110-103751](https://doi.org/10.1146/annurev-arplant-042110-103751).
- Seymour, G.B.; Ryder, C.D.; Cevik, V.; Hammond, J.P.; Popovich, A.; King, G.J.; Vrebalov, J.; Giovannoni, J.J.; Manning, K. A SEPALLATA Gene Is Involved in the Development and Ripening of Strawberry (*Fragaria×ananassa* Duch.) Fruit, a Non-Climacteric Tissue*. *Journal of Experimental Botany* **2011**, *62*, 1179–1188, doi:[10.1093/jxb/erq360](https://doi.org/10.1093/jxb/erq360).
- Shan, Q.; Wang, Y.; Chen, K.; Liang, Z.; Li, J.; Zhang, Y.; Zhang, K.; Liu, J.; Voytas, D.F.; Zheng, X.; *et al* Rapid and Efficient Gene Modification in Rice and Brachypodium Using TALENs. *Molecular Plant* **2013**, *6*, 1365–1368, doi:[10.1093/mp/sss162](https://doi.org/10.1093/mp/sss162).
- Shao, Y.; Wong, C.E.; Shen, L.; Yu, H. N6-Methyladenosine Modification Underlies Messenger RNA Metabolism and Plant Development. *Current Opinion in Plant Biology* **2021**, *63*, 102047, doi:[10.1016/j.pbi.2021.102047](https://doi.org/10.1016/j.pbi.2021.102047).

General references

- Shnaider, Y.; Elad, Y.; Rav David, D.; Pashkovsky, E.; Leibman, D.; Kravchik, M.; Shtarkman-Cohen, M.; Gal-On, A.; Spiegelman, Z. Development of Powdery Mildew (*Podosphaera Xanthii*) Resistance in Cucumber (*Cucumis Sativus*) Using CRISPR/Cas9-Mediated Mutagenesis of CsaMLO8. *Phytopathology*® **2022**, doi:[10.1094/PHYTO-06-22-0193-FI](https://doi.org/10.1094/PHYTO-06-22-0193-FI).
- Shu, L.; Lou, Q.; Ma, C.; Ding, W.; Zhou, J.; Wu, J.; Feng, F.; Lu, X.; Luo, L.; Xu, G.; *et al* Genetic, Proteomic and Metabolic Analysis of the Regulation of Energy Storage in Rice Seedlings in Response to Drought. *PROTEOMICS* **2011**, *11*, 4122–4138, doi:[10.1002/pmic.201000485](https://doi.org/10.1002/pmic.201000485).
- Shukla, V.; Gupta, M.; Urnov, F.; Guschin, D.; Both, M.J.D.; Bundock, P.; Sastry-Dent, L. Targeted Modification of Malate Dehydrogenase **2016**.
- Shukla, V.K.; Doyon, Y.; Miller, J.C.; DeKolver, R.C.; Moehle, E.A.; Worden, S.E.; Mitchell, J.C.; Arnold, N.L.; Gopalan, S.; Meng, X.; *et al* Precise Genome Modification in the Crop Species *Zea Mays* Using Zinc-Finger Nucleases. *Nature* **2009**, *459*, 437–441, doi:[10.1038/nature07992](https://doi.org/10.1038/nature07992).
- Snouffer, A.; Kraus, C.; van der Knaap, E. The Shape of Things to Come: Ovate Family Proteins Regulate Plant Organ Shape. *Current Opinion in Plant Biology* **2020**, *53*, 98–105, doi:[10.1016/j.pbi.2019.10.005](https://doi.org/10.1016/j.pbi.2019.10.005).
- Solano, R.; Stepanova, A.; Chao, Q.; Ecker, J.R. Nuclear Events in Ethylene Signaling: A Transcriptional Cascade Mediated by ETHYLENE-INSENSITIVE3 and ETHYLENE-RESPONSE-FACTOR1. *Genes Dev.* **1998**, *12*, 3703–3714, doi:[10.1101/gad.12.23.3703](https://doi.org/10.1101/gad.12.23.3703).
- Sonawane, P.D.; Pollier, J.; Panda, S.; Szymanski, J.; Massalha, H.; Yona, M.; Unger, T.; Malitsky, S.; Arendt, P.; Pauwels, L.; *et al* Plant Cholesterol Biosynthetic Pathway Overlaps with Phytosterol Metabolism. *Nature Plants* **2016**, *3*, 1–13, doi:[10.1038/nplants.2016.205](https://doi.org/10.1038/nplants.2016.205).
- Sousa-Baena, M.S.; Sinha, N.R.; Hernandez-Lopes, J.; Lohmann, L.G. Convergent Evolution and the Diverse Ontogenetic Origins of Tendrils in Angiosperms. *Frontiers in Plant Science* **2018**, *9*.
- Soyk, S.; Lemmon, Z.H.; Oved, M.; Fisher, J.; Liberatore, K.L.; Park, S.J.; Goren, A.; Jiang, K.; Ramos, A.; van der Knaap, E.; *et al* Bypassing Negative Epistasis on

- Yield in Tomato Imposed by a Domestication Gene. *Cell* **2017**, *169*, 1142–1155.e12, doi:[10.1016/j.cell.2017.04.032](https://doi.org/10.1016/j.cell.2017.04.032).
- Stitt, M.; Schulze, D. Does Rubisco Control the Rate of Photosynthesis and Plant Growth? An Exercise in Molecular Ecophysiology. *Plant, Cell & Environment* **1994**, *17*, 465–487, doi:[10.1111/j.1365-3040.1994.tb00144.x](https://doi.org/10.1111/j.1365-3040.1994.tb00144.x).
- Sun, W.; Xu, X.; Zhu, H.; Liu, A.; Liu, L.; Li, J.; Hua, X. Comparative Transcriptomic Profiling of a Salt-Tolerant Wild Tomato Species and a Salt-Sensitive Tomato Cultivar. *Plant and Cell Physiology* **2010**, *51*, 997–1006, doi:[10.1093/pcp/pcq056](https://doi.org/10.1093/pcp/pcq056).
- Sun, Y.; Chen, P.; Duan, C.; Tao, P.; Wang, Y.; Ji, K.; Hu, Y.; Li, Q.; Dai, S.; Wu, Y.; *et al* Transcriptional Regulation of Genes Encoding Key Enzymes of Abscisic Acid Metabolism During Melon (*Cucumis Melo* L.) Fruit Development and Ripening. *J Plant Growth Regul* **2013**, *32*, 233–244, doi:[10.1007/s00344-012-9293-5](https://doi.org/10.1007/s00344-012-9293-5).
- Sundaram, R.M.; Vishnupriya, M.R.; Biradar, S.K.; Laha, G.S.; Reddy, G.A.; Rani, N.S.; Sarma, N.P.; Sonti, R.V. Marker Assisted Introgression of Bacterial Blight Resistance in Samba Mahsuri, an Elite Indica Rice Variety. *Euphytica* **2008**, *160*, 411–422, doi:[10.1007/s10681-007-9564-6](https://doi.org/10.1007/s10681-007-9564-6).
- Symons, G.M.; Chua, Y.-J.; Ross, J.J.; Quittenden, L.J.; Davies, N.W.; Reid, J.B. Hormonal Changes during Non-Climacteric Ripening in Strawberry. *Journal of Experimental Botany* **2012**, *63*, 4741–4750, doi:[10.1093/jxb/ers147](https://doi.org/10.1093/jxb/ers147).
- Tarja Laaninen (2021). New genomic techniques, European Commission study and first reactions. European Parliament Research Service.
- Tassoni, A.; Watkins, C.B.; Davies, P.J. Inhibition of the Ethylene Response by 1-MCP in Tomato Suggests That Polyamines Are Not Involved in Delaying Ripening, but May Moderate the Rate of Ripening or over-Ripening. *Journal of Experimental Botany* **2006**, *57*, 3313–3325, doi:[10.1093/jxb/erl092](https://doi.org/10.1093/jxb/erl092).
- Thompson, A.J.; Tor, M.; Barry, C.S.; Vrebalov, J.; Orfila, C.; Jarvis, M.C.; Giovannoni, J.J.; Grierson, D.; Seymour, G.B. Molecular and Genetic Characterization of a Novel Pleiotropic Tomato-Ripening Mutant1. *Plant Physiology* **1999**, *120*, 383–390, doi:[10.1104/pp.120.2.383](https://doi.org/10.1104/pp.120.2.383).

General references

- Tian, M.S.; Prakash, S.; Elgar, H.J.; Young, H.; Burmeister, D.M.; Ross, G.S. Responses of Strawberry Fruit to 1-Methylcyclopropene (1-MCP) and Ethylene. *Plant Growth Regulation* **2000**, *32*, 83–90, doi:[10.1023/A:1006409719333](https://doi.org/10.1023/A:1006409719333).
- Tieman, D.M.; Klee, H.J. Differential Expression of Two Novel Members of the Tomato Ethylene-Receptor Family. *Plant Physiology* **1999**, *120*, 165–172, doi:[10.1104/pp.120.1.165](https://doi.org/10.1104/pp.120.1.165).
- Tigchelaar, E.; Tomes, M.L.; Kerr, E.A.; Barman, R.J. A New Fruit Ripening Mutant, Non-Ripening (Nor). *Rep. Tomato Genet. Coop.* **1973**, *23*, 33–34.
- Urrutia, M.; Bonet, J.; Arús, P.; Monfort, A. A Near-Isogenic Line (NIL) Collection in Diploid Strawberry and Its Use in the Genetic Analysis of Morphologic, Phenotypic and Nutritional Characters. *Theor Appl Genet* **2015**, *128*, 1261–1275, doi:[10.1007/s00122-015-2503-3](https://doi.org/10.1007/s00122-015-2503-3).
- Vallarino, J.G.; Osorio, S.; Bombarely, A.; Casañal, A.; Cruz-Rus, E.; Sánchez-Sevilla, J.F.; Amaya, I.; Giavalisco, P.; Fernie, A.R.; Botella, M.A.; *et al* Central Role of FaGAMYB in the Transition of the Strawberry Receptacle from Development to Ripening. *New Phytologist* **2015**, *208*, 482–496, doi:[10.1111/nph.13463](https://doi.org/10.1111/nph.13463).
- van der Vossen, E.A.G.; Gros, J.; Sikkema, A.; Muskens, M.; Wouters, D.; Wolters, P.; Pereira, A.; Allefs, S. The Rpi-Blb2 Gene from *Solanum bulbocastanum* Is an Mi-1 Gene Homolog Conferring Broad-Spectrum Late Blight Resistance in Potato. *The Plant Journal* **2005**, *44*, 208–222, doi:[10.1111/j.1365-313X.2005.02527.x](https://doi.org/10.1111/j.1365-313X.2005.02527.x).
- Varshney, R.K.; Pandey, M.K.; Janila, P.; Nigam, S.N.; Sudini, H.; Gowda, M.V.C.; Sriswathi, M.; Radhakrishnan, T.; Manohar, S.S.; Nagesh, P. Marker-Assisted Introgression of a QTL Region to Improve Rust Resistance in Three Elite and Popular Varieties of Peanut (*Arachis hypogaea* L.). *Theor Appl Genet* **2014**, *127*, 1771–1781, doi:[10.1007/s00122-014-2338-3](https://doi.org/10.1007/s00122-014-2338-3).
- Vegas, J.; Garcia-Mas, J.; Monforte, A.J. Interaction between QTLs Induces an Advance in Ethylene Biosynthesis during Melon Fruit Ripening. *Theor Appl Genet* **2013**, *126*, 1531–1544, doi:[10.1007/s00122-013-2071-3](https://doi.org/10.1007/s00122-013-2071-3).
- Vital, C.E.; Giordano, A.; de Almeida Soares, E.; Rhys Williams, T.C.; Mesquita, R.O.; Vidigal, P.M.P.; de Santana Lopes, A.; Pacheco, T.G.; Rogalski, M.; de Oliveira

- Ramos, H.J.; *et al* An Integrative Overview of the Molecular and Physiological Responses of Sugarcane under Drought Conditions. *Plant Mol Biol* **2017**, *94*, 577–594, doi:[10.1007/s11103-017-0611-y](https://doi.org/10.1007/s11103-017-0611-y).
- Vrebalov, J.; Ruezinsky, D.; Padmanabhan, V.; White, R.; Medrano, D.; Drake, R.; Schuch, W.; Giovannoni, J. A MADS-Box Gene Necessary for Fruit Ripening at the Tomato Ripening-Inhibitor (Rin) Locus. *Science* **2002**, *296*, 343–346, doi:[10.1126/science.1068181](https://doi.org/10.1126/science.1068181).
- Waltz, E. GABA-Enriched Tomato Is First CRISPR-Edited Food to Enter Market. *Nature Biotechnology* **2021**, *40*, 9–11, doi:[10.1038/d41587-021-00026-2](https://doi.org/10.1038/d41587-021-00026-2).
- Wang, H.; Yang, Y.; Zhang, Y.; Zhao, T.; Jiang, J.; Li, J.; Xu, X.; Yang, H. Transcriptome Analysis of Flower Development and Mining of Genes Related to Flowering Time in Tomato (*Solanum Lycopersicum*). *International Journal of Molecular Sciences* **2021a**, *22*, 8128, doi:[10.3390/ijms22158128](https://doi.org/10.3390/ijms22158128).
- Wang, J.; Tian, S.; Yu, Y.; Ren, Y.; Guo, S.; Zhang, J.; Li, M.; Zhang, H.; Gong, G.; Wang, M.; *et al* Natural Variation in the NAC Transcription Factor NONRIPENING Contributes to Melon Fruit Ripening. *Journal of Integrative Plant Biology* **2022**, *64*, 1448–1461, doi:[10.1111/jipb.13278](https://doi.org/10.1111/jipb.13278).
- Wang, R.; Angenent, G.C.; Seymour, G.; de Maagd, R.A. Revisiting the Role of Master Regulators in Tomato Ripening. *Trends in Plant Science* **2020**, *25*, 291–301, doi:[10.1016/j.tplants.2019.11.005](https://doi.org/10.1016/j.tplants.2019.11.005).
- Wang, X.; Aguirre, L.; Rodríguez-Leal, D.; Hendelman, A.; Benoit, M.; Lippman, Z.B. Dissecting Cis-Regulatory Control of Quantitative Trait Variation in a Plant Stem Cell Circuit. *Nat. Plants* **2021b**, *7*, 419–427, doi:[10.1038/s41477-021-00898-x](https://doi.org/10.1038/s41477-021-00898-x).
- Wang, Y.-H.; Thomas, C.E.; Dean, R.A. A Genetic Map of Melon (*Cucumis Melo* L.) Based on Amplified Fragment Length Polymorphism (AFLP) Markers. *Theor Appl Genet* **1997**, *95*, 791–798, doi:[10.1007/s001220050627](https://doi.org/10.1007/s001220050627).
- Wei, L.; Mao, W.; Jia, M.; Xing, S.; Ali, U.; Zhao, Y.; Chen, Y.; Cao, M.; Dai, Z.; Zhang, K.; *et al* FaMYB44.2, a Transcriptional Repressor, Negatively Regulates Sucrose Accumulation in Strawberry Receptacles through Interplay with FaMYB10. *Journal of Experimental Botany* **2018**, *69*, 4805–4820, doi:[10.1093/jxb/ery249](https://doi.org/10.1093/jxb/ery249).

General references

- Wilkinson, J.Q.; Lanahan, M.B.; Clark, D.G.; Bleecker, A.B.; Chang, C.; Meyerowitz, E.M.; Klee, H.J. A Dominant Mutant Receptor from Arabidopsis Confers Ethylene Insensitivity in Heterologous Plants. *Nat Biotechnol* **1997**, *15*, 444–447, doi:[10.1038/nbt0597-444](https://doi.org/10.1038/nbt0597-444).
- Woodward, J.R. Physical and Chemical Changes in Developing Strawberry Fruits. *Journal of the Science of Food and Agriculture* **1972**, *23*, 465–473, doi:[10.1002/jsfa.2740230406](https://doi.org/10.1002/jsfa.2740230406).
- Xie, X.; Chen, Z.; Cao, J.; Guan, H.; Lin, D.; Li, C.; Lan, T.; Duan, Y.; Mao, D.; Wu, W. Toward the Positional Cloning of QBlSr5a, a QTL Underlying Resistance to Bacterial Leaf Streak, Using Overlapping Sub-CSSLs in Rice. *PLOS ONE* **2014**, *9*, e95751, doi:[10.1371/journal.pone.0095751](https://doi.org/10.1371/journal.pone.0095751).
- Xie, Y.-G.; Ma, Y.-Y.; Bi, P.-P.; Wei, W.; Liu, J.; Hu, Y.; Gou, Y.-J.; Zhu, D.; Wen, Y.-Q.; Feng, J.-Y. Transcription Factor FvTCP9 Promotes Strawberry Fruit Ripening by Regulating the Biosynthesis of Abscisic Acid and Anthocyanins. *Plant Physiology and Biochemistry* **2020**, *146*, 374–383, doi:[10.1016/j.plaphy.2019.11.004](https://doi.org/10.1016/j.plaphy.2019.11.004).
- Yang, X.; Zhang, X.; Yang, Y.; Zhang, H.; Zhu, W.; Nie, W.-F. The Histone Variant Sl_H2A.Z Regulates Carotenoid Biosynthesis and Gene Expression during Tomato Fruit Ripening. *Horticulture Research* **2021**, *8*, 85, doi:[10.1038/s41438-021-00520-3](https://doi.org/10.1038/s41438-021-00520-3).
- Ye, X.; Al-Babili, S.; Klöti, A.; Zhang, J.; Lucca, P.; Beyer, P.; Potrykus, I. Engineering the Provitamin A (β -Carotene) Biosynthetic Pathway into (Carotenoid-Free) Rice Endosperm. *Science* **2000**, *287*, 303–305, doi:[10.1126/science.287.5451.303](https://doi.org/10.1126/science.287.5451.303).
- Yen, H.C.; Lee, S.; Tanksley, S.D.; Lanahan, M.B.; Klee, H.J.; Giovannoni, J.J. The Tomato Never-Ripe Locus Regulates Ethylene-Inducible Gene Expression and Is Linked to a Homolog of the Arabidopsis ETR1 Gene. *Plant Physiology* **1995**, *107*, 1343–1353, doi:[10.1104/pp.107.4.1343](https://doi.org/10.1104/pp.107.4.1343).
- Yesbergenova-Cuny, Z.; Dinant, S.; Martin-Magniette, M.-L.; Quilleré, I.; Armengaud, P.; Monfalet, P.; Lea, P.J.; Hirel, B. Genetic Variability of the Phloem Sap Metabolite Content of Maize (*Zea Mays* L.) during the Kernel-Filling Period. *Plant Science* **2016**, *252*, 347–357, doi:[10.1016/j.plantsci.2016.08.007](https://doi.org/10.1016/j.plantsci.2016.08.007).

- Zarid, M.; García-Carpintero, V.; Esteras, C.; Esteva, J.; Bueso, M.C.; Cañizares, J.; Picó, M.B.; Monforte, A.J.; Fernández-Trujillo, J.P. Transcriptomic Analysis of a Near-Isogenic Line of Melon with High Fruit Flesh Firmness during Ripening. *Journal of the Science of Food and Agriculture* **2021**, *101*, 754–777, doi:[10.1002/jsfa.10688](https://doi.org/10.1002/jsfa.10688).
- Zhang, M.; Yuan, B.; Leng, P. The Role of ABA in Triggering Ethylene Biosynthesis and Ripening of Tomato Fruit. *Journal of Experimental Botany* **2009**, *60*, 1579–1588, doi:[10.1093/jxb/erp026](https://doi.org/10.1093/jxb/erp026).
- Zhang, Y.; Yin, X.; Xiao, Y.; Zhang, Z.; Li, S.; Liu, X.; Zhang, B.; Yang, X.; Grierson, D.; Jiang, G.; *et al* An ETHYLENE RESPONSE FACTOR-MYB Transcription Complex Regulates Furaneol Biosynthesis by Activating QUINONE OXIDOREDUCTASE Expression in Strawberry. *Plant Physiology* **2018**, *178*, 189–201, doi:[10.1104/pp.18.00598](https://doi.org/10.1104/pp.18.00598).
- Zhao, G.; Lian, Q.; Zhang, Z.; Fu, Q.; He, Y.; Ma, S.; Ruggieri, V.; Monforte, A.J.; Wang, P.; Julca, I.; *et al* A Comprehensive Genome Variation Map of Melon Identifies Multiple Domestication Events and Loci Influencing Agronomic Traits. *Nat Genet* **2019**, *51*, 1607–1615, doi:[10.1038/s41588-019-0522-8](https://doi.org/10.1038/s41588-019-0522-8).
- Zheng, X.; Wolff, D.; Crosby, K. Genetics of Ethylene Biosynthesis and Restriction Fragment Length Polymorphisms (RFLPs) of ACC Oxidase and Synthase Genes in Melon (*Cucumis Melo* L.). *Theor Appl Genet* **2002**, *105*, 397–403, doi:[10.1007/s00122-002-0880-x](https://doi.org/10.1007/s00122-002-0880-x).
- Zhong, S.; Lin, Z.; Grierson, D. Tomato Ethylene Receptor–CTR Interactions: Visualization of NEVER-RIPE Interactions with Multiple CTRs at the Endoplasmic Reticulum. *Journal of Experimental Botany* **2008**, *59*, 965–972, doi:[10.1093/jxb/ern021](https://doi.org/10.1093/jxb/ern021).
- Zhou, D.; Kalaitzis, P.; Mattoo, A.K.; Tucker, M.L. The MRNA for an ETR1 Homologue in Tomato Is Constitutively Expressed in Vegetative and Reproductive Tissues. *Plant Mol Biol* **1996**, *30*, 1331–1338, doi:[10.1007/BF00019564](https://doi.org/10.1007/BF00019564).
- Zhou, H. Fiscal Decentralization and the Development of the Tobacco Industry in China. *China Economic Review* **2000**, *11*, 114–133, doi:[10.1016/S1043-951X\(00\)00013-4](https://doi.org/10.1016/S1043-951X(00)00013-4).

General references

Zhou, L.; Tang, R.; Li, X.; Tian, S.; Li, B.; Qin, G. N6-Methyladenosine RNA Modification Regulates Strawberry Fruit Ripening in an ABA-Dependent Manner. *Genome Biology* **2021**, *22*, 168, doi:[10.1186/s13059-021-02385-0](https://doi.org/10.1186/s13059-021-02385-0)

Conclusions

1. Two reciprocal introgression line (IL) populations with ‘Védrantais’ and ‘Piel de Sapo’ as parental lines have been developed. In six generations, around thirty-five lines were developed of each population, covering 98% of the recurrent parent with introgression of the donor parent.
2. Several QTLs and major genes have been mapped in the IL populations controlling fruit morphology, fruit quality and fruit ripening related traits.
3. Two major previously identified QTLs for fruit ripening have been mapped and validated in both genetic backgrounds: *ETHQV8.1* and *ETHQV6.3*.
4. With a fine-mapping strategy, *ETHQV8.1* has been narrowed down to a 3.6 Kbp region in chromosome 8, containing a single annotated gene: *MELO3C024520.2* or *Ethylene responsive transcription factor 024 (ERF024)*.
5. *CmERF024* has been validated as the causal gene of *ETHQV8.1* using introgression lines and CRISPR/*Cas9* gene editing. High expression of *CmERF024* induces a climacteric behavior, while lower or absence of expression leads to a much milder climacteric behavior.
6. *CmERF024* seems to somehow control epigenomic changes at the onset of ripening, mainly chromatin structure and DNA accessibility by regulating the expression of histones.
7. QTL stacking is a powerful strategy to study QTL x QTL interactions shaping quantitative traits. Minimizing the genetic background effects, interactions are detected more clearly, simplifying phenotype predictions.
8. A few QTLs are sufficient to cover a wide range of ripening behavior in both ‘Védrantais’ and ‘Piel de Sapo’ genomic backgrounds, proving that QTL stacking may also be a powerful strategy for breeders.
9. There is a crosstalk between ethylene production, respiration rate and primary metabolism, although the leading process for melon fruit ripening is still unidentified.
10. Metabolic profiling can help melon breeders to develop new varieties with improved nutritional content.

